University of Plymouth

PEARL **https://pearl.plymouth.ac.uk**

04 University of Plymouth Research Theses 01 Research Theses Main Collection

2008

Mathematical modelling of shoreline evolution under climate change

Zacharioudaki, Anna

http://hdl.handle.net/10026.1/473

http://dx.doi.org/10.24382/3350
University of Plymouth

All content in PEARL is protected by copyright law. Author manuscripts are made available in accordance with publisher policies. Please cite only the published version using the details provided on the item record or document. In the absence of an open licence (e.g. Creative Commons), permissions for further reuse of content should be sought from the publisher or author.

University of Plymouth

School of Engineering, Faculty of Technology

Mathematical Modelling of Shoreline Evolution under Climate Change

by

Anna Zacharioudaki

Doctor of Philosophy

May 2008

To my father

Mathematical Modelling of Shoreline Evolution under Climate Change

Abstract

Anna Zacharioudaki

This study focuses on the impact of potential changes in the wind-wave climate on shoreline change. The 'one-line' model for medium to long-term prediction of coastline evolution is employed. New analytical and numerical solutions of this important model are described. Specifically: 1) original semi-analytical solutions are derived that relax the unrealistic assumption of existing analytical work that a constant wave condition drives shoreline change and, 2) a more general form of the one-line model is solved with a novel application of the 'Method of Lines'. Model input consists of 30-year nearshore wave climate scenarios, corresponding to the 'present' (1961-1990) and the future (2071-2100). Winds from a high resolution, (12km *x* 12km), regional climate model, obtained offshore of the south-central coast of England at a dense temporal resolution of 3 hours, are used to develop the aforementioned wave climate scenarios, through hindcast and inshore wave transformation. A hypothetical shoreline segment is adopted as a 'benchmark' case for comparisons. Monthly and seasonal statistics of output shoreline positions are generated and assessed for relative changes of 'significance' between 'present' and future. Different degrees of evidence that such changes do exist are found. This study is the first application of such high resolution climate model output to investigate climate change impact on shoreline response. Major findings include: 1) shoreline changes of 'significance' are strongly linked to 'significant' changes in future wave direction, 2) future changes appear smaller for entire seasons than for individual months, 3) shoreline position variability is often smaller in the future, 4) different climate model experiments produce diverging results; however, general trends are largely similar.

The present study, at a fundamental level, offers analytical solutions of the 'one-line' model that are closer to reality and a numerical solution that is of increased efficiency. At a practical level, it contributes to better understanding of the patterns of shoreline response to changing offshore wave climate through: 1) the use of fast and straightforward methods that can accommodate numerous climate scenarios without need for data reduction, and 2) the development of a methodology for using climate model output for coastal climate change impact assessment studies.

Contents

List of Figures

List of Tables

Abbreviations

A2	medium-high future climate scenario (referred as A2 'scenario')
A12	HIRHAM-H simulation of the A2 'scenario' at 12km resolution
AGCM	Atmosphere General (or Global) Circulation Model
AOGCM	Atmosphere-Ocean General (or Global) Circulation Model
B2	medium-low future climate scenario (referred as B2 'scenario')
C	present climate simulation (referred as 'control')
C12	HIRHAM-H simulation of the 'control' at 12km resolution
DEFRA	Department for Environment, Food and Rural Affairs
DHI	Danish Hydraulic Institute
DNMI	Norwegian Meteorological Institute
E	Explicit finite difference solution
EC50	HIRHAM-E simulation of the 'control' at 50km resolution*[1]
EMO	Met Office European waters wave MOdel
GCM	General (or Global) Climate model
HC50	HIRHAM-H simulation of the 'control' at 50km resolution*[2]
HIRHAM-E	HIRHAM RCM driven by ECHAM4/OPYC GCM
HIRHAM-E50	HIRHAM-E at 50km resolution
HIRHAM-H	HIRHAM RCM driven by HadAM3H GCM
HIRHAM-H12	HIRHAM-H at 12km resolution
HIRHAM-H50	HIRHAM-H at 50km resolution

IPCC	Intergovernmental Panel on Climate Change
JERICHO	Joint Evaluation of Remote Sensing Information for Coastal Defence and Harbour Organisations
LHB	Left Hand Boundary
M	MOL solution
MOL	Method of Lines
MSL	Mean Sea Level
NAO	North Atlantic Oscillation
NWP	Numerical Weather Prediction
ODE	Ordinary Differential Equation
ODN	Ordinance Datum Newlyn
PDE	Partial Differential Equation
PESETA	Projection of Economic impacts of climate change in Sectors of the European Union based on boTtom-up Analysis
PRUDENCE	Prediction of Regional scenarios and Uncertainties for Defining EuropeaN Climate change risks and Effects
RCM	Regional Climate Model
RHB	Right Hand Boundary
RMSE	Root Mean Square Error
SANDS	Shoreline and Nearshore Data System
SLR	Sea Level Rise
SPMs	Shore Management Plans
SRES	Special Report on Emission Scenarios
SST	Sea Surface Temperature
STOWASUS – 2100	STOrm, Wave and Surge Scenarios for the 2100 century

UKCIP	United Kingdom Climate Impacts Project
WASA	Waves and Storms in the North Atlantic
WG	Working Group

*[1] Similarly, EA50 and EB50 for the A2 and B2 climate scenarios respectively

*[2] Similarly, HA50 and HB50 for the A2 and B2 climate scenarios respectively

Symbols

a	distance between the groynes in a groyne compartment.
a, b	length parameters
A	cross-sectional area
C_g	wave group velocity
D	vertical extension of the active part of the shoreline
D'	sea level
D_{50}	mean grain size
D_B	berm height
D_c	depth of closure
D_e	uniform wave energy dissipation per unit volume
D_{lt}	depth of active longshore transport
$erf(x)$	error function
$erfc(x)$	complementary error function
E	wave energy per unit length
f	spatial differential operator
F	wave energy flux in shallow water
$F_c[]$	finite Fourier cosine transform
F_c^{-1}	inverse finite Fourier cosine transform
$F_s[]$	Fourier sine transform
F_s^{-1}	inverse Fourier sine transform

g	acceleration of gravity
h	still water depth
H	wave height
H_e	non-breaking significant wave height that is exceeded 12 hours per year
H_{rms}	root-mean-square wave height
H_s	significant wave height
I	alongshore immersed weight sediment transport rate
k	constant
k	proportionality coefficient
K, K', K_1, K_2	dimensionless constants
L	cross-shore distance to the depth of closure
L_g	groyne length
m	derivative order
MSL	mean sea level $\equiv D'$
P	wave power
q	point sources/sinks of sediment along the shoreline
$q_{y,dune}$	sediment exchange of the upper shoreface with the backshore
$q_{y,sea}$	sediment exchange of the upper shoreface with the lower shoreface
Q	alongshore sediment transport rate
Q_0	amplitude of longshore sediment transport
Q_b	sediment bypassing rate
Q_y	cross-shore net gain or loss of sediment
$r(t)$	source/sink function
R	shoreline retreat rate
RC	an arbitrary constant rate of change

$s(x,t)$	source/sink function
S	sea level rise
t	time
T_e	wave period associated with H_e
T_p	peak wave period
u	vector of dependent variables
u	zonal component of the wind vector
u_m	maximum horizontal near bottom wave orbital velocity evaluated at the breaker zone
v	Fourier transform variable
v	meridional component for the wind vector
$\bar{v}$	average longshore current velocity in the surf zone
w	dummy variable
x	represent a three vector (x, y, z)
x, y, z	ordinates in horizontal and vertical directions (denote alongshore and offshore distance respectively)
y_0	initial width of a rectangular beach fill
y_b	cross-shore position of D_B
y_c	cross-shore position of D_c
y_s	shoreline position
α	angle between the breaking (or nearshore) wave crest and the shoreline
α_0	angle between the breaking (or nearshore) wave crest and the x-axis (set parallel to the shoreline trend)
β	beach slope
γ	breaker index

ε	diffusion coefficient
ε_s	small angle approximation diffusion coefficient
ε_w	wide angle approximation diffusion coefficient
θ_0	deep water wave angle
μ	Gaussian distribution mean
ξ	dummy variable
ρ	sea-water density
ρ_s	sediment density
σ	Gaussian distribution standard deviation
σ	sediment porosity

Subscript *b* value of parameter at breaking

Symbols related to numerical solutions

dt	time-step
dx	spatial grid cell size
eps	integration local error tolerance
h	integration stepsize
h'	stepsize variable
hdid	integration stepsize accomplished
hmin	minimum integration stepsize
hnext	next integration stepsize to be taken
maxstp	maximum number of calls to a subroutine
n	number of integration steps
neqn	number of ODEs

N	number of grid points
t_0	initial time of integration
t_f	final time of integration

Symbols related to hypothesis tests

alpha	significance level
ci	confidence interval
h	constant denoting acceptance of rejection of the "null hypothesis"
ne	equivalent sample size
N	number of data points in a sample
p (p-value)	probability of obtaining by chance a value of the hypothesis test statistic as extreme or more extreme than the value computed from the sample
r_1	lag-1 autocorrelation coefficient
x, y	population samples

Acknowledgments

I would like to express my gratitude to my supervisor, Prof Dominic Reeve for his tremendous support, guidance and encouragement over the years. His peaceful approach to every problem helped keep me composed and positive over stressful periods. My sincere gratitude should also go to Dr Julian Stander who spent lengthy time improving my understanding of relevant statistics and exploring different possibilities with me.

I would like to thank everyone in the Coastal Engineering Research Group of the University of Plymouth for being welcoming and supportive. I especially thank Dr Jose Horrillo-Caraballo, my officemate for his frequent I.T and scientific advice. In this respect, I also thank Dr John Lawrence and Dr Adrian Pedrozo-Acuna. Thanks also to Dr Harshinie Karunarathna for kindly offering the explicit 'one-line' numerical code I used in my thesis.

With respect to information and data for the project, I should like to thank the Channel Coastal Observatory and the Bournemouth Council for kindly granting me access to the Poole Bay data sets in SANDS. Particular thanks going to Travis Mason for responding to my frequent data related questions. Further thanks to Ole Bøssing Christensen at DHI for the climate model data sets and his support on these data; and to Michael Stickley for his help on certain aspects of the SANDS software.

I would like to thank Dr Phil James for his thoughts on the Gibb's phenomenon present in my results. Also, I thank Mr Paul Thompson for kindly explaining to me mathematical concepts. I am really sorry to both of them if it was obvious that I do not get pure mathematics easily.

I would like to thank with all my heart the people that have not necessarily been directly linked to any aspect of my research but have generously offered moments of happiness and laughter, 'seriously' supported me, or hugged me in moments of panic or depression. Thank you for not abandoning me during dull periods of life, having little to say or offer. For inexplicable reasons I would like to especially thank Nadine Schaefer, Joao Magalhaes Martins, Miriam Vadillo, Lari Vainio, and David Forber.

Last but not least, I would like to thank Frederic Verret for loving all my moods (nearly!), for being always there and for giving me plenty of reasons to love him. My future 'research' will definitely focus on him as to date the relevant results have been the most rewarding.

Author's Declaration

At no time during the registration for the degree of Doctor of Philosophy has the author been registered for any other University award without prior agreement of the Graduate Committee.

Conferences attended and presentations:

2006 Young Coastal Scientists and Engineers Conference (YCSEC'06), 19th and 20th April, Southampton, UK.

2007 Young Coastal Scientists and Engineers Conference (YCSEC'07), 19th and 21th April, Plymouth, UK.

2007 RCEM 2007: 5TH IAHR Sympsoium on River, Coastal and Estuarine Morphodynamics, 17-21 September, Twente, Netherlands.
Poster presentation: "Explicit formulae of shoreline change under time-varying forcing".

Publications:

Zacharioudaki, A. and Reeve, D. E., 2007. Explicit formulae of shoreline change under time-varying forcing. *Proceedings of the Conference on River, Coastal and Estuarine Morphodynamics: RCEM2007*, Twente, Netherlands, pp. 1067-1074.

Zacharioudaki, A. and Reeve, D. E., 2008. Semi-analytical solutions of shoreline response to time-varying wave conditions. *Journal of Waterway, Port, Coastal, and Ocean Engineering* (in press).

Zacharioudaki, A. and Reeve, D. E., 2008. A note on the numerical solution of the One-line model. Submitted to *Journal of Coastal Engineering.*

Word count of main body of thesis: ≈ 56,000 words

Signed ..... Zacharioudaki .....

Date ..... 01/10/08 .....

Chapter 1

Introduction

1.1 Shoreline erosion and its threats

Shoreline erosion is a common problem in UK and elsewhere (e.g. Bird, 1993). Sandy shorelines in particular, shaped predominantly by net gradients in the alongshore sediment transport and sediments induced through land erosion, are amongst the most prone to erosion. Bird (1985) stated that at least 70% of sandy beaches around the world are recessional. A number of later studies (see e.g. Zhang *et al.*, 2004) also document a widespread trend of erosion. Sea-Level Rise (SLR) and changes in the storm climate have been reported as plausible causes of this general trend besides localized human interference.

Shoreline erosion is a problem for a number of reasons. Most importantly, as the protective shore narrows the risk to coastal assets increases because of storms and flooding. Breaching might occur at certain coastal environments (e.g. barrier islands, spits). In addition, existing defensive coastal engineering structures often fail under coastal erosion (e.g. enhanced scour or overtopping), leading to an amplification of the above risks. Adverse impacts on tourism and coastal recreational activities may also occur. Figure 1.1 shows examples of severe shore erosion and associated problems.

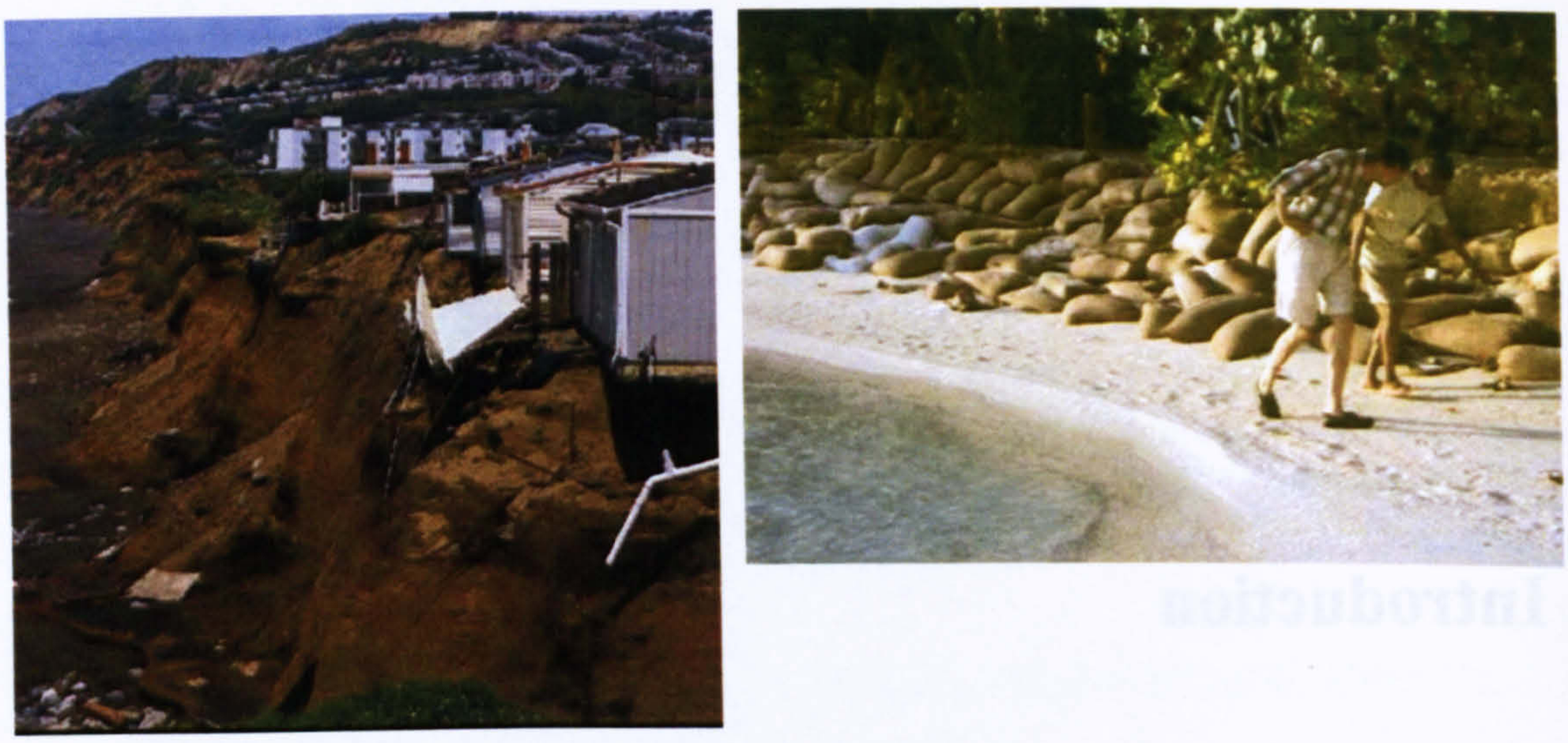

Figure 1.1 Coastal erosion in Pacifica, California is a pervasive problem that threatens many homeowners (left) (adopted from http://solidearth.jpl.nasa.gov/PAGES/sea01.html, 2003). Sandbags piles against the eroding sand at Maldives (right) (adopted from Goreau *et al.*, 2004)).

In the future, beach erosion is anticipated to exacerbate because of accelerated SLR due to climate change. According to Bird (1993) and Leatherman *et al.* (2000) even shorelines that are accretional at present will stabilize or even retreat. Nevertheless, accelerated SLR is not the only climatic change with severe implications on long-term shoreline evolution. Potential climatic changes in wave climate, storm frequency and intensity, tidal range, and precipitation are all important in determining future shoreline trends at open sandy beaches and could enhance or counter the effects of SLR alone (e.g. Bell *et al.*, 2001; Douglas *et al.*, 2001; Stive *et al.*, 2002; Walsh *et al.*, 2004; Cowell *et al.*, 2006). Evidence of accelerated SLR in the future is growing (e.g. IPCC WG1, 2007). Evidence of change in the other factors responsible for shaping coastlines is less strong; however, numerous studies have reported changes beyond the limits of natural variability (e.g. IPCC WG1, 2001; Kaas *et al.*, 2001; Hulme *et al.*, 2002; Alexander, 2005).

It is apparent from the above that Shoreline Management Plans (SPMs) - initiated by the UK government to bring a more strategic approach to coastal planning and development and consisting of: 1) a large-scale assessment of the risks associated with

coastal processes and, 2) a policy framework to reduce these risks to people and the developed, historic and natural environment in a sustainable manner - need to account for potential climatic changes in order to be effective in the long-term. More precisely, they should account for any change in the main processes shaping any particular coastline expected to occur within time-scales of coastal evolution approximately equal to the design life of coastal engineering projects (Reeve and Spivack, 2004; Cowell *et al.*, 2006). In general, the capability of predicting shoreline evolution at these large timeframes, i.e. years to decades or even centuries, is important.

1.2 Predicting long-term coastal change

1.2.1 Difficulties

Although important, prediction of long-term coastal evolutionary tendency is difficult. This is because of the high complexity of the coastal system. Different forcing agents act at different spacial and temporal scales, vary continuously, and interact in a complex non-linear way. In addition, they are often of an unpredictable character (e.g. Larson *et al.*, 2003; Southgate *et al.*, 2003; De Vriend, 2003). The relative importance of the different processes and associated scales in the aggregated long-term response of the beach is not well-known. Ignoring climatic changes other than SLR, it has been suggested that long-term shoreline adjustment is essentially forced by large-scale processes, e.g. changes in sediment supply and transport patterns caused by changes in mean water levels or/and coastal engineering projects. The impact of time-varying processes, like fluctuating waves or tides has been thought to be smoothed in the long-term perspective (Hanson *et al.*, 2003). Nevertheless, as mentioned above, long-term shifts in wave climate, tidal levels,

extreme events, and precipitation statistics caused by climate change have been reported and these will also alter sediment transport patterns and sediment budgets (e.g. Halcrow, 2002). In fact, accelerated rates of SLR in combination with the aforementioned climatic shifts might severely impact future coastal evolution (e.g. Beniston *et al.*, 1998; IPCC WG2, 2001; Nicholls, 2002). Climate change introduces extra difficulties in the prediction of beach response on the relevant timescales. They arise from the intrinsic uncertainties involved: 1) uncertainty about the magnitude of climate change, and 2) uncertainty of its effect on sea-level, waves, tides, and other time-varying processes (Cowell *et al.*, 2006). Nevertheless, despite difficulties and uncertainties, decadal prediction of coastal change remains imperative in view of the potential threats of coastal erosion, described in the previous section.

1.2.2 Approaches

To date, few approaches to long-term beach evolution exist. By far the most popular ones involve mathematical modelling and this is the approach described in the following paragraph. Non mathematical approaches have also been investigated. Uncertainties associated with all approaches increase with time-scale. Prediction of beach evolution at timescales relevant to climate change has been the subject of a number of recent studies (e.g. Nicholls *et al*, 2007). However, on these timescales present methodologies are not well developed and the subject remains one of active research.

Mathematical models for the prediction of beach evolution include: 1) Quasi-3-Dimensional (Q3D) and 3D beach change models, 2) 'behaviour-oriented' models, 3) 1D shoreline models and 2DH multi-line models, and 4) hybrid models. The first models in this list are complex, based on deterministic dynamical equations for fluid flow and sediment transport. They have prohibitive computational demands in long-term forecasting

whilst it is unclear whether they include the relevant physics for long-term predictions as they often fail to produce reasonable results at these time-scales (De Vriend *et al.*, 1993; Hanson *et al.*, 2003). Furthermore, data requirements are high (Larson, 2005). 'Behaviour-oriented' models are simple empirical models that rely on equations that reproduce the type of behaviour observed in measurements. Although they may account for large time and space scales they also suffer from high data requirements and are of limited applicability because they are totally unrelated or weakly related to the physics of the coastal system. One-dimensional shoreline models, known as 'one-line' models, are simplified semi-empirical models whose fundamental assumption is that the shape of the beach profile is in equilibrium and where the shoreline evolves in response to the spatial gradients of the alongshore component of the sediment transport. Non-linear interactions and feed-back mechanisms between different processes are ignored or parameterized in a simplified manner (Gravens *et al.*, 1991; Hanson *et al.*, 2003). 'One-line' models have been routinely used since 1956 for the prediction of long-term shoreline evolution and are still very important for a number of reasons. In comparison to the models mentioned above they are computationally cheap, have reasonable data requirements for calibration and validation, are physics based and thus have a level of generality, and have performed well in numerous projects of long-term shoreline evolution (e.g. Gravens *et al.*, 1991; Reinen-Hamill, 1997; Dabees and Kamphuis, 1998). 'Multi-line' models are an extended version of 'one-line' models that account for shore profile changes. They are not preferred for long-term predictions of shoreline change because they are more complex but not necessarily more accurate than 'one-line' models. Hybrid models consist of a collection of models linked together so that a range of time and space scales maybe simulated simultaneously through a cascade of information between 'sub-models' (Hanson *et al.*, 2003). Although promising, hybrid models require parameterisation of various processes; however, the process of

parameterisation is not established. In addition, it is often difficult for the individual researcher to access, link, operate, and understand the broad range of models needed for predictions relevant to climate change.

1.3 Motivation – Objectives

Ideally, climatic changes in all factors that are important in shaping future coastlines, in addition to local topography and human activities and interference on the beach, should be taken into account when conducting a shoreline vulnerability assessment. I.e. when estimating the susceptibility of the coastal community to shoreline change, with this susceptibility determined from the level of impact of the aforementioned factors on shoreline change and the ability of the coastal system/community to cope with or adapt to the risks induced. However, incorporation of all factors is rarely possible because of limitations in data availability, computer resources, largely increased complexity, possibly increased uncertainty, and time. Only very recently, with the development of hybrid models, has a highly integrated approach to climate change and its impacts been attempted (Nicholls *et al.*, 2007). Traditionally, SLR impacts on shoreline evolution have been studied in isolation as, in contrast to the other climatic variables, sufficient evidence of change existed. However, an increasing number of studies on the impact of global warming in future wind, storm, and wave climates, using either historical trends (e.g. Gunther *et al.*, 1998; Gulev and Hasse, 1999; Cotton *et al.*, 1999; Alexander *et al.*, 2005) or climate model output (e.g. Kaas *et al.*, 2001; Hulme *et al.*, 2002; Räisänen *et al.*, 2003), suggests that future change is very likely. Such changes, particularly those in wave heights and directions resulting from changes in wind climate, are expected to contribute the most in altering future shoreline evolution patterns, since wave conditions are the main regulator of

longshore drift rates and direction. Therefore, the increased evidence of future change in these parameters has initiated, within the last few years, assessments of the potential effects of a changing wave climate on shoreline change.

The studies investigating the effect of SLR on future shoreline recession have routinely used a simple conceptual model, known as the Bruun Rule, and modifications of it (e.g. Richmond *et al.*, 1997; Lanfredi *et al.*, 1998; Leatherman *et al.*, 2000; Zhang *et al.*, 2004). Amongst the studies available at present on the investigation of the potential effect of climatic changes other than SLR on coastal evolution, only two, one by Ruggiero *et al.* (2006) on a sandy shore and one by Dickson *et al.* (2007) on a soft-rock shore, have explicitly forecasted future shoreline shapes in response to potential changes in future wave climate. The 'one-line' model is the basis of the modelling approach of these studies whilst both use incremental wave climate scenarios, i.e. when the variable of interest is changed incrementally by plausible but arbitrary amounts. Incremental scenarios are not physically based and often lack realism (IPCC WG1, 2001). Other reports, using incremental scenarios or coarse resolution climate model output have explored the effect of a changing wave climate on modifications of the littoral drift (e.g. Lorenzo and Texeira, 1997; Hosking and McInnes, 2002; Sutherland and Gouldby, 2002). Coarse resolution climate simulations are unable to capture changes in short range variability or extremes. Since such changes may show a very different pattern compared to average changes in climate, the reliability of the results of coarse resolution studies is constrained (Feyen *et al.*, 2006).

The five elements that motivate the present work are:

- The paramount importance of predicting decadal shoreline evolution.
- The scarcity of studies on shoreline evolution under climatic changes other than SLR.
- The use of incremental scenarios in these studies.

- The increasing availability of high spatial and temporal resolution output from comprehensive, advanced physically-based climate models
- The belief that changes in wave heights and directions along with SLR will contribute the most in altering future shoreline evolution patterns,

Thus, the relative changes in the evolution of a shoreline segment under various wave climate scenarios generated from high spatial and temporal resolution wind output from climate models are studied here. The 'one-line' model is employed in the study. In view of the chronic importance of this model in long-term predictions of shoreline change, certain improvements to its analytical and numerical solutions are also performed before its application.

Basic features of this study include:

- Potential changes in SLR, tidal range and precipitation are ignored. Impacts of changes in storm frequency and intensity other than on the littoral drift are also neglected.
- Although the location of the original data, used in this study, is situated offshore the south-central coast of the United Kingdom, the results produced are not site-specific as a common but hypothetical stretch of shoreline is adopted. This is to simplify the modelling, focus on the methodology proposed, and provide qualitative results that are broadly representative of stretches of coastlines having a similar setting. Thus, although wave climate changes are site-specific, it is possible that other similar coastlines where predicted changes in the wave climate are of a comparable magnitude will experience similar rates of change.
- The study focuses on open predominantly sandy shores, where alongshore sediment transport is the main mechanism determining long-term evolution. This is because this type of coastal environment is the most suited for 'one-line' modelling.

1.4 Thesis layout /Methodology outline

The work carried out in this study is organized as follows:

Chapter 2: This chapter focuses on the mathematical modelling. Thus, present approaches to long-term predictions of coastal change are presented in some greater detail with the focus on the 'one-line' model for long-term shoreline change which this study improves and applies.

Chapter 3: This chapter gives a review of the science of climate change. Thus, climate change scenarios and their potential impacts on shoreline evolution are described. The review focuses on sandy shores and UK climate.

Chapter 4: New generalized analytical solutions to the 'one-line' model are derived for certain cases of shoreline change. The new solutions, in contrast to existing ones, can account for time-varying wave forcing. As a result, they are considerably more realistic.

Chapter 5: An improved numerical solution to the 'one-line' model is proposed. Specifically, a well-established, particularly efficient and versatile numerical scheme is applied for the first time towards solving the model numerically. Certain benefits arise from this application.

Chapter 6: In this chapter, the analytical and numerical solutions derived in the two previous chapters are compared. The aim is to investigate how assumptions and errors associated with each of these solutions affect their relative performance under time-varying wave conditions.

Chapter 7: Wind data sets (8 30-year 3-hourly time-series corresponding to the 'present', 1961-1990, and a future period, 2071-2100) from climate models are used to hindcast offshore waves which are then transformed nearshore to form the wave climate scenarios needed to achieve the main objective of this study, i.e. assess shoreline change under a

changing wave climate. Aiming to retain the full information of the original data but at the same time being capable of accommodating a broad range of scenarios, simple, fast, and straightforward modelling techniques are proposed. A rigorous statistical test is carried out to identify differences of 'significance' in the mean characteristics of the various nearshore wave climate scenarios.

Chapter 8: The nearshore wave scenarios generated in Chapter 6 are input in the 'one-line' models, developed in Chapters 3 and 4, to produce monthly and seasonal shoreline statistics corresponding to each input scenario. Rigorous statistical tests are performed to identify evidence of change between 'present' and 'future' patterns of shoreline evolution. Results are qualitative, given in terms of general trends.

Chapter 9: The key attributes and conclusions of this study are summarized. In addition, suggestions for future complementary research are made.

It is highlighted that accurate prediction of the impacts of climate change on future shoreline evolution is difficult and inherently uncertain irrespective of the method used. In this context, the present study serves as an early assessment of shoreline change and also as a proposition of simple but often preferable methods to this problem. However, its simplifications and assumptions should be kept in mind when interpreting the results.

Chapter 2

Mathematical modelling of shoreline change

In this chapter, methods and processes relevant to the prediction of shoreline evolution are dealt with in some detail. Firstly, the different mathematical methods available to date for the prediction of long-term shoreline changes are better introduced. Non-mathematical techniques are also described. The relative advantages and disadvantages of these two general approaches are outlined. Secondly, the 'one-line' model, the method chosen for use in the present study, is described in detail. Initially, the model theory is explained and model related expressions are presented. Then, analytical and numerical solutions to these expressions are described. The pros and cons of the two types of solutions are outlined, solution techniques are explained, and example solutions/models are presented. The required model inputs/outputs are then introduced along with some methods for obtaining the necessary wave input. The chapter finishes with a discussion relevant to the choices and objectives of this study.

2.1 Approaches to long-term predictions of shoreline change

2.1.1 Mathematical modelling

At present, mathematical modelling is definitely the most widespread method used for the prediction of coastal change at all time and space scales. This is for a number of reasons:

- Mathematical modelling can further assist in the understanding of the processes governing coastal evolution. Models involve assumptions typically made to reduce the overwhelming complexity of the coastal system. Hence, they may be seen as a tidy and concise means of testing the validity and generality of these assumptions through the process of calibration and validation at a broad range of locations and with respect to scale (Cowell and Bruce, 2006; Hanson *et al.*, 2003).
- They can provide guidance on the kind and scale of measurements needed to improve assumptions, understanding, and thus predictions of coastal change.
- They offer a systematic framework for the collection and analysis of data and for the evaluation of alternative future scenarios of coastal evolution. For example, medium to large scale models are especially useful for the design of engineering works through the investigation of the possible impact of different designs and the optimization of the best option (Hanson *et al.*, 2003).
- They are time and cost efficient.

Mathematical models are not perfect. They are simplified representations of nature which is extremely complex, often chaotic (Southgate *et al.*, 2003). As a result, their forecasts do not necessarily represent the truth and should be treated with caution. This is particularly true in the long-term engineering scale when characteristic features of the

system (e.g. a representative wave climate) may change. That is why applied long-term mathematical models have being severely questioned (Young *et al.*, 1995; Thieler *et al.*, 2000; Cooper and Pilkey, 2004; Pilkey and Cooper, 2006), although by a small scientific group. Alternatives to mathematical modelling will be discussed in the second part of this section. Here, a brief description of the models that are presently available for shoreline prediction and of their capabilities continues from Section 1.2.2.

Q3D and 3D beach change models.

These complex, first principle process-based models can account for strong non-linearities and feedback mechanisms (e.g. bed topography updating) and make the least assumptions compared to any other models of coastal evolution. Although skillful at hydrodynamic time-scales, even the simpler of these models, e.g. schematic or quasi three dimensional (Q3D) models, are not suited for time-scales larger than some years and space scales larger than a few kilometres (Figure 2.1), (Larson, 2005). A number of problems appear at these scales. Hence, one problem is that they have prohibitive computational demands. Although a number of reduction techniques, e.g. input reduction, have been introduced to overcome this problem, still the decadal time-scales are out of reach. But even if computer power was not an issue, it is unclear whether these models include the relevant physics for long-term predictions. Longer-time evolution is considered to depend mainly on weak residual effects, which are often disregarded in short-term models, whilst it is uncertain which short-term processes are important in the long-run (De Vriend *et al.*, 1993; Hanson *et al.*, 2003). In addition, at present, there is limited knowledge on the interaction between complex fluid motion and sediment particle motion over an irregular bed. Consequently, results obtained after up-scaling of first physical principle models are extremely uncertain (Hanson *et al.*, 2003). Finally, a large amount of data for calibration

and validation are required due to the fact that this type of models simulates fine details of natural processes (Larson, 2005)

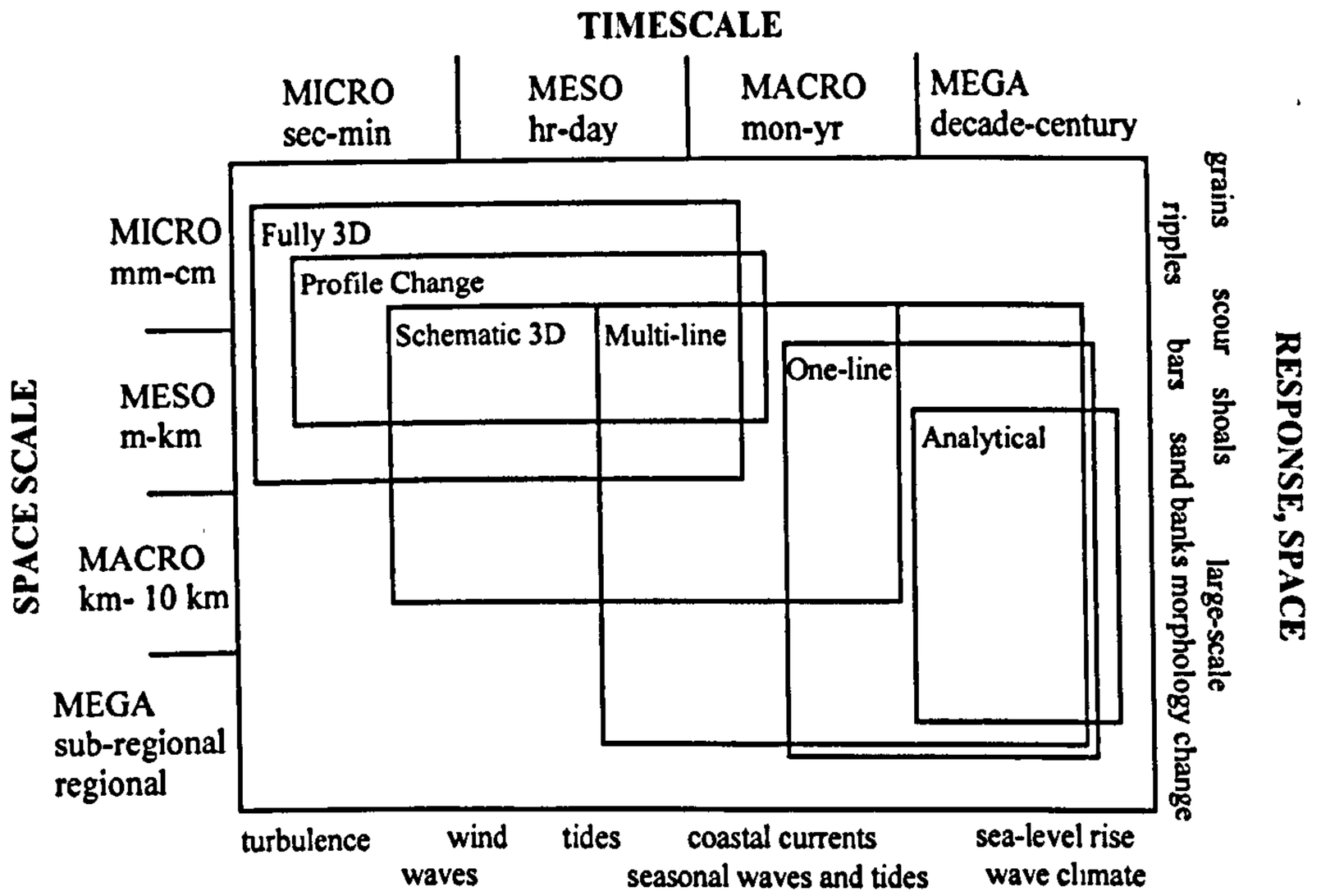

Figure 2.1 Classification of coastal evolution models in terms of characteristic spatial and temporal scales (adopted from Larson, 2005)

'Behaviour-oriented' models

These are simple mathematical models that are essentially phenomenological (De Vriend *et al.*, 1993), i.e. they can simulate coastal behaviour, without necessarily having any relation with the underlying physical processes. Analysis of a rich set of field observations and information obtained through process-based model runs with real-life input conditions, are used to map the behaviour of the coastal system. Then, mathematical formulations are derived that are able to reproduce certain aspects of the observed behaviour relevant to the time and space scales of interest (Capobianco *et al.*, 1999; Larson *et al.*, 2003).

The simplicity of this model type allows for space-scales of hundred of kilometres and time-scales of decades to centuries to be simulated. However, predictions are poor if

the amount and/or quality of the data used to generate the model do not well reflect the basic features of the process under study in a particular time and space scale. Accurate, complete and long data sets are rare, especially if prediction over several decades is of interest. Inevitably, the development of 'behaviour-oriented' models is obscured by a lack of data, particularly for prediction within larger scales. Another drawback related to these models is that they are not generally applicable. This is especially true when they are totally unrelated to physics. Thus, they might perform well at a particular site but give poor predictions for another location with different mechanisms acting at different time-scales. Nevertheless, some physical consideration in 'behaviour-oriented' models is possible, hence increasing their applicability (Larson *et al.*, 2003).

'Behaviour-oriented' models have been developed mostly for profile change. A simple example of this type of models is the well-known Bruun Rule (see Section 3.3.1) which predicts shoreline recession under sea-level rise (Bruun, 1962). In this case, although the formulation is not related to physics, it can still be explained though physical reasoning (see Sections 2.2.1.4 and 3.3.1). The evolution of the shoreline and bed contours was estimated as part of the Dutch Kustegenese program (Stive *et al.*, 1990), using 'behaviour-oriented' modelling. This was done by considering several profiles alongshore connected and exchanging sediments through the process of longshore drift.

<u>1D shoreline models and 2DH multi-line models</u>

These are quite simplified models, used to predict the evolution of the shoreline alone, 'one-line' models, or the evolution of two or more depth contours, typically including the shoreline, 'multi-line' models. Their fundamental assumption is that there is an explicit equilibrium state under constant external forcing.

As mentioned in Section 1.2.2, 'one-line' models assume that the shape of the beach profile is an equilibrium constant shape and that the shoreline evolves in response to the spatial differentiation of the alongshore component of the sediment transport. 'Multi-line' models divide the beach into multiple subsections and a 'one-line' calculation is performed for a depth contour from each division. In this way some 2D aspect is introduced compared to one-line models. The depth contours evolve in response to a combination of net cross-shore and longshore sediment transport. The equilibrium single profile, used in 'one-line' models, is now used for the assessment of the cross-shore interaction between the different layers (Kamphuis, 2000; Hanson *et al.*, 2003).

'One-line' models are the most developed, well-documented, and by far the most applied models for medium to long-term predictions of shoreline change (Figure 2.1). Their predictive capabilities have been proven good (e.g. Hanson, 1987; Reinen-Hamill, 1997; Dabees and Kamphuis, 1998; Szmytkiewicz *et al.*, 2000). 'Multi-line' models have become applicable only recently, after significantly improving the cross-shore transport parameterizations (Steetzel, 1995; Steetzel *et al.*, 2000). However, they are still rarely used in engineering practice, especially when long-term prediction of shoreline change is the objective (Figure 2.1). As noted in Section 1.2.2, this is because despite their increased complexity, compared to 'one-line' models, they do not significantly improve the predictions (Hanson *et al.*, 2003).

The fact that models in this category are computationally cheap, are physics related and thus of sufficient generality, have reasonable data requirements for calibration and validation, and have performed well in numerous projects (mainly the 'one-line' model), makes them actually the only mathematical tool one can readily resort to at present for prediction of shoreline position changes in the very long time-scales, i.e. decades. In this large timeframe, analytical solutions of the 'one-line' model for idealized cases are

especially useful, since they do not suffer from accumulation of errors inherent in numerical schemes.

The simplified relations and assumptions of the 'one-line' model in combination with its deterministic nature which does not provide with uncertainty bands have naturally provoked considerable criticism against its extensive use (Young *et al.*, 1995; Thieler *et al.*, 2000). Modellers do accept its drawbacks. However, in view of its good performance, of the general advantages of the use of mathematical models outlined at the beginning of this section, and the need for long-term predictions, they believe in the model and encourage its further improvement and its correct application, i.e. respecting its application limits. In addition, steps are currently made to relax the deterministic nature of the model by using it in a probabilistic manner, thus providing uncertainty estimates (Dong and Chen, 1999; Reeve and Spivack, 2004; Payo *et al.*, 2004; Ruggiero *et al.*, 2006; Cowell *et al.*, 2006). A common approach is to run the 'one-line' model in a Monte Carlo setting (e.g. Ruggiero *et al.*, 2006). Nevertheless, even if decadal deterministic output might not be appropriate for quantitative studies it can still give a valuable qualitative insight into the evolution of the system

Hybrid or 'system' models

The term 'system' refers here to a collection of generalized computer models. In a 'system' various model types are linked so that a range of time and space scales, typically found in large scale morphodynamic problems, may be simulated simultaneously by matching model type and relevant scale of applicability and then allow for the information to pass between models. In general, when time-scale is considered, smaller scale models give input to larger scale models, e.g. an initial transport field or an indication of the equilibrium state (Hanson *et al.*, 2003), whilst in space, regional characteristics 'cascade' to

local shoreline stretches. A very recent example of the hybrid modelling approach is the 'integrated coastal simulator', which is under development for the UK by the Tyndall Centre for Climate Change Research in partnership with the Environmental Agency (Nicholls *et al.*, 2007). This adopts an integrated approach, combining models of global, regional (e.g. North Sea), and local (e.g. coastal cell) scale. The linked models may describe climate (waves, surges, and mean sea-level), sand-bank morphodynamics, wave transformation, shoreline morphodynamics, built environment changes, ecosystem changes, and erosion and flood risk. In addition, non-mathematical approaches (see following section) are incorporated to cover cases where mathematical modelling is not appropriate or inadequate. Time-scales of up to centuries may be simulated.

Further development of 'system' models is expected to greatly improve long-term forecasts of coastal evolution. However, as mentioned in Section 1.2.2, the development of such an approach requires large funds and collaboration between researchers. It is extremely difficult for the individual scientist to develop or even understand the details of this kind of approach, except probably for the coupling of a very small number of simple models. In addition, hybrid models require parameterisation of various processes, a procedure that is not well established.

2.1.2 Non-mathematical modelling

Non mathematical approaches are all based on some sort of extrapolation of historical data, quantitative or qualitative.

<u>Quantitative extrapolation of historical data</u>

At the simplest, quantitative predictions of large-scale, long-term shoreline evolution has been made through extrapolation of historical measurements without taking

into account the behaviour and interaction of the different components that make up the system (Southgate *et al.*, 2003; Burgess *et al.*, 2004).

This approach is severely limited by data availability. Predictions can be accurate only at time-scales much shorter than those covered by the data time-series. Thus, long-term predictions would require an excessive amount of data not even available in the most comprehensive data sets to date (Southgate *et al.*, 2003). Furthermore, since no physical considerations are involved, the method applies only to the specific study site and predictions rely on the implicit assumption that the statistics of the forcing will remain the same. Finally, the method can not account for changes in the sediment budget since shoreline evolution is predicted in isolation from the rest of the coastal system.

'Behavioural systems' approach

This approach was developed not long ago as part of a study called 'Futurecoast', commissioned in 2000 by the UK national government Department for Environment, Food and Rural Affairs (DEFRA) to provide qualitative predictions of coastal evolution tendencies over the next century for the whole coast of England and Wales (Burgess *et al.*, 2004). It is somehow the equivalent of the 'systems model' mathematical approach but based mostly on field observations and experience and less on mathematical model output. Specifically, the approach seeks to understand the processes and their interactions at the different time and space scales that might contribute to the long-term evolution of the system. This is done though the collation, collection, and analysis of a large amount of data and information. A 'top-down' description of the coastal environment is then possible, starting with the knowledge of the characteristics of the wider scale involved, normally beyond the limits of a coastal cell, and gradually focusing on the smaller local scale allowing for information to cascade between scales. Ultimately, after qualitative sediment

budget estimates are obtained, i.e. sources, sinks, and pathways, and past evolution of the shoreline is investigated to identify long-term controls and behaviour, an appreciation of the most likely shoreline change over the next century is possible. A similar approach is proposed by Cooper and Pilkey (2004), who further strengthen the importance of experience on similar types of beaches, in the regional and global scale.

Data limitation is again a serious problem. To characterize the system correctly at the desired time and space scales, a large amount of data is required. In addition, data sets of a diverse nature are needed in this case in order to capture the complex interactions within the system. Furthermore, such a method is of overwhelming complexity and as for 'system models' is better pursued by a team of researchers as part of a highly funded project. Cowell and Bruce (2006) refer to a case of coastal development in New Zealand where researchers after examination of the same information on the history of the coastal system produced a "notable absence of consensus" (Thompson, 2006, cited in Cowell and Bruce, 2006). This means that such an approach is subjective. In addition, although results may help to understand other cases, it is still of limited generality.

It is concluded that the constraints to the application of non-mathematical methods for the prediction of decadal shoreline evolution are even more severe than those associated with mathematical models. An inclusive approach, involving both mathematical and non-mathematical techniques, would probably be the best practice for sound coastal management.

2.2 The 'one-line' model of shoreline evolution

2.2.1 Model theory and related expressions

2.2.1.1 Basic concept

The foundation of the 'one-line' theory is that the cross-shore beach profile is essentially unchanged in the long-term perspective. This relatively stable profile is referred as "equilibrium beach profile". Its concept is based upon the analysis of numerous beach profiles which has indicated that a specific beach has a characteristic profile depending mainly on the sediment properties and being almost independent of the temporal variations of wave climate (Bruun, 1954; Dean, 1977). Short-term beach profile fluctuations in response to on-shore off-shore sediment transport due to varying incident wave conditions and especially due to storm events do exist. If not considerably great, these seasonal or storm-induced profile changes do not cause the long-term average beach profile to vary substantially as they essentially cancel out. Based upon the equilibrium profile concept 'one-line' theory assumes that the bottom profile moves parallel to itself without changing its shape during erosion or accretion. Hence, only one contour line, the shoreline in this case, is needed for determining the location of the entire cross-section (Pelnard-Considère, 1956). The concept of equilibrium beach profile will be examined closer in Section 2.2.1.4.

Shoreline position changes over a long enough simulation period are assumed to be primarily caused by the temporal evolution of spatial differences in the longshore sediment transport rates. Consequently, 'one-line' models are best suited when there is a systematic trend in shoreline evolution, e.g. erosion down-drift of a groyne (Hanson, 1987; Larson *et al.*, 1997). Cross-shore transport is taken into consideration when short-term shoreline

fluctuations are significant. Otherwise, cross-shore effects on longer-term shoreline evolution are assumed negligible compared to longshore effects. Inclusion of cross-shore sediment transport is achieved though external calculation or through 'one-line' compatible methods (Reinen-Hamill, 1997; Dabees and Kamphuis, 1998; Hanson and Larson, 1998; Karambas *et al.*, 2001).

Pelnard-Considère (1956) was the first to derive a mathematical model governing the evolution of the shoreline in response to longshore sediment transport, now called the 'one-line' model. The simplest form of a 'one-line' model is a linear diffusion equation with constant coefficient (Equation 2.1).

$$\frac{\partial y}{\partial t} = \varepsilon \frac{\partial^2 y}{\partial x^2} \tag{2.1}$$

In Equation 2.1, $y(x,t)$ is the position of the shoreline from a fixed datum line, usually taken to be the x-axis which runs parallel the shoreline trend so that x is the alongshore distance. The variable t is the time, and ε is a diffusion coefficient that is a measure of the rate at which sediment is transported alongshore. The derivation of Equation 2.1 will be examined in Section 2.2.2.2.

2.2.1.2 Fundamental relations

A key ingredient of the 'one-line' formulation is the principle of mass conservation. Applying the continuity of sand along an infinitely small length, dx, of shoreline (Figure 2.2) gives (Hanson, 1987; Bonnett, 2002)

$$dt\frac{\partial}{\partial t}(Adx) = Qdt - (Q + \frac{\partial Q}{\partial x}dx)dt,$$

$$\frac{\partial A}{\partial t} = -\frac{\partial Q}{\partial x} \tag{2.2}$$

where A is the cross-sectional area, and Q is the longshore particulate sand transport rate.

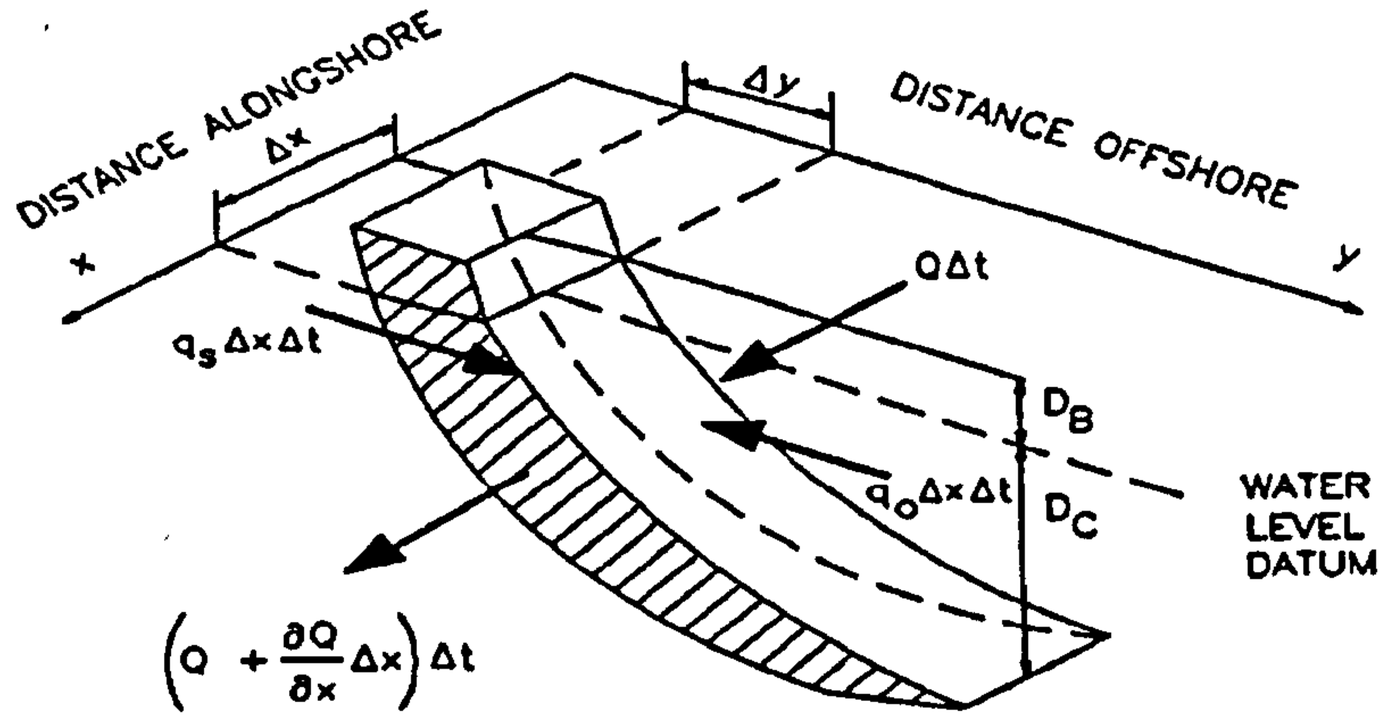

Figure 2.2 Cross-section view (adopted from Gravens *et al.*, 1991)

Assuming an equilibrium beach profile, Equation 2.2 can be written as (see Figure 2.2)

$$D\frac{\partial y}{\partial t} = -\frac{\partial Q}{\partial x} \tag{2.3}$$

where D is the vertical extension of the active part of the shoreline and is given by $D = D_c + D_B$, where D_c is known as the "depth of closure" and D_B is the berm height, taken as the upper profile limit. The depth of closure is the depth below which no appreciable profile change takes place (Kamphuis, 2000). It enters all applications, where it is taken as constant. A closer examination of the depth of closure concept is presented in Section 2.2.1.5. Equation 2.3 can be extended to include line sources and/or sinks of sediment along the coastline (Hanson, 1987; Larson *et at.*, 1997; Bonnett, 2002)

$$D\frac{\partial y}{\partial t} = -\frac{\partial Q}{\partial x} + q \tag{2.4}$$

where $q(x,y,t)$ can be positive or negative, depending on whether it is a source or sink term respectively. It is usually taken as constant. Equation 2.4 is very useful and can describe situations such as river sediment supplies, the effect of land subsidence or sea-level rise, offshore sediment loss, artificial sand bypass and beach mining. The q term has also been used by researchers to represent an overall (average) on-offshore sand transport rate. Their

methods suggest that shoreline retreat or advance due to the cross-shore sediment transport component can be calculated without violating the assumption of an equilibrium beach profile and are basically aimed towards shorter-term prediction of shoreline position, e.g. seasonal variation (Hanson *et al.*, 1997; Dabees and Kamphuis, 1998; Hanson and Larson, 1998; Karambas *et al.*, 2001).

Accounting for cross-shore transport and sea-level variations, Le Mehaute and Soldate (1978) suggested the following equation to express the sand budget balance

$$\frac{\partial Q}{\partial x} + Q_y = D\frac{\partial y_s}{\partial t} + (y_c - y_b)\frac{dD'}{dt} \qquad (2.5)$$

where Q_y represents cross-shore net gain or loss of sediment, $\frac{dD'}{dt}$ is the rate of change of sea-level, and y_c, y_b are the cross-shore positions of the depth of closure and the berm height respectively.

To solve the above equations, expressions for Q, q (or Q_y), and D_c must be formulated. An introduction to the expressions relevant to the alongshore movement of sediments is presented in the following sections. It is noted here that although certain studies suggest that cross-shore expressions enhance the quality of shoreline predictions (e.g. Karambas, 2001), they have not always been particularly successful (e.g. Hanson and Larson, 1998). Moreover, their inclusion in the 'one-line' formulation is thought questionable because no consideration of the profile shape is made which has been found to be the key parameter for the cross-shore sediment transport magnitude and direction. Since no cross-shore component is included in this study, reference to cross-shore processes will be limited in the remainder of this chapter. The berm height, D_B, is taken from the measured or assumed profile in applications.

2.2.1.3 Longshore sand transport formulae

There is a variety of expressions in the literature for the longshore sand transport rate, Q. The most extensively used in applications is known as the "CERC formula" (CERC, 1984), is empirical, and follows the expression

$$I = KP \tag{2.6}$$

where I is the alongshore immersed weight sediment transport rate, K is a proportionality coefficient and P is the "longshore component of the wave power" (Komar, 1998), given by

$$P = (EC_g)_b \sin\alpha_b \cos\alpha_b \tag{2.7}$$

where E is the wave energy per unit length, C_g is the wave group velocity and α is the angle between the wave crests and the shoreline. The subscript b denotes these quantities at breaking. The immersed weight transport rate I (Equation 2.6) is related to the volumetric transport rate Q by the equation

$$I = (\rho_s - \rho) g \sigma Q \tag{2.8}$$

Where ρ_s, ρ are the sea-water density and sediment density respectively, σ is the sediment porosity and g is the acceleration of gravity. Equations 2.9, 2.10 and 2.11 combine to give Equation 2.9 which is the commonly used form of the CERC formula.

$$Q = Q_0 \sin 2\alpha_b \tag{2.9}$$

$$Q_0 = K \frac{\rho}{16(\rho_s - \rho)\sigma} H_b^2 C_{gb}$$

where Q_0 (m^3/sec) is the amplitude of the longshore sand transport rate, Q, and H is the wave height.

Different values have been suggested for the K coefficient using different data sets (Komar, 1998). The value of K = 0.77, suggested by Komar and Inman (1970) using the

mean root square wave height, H_{rms}, in Equation 2.9, is commonly used in applications. This value is essentially the same with the one ($K = 0.39$) suggested by CERC (1984) using significant wave height, H_s ($H_{sb}/H_{rmsb} \approx 1.41$) (Longuet-Higgins, 1952). Schoones and Theron (1993) found $K = 0.41$ (using H_s) analysing a high quality data set.

Equation 2.9 assumes that sand transport solely results from oblique wave breaking and indirectly from the longshore currents generated by those waves. It describes potential sediment transport rates and assumes fully developed wave-induced longshore current. Thus, it ignores the contribution of tidal currents, rip currents, or wind-generated currents in the nearshore (CERC, 1984; Hanson, 1987; Komar, 1998) and gives poor results when the longshore current varies considerably due to obstacles in the flow (Galvin and Eagleson, 1965; Kumar *et al.*, 2002). CERC formula has been criticized for over-predicting Q, particularly at high-energy conditions and has a high degree of uncertainty which can reach 50% for hindcast wave data (CERC, 1984; Kamphuis, 2000). However, low accuracy is a common problem of predictive longshore sand transport formulae.

Another empirical formula, used in 'one-line' applications, obeying the same assumptions as above, is Kamphuis' (1991) formula. This formula was derived from small-scale hydraulic model tests, includes directly the effects of wave period, beach slope and grain size and is given by

$$Q = 2.27 H_{sb}^2 T_p^{1.5} \beta_b^{0.75} D_{50}^{-0.25} \sin^{0.6} 2\alpha_b \qquad (2.10)$$

where T_p is the peak wave period, β is the beach slope in the breaking zone, D_{50} is the mean grain size, and Q is in m^3/sec. Schoones and Theron (1994) found that Kamphuis' formula has better predictive capabilities than the CERC formula.

To overcome the assumption of wave-induced longshore currents alone Hanson *et al.* (2001), following the formula proposed by Bagnold (1963) and Inman and Bagnold

(1963), suggested that Equations 2.9 (having P substituted from Equation 2.7) can be modified to explicitly represent a longshore current as

$$I = K'(EC_g)_b \cos\alpha_b \frac{\bar{v}}{u_m} \tag{2.11}$$

where K' is a dimensionless constant, $\bar{v}$ is the average long-shore current velocity in the surf-zone and u_m is the maximum horizontal near-bottom wave orbital velocity evaluated at the breaker zone. In Equation 2.11, longshore sand transport rate is allowed to be generated by currents originated from other mechanisms, e.g. tide or wind, apart from breaking waves. It is also built upon considerations of the processes of sand transport rate rather than being completely empirical. Different values for K' have been suggested based on different assumptions made and different expressions used for the average longshore current velocity in the general sediment transport model of Bagnold (1963), (Komar, 1998).

Kraus *et al.* (1982) and Kraus and Harikai (1983) have illustrated that in the sheltered region of a breakwater the combined effects of oblique incident waves and longshore variation in the wave heights due to diffraction should be taken into account for realistic shoreline evolution and longshore sediment transport calculations. To achieve that they suggested the following predictive longshore sand transport formula which is a variant of the CERC formula

$$Q = H_b^2 C_{gb}(a_1 \sin 2\alpha_b - a_2 \cos\alpha_b \frac{\partial H_b}{\partial x}) \tag{2.12}$$

The dimensionless parameters a_1 and a_2 are given by

$$a_1 = \frac{K_1}{16(\rho_s/\rho - 1)(1-\sigma)1.416^{5/2}}$$

$$a_2 = \frac{K_2}{8(\rho_s/\rho - 1)(1-\sigma)(\tan\beta)1.416^{5/2}}$$

where K_1 and K_2 are dimensionless constants, tanβ is the average beach slope and the factor $1.416^{5/2}$ converts significant wave height to root mean square wave height. In the same manner, Kamphuis' formula (Equation 2.10) has been modified to account for the longshore variation in the wave height.

The first term in Equation 2.12 describes longshore sand transport due to oblique incident waves and is identical to the CERC formula ($K \equiv K_1$). The second term, introduced by Ozasa and Brampton (1980), accounts for longshore sediment transport produced by alongshore variation in breaking wave height. The first term is the dominant one on natural straight beaches, whilst the second becomes important in the vicinity of structures and headlands where diffraction is significant.

The use in 'one-line' modelling of relative more complex formulae adapted to calculate the cross-shore distribution of the sand transport rate has been recently adopted in applications (e.g. Reinen-Hamill, 1997). Well-known formulae in this category can be found in Bayram *et al.* (2001) along with their predictive capabilities.

2.2.1.4 Equilibrium beach profile

As explained in Section 2.2.1.1, a very useful concept in 'one-line' modelling of beach evolution is the concept of "equilibrium beach profile". To better understand this concept one of the main equilibrium shape expressions is given below

$$h = Ax^{2/3} \tag{2.13}$$

$$A = \left(\frac{24 D_e}{5 \rho \gamma^2 g^{3/2}} \right)$$

where h is the still water depth at a horizontal distance x from the shoreline, D_e is the wave energy dissipation per unit water volume due to wave breaking over an equilibrium profile, and γ is the breaker index, i.e. $\gamma = H_b/h_b$ ($\gamma \cong 0.8$). Equation 2.13 was derived empirically

by Bruun (1954) and subsequently explained by Dean (1977), using the constant wave energy dissipation assumption given by

$$D_e = \frac{1}{h}\frac{dF}{dx} \tag{2.14}$$

where F is the wave energy flux in shallow water and D denotes uniform breaking wave energy dissipation per unit volume which is the mechanism that determines the profile shape. Equation 2.13 is the most commonly used equilibrium beach profile expression. A number of other expressions have followed (e.g. Larson and Kraus, 1989; Bodge, 1992; Komar and McDougal, 1994). For example, the last two studies in the parenthesis explore exponential equilibrium profile models that according to Komar (1998) have shown better agreement with measured profiles.

The assumption of an equilibrium beach profile may be reasonable for long-term averages of uniform undisturbed coasts. However, this assumption seems to be considerably violated in the vicinity of structures. For example, the profile slope on the updrift side of a groyne is usually gentler than away from it (Young *et al.*, 1995).

2.2.1.5 Depth of closure

The depth of closure is a fundamental parameter entering all 'one-line' modelling applications of shoreline evolution. It is commonly defined as the depth seaward of which changes in bed elevation are insignificant and as such divides the beach profile into two discrete zones: (1) the nearshore morphologically active zone, and (2) the offshore nearly inactive zone. Its concept has been based upon the observation that there is a depth beyond which individual profiles converge in a profile envelope (Capobianco *et al.*, 1997; Kamphuis, 2000; Hanson *et al.*, 2003).

In 'one-line' modelling it is assumed that no significant transport of sediment takes place beyond that depth. This assumption is disputed by coastal geologists who find evidence of sand exchange across the entire shoreface. Thus, the existence of a morphologically inactive zone is questioned (Young *et al.*, 1995; Thieler *et al.*, 2000). Recent high quality studies have proven the existence of a closure depth for short-term erosional and accretional events up to several years (Nicholls and Birkemeier, 1997; Nicholls *et al.*, 1998). However, they do support the finding that cross-shore sediment exchange within the entire shoreface becomes important as time-scale increases, often resulting in net profile translation which affects considerably the closure position (Nicholls and Birkemeier, 1997). Depth of closure is thus time-dependent and it is important to be able to predict it at different time-scales (Capobianco *et al.*, 1997).

Predictive formulae have typically related the depth of closure to the wave climate. The most well-known formula has been derived by Hallermeier (1981) who found that closure depth at an annual scale is a function of the extreme wave conditions as

$$D_c = 2.28H_e - 68.5\left(\frac{H_e^2}{gT_e^2}\right) \tag{2.15}$$

where H_e is the non-breaking significant wave height that is exceeded 12 hours per year, and T_e is the associated wave period. The dominant term in Equation 2.15 is the first term, whilst the second term provides a small correction associated with the wave steepness. A variation of Equation 2.15 (altered coefficient values) was proposed by Birkemeier (1985) The adjusted equation produces a smaller closure depth than Equation 2.15. Birkemeier further suggested that the simple relation $D_c = 1.57H_e$ provides a satisfactory prediction.

To date, Hallermeier's method is the only analytical method to estimate closure depth. Equation 2.15 can be generalized for any time interval (Nicholls *et al.*, 1998; Hanson *et al.*, 2003). Nicholls *et al.* (1998) found that in an event-by-event basis Hallermeier's relation

provided a robust limit to the observations. Scatter below the predicted limit was partly attributed to pre-storm profile morphology associated with internal bar dynamics, particularly the position and volume of the outer bar. When time interval depth of closure was considered, Equation 2.15 produced again a reasonable limit to the observations. However, it appeared that closure depth was underpredicted in accretion-dominated cases, which implies that Equation 2.15 might not be suitable for swell-dominated environments (Nicholls *et al.*, 1998). It might also not be suitable in the very long time-scale when, as mentioned above, net profile translation might occur. Capobianco *et al.* (1997) analysed data from the same location and further observed that as time-scale increased from one year to 30 months predictions grew faster than the observations, constituting Equation 2.15 a less valuable practical tool. In general, depth of closure has been found to increase with time-scale. From the above, it is clear that determining the time-scale of an engineering application is essential.

Depth of closure does not only vary in time but in space as well. It has been shown that steeper profiles have a shallower depth of closure than gentler ones (Kraus and Harikai, 1983; Nicholls *et al.*, 1998). This is particularly apparent in the vicinity of structures. For example, a gentler beach profile on the updrift side produces a deeper depth of closure than the one observed away from the structure (Kraus and Harikai, 1983). This variation might be important in sediment bypassing estimations. In summary, when a time-scale from erosional events to some years is considered, depth of closure seems to be an integrated product of three interacting processes: (1) cross-shore sediment distribution as controlled by extreme wave conditions, (2) Internal bar dynamics, and (3) net profile translation due to longshore sediment transport gradients. At longer time-scales net profile translation due to net cross-shore sediment exchange becomes important. Finally, dependence on grain size should be considered, particularly in the case of nourishment projects, as a different

nourishment grain size than the native alters significantly the profile shape (Jenkins and Keehn, 2001).

Further research is needed to evaluate the depth of closure in coastal systems where tidal currents, rip currents or other non-wave-induced currents become important, e.g. near inlets. Research is also needed to better estimate depth of closure at longer time-scales, especially in situations when an accretional coastal trend is apparent.

2.2.1.6 Assumptions and limitations

The basic limitations and assumptions of the 'one-line' theory can be summarized as:

- The shape of the beach profile is assumed not to change with time so that only one contour line can determine the profile position. This shape is the "equilibrium beach profile" shape.
- Commonly used models account only for longshore sand transport rate. Cross-shore sand transport has been included in the 'one-line' formulation but is often oversimplified and independent of the actual profile shape which is a significant parameter in this case.
- A systematic trend in the shoreline evolution is preferable.
- Sand is assumed to move down to the depth of closure, beyond which the profile stays essentially unchanged.
- Availability of sand is generally considered unrestricted unless explicitly restricted by boundary or/and initial conditions.
- Short-term dynamics are assumed to average out in the longer-term and details of the nearshore circulation are essentially ignored.

2.2.2 Analytical solutions

2.2.2.1 Critical appraisal of analytical solutions

The continuity of sand equation, under certain assumptions, reduce down to a diffusion equation of the form of Equation 2.1 (at its simplest). The resulting diffusion equation can then be solved analytically to describe systematic trends of shoreline evolution for simple cases. Analytical solutions have been derived by several researchers for idealized situations of shoreline change at groynes, jetties, detached breakwaters, rivers, and nourished or sand-mined beaches (e.g. Walton and Chiu, 1979; Larson *et al.*, 1987; Larson *et al.*, 1997). An overview of previous analytical work is presented in Section 2.2.2.3.

Despite their simplicity, analytical solutions have been proven to be very useful with certain advantages over numerical solutions. These can be summarised as follows:

- They help understanding and investigation of the physical processes controlling beach response by enabling essential features to be isolated and thus more readily comprehended than in complex numerical or laboratory models. Consequently, analytical models of shoreline response are a valuable educational tool.
- Only one evaluation is needed to obtain shoreline position at any particular time. This has two advantages over numerical time-stepping finite difference solution schemes, which increase with time:
    1. quick estimate of shoreline change
    2. cumulative errors associated with the accuracy of the numerical approximation scheme are avoided.
- Numerical stability problems are avoided.

- Characteristic parameters associated with particular cases of shoreline response are easy and direct to estimate at an early design stage, e.g. the percentage of volume lost from a beach fill, or a preliminary estimate of the time elapsed before bypassing of the groyne occurs.
- Equilibrium conditions may be determined from asymptotic solutions.
- They provide an independent means of validating numerical solutions for idealized situations.

However, analytical solutions can not be expected to produce an accurate result when complex wave inputs or boundary conditions are involved, whilst it is almost impossible to derive such solutions when many physical phenomena are included in the original formulation. As a result, numerical modelling of shoreline evolution is more appropriate in engineering design (Hanson and Larson, 1987; Larson *et al.*, 1987; Larson *et al.*, 1997; Reeve, 2006).

2.2.2.2 Analytic solution technique

Equation 2.1 is derived from Equation 2.3 using a general expression for the sand transport rate of the form

$$Q = Q_0 \sin 2\alpha_b \tag{2.16}$$

The angle α_b may be expressed by (Figure 2.3)

$$\alpha_b = \alpha_0 - \arctan\left(\frac{\partial y}{\partial x}\right) \tag{2.17}$$

where α_0 is the angle between the breaking wave crests and the x-axis, set parallel to the shoreline trend (Figure 2.3), and $\partial y/\partial x$ is the local shoreline orientation. By substituting Equation 2.17 in Equation 2.16, the sand transport rate becomes

$$Q = Q_0 \sin\left\{2\left[\alpha_0 - \arctan\left(\frac{\partial y}{\partial x}\right)\right]\right\} \tag{2.18}$$

At beaches with mild slope, wave crests tend to parallel the shoreline due to refraction and

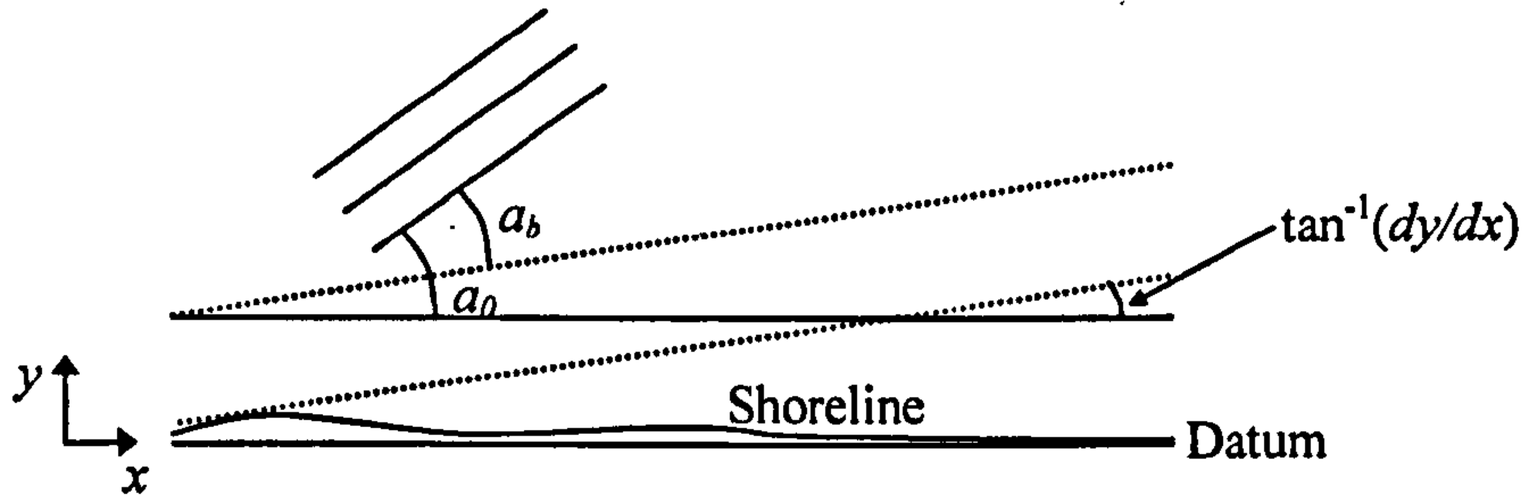

Figure 2.3 Definition of geometric properties of the 'one-line' shoreline change model.

shoreline perturbations tend to even out. It is thus reasonable to assume that α_0 and $\partial y/\partial x$ are small. Using a first order Taylor series approximations and the small angle assumption, Equation 2.18 can be linearized as

$$Q = Q_0\left(2\alpha_0 - 2\frac{\partial y}{\partial x}\right) \tag{2.19}$$

If it is further assumed that wave conditions remain constant alongshore so that Q_0 and a_0 are constant in the x-direction, then, substituting Equation 2.19 into Equation 2.3, the diffusion equation (Equation 2.1) is derived as

$$\frac{\partial y}{\partial t} = \varepsilon \frac{\partial^2 y}{\partial x^2} \tag{2.20}$$

$$\varepsilon = \frac{2Q_0}{D}$$

As already mentioned, ε is a diffusion coefficient which expresses the time-scale of shoreline change following a disturbance. Carslaw and Jaeger (1959) provide many solutions to the heat conduction equation which is identical to Equation 2.20. Crank (1975) gives solutions to the diffusion equation.

Allowing wave conditions to vary alongshore, the following differential equation is derived from Equations 2.3 and 2.18

$$\frac{\partial y}{\partial t} = \varepsilon \frac{\partial^2 y}{\partial x^2} + \frac{\partial \varepsilon}{\partial x}\frac{\partial y}{\partial x} + \frac{\partial}{\partial x}(\alpha_o \varepsilon) + q(x,y,t) \qquad (2.21)$$

where the source/sink term, q, is in addition. Equation 2.21 makes it possible to include, for example, longshore variation of wave height or wave angle as caused by diffraction. However, such a variation should be described in a simple form for an analytical solution to be feasible (Hanson *et al.*, 1997).

By expanding the trigonometric term in Equation 2.16, assuming $\partial y/\partial x$ is very small, but not α_0, Dean and Dalrymple (2002) derived the following expression for the longshore sediment transport

$$Q = Q_0 \sin 2a_0 - 2Q_0 \cos 2a_0 \frac{\partial y}{\partial x} \qquad (2.22)$$

where the first term represents longshore transport rate for a straight shoreline, thus it is constant alongshore, and the second term represents the transport induced by the alongshore shoreline slope. Substituting Equation 2.22 into Equation 2.3 gives Equation 2.1 but with ε as

$$\varepsilon = \frac{2Q_0 \cos 2\alpha_0}{D} \qquad (2.23)$$

If α_0 is very small, Equation 2.23 reduces to Equation 2.20. If $\alpha_0 > 45^0$ or $\alpha_0 < -45^0$ (the sign denotes waves coming from the east or the west respectively, relative to the shoreline normal) then Equation 2.23 would produce a negative diffusion coefficient. Nevertheless, reasonable breaking wave angles are not expected to be greater than about 32^0 (Falqués, 2003). However, Ashton *et al.* (2001) and later Falqués and Calvete (2005), Falqués (2006), and Uguccioni *et al.*, (2006) do support the idea of negative diffusivity. In particular they pick up on the inability of the classical diffusion equations to account for feedback between

the changing shoreline orientation and the wave characteristics (wave height and direction) at breaking and suggest that this process is very important for obtaining the correct diffusivity of shoreline irregularities. Accounting for this feedback, Murray and Ashton (2004) and Falqués (2003) proposed diffusion coefficients that depend on deep water wave quantities and local shoreline orientation whilst Falqués and Cavete (2005) and Falqués (2006) extended the 'one-line' model so that nearshore wave transformation is affected by the feedback between shoreline perturbations and bathymetry; their final equation is not anymore a diffusion equation and it is non-local (i.e. it depends on integration of wave characteristics in the whole nearshore domain). These studies find negative diffusivity for $\theta_0 > 43^0$, where θ_0 is the deep water wave angle. The formation of sand waves (Ashton *et al.*, 2003; Falqués and Cavete, 2005) or large scale cuspate features on the shoreline (Murray and Ashton, 2004) is attributed to this longshore instability under high wave angle approach.

Falqués and Cavete (2005) and Falqués (2006) finally conclude on the conditions under which the diffusion coefficient given by equation 2.23 works well. These are:

- Large waves and moderate angles.
- Bathymetric perturbations confined very close to the shore.
- Perturbations with wavelength smaller than 2 km.

It is noted here that despite being mentioned in this section, the formulae derived by these studies are not easily amenable to analysis.

2.2.2.3 Overview of previous analytical work

Assumption of time-invariant wave forcing

As mentioned above, Pelnard-Considère (1956) was the first to derive the 'one-line' mathematical model for shoreline change (Equation 2.1) which he verified against laboratory experiments of shoreline evolution at a groyne. His analytical solutions were for the case of shoreline advance updrift of the groyne, with and without bypassing, and the case of an instantaneous release of sand on the beach. Since then, several researchers have worked on the development of Pelnard-Considère's work. Grijm (1961) and Bakker and Edelman (1965) studied delta formation from rivers discharging sand. Le Mehauté and Brebner (1961) more thoroughly presented the analytical solutions derived by Pelnard-Considère (1956), providing more detail in the geometric aspects of shoreline change. They also treated the cases of the decay of an undulating shoreline and of the equilibrium shape shoreline between two headlands. Le Mehauté and Soldate (1977) studied the spread of rectangular beach nourishment. Walton and Chiu (1979) postulated three models for the sand transport rate equation: the CERC formula, an expression considering only suspended load transport, and a non-linear one in its bedload component. The first two models produced a linearized shoreline change equation whilst the last gave a non-linear one. They also presented a review of analytical solutions and derived new for cases like a triangular shaped beach fill, a rectangular gap in a beach and a semi-infinite rectangular fill. A short survey of analytical solutions applicable to beach nourishment calculations was given by Dean (1983). He especially focused on characteristic quantities describing fill loss percentages. Larson *et al.* (1987) presented a great number of analytical solutions, including previous work and new solutions derived using the Laplace transform technique and analogies with heat conduction. They also extended the 'one-line' equation to the form

of Equation 2.21 to allow for longshore variation in wave height and angle and derived solutions for shoreline evolution at regions of diffraction. In general, the solutions they presented fall into three groups: (1) shoreline evolution without structures, applicable both to natural and artificial beach forms, (2) river delta growth, and (3) shoreline change near coastal structures. Wind (1990) gave again a summary of solutions for the situations of updrift accretion at a groyne, sediment bypassing, and river discharges as point sources. Bodge and Kraus (1991) derived values for the diffusion coefficient, ε, using the analytical solution describing accretion updrift of a groyne. They concluded that it is related to the mean significant wave height at the site to a power of 2.8. Walton (1994) presented an analytical solution for the case of a rectangular beach fill with tapered ends. Larson *et al.*, (1997) included some new situations to their previous analytical work, Larson *et al.* (1987), such as a different expression for jetty bypassing.

Consideration of time-varying wave conditions

Larson *et al.* (1997) included the situation of a sinusoidaly time varying breaking wave angle at a single groyne and at a groyne compartment. Dean and Dalrymple (2002) studied the longevity of beach nourishment projects by allowing the diffusion coefficient of the 'one-line' model to vary arbitrarily with time, implying time varying wave conditions. By assuming an initially straight, undisturbed coastline and applying a Fourier decomposition of the shoreline position, they derived an analytical solution for the n^{th} Fourier component. They aimed to show that fill evolution does not depend on the sequence of events (storms) but on their cumulative effect. Reeve (2006) also examined time varying wave conditions. By using cosine Fourier transforms and considering a time varying diffusion coefficient and a spatially and temporally varying source term he derived

a general solution in terms of closed-form integrals for the case of shoreline evolution at a single groyne.

2.2.2.4 Examples of analytical solutions

Straight impermeable groyne before bypassing

Solution method: Laplace transform

Initial condition: $y(x,0) = 0$

Boundary conditions:

1. $\frac{\partial y(0,t)}{\partial x} = \tan\alpha_0$ which results from Equation 2.18 for $Q = 0$ (at the groyne location, $x = 0$).

2. $y(x,t) \to 0$ when $x \to \infty$, a boundary condition assumed to be valid for any case an analytical solution is derived for

$$\textit{Solution: } y(x,t) = 2\tan\alpha_0\left[\sqrt{\frac{\varepsilon t}{\pi}}e^{-x^2/4\varepsilon t} - \frac{x}{2}erfc\left(\frac{x}{2\sqrt{\varepsilon t}}\right)\right] \tag{2.24}$$

Example solutions are shown in Figure 2.4.

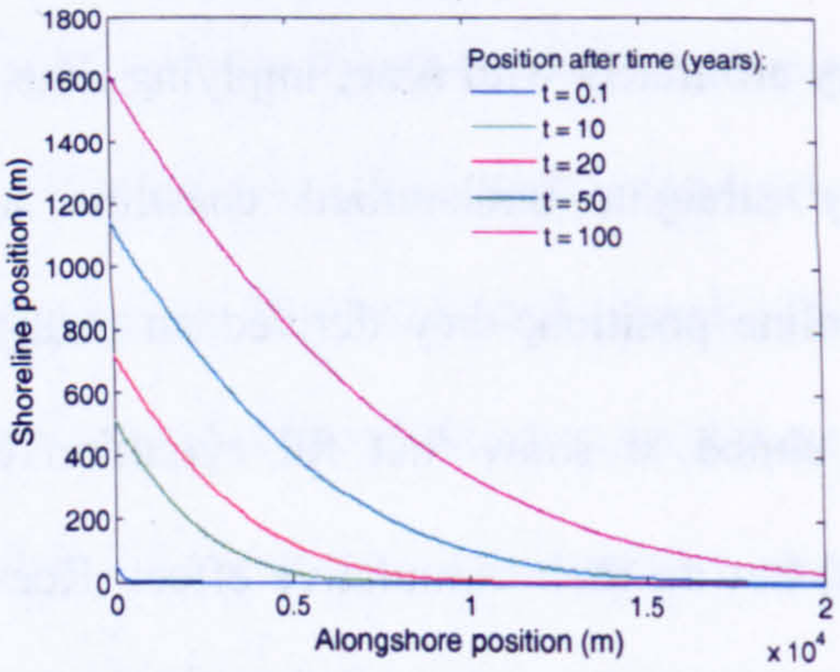

Figure 2.4 Analytical solution for an infinite breakwater positioned at x=0 at selected times for ε=500000m^2/year and a wave angle of 0.2 radians.

If Equation 2.24 represents accretion at the updrift side of the groyne, the same equation with a minus sign on the right hand side will represent erosion at the downdrift side of the groyne if diffraction is neglected.

Rectangular beach fill

Solution method: Laplace transform

Initial conditions: $y(x,0) = \begin{cases} y_0 & |x| < a \\ 0 & |x| > a \end{cases}$ where y_0 is the width of the fill and a is half its length (the middle of the fill is located at $x = 0$)

Solution: $$y(x,t) = \frac{y_0}{2}\left[erf\left(\frac{a-x}{2\sqrt{\varepsilon t}}\right) + erf\left(\frac{a+x}{2\sqrt{\varepsilon t}}\right)\right] \qquad (2.25)$$

Example solutions are shown in Figure 2.5.

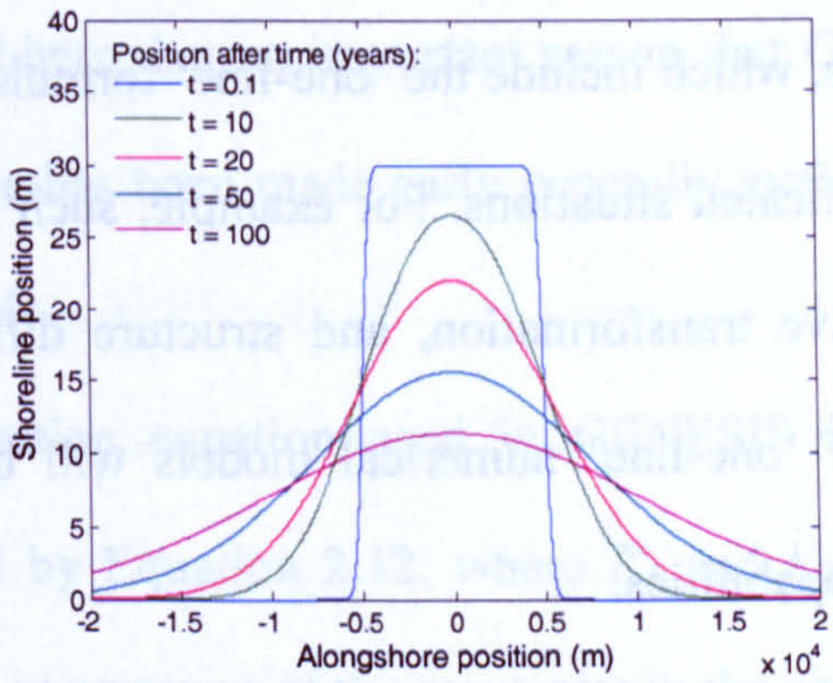

Figure 2.5 Analytical solution for a beach nourishment (rectangular at t=0 with width 5000m and depth 30m) for ε=500000m^2/year.

For a collection of analytical solutions along with some derivations the reader is prompted to Walton and Chiu (1979), Larson *et al.* (1987), and Larson *et al.* (1997).

2.2.3 Numerical modelling

2.2.3.1 General capabilities

In engineering practice the problems encountered are complex, involving a variety of natural processes varying both in time and space. As a result, numerical simulation models have been developed to account for the variability of nature. These models have the capacity to examine shoreline evolution in response to time and space varying wave conditions, changes in sediment supply, and variable structure configuration. Most consider only wave-induced longshore transport of sand, although alongshore transport originated from currents other than wave-generated has been considered (Szmytkiewicz *et al.*, 2000; Hanson *et al.*, 2001; Larson *et al.*, 2006). As mentioned above, attempts have been made to include cross-shore sediment transport in the 'one-line' formulation. Morphodynamic modelling prediction suites, which include the 'one-line' formulation, have been developed to account for more complicated situations. For example, such models may include wave hindcasting, nearshore wave transformation, and structure diffraction. In the following section some examples of 'one-line' numerical models will be given along with their assumptions and specific capabilities.

2.2.3.2 Examples of 'one-line' numerical models

The first numerical 'one-line' model for predicting shoreline evolution was developed by Price (1972). Willis (1977) evaluated different longshore transport formulae by applying a 'one-line' numerical model to prototype conditions, and Perlin (1979) simulated the shoreline evolution around detached breakwaters. Le Mehauté and Soldate (1978) accounted for sea level, wave refraction and diffraction, losses of sand, and effects

of structures and beach nourishment projects. Since then, a number of 'one-line' models have been developed; however, the most well-known is called GENESIS, an acronym for Generalized Model for Simulating Shoreline Change, developed jointly by the Waterways Experiment Station at Vicksburg, USA, and the Lund Institute of Technology, Sweden. It was presented by Hanson (1987). GENESIS can be applied to a diverse variety of situations involving almost arbitrary numbers, locations, and combinations of groynes, jetties, detached breakwaters, seawalls and beach fills. It accounts for wave shoaling, refraction, diffraction, sand bypassing through and around a groyne, and sources and sinks of sand (Hanson, 1987). As it is by far the most extensively used numerical model for shoreline evolution and one of the most developed, some basic features of GENESIS are referred in the following paragraphs. For comparison, characteristics of some other models are mentioned. For a detailed description of GENESIS the reader is prompted to Gravens *et al.* (1991). It should be noted here that an important reason that GENESIS has dominated in applications is that its code has been made early generally available in contrast with other 'one-line' numerical models.

The mass conservation equation used in GENESIS is Equation 2.4. Sediment transport rate is described by Equation 2.12, where K_1 and K_2 are calibration parameters that determine the relative importance of the two terms in the equation and the time-scale in the model. Wave refraction is calculated using Snell's law, assuming parallel bottom contours whose shape is given by smoothing the shoreline configuration. For advanced refraction calculations GENESIS can interact with RCPWAVE model which refracts linear waves over irregular bottom topography. Diffraction calculations are made using the directional spreading of the incident waves (Goda, 2000). Ultimately, combined refraction and diffraction determine the breaking wave height.

Genesis uses three characteristic depths:

- "Depth of active longshore transport", D_{ll}, which is related to the width of the surf zone and is the depth of breaking of the highest one-tenth of waves at the updrift side of the structure. It is used for by-passing calculations.
- "Maximum depth of longshore transport" given by Equation 2.15 (Hallermeier's expression) but with H_e being the significant deep water wave height. It is used for estimating the average beach slope, $\tan\beta$, in Equation 2.12, using Equation 2.13 (equilibrium profile). Equation 2.15 is calculated for each time-step from input deep water wave data. The use of a varying "maximum depth of longshore transport" in response to varying wave climate reflects changes, especially seasonal, in profile shape and slope.
- "Depth of closure", D_c, which is either derived from profile measurements or again from Equation 2.15 but using the formal definition for wave inputs.

The GENESIS model has been applied to several example analysis (e.g. Gravens *et al.*, 1991; Hanson and Kraus, 1991; Szmytkiewicz *et al.*, 2000). In general, the agreement between measured and computed shoreline has been good. However, it must be kept in mind that a number of empirical coefficients may be adjusted in the model to maximize the fit (Komar, 1998; Young *et al.*, 1995), although a smaller number than in other widely available 'one-line' numerical models (e.g. UNIBEST).

Larson *et al.* (2006) describe a 'one-line' numerical model, called "Cascade", to simulate complex regional (e.g. encompassing barrier islands or inlets) sediment transport and coastal evolution over centuries and hundred of kilometres. In their model information is "cascading" from the regional to the local scale. A modified CERC formula that accounts for the regional component in local shoreline evolution is proposed. Other sand transport sub-models that account for bypassing and inlet sediment storage and transfer are included. Weesakul and Rasmeemasmuang (2002) have applied combined polar and Cartesian

coordinates in order to improve estimates of shoreline change at crenulated bays, where shoreline curvature near the headland is poorly predicted due to the limiting Cartesian coordinate system typically adopted in 'one-line' models.

Other advanced 'one-line' models, generally available, are contained in model packages such as LITPACK, developed by the Danish Hydraulic Institute (DHI), UNIBEST, developed by Delft Hydraulics, and SAND94 developed at the Polish Academy of Sciences' Institute of Hydro-Engineering. The major differences between models consist in the determination of the longshore sediment transport, i.e. in the number and complexity of the processes involved. For instance, in LITPACK, sediment transport as bedload and vertically distributed suspended load is considered. Regular and irregular waves, the impact of tidal currents, wind-stress and non-uniform bottom friction can be accounted for. This model further accounts for the linking of the water level and the profile at every wave incident (Szmytkiewicz *et al.*, 2000). In UNIBEST, the longshore sediment transport may be determined using 5 theoretical approaches (e.g. formulae for sand or shingle beaches, inclusion of cross-shore sediment distribution, current-induced transport) (Szmytkiewicz *et al*, 1998, cited in Szmytkiewicz *et al.*, 2000). Table A1 in Appendix A, adopted from Szmytkiewicz *et al.* (2000), shows the main features of the numerical 'one-line' models mostly used to date and help identify the main differences between them.

The general numerical solution procedure used to solve the continuity equation is presented in the following section. The procedure is similar for most 'one-line' models. Some boundary conditions applied in models, necessary for the numerical evaluation of the shoreline position, are mentioned.

2.2.3.3 Finite difference representation

Grid specification

To solve the continuity of sediment equation and the longshore sand transport rate equation numerically finite differences are used, i.e. the shoreline is discretized into a series of cells of finite length, Δx, as shown in Figure 2.6. In Figure 2.2 one of these cells in three dimensions was shown; this figure helps to see that the change of the shoreline position over one cell, i.e. Equation 2.3 over a cell, may be expressed as

$$\Delta y = (Q_{IN} - Q_{OUT})\frac{\Delta t}{\Delta x D} \tag{2.26}$$

$$Q_{IN} = Q + q\Delta x, \qquad Q_{OUT} = Q + \frac{\partial Q}{\partial x}\Delta x$$

The above equations are solved for every alongshore cell, Δx. Also, Equation 2.17 for α_b (which participates in the sediment transport formulae) has to be solved at each cell. The grid adopted is one where the transport quantities Q_i are specified at the cell walls (grid lines) and the y_i values at the cell midpoints, i.e. a staggered grid. The subscript i denotes

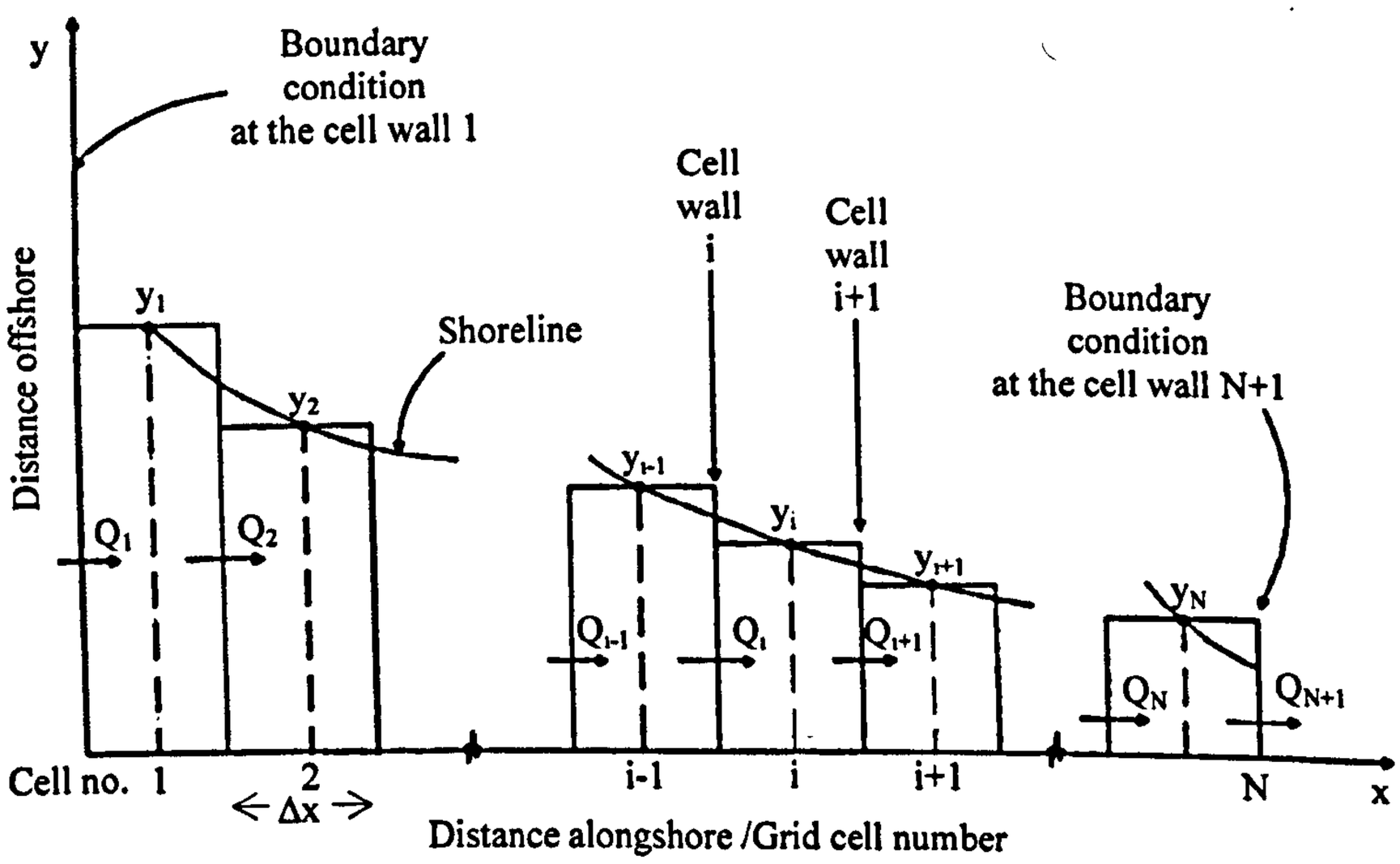

Figure 2.6 Finite difference staggered grid (adopted from Gravens *et al.*, 1991)

the location (cell number) along the shoreline. The computation is stepped forward in time using increments of Δt.

Explicit and implicit finite-difference method

Two types of time stepping finite difference solution schemes are typically employed, the explicit and the implicit method. In the explicit numerical scheme, the relation

$$\frac{\partial Q_i}{\partial x} = \frac{Q_{i+1} - Q_i}{\Delta x} \tag{2.27}$$

combines with Equation 2.26 to give

$$y_i^{t+\Delta t} = \frac{\Delta t}{D\Delta x}(Q_i - Q_{i+1} + q_i \Delta x) + y_i \tag{2.28}$$

Therefore, the new value of y at the new time ($t + \Delta t$) is computed from known values at the previous time t. Equation 2.27 is a first order upwind numerical approximation of the sediment flux.

In the implicit scheme, the relation

$$\frac{\partial Q_i}{\partial x} = \frac{1}{2}\left(\frac{Q_{i+1}^{t+\Delta t} - Q_i^{t+\Delta t}}{\Delta x} + \frac{Q_{i+1} - Q_i}{\Delta x}\right) \tag{2.29}$$

combines with Equation 2.26 to give

$$y_i^{t+\Delta t} = \frac{\Delta t}{2D\Delta x}\left(Q_i^{t+\Delta t} - Q_{i+1}^{t+\Delta t} + Q_i - Q_{i+1} + (q_i^{t+\Delta t} + q_i)\Delta x\right) + y_i \tag{2.30}$$

Therefore, the new values of y and Q at time ($t + \Delta t$) depend on values calculated on the old as well as the new time step and are computed simultaneously all along the shoreline (Kamphuis, 2000).

The explicit numerical scheme has certain advantages over the implicit. It is considerably easier to program, allows for simpler expression of boundary conditions, and

needs a shorter computer run time. However, a major disadvantage of this scheme is that it becomes easily unstable as time step increases. In contrast, the implicit scheme is unconditionally stable although accuracy of the solution decreases with increasing time step (Hoffman, 2001). The stability criterion of the explicit method is taken to be the one for the diffusion equation (Equation 2.20), where the diffusion coefficient can be of different forms. It is given by

$$K\frac{\Delta t}{\Delta x^2} < \frac{1}{2} \tag{2.31}$$

However, as seen in Section 2.2.2.2, the diffusion equation was obtained by linearization of the sediment transport equation and thus of the continuity of sediment equation. This linearization was achieved by employing a small angle approximation. Numerical models do not assume small angle so that the governing equations are non-linear. As a result, Equation 2.31 is an approximate stability condition for the explicit numerical solution of shoreline change since a precise condition could only be determined by trial and error (Kraus and Harikai, 1983). Nonetheless, despite the small angle approximation inherent in Equation 2.31, it was found that the criterion is still valid for wider angles ($<45^0$) (Hanson, 1987). Equation 2.31 implies that when the time interval between wave inputs is very long or when a big diffusion coefficient results from them the use of an explicit scheme may be prohibited. Both explicit and implicit schemes use simple first order upwind numerical approximations which are expected to introduce numerical diffusion, i.e. an artificial reduction of the amplitude of shoreline irregularities or in other words a smoothing of the shoreline (e.g. Press *et al.*, 1992; Gallagham *et al.*, 2006). Nevertheless, this scheme has been found the most robust in problems involving transport properties (Press *et al.*, 1992).

Details on finite difference expressions used in the two solution schemes can be found in a number of studies, e.g. Hanson (1987), Kamphuis (2000) (implicit method),

Weesakul *et al.* (2004) (explicit method, polar coordinates). As an example, it is mentioned here that GENESIS can use either an explicit or implicit method.

Boundary conditions

To solve the finite difference approximations of the governing equations, the initial shoreline configuration, $y_1, y_2,\ldots\ldots,y_N$ at time $t = 0$ (Figure 2.6), should be known, and boundary conditions should be set. Several types of boundary conditions and possibly internal constraints may be implemented (e.g. Hanson, 1987; Miura *et al.*, 2006). These may involve bounded values of Q or of y. For example, the shoreline position may be fixed at the boundaries of the computational domain, i.e. y_1, y_N values are held constant in time. A pinned beach may be assumed where $Q_1 = Q_2$ and $Q_{N+1} = Q_N$, or a moving beach may be specified by letting $y_N^{t+\Delta t} = y_N + RC$, where RC is a constant rate of change. The placement of a groyne at the boundary or inside the computational domain would impose a boundary condition or an internal constraint respectively either by trapping sediment transport alongshore so that $Q = 0$ at the groyne location, or by allowing sand bypassing so that a bypassing rate can be specified (e.g. $Q_b = 2Q_0\alpha_0 y/L_g$, where L_g is the length of the groyne). This is a time-dependent boundary condition. Detailed examples along with their numerical formulation for the explicit and the implicit methods can be found in Hanson (1987).

2.2.3.4 Model input/output

Data required and related model sensitivity

In summary, the basic inputs needed to run 'one-line' numerical models are:

- The initial shoreline configuration.

- Wave conditions (wave height, period, and direction) at breaking.
- The location of engineering structures and activities.
- Beach material along with measured and calculated beach profiles in order to define average slopes, characteristic depths, and wave refraction patterns.
- Boundary conditions and estimates of structure permeability.

In addition to the above, at least two measured shorelines are needed for model calibration and more than two for the validation process (Hanson, 1987). Essentially, most of the input parameters, both dynamic and morphological, vary randomly in time and space so that the best approach to shoreline evolution modelling would probably be the assignment of a suitable probability distribution to each of these inputs (Dong and Chen, 2001, Cowell *et al.*, 2006) resulting in a probabilistic output which provides with uncertainty estimates in contrast to the deterministic approach. As mentioned in Section 2.1.1, running the 'one-line' model in a Monte Carlo setting is becoming popular (e.g. Dong end Chen, 1999; Ruggiero *et al.*, 2006). In this track researchers have examined the sensitivity of 'one-line' models to input variation. For example, Monte Carlo simulations (Hanson, 1987) and numerical experimentation (Jayakumar and Mahadevan, 1993) have agreed in that random variation of wave angle around the mean value leads to small shoreline variation away from groynes but significant near them. Studies also suggest that wave height sequencing in the long-term has minor influence on shoreline change (e.g. Hanson, 1987; Southgate and Capobianco, 1997; Dong and Chen, 2001). In general, by running the models for different sequences of wave characteristics and for their mean and extreme values, a band of shorelines may be generated within which the "true" shoreline is expected to lie.

Wave input – Wave hindcast and inshore transformation

The sediment transport formulae, involved in the 'one-line' model, ideally require breaking wave characteristics. For simplicity, it is common that wave conditions at a reference depth nearshore are used instead of those at breaking. In any case, nearshore wave conditions are needed. These can be either measured, directly hindcasted from winds, or obtained from deep water waves through their transformation inshore. Deep water waves can be again measured or hindcasted from wind records (wind speed and direction). Availability of very long-term (decadal) measured wave data is rare, both offshore and nearshore. Thus, wave hindcast from winds, measured or most commonly derived from numerical weather forecast models, is an ordinary procedure in engineering practice. Numerous wave hindcast and nearshore wave transformation models exist. However, this is not the main objective of this study so that a brief description of the models used herein, which are well-established simple models suitable for long-term (decadal) predictions, follows. The long-term suitability is attributed to their small computational demands compared to more sophisticated models.

Wave hindcast models can be point (e.g. Donelan, 1980), regional, or even global models (e.g. WAMDIG, 1988). Point models make use of semi-empirical formulae which calculate wave characteristics (significant wave height, wave period, and direction) at a single point from wind characteristics (wind speed, wind direction, fetch length, and wind duration). Swell from distance sources cannot be accounted for. Two-dimensional regional and global models numerically solve a wave energy spectrum evolution equation on a regular grid. They may account for a number of physical processes that could impact wave generation and growth (e.g. wave-wave interaction, wave-current interaction, dissipation due to breaking), incorporate swell, and are in general considerably more complex than the point models. For the need of this study, a point model is used to hindcast waves at deep

water. In the model, the deep water hindcast formulae for significant wave height and wave period are based on the well-known SMB method developed during the Second World War by Sverdrup and Munk and subsequently refined by Bretschneider (1952, 1958). The method is fully described in CERC (1977). However, the method has been modified by Donelan (1980) so as to allow for non-coincidence wind and wave directions for fetch-limited waves, i.e. wave direction is biased towards the longer fetch distances (Donelan, 1985). Thus, the fetch length is measured along the wave direction rather than the wind direction. To estimate the predominant wave direction it is assumed that this is the one that produces the maximum value of wave period for a given wind speed. A process of trial and error is needed to calculate the wave direction that maximizes the wave period. After determining the wave direction, the SMB formulae are used but with the wind speed at 10m above the sea surface, U_{10}, replaced with $U_{10}\cos(\theta_{wind}-\theta_{wave})$. If the fetch length is not a restrictive factor for wave development, wave and wind directions coincide. The model used here is a parametric 'long-term' wave hindcasting model, which means that also accounts for wave growth lag and wave decay due to changing wind direction and speed (see e.g. Kamphuis, 2000). It therefore includes 'local swell'.

Bishop (1983) compared different wave hindcast expressions with data from Lake Ontario, Canada, and suggested that the Donelan formulae (Donelan, 1980; Donelan, 1985), used here, outperform the well-known SMB and JONSWAP methods (see CERC (1977) and CERC (1984) for a description of the methods). Therefore, on Great Lakes the wave direction is biased towards the longer axis of the lake. With respect to 'one-line' modelling, the often invalid assumption that wind and wave directions coincide, made in the routinely used SMB or JONSWAP methods, may lead to large errors in estimates of shoreline positions because of the sensitivity of alongshore sediment transport formulae on wave direction. In general, all hindcast formulae are approximations. At the same time,

wind speed, direction, and duration are highly uncertain parameters. As a result, wave hindcast models should always be calibrated and their results interpreted with caution (Kamphuis, 2000).

For a review on the different wave transformation model types and their capabilities the reader is prompted to Dodd and Brampton (1995) and Andrew (1999). In general, a fundamental difference between models is the inclusion or not of diffraction. Thus, only two model types, the mild-slope equation and Boussinesq models, simultaneously solve refraction and diffraction. The rest assume an artificial separation of refraction and diffraction, and usually calculate refraction only. Here, a simple spectral ray-tracing model was used to transfer the waves from offshore to an inshore point using back-tracking (see Abernethy and Gilbert, 1975). The model is called REFPRO and was developed by Halcrow. Ray-tracing wave transformation models, like REFPRO, are essentially computerized versions of the well-established graphical ray-tracing techniques described in most relevant textbooks (Chadwick *et al.*, 2004). These simple refraction models are extremely cost effective in terms of computational time and provide reasonable results in regions of largely uniform sea-bed where diffraction is not important.

2.2.4 Comparison of analytical and numerical solutions

Hanson (1987) compared analytical and numerical solutions of the 'one-line' model and showed that the linearization required to derive analytical solutions produces only small errors if the incident wave angle is kept within the order of 30 degrees. The error is generally the prediction of a faster rate of shoreline response. By applying two types of numerical models, one accounting for the effects of wave refraction and one neglecting this process thus assuming constant wave characteristics along the breaker line, they also concluded that the omission of wave refraction can potentially cause considerable errors in

the prediction of shoreline positions. This is because wave height and angle are expected to change continually with space and time even for constant offshore wave conditions as the bottom contours vary alongshore and change with changes in the shoreline position. They showed that exclusion of wave refraction results in a flattening of shoreline irregularities. For example, a beach fill will erode more rapidly or accumulation rate on the updrift side of a groyne will be underestimated.

2.3 Discussion

The review of the different approaches available to date for the prediction of shoreline change clearly indicates that in the very long-term, i.e. over decades, no method exists that can produce accurate results. However, long-tem predictions are important. Therefore, apart from improving existing methods and investigating new approaches, one has to balance the advantages and disadvantage of present techniques for his specific application. This chapter showed that between mathematical and non-mathematical approaches, the former are preferred. Also, it revealed that amongst mathematical models, the 'one-line' model appears to be the best suited for decadal predictions if data availability is limited, resources are restricted, and a sufficient level of generality is required. If no restrictions as such are present, then 'behaviour-oriented' models or 'hybrid' models could be an option.

The 'one-line' model is the approach used in this study and was reviewed in greater detail. This simplified model based on the continuity of sediment equation, dates back to 1956 and has performed well in numerous applications. Because of its assumptions, it works better on open sandy shores that are predominately shaped by the alongshore variation of the littoral drift, determined mostly by wave-induced currents. Consequently,

the present study better applies to coastal environments with the aforementioned characteristics.

Like all the methods described, model predictions become increasingly uncertain with time-scale. Ignoring uncertainty in input data, the reason lies in the basic assumptions of the model that are likely to be violated in the very long-term. Thus, the fundamental assumption of a constant depth of closure might be violated as depth of closure has been found to increase with time. In addition, as it will be seen in the following chapter, the assumption of a constant equilibrium profile might also be violated in the long-term, especially under climate change. Restricted sediment availability and/or altered sediment exchange at the boundaries might also become a problem. Uncertainties in data input will also deteriorate the accuracy of any long-term shoreline forecast, irrespectively of the method used. This type of uncertainty will be also described in the following chapter. Here, it is noted that changes in the statistics of the forcing, predicted due to climate change (Chapter 4), further justify the choice of a physics-based modelling approach.

Apart from applying the 'one-line' model, the present study further aimed to improve certain aspects of it. In particular, the highly unrealistic assumption that a constant wave condition drives shoreline evolution, adopted in analytical solution derivations, is relaxed in Chapter 4. In addition, the stability problem of the explicit numerical scheme and the problem of increased complexity and reduced accuracy of the implicit numerical scheme, used to date to solve the model numerically, are solved in Chapter 5 through the application of an alternative, highly efficient numerical solution technique.

Chapter 3

Climate change and its implications on shoreline evolution

In this chapter, the reasons why certain aspects of climate change are important for beach evolution are given. Then, evidence that climate change is happening is presented. Specifically, "greenhouse gas" emission scenarios and associated scenarios of change in sea-levels, winds, and waves, predicted by recent studies, are described. The focus is on UK climate. A briefing to the methods available for the development of climate change scenarios is also included. Scenario uncertainties are discussed. The chapter continues with reference to existing studies on the impact of climate change, SLR and/or wave climate shifts in particular, on shoreline evolution or sediment transport patterns. A discussion relevant to the choices and objectives of this study follows. The focus is on open coast environments and sandy shores.

3.1 Beach response to SLR and other climatic changes

As mentioned in Chapter 1, the aspects of climate change that are more likely to impact shoreline change at open sandy beaches include changes in relative sea-level, wave

climate, storm frequency and intensity, tidal range, and precipitation. The mechanisms through which each of these factors affects shoreline evolution are summarized in this section.

SLR often initiates or exacerbates beach erosion because:

- Waves break closer to the shore because of higher water levels, dissipating their energy within a smaller distance.
- Wave refraction is reduced because of deeper waters, generating greater potential for longshore sediment transport.
- Wave and current erosion processes act further up the beach profile causing its readjustment (Douglas *et al.*, 2001; Paskoff, 2004).

Relative SLR is a very important driver of shoreline change, leading to erosion of about 50 to 100 times greater than the amount of sea-level rise itself (result obtained from the Bruun Rule described in Section 3.3.1). Wave heights and directions, the climatic aspect whose changes are expected to contribute the most in altering future shoreline evolution patterns, largely determine the magnitude and direction of the littoral drift which is the main regulator of shoreline shape on open sandy shores. Increased storm frequency and intensity will enhance the back and forth movement of the shoreline and might eventually lead to a long-term residual movement of erosion (Nicholls, 2000). In addition, natural features protecting the shore from increased wave energy may be eliminated for extended periods or breached leaving the shoreline highly exposed. Human made stabilization defences will also be prone to breaching. It is also possible that increases in the storage of sediments below low water will occur, causing enhanced long-term erosion. Increased tidal range might affect long-term shoreline evolution by changing relative sea-levels. Finally, changes in precipitation rates are expected to contribute to the establishment of shoreline response patterns by altering sediment discharge. In general, an increase in run-off is predicted for

northern Europe and a decrease for the south (Nicholls, 2000). Climatic variability will add to long-term changes to produce an aggregated effect (Forbes *et al.*, 1997; Nicholls, 2000). According to Hulme *et al.* (2002) the worst scenario for the coastal zone would be one of increased sea-level and higher tidal water combined with amplified wind speed and changes in wind direction such that exposure of offshore energetic waves is greater, enhancing their erosive potential. Since this study is interested principally in wave climate changes and then on SLR, the remainder of this chapter focuses on these two processes.

3.2 Climate change scenarios

3.2.1 IPCC and emission scenarios

The Intergovernmental Panel on Climate Change (IPCC) reports, based on peer reviewed and published scientific/technical literature, are considered today as the 'bible' of climate change, as they are the most comprehensive and up to date assessments on climate change around the globe. These include information on the development, application, and uncertainty of different climate change scenarios. It is only the latest assessment of IPCC Working Group 1 (WG1), completed in 2007 (IPCC WG1, 2007), that gives a conclusive statement about climate change. Specifically it states: "Warming of the climate system is unequivocal, as it is now evident from observations of increases in global average air and ocean temperatures, widespread melting of snow and ice, and rising global average sea level."

Climate change scenarios for use in impact assessment studies can be developed in different ways as it will be seen in the following subsection. However, most commonly, climate change scenarios are based on scenarios of future CO_2 concentration in the

atmosphere. The most comprehensive and recent assessment of possible emission scenarios is the Special Report on Emissions Scenarios (SRES) of the IPCC, completed in 2000 (IPCC SRES, 2000). A range of possible "greenhouse gas" emissions (35 scenarios) were developed based on estimates of socio-economic drivers, i.e. how population, economies, energy technologies and societies develop. Ultimately, four representative and equally plausible global social - emission 'storylines' were extracted, known as A1, A2, B1, and B2. These storylines, modified to represent UK in particular, are shown in Figure 3.1 and

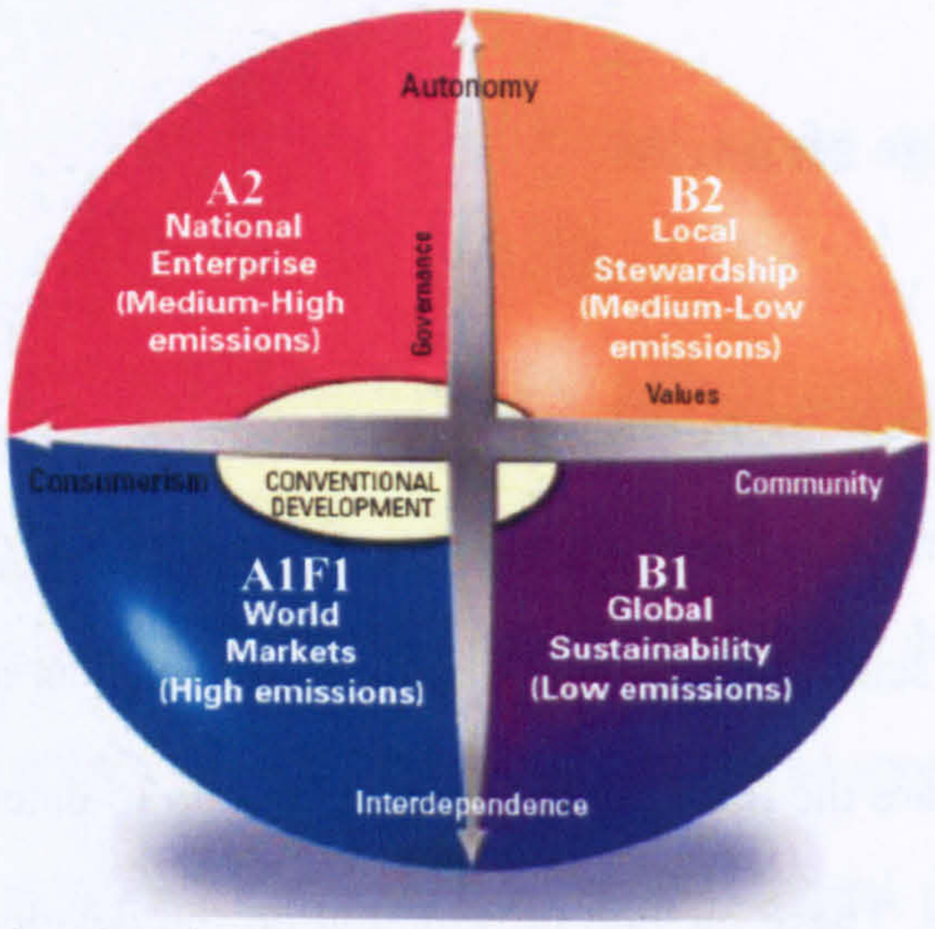

Figure 3.1 Future social and emission scenarios for the UK. The vertical axis shows the system of governance, ranging form autonomy, where power remains at the local and national level, to interdependence, where power increasingly moves to international institutions. The horizontal axis shows social values, ranging from consumerist to community-oriented (adopted from FORESIGHT, 2003)

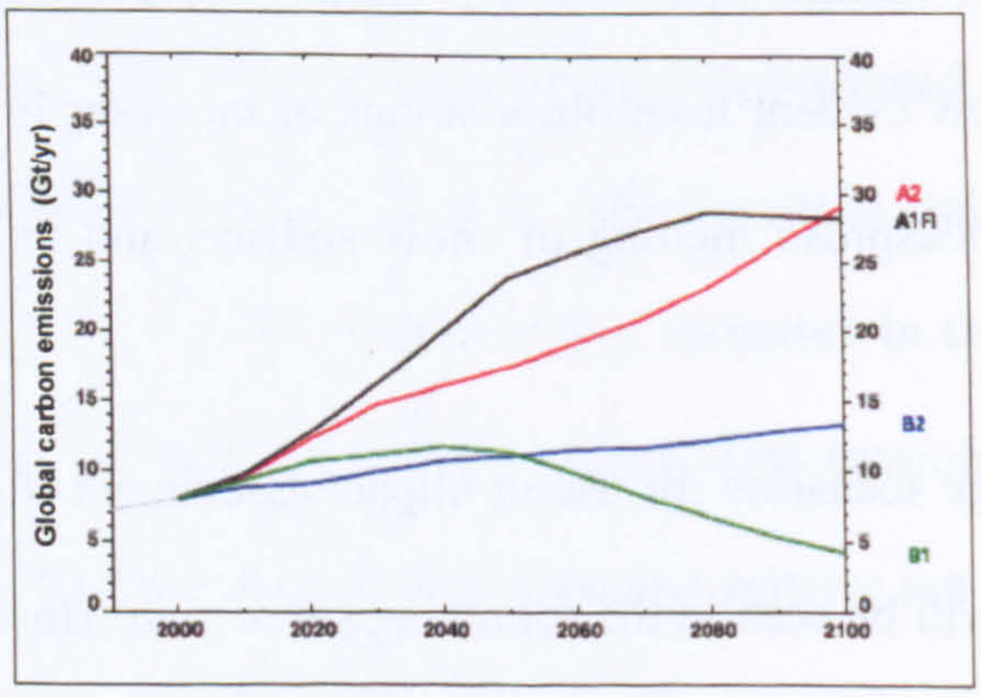

Figure 3.2 Global carbon emissions from 2000 to 2100 for the four SRES emission scenarios. Observed data to 2000 (adopted from FORESIGHT, 2003).

described in Table A2 in the Appendix A. A1F1 is a group within the A1 scenarios 'family' (characterizing alternative developments of energy technologies) based on fossil intensive energy technologies. Associated global carbon emissions are presented in Figure 3.2.

3.2.2 Development of climate scenarios

There are a number of ways to develop future climate scenarios, resulting in different scenario types, each with its advantages and disadvantages. Similarly to the approaches to long-term predictions of shoreline change (Section 2.1), the approaches to generating climate scenarios can be based on mathematical modelling or not. For example, a scenario type that has been used in impact assessment studies relevant to shoreline change (Slott *et al.*, 2005; Dickson *et al.*, 2007) and is not directly based on mathematical modelling is the incremental scenarios. In these, the variable of interest is changed incrementally by plausible but arbitrary amounts (e.g. ± 10%, ±20% etc) and thus the sensitivity of an exposure unit to a wide range of potential future changes may be studied (IPCC WG1, 2001). Often, mathematical modelling outputs are used to determine the direction and range of variation of the incremental scenarios (e.g. Dickson *et al.*, 2007). Other types of scenarios, not based on the modelling of physical processes, that have been used in impact assessment studies (e.g. for agriculture) and could potentially be employed in shoreline evolution impact assessments include:

- Instrumental temporal analogues, i.e. use system response in a period of warmer climate during the past as an analogue for system response in a warmer period in the future.
- Extrapolation of current trends in climate.
- Expert judgment.

- Stochastic weather generators, which produce synthetic time-series of weather data of unlimited length for a location based on the statistical characteristics of observed weather at that location.

However, thinking of the above techniques especially with regard to future wave scenarios - what this study requires to pursue its objective - some basic problems are identified. One, which pertains to all of the non-mathematical techniques, is that they are not directly related to greenhouse forcing (i.e. emission scenarios) so that generation of unrealistic scenarios is possible. In particular, unrealistic scenarios maybe be the result of ranging the variables outside a realistic range (incremental type scenarios) or of relating periods of small climate change magnitude in the past with periods of potential much stronger change in the distant future (temporal analogues, extrapolation of current climate trends). Another vital problem of non-mathematical techniques is their requirement for long-observational data sets (temporal analogues, trend extrapolation, and weather generators). In addition, stochastic weather generators usually need information on climate change from mathematical models (e.g. change in natural variability) in order to be able to reproduce weather scenarios with different statistical properties than those at present. It is because of these limitations of non-mathematical techniques that climate scenarios derived from comprehensive, physically-based numerical climate models are the most popular at present and those most extensively used in impact assessment studies. In contrast with non-mathematical approaches, computerised climate models are able through mathematical formulations to calculate explicitly the impact that altered concentrations of "greenhouse gases" in the atmosphere will have on the climate system. Most if not all of the key processes operating in the climate system may enter a climate model computation. In addition, the requirement for observational data, which now serves mainly for model

validation, is reduced. As a result, climate models are presently considered as the best tool available to estimate climatic changes (Houghton *et al.*, 1995).

At present, there is a substantial set of climate models available. These may differ in their mathematical representations of the climate system, in their complexity, and/or in their resolution. A short introduction to some aspects of climate modelling is given in the following section. It is noted here that this project makes use of climate scenarios but does not go into the details of their development and application, so that the present discussion on the different emission scenarios (previous section), types of climate scenarios (present section), and climate models (following section), is relatively brief aiming to introduce the reader to the subject and to justify choices made in this study. For a more detailed description on the development of climate scenarios, their advantages and disadvantages, and their application in impact assessments the reader is prompted to Chapter 13 of the IPCC Third Assessment WG1 report and Chapter 3 of the IPCC Third Assessment WG2 report (IPCC WG1, 2001; IPCC WG2, 2001). Table A3 (Appendix A) provides a good summary of part of the context of Chapter 13, IPCC WG1 (2001).

3.2.3 Climate models

As mentioned above, climate models exist at different spatial scales and levels of complexity. They can be global or regional, complex three-dimensional or simplified models that attempt to model complex 3D behavior in fewer dimensions (see Table A3, Appendix A). In earlier days, climate scenarios developed with state of the art global coupled Atmosphere – Ocean General (or Global) Circulation Models (AOGCMs), which are the most complex 3D climate models, were used directly in quantitative impact assessment studies. For example, in the United Kingdom Climate Impacts Program (UKCIP) assessment of 1998 (Hulme and Henkins, 1998), UK climate scenarios came

directly from a AOGCM. Also, Kaas and Andersen (2000) refer to a number of studies that investigated changes in extra-tropical storm activity using output directly from AOGCMs. However, the spatial resolution of these models is coarse, typically between 125 and 250 km (IPCC WG1, 2001), and thus not ideal for regional impact assessment studies that depend on climatic variables whose changes take place over finer scales than those resolved by AOGCMs (e.g. wind climate scenarios or cloud formation and development). Simulation of extreme events is also prevented. For example, Kaas and Andersen (2000) note that the studies that used AOGCM output directly could not conclude on any changes in the frequency and intensity of extreme events. Also, Hulme *et al.* (2002) say that storm tracks over northwest Europe were displaced too far south with the use of AOGCMs in UKCIP98. To overcome these problems, techniques to improve the spatial resolution of climate models, known as regionalization techniques, have been developed. These include:

- Global high resolution/variable resolution Atmospheric GCM (AGCM).
- Regional climate modelling.
- Statistical downscaling.

Before, going to a short description of the regionalization techniques, it is important to note that AOGCMs are the starting point of all of them (IPCC WG1, 2001).

The global high and variable resolution AGCMs are atmosphere stand-alone models with resolution 2 to 3 times finer than in AOGCMs. In the global scale resolution of 100 to 150 km is common whilst in the local/regional scale resolution as little as 50 km can be achieved (IPCC WG1, 2001; Christensen and Christensen, 2007). AGCMs are computationally very demanding so that only time-slice simulations have been performed, i.e. regional information on climate or climate change is produced for at most several decades selected from a transient AOGCM simulation. This is sufficient for many regional impact assessment studies. In a typical climate experiment, two time windows are selected,

one representing 'present' conditions, known as 'control' time-slice, and one representing future climate conditions, known as 'scenario' time-slice. Most if not all of the big projects on climate change over the European domain (e.g. STOWASUS 2100, PRUDENCE, UKCIP, PESETA) involve AGCM runs for the control period, 1961-1990, and the future period, 1971-2100. For the control time-slice, AGCMs lower boundary conditions, i.e. sea surface temperature (SST) and sea ice conditions, are obtained either from AOGCMs simulations or directly from observations, thus avoiding systematic errors associated with AOGCMs. For the scenario time-slice, SST and sea ice conditions at the lower boundary are usually obtained by extracting the anomalies between control and scenario from AOGCM simulations and adding them to the observed conditions used for the control AGCM run. Monthly means over the 30 year time-slices are commonly used in the calculations. A possible problem of AGCMs is that they generally use the same formulations as AOGCMs, which might not be optimal for the higher resolution of the former models (IPCC WG1, 2001). Another problem, related to impact assessment studies, is that even higher resolution is often required. For example, Kaas and Andersen (2000) suggest that although AGCMs can better simulate intense climatic variables than AOGCMs, storms like those in December 1999 in Europe can still not be resolved. Since the computational demands of AGCMs do not allow for an increase of AGCMs present resolution (IPCC WG1, 2001) another method to further increase the resolution of climate information is required. The most common approach is the use of regional climate models.

Regional climate models (RCMs) have nowadays a resolution as high as 12 km (Christensen *et al.*, 2002; http://prudence.dmi.dk/). As a result, they account for processes not resolved by global climate models (AOGCMs and AGCMs) such as the impact of complex topography and land-sea contrast on atmospheric circulation and climate variables. In addition, finer spatial resolution leads to improved information at high

frequency temporal scales (e.g. Mearns *et al.*, 1997, cited in IPCC WG1 (2001)) so that RCMs can provide useful information at high temporal resolution (e.g. 3-hourly output of climatic variables). This makes temporal variability considerations possible in impact assessment studies (before RCM applications, normally only changes in the mean of a climatic variable were examined in impact assessments). Changes in climate variability on daily to interannual time-scales have been found in RCMs runs (e.g. Mearns, 1999, cited in IPCC WG1, 2001). RCMs cover only limited areas of the globe and therefore need a GCM (AOGCM or AGCM) as parent to provide the weather conditions at the boundaries of the area covered by the RCM. A consequence of this is that high temporal resolution RCM output is uncommon because of the rarity of high resolution GCMs output. The nesting of RCMs is one way so that no feedback exists back to the driving GCMs. Thus, although they are better suited for small scale intense events, simulations of larger scale processes are not necessarily different that those performed with GCMs. Like all 3D climate models, RCMs are also very computationally expensive, so that time-slice climate experiments exactly like the ones described in the above paragraph are typically performed.

Statistical downscaling is another method for developing high spatial resolution climate scenarios using the output of GCMs. In contrast with the methods described above, this method is empirical and is based on establishing statistical relations between regional or local scale climate variables and large-scale variables derived from GCMs. Although the method is computationally cheap and gives the potential of addressing a wide range of variables, its theoretical basis, which is that the empirical relations developed for present day climate also hold unchanged under different forcing conditions of possible future climates, cannot be verified. In addition, an extensive data set is required to develop the statistical relations (IPCC WG1, 2001). As a result, the method is not very well accepted for climate impact assessment studies. For further details on climate models and

regionalization techniques, the reader is prompted to IPCC WG1 (2001), Chapters 10 and 13. Also, to Table A3 (Appendix A) for a briefing. For the remainder of this chapter, only climate scenarios developed with climate models (GCMs and RCMs) are dealt with.

3.2.4 Uncertainties in climate scenarios

When examining the impacts of climatic changes on a natural system along with possible adaptation and mitigation responses, it should be bear in mind that a cascade of uncertainties is pertained to such an examination, starting from the emission scenarios, through climate modelling, to the impacts.

Firstly, we cannot be certain how socio-economic parameters will change in the future and as a consequent what the future "greenhouse gas" emissions will be. However, the range of emission scenarios described in Section 3.2.1 cover the possibilities which seem realistic with respect to modern societies. Uncertainty also exists in the conversion of emission scenarios to "greenhouse gas" concentrations in the atmosphere and in turn to radiative forcing (IPCC WG1, 2001; Hulme *et al.*, 2002).

Secondly, predicting both atmospheric forcing and ocean response is not easy introducing uncertainty to the mathematical formulations. Different GCMs and RCMs have different formulations and thus different climate sensitivities, which is a key source of uncertainty in simulated climate scenarios. Also, differences in spatial and/or temporal resolution between models or model runs and different lengths of integrations contribute to variation of the predictions and increase of uncertainty (IPCC WG1, 2001; Nicholls, 2000). An extra source of uncertainty relevant to climate modelling is due to the internal climate variability of the model, i.e. in each simulation there is an unpredictable component (noise) along the response (signal) to a specified forcing. Internal climate variability may be seen as an imperfect replica of true climate variability (IPCC WG1, 2001).

Studies on uncertainty estimates have recently appeared in the literature (e.g. Jenkins and Lowe, 2003; Rowell, 2006; Christensen and Christensen, 2007). Typical approaches to the quantification of uncertainty involve running a wide range of GCMs, RCMs, and combinations of both, at a range of spatial and temporal resolutions, for a wide range of emission scenarios. In addition, nowadays, 'ensemble' modelling is carried out to address uncertainty due to natural climate variability, i.e. climate experiments with different initial conditions (different points in the control run) are performed. Although, such studies have been made possible today because of the ever increasing and improved global and regional climate experiments carried out by highly funded and collaborative project on climate change (see following section), incorporation of all sources of uncertainty still seems impossible. Climate model runs are expensive thus it is extremely difficult to perform ensemble simulations for all possible models and combinations of them and all the possible range of future emission scenarios. Impact assessment studies performed by the individual researcher necessarily use a small subset of the available model experiments (subset choice suggestions are made by Christensen and Chistensen (2007)).

Despite uncertainty, it has been made clear in the introduction of this study and in Section 3.1 that the incorporation of climate change in coastal planning is essential and should not be deferred. This is so, even if results are in terms of general trends rather than exact magnitude estimates. To this point, it is worth adding that although different models produce different results, qualitative results are often in agreement showing similar trends, especially those from RCMs. Consequently, despite the fact that the climatic changes of interest to this study, which are changes in future wind and wave fields, are associated with a high level of uncertainty (Hulme *et al.*, 2002), it is still expected to get an insight into future trends of shoreline evolution in response to these aspects of climate change. A high

level of confidence is associated with sea-level predictions, also of interest, under different emission scenarios (IPCC WG1, 2007, Hulme *et al.*, 2002)

3.2.5 Major projects on climate change over Europe

The European Union project for the Prediction of Regional scenarios and Uncertainties for Defining EuropeaN Climate change risks and Effects, know as PRUDENCE project (Christensen *et al.*, 2002; http://prudence.dmi.dk/), provides perhaps the best existing information on GCM and RCM integrations available over Europe, containing a series of high-resolution regional control simulations for 1961-1990, and climate change simulations for 2071-2100. The SRES A2 and B2 emission scenarios are used in the simulations. At present, PRUDENCE experiments are carried out with 10 RCMs, 4 AGCMs, and 2 AOGCMs. A great source of information on the PRUDENCE project and its findings is the Special Issue of the Climatic Research journal on the PRUDENCE project (Vol.8, Supplement 1, May 2007). Output from PRUDENCE is often used in impact assessment studies.

PRUDENCE project's main objective is to quantify the uncertainty originating from the choice of GCM and RCM formulation in climate-change downscaling experiments rather than explicitly develop climate change scenarios over Europe. Large projects whose basic aim is the projection of climate variables in the future and the analysis of their changes include: (1) the United Kingdom Climate Impacts Programme (UKCIP) (Hulme *et al.*, 2002; http://www.ukcip.org.uk/), which provides climate change scenarios specifically for the UK and coordinates research on their impacts and on adaptation policies, and (2) the regional STOrm, Wave and Surge Scenarios for the 2100 century (STOWASUS-2100) EU project (Kaas *et al.*, 2001; http://web.dmi.dk/pub/STOWASUS-2100/), which was a joint atmospheric/oceanographic numerical modelling effort that aimed to examine future

changes in frequency, intensity or area of occurrence of severe storms, waves and surges over Europe and the North Atlantic. A different objective, which is the assessment of the impacts of climate change on a variety of sectors (e.g. coastal systems, floods, agriculture, energy demands) for the 2011-2040 and 2071-2100 time horizons, is currently pursuit by the EU project on Projection of Economic impacts of climate change in Sectors of the European Union based on boTtom-up Analysis (PESETA) (Feyen *et al.*, 2006; http://peseta.jrc.es/index.html/). STOWASUS-2100 and PESETA projects rely mainly on high-resolution output from PRUDENCE project. UKCIP climate simulations have actually determined the time window (1961-1990 and 2071-2100) of subsequent PRUDENCE experiments.

3.2.6 Scenarios of future sea-level, wind and wave climate changes around UK

3.2.6.1 Global mean and relative SLR

Sea-level is rising since 20000 years ago (Last Glacial Maximum). However, long tide gauge records have revealed that over the 20th century SLR rates were higher than those of the 19th century whilst further acceleration is anticipated for the 21st century (Komar, 1998; IPCC WG1, 2001). Table 3.1, obtained from the latest (4th) IPCC WG1 assessment in 2007, shows projections of global mean SLR at the end of the 21st century, 2090-2099, relative to the period, 1980-1999, for the SRES emission scenarios. In general, SLR rate over the 21st century is predicted to be about 2 to 4 times greater than that of the 20th century.

Here, SLR scenarios produced by the latest UKCIP report for the UK, known as UKCIP02 (Hulme *et al.*, 2002), are used. Results are from the global climate model, HadCM3, developed by the Tyndall Centre for Climate Change Research (East Anglia

Table 3.1 Projected global average surface warming and SLR at the end of the 21st century (adopted from IPCC WG1, 2007).

Case	Temperature Change (°C at 2090-2099 relative to 1980-1999)[a]		Sea Level Rise (m at 2090-2099 relative to 1980-1999)
	Best estimate	*Likely* range	Model-based range excluding future rapid dynamical changes in ice flow
Constant Year 2000 concentrations[b]	0.6	0.3 – 0.9	NA
B1 scenario	1.8	1.1 – 2.9	0.18 – 0.38
A1T scenario	2.4	1.4 – 3.8	0.20 – 0.45
B2 scenario	2.4	1.4 – 3.8	0.20 – 0.43
A1B scenario	2.8	1.7 – 4.4	0.21 – 0.48
A2 scenario	3.4	2.0 – 5.4	0.23 – 0.51
A1FI scenario	4.0	2.4 – 6.4	0.26 – 0.59

Table notes:
[a] These estimates are assessed from a hierarchy of models that encompass a simple climate model, several Earth System Models of Intermediate Complexity and a large number of AOGCMs.
[b] Year 2000 constant composition is derived from AOGCMs only.

University), and are shown in Figure 3.3. The SRES emission scenarios have been used.

The IPCC results shown in the figure (coloured bars on the right) come from the previous (3rd) IPCC WG1 assessment in 2001. SLR is anticipated to occur for many centuries beyond the 21st even if atmospheric concentrations of "greenhouse gases" were to stabilize (Nicholls, 2000; IPCC WG1, 2001; Nicholls, 2002).

To assess the impact of SLR on any particular coastal region, projections of the

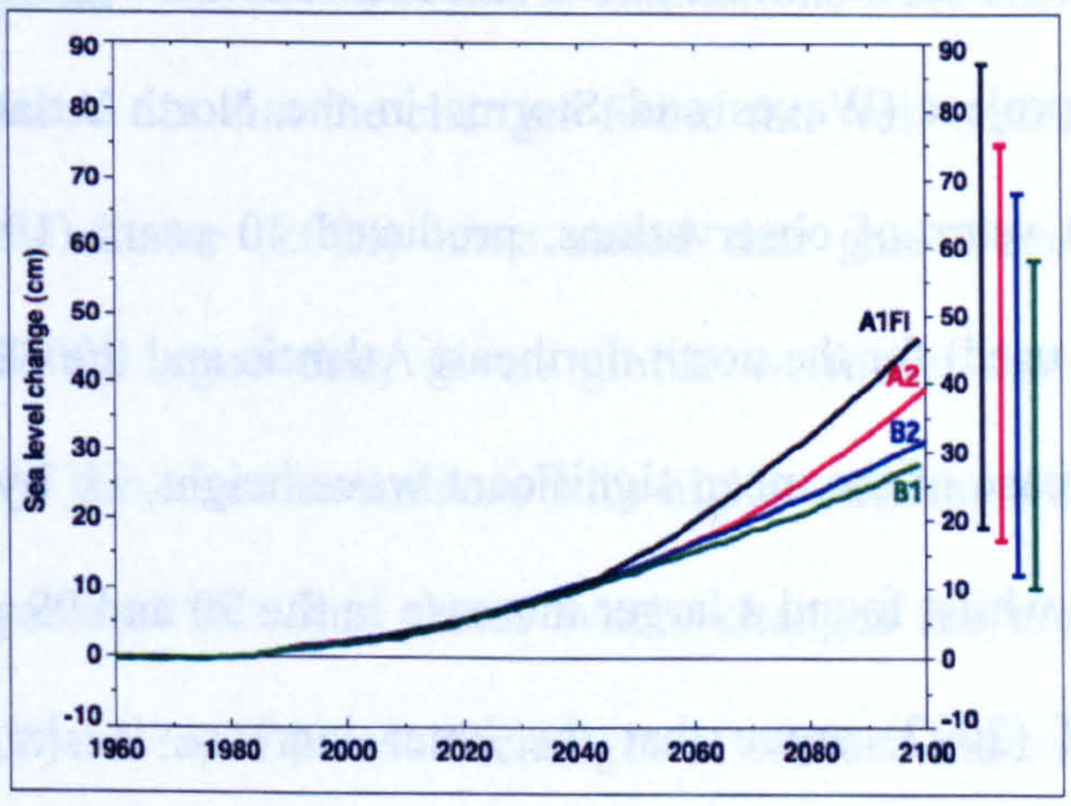

Figure 3.3 Global sea-level change (wrt 1961 – 1990 average) plotted from 1960 to 2100. Time-series show the HadCM3 results. Range bars to the right show the full IPCC range for each emissions scenario by 2100, the result of using different models climate models and different values for the ice melt parameters (adopted from Hulme *et al.*, 2002)

relative level of the sea to the land, i.e. relative sea-level, should be known. For the UK, the time mean local SLR is predicted to be very similar to the time mean global average during the next 100 years. Relative sea-level will be spatially variable with much of the southern Britain sinking (1-2 mm/yr) and much of the northern part rising (0.5 – 1mm/yr). Table A4 (Appendix A) shows UK regional net SLR allowances (DEFRA, 2006).

3.2.6.2 Changes in wind and wave climate and their extremes

A number of studies have aimed to improve our understanding of and to quantify changes in winds, storms, and wave climatology due to present and future changes in climate. Present trends are studied on the basis of long-term observations and measurements. For comparison of 'control' (or 'present') and 'scenario' climate, the most recent studies use output from high resolution RCM or AGCM time-slice experiments. Earlier ones used directly coarse resolution output from AOGCM. In all approaches, the data are analyzed to detect any changes in the long-term trend of the variables of interest and/or to investigate changes in their extremes (better done with high resolution data sets, see Section 3.2.3). In the following paragraphs examples of such studies are presented, starting from the earlier ones and those based on observations.

The WASA project (Waves and Storms in the North Atlantic) (Günther *et al.*, 1998), based on 100 years of observations, produced 40 years (1955-1994) of hindcast waves (WAM model used) for the north-northeast Atlantic and the North Sea. The project observed a small increase of the mean significant wave height, H_s, by about 0.2% per year over the last 30 years whilst found a larger increase in the 90 and 99 percentiles. However, Sutherland and Wolf (2002) argue that the latter increase is simply the result of an improved resolution of events within the long data set as time evolves and thus it is not real. Increases in wave height over the north Atlantic and the northern Europe have also

been reported by a number of smaller studies (e.g. Environmental Agency, 1999; Gulev and Hasse, 1999; Regnauld *et al.*, 1999; Grevemeyer *et al.*, 2000). Nonetheless, an important finding by Bouws *et al.* (1997) and Gulev and Hasse (1999) is that wave height increases are connected with growing swell rather than wind sea which actually shows significant negative tendencies in the 50% and higher percentiles exceedances. However, in general, the 100-year long record revealed that changes of this order are most probably because of significant interannual and interdecadal variability showing little evidence of long-term trends (Günther e al., 1998; Holt, 1999; Zhang *et al.*, 2000). Part of this variability is accredited to changes in the North Atlantic Oscillation (NAO) (i.e. a measure of the strength of the westerly flow over the North Atlantic), which has been found to increase over the last 30 years (Günther e al., 1998, IPCC WG1, 2001). An example of this effect is given in a study by Wolf and Woolf (2005) who concluded that a NAO increase, i.e. moderately strong westerly winds, results in large wind-seas both in the west coast of Scotland and south coast of England whilst a decrease, i.e. light easterly winds, results in fetch limited low waves in both locations. A second step of the WASA project was to perform a climate-change time-slice experiment with an AGCM at 125km resolution. However, the length of the control and scenario simulations were only 5 years and Beersma *et al.* (1997) have pointed out that the changes found fall well within the limits of natural variability. Hulme and Carter (2000) have stated that gale frequencies will probably increase. Nicholls (2000) argue that, given global warming, the balance of evidence suggests that a trend of increased storminess with higher extreme waves does exist for the northern Europe in contrast to other places where changes are uncertain. The study of Alexander *et al.* (2005) on rapid pressure changes at stations indicated an increase in the number and intensity of severe storms over the southern UK since the 1950s.

As part of the JERICHO project (Joint Evaluation of Remote Sensing Information for Coastal Defence and Harbour Organisations) (Cotton *et al.*, 1999), whose principal objective was to investigate whether UK coastlines have been experiencing increased wave heights over the last centuries, satellite recordings of wave heights since 1985 were analysed. The long-term record shows a clear signal of a 10% increase in wave height over the last decade. To obtain the nearshore wave heights from the offshore satellite and buoy measurements, the project employed wave transformation models (STORM and SWAN). They found that nearshore waves show lesser increase in wave height compared to the offshore increase. The reason lies on the strong control water depth exerts on the waves as they propagate inshore.

The STOWASUS-2100 30-year time-slice climate experiments (see Section 3.2.5) employed output from the ECHAM4 AGCM at about 125km spatial resolution and 6-hours temporal. Waves were studied by the Norwegian Meteorological Institute (DNMI) using the WAM model with wind fields from ECHAM4 as input. The 'scenario' used is the IPCC IS92a, developed in the 1992 IPCC assessment, which is very similar to the A2 emissions scenario. The 6 times longer integrations of this project, compared to the WASA project, provide more confidence in the assessment of long-term changes. Main findings of the STOWASUS-2100 project, related to wind and wave climate, include: (1) a downstream (i.e. north-east) displacement of the storm track which translates to an increase in storm activity over the North Sea and Britain. This finding is consistent with a number of other climate experiments (e.g. Beersma *et al.*, 1997; Lunkeit *et al.*, 1998) and lies beyond the limits of natural variability (significance on a 1% level), (2) no robust conclusions with respect to extreme wind speeds with a general, large scale small increase in extreme speeds along the north western European coasts but with considerable variability in the regional/local scale which by and large falls within natural variability. For example, the 50

year return period wind speed increased with 0.5 – 3.5m/sec in the North Sea while it decreased in the English Channel and west of UK and Ireland, and (3) higher changes in significant wave height, H_s, are observed in autumn with virtually no change in summer. H_s increases in the North Sea by 5% in autumn. Some increase in extreme events also occurs there. Both average and extreme H_s seem to decrease west and southwest of the British Isles.

Sutherland and Gouldby (2002) also used the two 30-year time slice experiment, mentioned above, to produce future wave time-series for five coastal locations around the UK and assess overtopping of sea defenses in 2075. Wave hindcasting was performed by a local wind wave model, called HINDCAST, so that swell was not included in the predictions. They found that in most of the cases wave heights of small return periods are slightly higher in the future but as return period increases they reduce and finally become smaller than present waves. In general, future wave heights were estimated to be within 5% of present-day values while differences in average annual offshore wave angles were all less than 5^0.

The latest assessment of the UKCIP, UKCIP02 report (Hulme *et al.*, 2002) provides some quantification of future changes in wind speed but not in wind direction because of the high uncertainty related to this variable. Output is from the Hadley Centre RCM, HadRM3, at 50km horizontal resolution, for the two time-slice experiment, and for the four SRES emission scenarios. A three-member ensemble run was performed for the A2 emission scenario. Results are given in terms of daily averages. UKCIP02 predicts a 2-8% increase in wind speeds by the 2080's, depending on scenario, over the south and east coasts of England in winter and spring. For the rest of the UK small changes are anticipated. Summer and autumn wind speeds decrease for most of the coastal areas reaching a 10% reduction off the west coast. Considering that waves largely follow wind

patterns, the latter result is consistent with the pattern of significant wave height changes, estimated by the STOWASUS-2100 project.

Pryor *et al.*, (2005) run the Rossby Centre coupled RCM, RCAO, over north-east Europe at about 50km horizontal resolution, forced by two different GCMs (higher resolution HadAM3 (AGCM) and coarser resolution ECHAM4/OPYC3 (AOGCM)). Their aim was to assess the impact of climate change on wind energy availability. The typical 30-year time-slice experiment was performed at a temporal resolution of 6 hours. The study obtained different results for HadAM3 and ECHAM4/OPYC boundary conditions. Wind directions were more sensitive to the change of driving global model than wind speeds. Another interesting finding is that on an annual basis the differences identified between 'control' runs for the two GCMs were of similar magnitude to those estimated between 'control' and 'scenario'. Simulations with boundary conditions forced with ECHAM4/OPYC3 revealed considerably higher climate sensitivity. Räisänen *et al.* (2003) found similar results using boundary conditions from the same GCMs. Another study by Hanson and Goodess (2004) analyzed daily mean wind speed and direction simulated with HadRM3 at 50km resolution (30-year time-slice experiment) aiming to assess the ability of the model to reproduce realistic wind fields. They found that the RCM reproduces considerably slower winds and highly spread in directions compared with observations. Poor model performance was attributed to its inability to accurately simulate wind speed with height and to the coarse spatial (50km) and time resolution (daily). However, modeled wind components were significantly more accurate within low lying regions and along the coast. Future wind speed changes were found to agree with the UKCIP report while winds from present dominant directions were found to decrease.

Beniston *et al.* (2007) using output from most of the RCMs of the PRUDENCE project found that the 90th percentile of daily winter wind speeds increase by 2.5% to more

than 10% in a European latitude band extending approximately from 45-55° N (including UK, France, northern Switzerland and Germany). In contrast, smaller increases or even negative change was found outside the specified band. Finally, the latest assessment of the IPCC WG1 in 2007 suggests that confidence in future windiness is not very high due to a relatively high range of results from different studies and climate models. However, it concludes that most of the projected pressure changes over Europe fall between two PRUDENCE simulations, shown in Figure 3.4, so that mean wind changes in Europe are expected to be between these two cases.

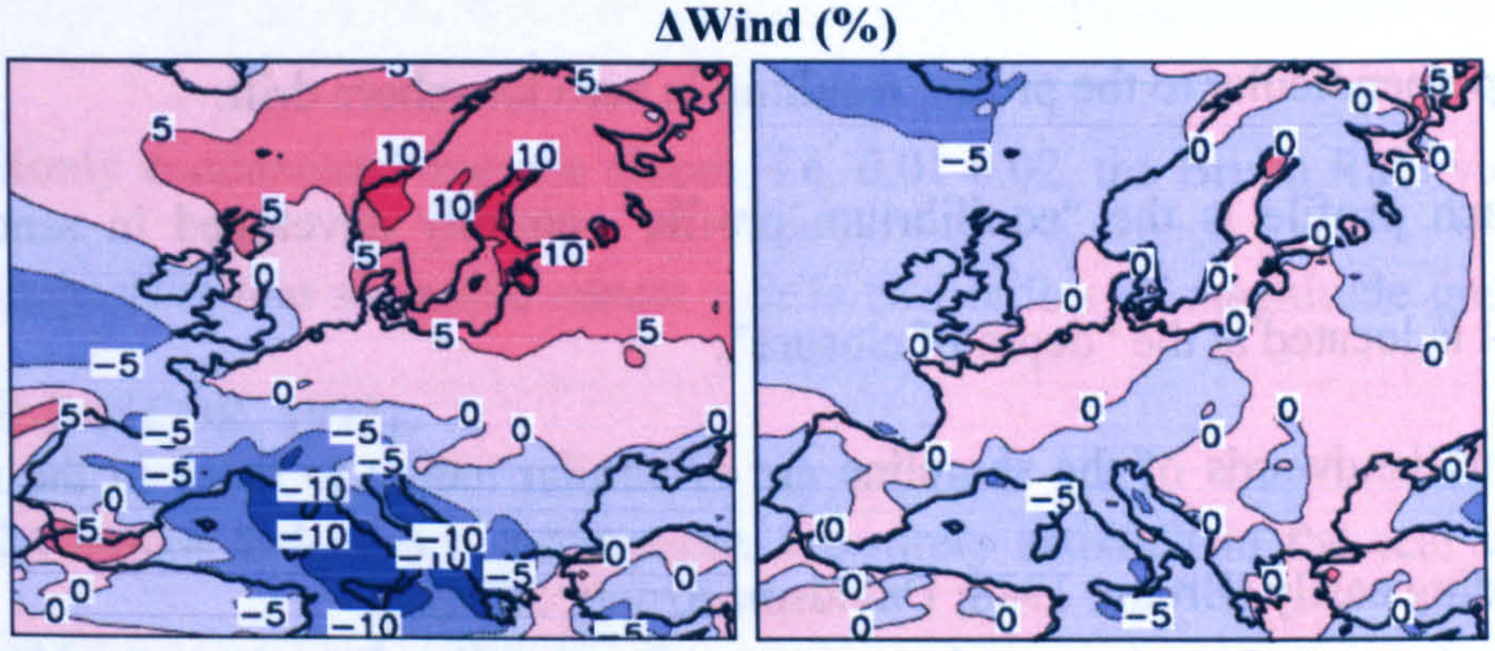

Figure 3.4 Simulated changes in annual mean 10m level wind speed (ΔWind) for the years 1961 to 1990 to the years 2071 to 2100. The results are based on the SRES A2 scenario and produced by the same RCM (RCAO) using boundary conditions from 2 global models, ECHAM4/OPYC3 (left) and HadAM3H (right), (adapted from Rummukainen *et al.*, 2004).

3.3 Calculating the impact of climate change on shoreline evolution

3.3.1 Estimates of SLR impact

At the beginning of this chapter (Section 3.1) the mechanisms which cause shoreline to retreat under a rise in the relative sea-level were listed. To calculate this retreat, the best-known model available at present is the so-called "Bruun Rule" and its

modifications (Bruun, 1962; Bruun, 1988; Cowell *et al.*, 2003). In its simplest form the Bruun Rule is given by

$$R = \frac{L}{B + D_c} S \tag{3.1}$$

where R is the shoreline retreat rate, S is the SLR, and L is the cross-shore distance to the depth of closure (SCOR, 1991), (Figure 3.5).

The Bruun Rule obeys the following conditions:

- It applies to a two-dimensional profile over which integrated material inputs and outputs equal zero. Net sediment transfer is onshore-offshore and wave action is always perpendicular to the profile resulting in zero longshore drift.
- The beach profile is the "equilibrium profile", entirely developed in sand, and its endpoint is located at the "depth of closure".
- Sediments landwards of the shoreline are of similar nature to those in the nearshore thus eroding easily (Bruun, 1988; Davidson-Arnott, 2005).

Apparently, the Bruun Rule does not suggest erosion is merely caused by SLR but by high energy short period storm waves that act closer to the shore due to deeper water (Douglas *et al.*, 2001). In case of waves with no sediment transport efficiency SLR would simply cause inundation of the landward profile (Davidson-Arnott, 2005).

The idea that the "equilibrium profile" shape is maintained with SLR, led Bruun to the following hypotheses, schematized in Figure 3.5:

1. The upper beach is eroded and the profile translates shorewards.
2. The eroded material is transported and deposited on the near offshore bottom of the profile.

3. The deposited material results in a seabed rise, equal to the SLR, thus maintaining a constant water depth (Bruun, 1988).

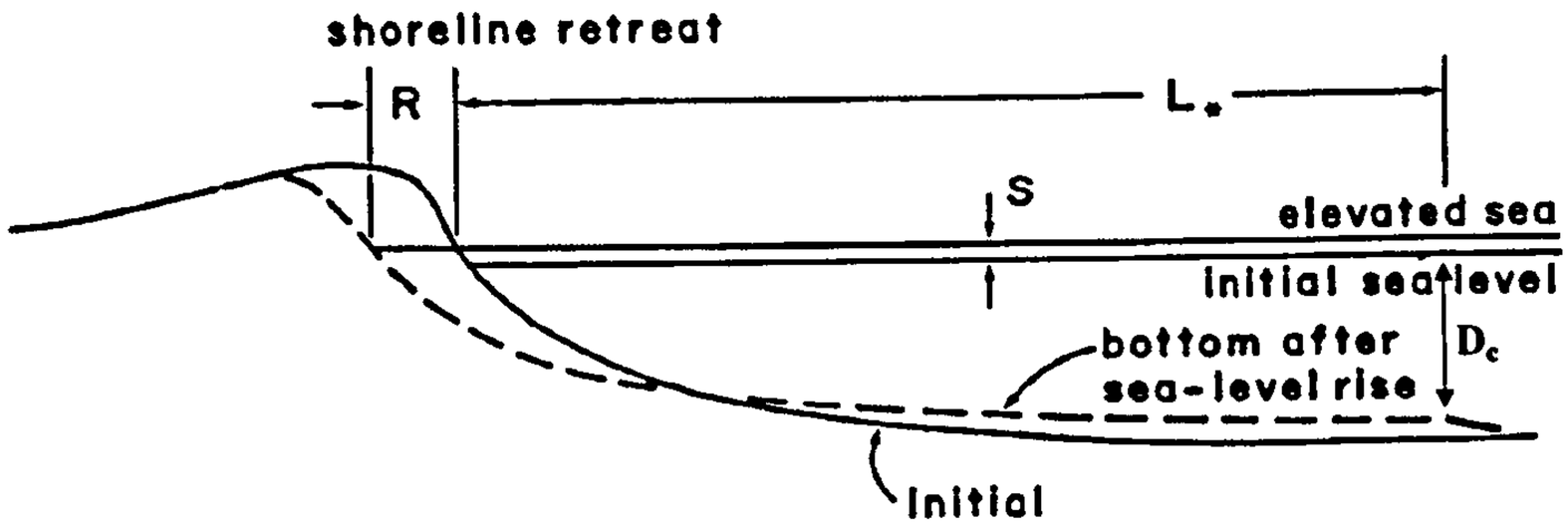

Figure 3.5 The net change in beach profile position due to a rise in sea-level, *S*, according to the Bruun rule, resulting in a zone of offshore deposition and erosion of the upper beach, with an overall recession rate, *R* (adopted from Komar, 1998)

For commonly encountered average slopes, i.e. 0.01-0.02, the Bruun Rule yields $R = 50S$ to$100S$, suggesting that shoreline retreat rate is two orders of magnitude greater than the causing SLR (SCOR, 1991).

The Bruun Rule basic assumptions are rarely satisfied in the real world mainly because of losses/gains of sediments alongshore and cross-shore beyond the limits of the Bruun profile (Bruun, 1988; Eitner, 1996). Nonetheless, the Rule has been extensively used in coastal vulnerability assessments under SLR (e.g. Richmond *et al.*, 1997; Lanfredi *et al.*, 1998) because of its simplicity and heuristic appeal. In fact, there is considerable controversy over whether it produces reasonable results. For example, Leatherman *et al.* (2000) and Zhang *et al.* (2004) are two studies that conform to the Brunn Rule whilst Dean (1990) and Cooper and Pilkey (2004) defy the Rule.

Controversial studies with respect to the validity of the Bruun Rule most probably exist because the Bruun effect is often subordinate to other effects under present day slow rates of SLR (Stive, 2004), most plausible being the sediment availability effect. This controversy is much more pronounced when the Rule is tested in open coast environments

which, in contrast to laboratories and lakes, pose many complexities and by and large break the Rule's assumptions. This is why validation studies that obey the Bruun Rule assumptions (e.g. Zhang *et al.*, 2004) are more likely to observe recession rates as predicted by the Rule. In any case, it is probable that an accelerated SLR, as anticipated, will override other effects, and shoreline recession similar to the one predicted by the Bruun Rule will be observed in the long-term (Stive, 2004). An indication of the latter is for instance a study by Minura and Nobuoka (1995) who confirmed the Bruun Rule along a coast where relative SLR was significant.

Several studies attempted to relax the Bruun Rule assumptions by introducing some sediment budget considerations in the original model. Although such models are still relatively underdeveloped, they normally improve comparisons between measured and predicted shoreline retreat rates (Komar, 1998; Douglas *et al.*, 2001). For instance, Hands (1983) and Bruun (1988) refer to modified equations that include potential losses of very fine sand offshore. Dean and Maurmeyer (1983) produced a modified Bruun Rule that accounts for longshore sediment transport. A similar model was derived recently by Cowell *et al.* (2003) and is given by

$$\frac{\partial y}{\partial t} D_c = \frac{\partial MSL}{\partial t} L - (q_{y,sea} - q_{y,dune}) - \frac{\partial Q}{\partial x} - q \qquad (3.2)$$

where MSL is the Mean Sea-level, $\partial y / \partial t = R$, $q_{y,sea}$, $q_{y,dune}$ is the sand exchange of the upper shoreface with the lower shoreface and the backshore respectively, and q is a local source or sink term, e.g. a river, estuary, or tidal lagoon. Relative sea-level change is introduced as a global source/sink term. Equation 3.2 is virtually the same as the sand budget balance equation suggested by Le Mehauté and Soldate (1978) (Equation 2.5), a form on which 'one-line' modelling of long-term shoreline evolution is based. In the

absence of longshore transport and other sources/sinks of sand Equation 3.2 reduces to the simple Bruun Rule.

In nature, it is expected that the last three terms of Equation 3.2, related to sediment availability, will considerably affect shoreline evolution. Stive (2004) compared cross-shore and longshore effects against the Bruun Rule effect and concluded that they are of similar magnitude both on low and high energy coasts apart from the case of human interference on high energy coasts when Bruun Rule effect is subordinated; this is often the case along tidal-inlet influenced shorelines, which can act as a source or sink of sediment (Stive, 2004).

3.3.2 Complications due to net profile changes

A further complication with respect to the validity of the Bruun Rule but also to the validity of the assumptions of the 'one-line' model at time-scales relevant to climate change is that the concept of the "equilibrium profile" might be violated at these time-scales. In particular, a steepening of the profile has been observed in several locations. For instance, Soulsby *et al.* (1999) and later Taylor *et al.* (2004) have shown that the intertidal width decreases around the British coastline, a manifestation of coastal steepening. Results from the latter study, which used 1084 profile lines around England and Wales covering an average period of 113 years, suggest that 61% of the profiles have steepened (66% at the south coast), 33% have flattened, and 6% did not change. Most of the steepening profiles were found at locations where long-term shoreline retreat has been observed, suggesting the coastal steepening occurs because of removal of sediments from the profile (Soulsby *et al.*, 1999). Although the original cause of the phenomenon is not well understood it is most probably the result of engineering structures interrupting the landward transgression of the high water mark (Sutherland and Wolf, 2002; Taylor *et al.*, 2004). In a different

perspective, a study by Walkden and Dickson (2006) found that accelerated SLR resulted in coastal steepening along a soft-rock shore at Norfolk. Their physical explanation is that since waves tend to flatten the beach profile and SLR causes the zone of wave attack to move to higher elevations along the profile, under an accelerated SLR the period that each profile elevation is exposed to wave attack is less so that the flattening effect of the waves reduces. However, their findings are specifically for soft rock shores overlain by a low volume beach and may not apply to deep beach shores for which the Bruun Rule was developed. In addition, the time elapsed between two successive equilibrium states for a change in the SLR rate is large (1000 years for a change from 2 to 6 mm/yr). In addition to coastal steepening, 'depth of closure' has also been found to increase with time-scale (Section 2.2.1.5), again contrasting the assumptions of the Bruun Rule and of the 'one-line' model. Cowell *et al.* (2006) and Dickson *et al.* (2007) investigated uncertainty in profile shapes and magnitude of shoreline recession by varying the values of 'closure depth' and 'length of active profile' in 'one-line' model simulations (at a single profile). Forecast envelopes similar to that shown in Figure 3.6 (following section) were generated allowing for a probabilistic analysis of future shoreline positions.

3.3.3 Estimates of the impact of changes in wind and wave climate

As mentioned in Section 1.3, to date, few studies have dealt with the implications of a changing wave climate on alongshore sediment transport and hardly any on the eventual impact on shoreline evolution. The few studies available may be divided into three categories:

- Studies describing the impact of observed shifts in the past.
- Those which use incremental future scenarios (with some using only one increment).
- Those who use output from climate models.

A further division could be done between those who estimate uncertainty at a high degree and those who estimate a small part of the uncertainty or do not consider uncertainty at all. A review follows.

Stive *et al.* (2002) refer to the work of Van Straaten (1961) who found that a small shift in dominant wind directions along the Holland coast during the period 1855 and 1900 resulted in a shore retreat of 50 to 100m. A phase difference of 5 years was observed between shoreline response and meteorological change. Peerbolte *et al.* (1991) estimated that an adverse 5% change in wind direction with consequent adverse change in wave direction would require response expenditures equivalent to a 60cm rise in sea-level for the Netherlands. Lorenzo and Teixeira (1997) used a sequence of hourly winds over a 2-year period and performed wave hindcast and wave transformation assuming a 10% increase in future wind strength (with no direction change), 1m rise in sea-level, and 1m increase in tide elevation. He concluded that storm waves approaching the Montevideo coast would increase in height while their wave angle would change within a range of $\pm 4^0$. Hosking and McInnes (2002) showed that for a small change in mean wave energy direction ($\approx 1.6^0$) at West Bexington, Dorset, net drift changed from east to west. For their study, they performed wave hindcast and inshore transformation using wind data output from the Hadley Centre RCM covering a 10 year 'control' period and a 10 year 'scenario' period representing the 2080s and the medium-high UKCIP98 climate change scenario. Sutherland and Gouldby (2002) produced time-series of future drift rates at five coastal sites around the UK and found that in most of the cases future annual drift rates increase by an average of 15% whilst standard deviations reduce by an average of 14% (i.e. reduced future variability). However, they concluded that future changes are unlikely to be greater than current levels of uncertainty. As mentioned in Section 3.2.6.2, Sutherland and Gouldby (2002) used winds produced by the ECHAM4 AOGCM at 125km horizontal resolution and

6-hours temporal (see Section 3.2.6.2 for further details) under the IS92A climate change scenario of the IPCC 1992 first assessment (Leggett *et al.*, 1992). A sediment transport model (DRCALC) was used to calculate annual drift rates. The model accounts for simplified refraction and uses the CERC formula.

A study that explicitly forecasts future alongshore shoreline positions was carried out by Ruggiero *et al.* (2006). The starting point of this study was a 10-year long data set of measured deep water waves offshore from Long Beach Peninsula, Washington, at the East Pacific Ocean. The probability distribution function of each wave characteristic in this data set was generated and the wave climate was discretized into bins of approximately equal probability to create a manageable number (1121) of realistic combinations of wave height, period, and direction, for input to a spectral wave energy model (SWAN) for wave transformation to a reference line (15m). A lookup table was generated where any of the events in the original 10-year data set could be represented. For shoreline hindcasts, 5 nearshore wave climates (≈ 100 wave conditions each) with the appropriate probability of occurrence were developed for input into UNIBEST 'one-line' model (≈ 10km alongshore discretisation, refraction performed up to the breaker point). For shoreline forecasts, the original 10-year time-series was modified by randomly varying the mean wave height, period, and direction, generating a number of incremental scenarios (± 0.5m for wave height, ± 2s for wave period, and ± 3 degrees for direction). Then, the methodology described above was repeated. Ultimately, the Monte Carlo technique was used to generate approximately 70 wave climates of 25 years each for input into UNIBEST. The 70 wave climates were combined with three sediment supply scenarios for a total of 210 shoreline change simulations, generating an envelope of possible future shorelines as seen in Figure 3.6. Finally, shoreline change prediction probability distribution functions at specific alongshore locations were assigned (e.g. at 130km alongshore 100% of model simulations

shows shoreline propagation by 2020). The authors state that future shoreline changes are highly sensitive to changes in wave direction and that sediment supply changes at the boundaries are as important in the resulting shoreline positions as wave changes. A second study on future shoreline evolution under climate change scenarios was performed by Dickson *et al.* (2007), for the soft-rock shore of northeast Norfolk. In this study, a range of incremental wave climate scenarios, SLR scenarios, and management scenarios for the period 2000-2100, were considered. These can be seen in Table A5 in the Appendix. To constrain the scenarios within a realistic range, guidance from the UKCIP02 report (Hulme *et al.*, 2002) was used. 'Present' wave data - a starting point in the study - was a 23-year record of hindcast wave characteristics. Wave transfer functions at the study location (previously calculated using a spectral wave transformation model (TOMOWAC)) were employed to transform the waves to a reference line (15m). These were then input to a

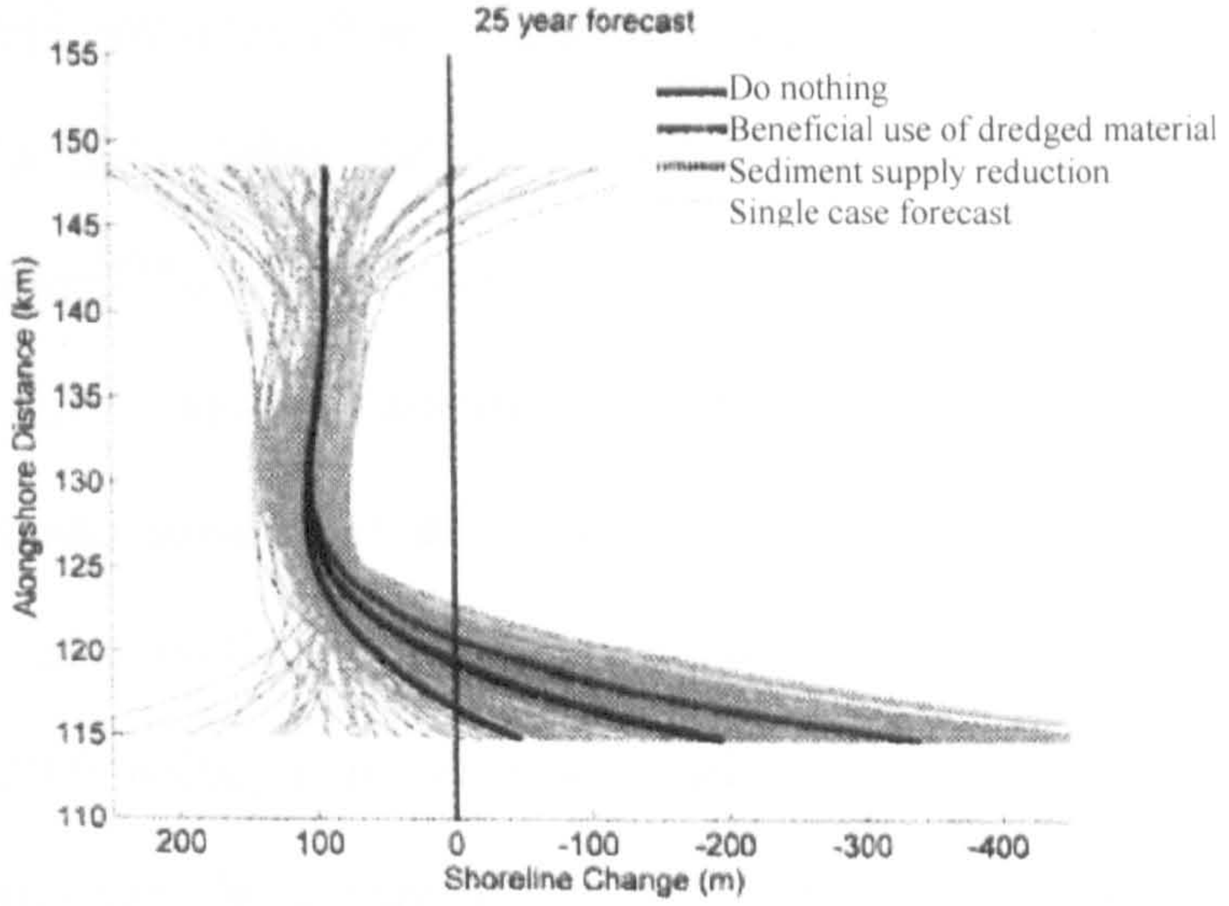

Figure 3.6 Decadal-scale shoreline forecasts for 210 wave climate and sediment supply scenarios. Black lines indicate the mean shoreline position for each sediment supply scenario (adapted from Ruggiero *et al.*, 2006)

relatively simple process-based model for soft cliff and platform erosion (SCAPE) (Walkden and Hall, 2005), which ultimately uses the 'one-line' approach and the CERC formula to compute shoreline change rates (a 12h and 25min model timestep was adopted).

It was found that model output was relatively insensitive to changes in wave height, moderately sensitive to changes in wave direction, with the most important effects associated with accelerated SLR. The study of Dickson *et al.* (2007) is part of the 'integrated coastal simulator', described in Section 2.1.1. As already mentioned, this is a 'system' models approach which accounts for many processes at different scales. With respect to future scenarios of change, the 'integrated coastal simulator' uses output from the Hadley Centre RCM corresponding to the SRES emission scenarios along with a large range of incremental and management scenarios (Nicholls *et al.*, 2007)

3.4 Discussion

The review of UK climate change scenarios – emission, SLR, wind and wave climate scenarios – reveals the truth of climate change but also highlights that uncertainty in the prediction of the different climatic variables in the future is substantial so that these variables are better thought to vary within a possible range, often wide. The higher evidence of change is associated with SLR whilst less evidence of change exists for wind and wave climatology because of the lack of consensus between results from different studies. Nevertheless, the fact that several studies have predicted changes in the latter variables that lie beyond the limits of natural variability in addition to the fact that similar trends are common between different studies, justify the investigation of the impact of such changes on coastal vulnerability, in view of the importance of wave climate in shaping shorelines. To date, relevant studies are rare.

This chapter also shows that amongst the different methods available to date to produce climate scenarios, climate model output is considered the best, since, in contrast to other techniques, climate models are physically-based and can explicitly account for altered

concentrations of "greenhouse gases" in the atmosphere. For a regional impact assessment study, RCM output is preferable since RCMs account for climatic changes that take place over finer scales than those resolved by GCMs. The finer the spatial scale the better extreme events can be simulated. Furthermore, high spatial resolution enhances the quality of high frequency output so that temporal variability can be assessed. Both extreme events and temporal variability are important in determining shoreline change so that high spatial and temporal resolution output from physically-based climate models would be the best option available to date for conducting a shoreline impact assessment study under climate change. This is the option employed in this study, in contrast to existing studies on the impact of a changing wave climate on littoral drift or eventually shoreline evolution which have been using incremental scenarios or coarse resolution climate model output.

The possibility for violating the assumptions of the 'one-line' model at time-scales relevant to climate change, summarized in the "Discussion" of the previous chapter and further described above, along with the uncertainty pertaining to climate change scenarios, input in 'one-line' model simulations, should be kept in mind when interpreting the results of this work.

Chapter 4

Semi-analytical solutions of shoreline response to time-varying wave conditions

As described in Chapter 2, solutions to the 'one-line' model can be analytical or computational. In this study, the aim is to improve both types of solutions as each has its advantages over the other and thus are complementary and both have an important role in research and practice (Sections 2.2.2.1 and 2.2.3.1). In brief, in practical engineering terms, numerical solutions are preferable because they are free from the assumptions associated with analytical solutions; however, in the preliminary design stage analytical solution are often used because they are quick and straightforward. Being exact, quick, and straightforward analytical solutions are also valuable for research and education. But in any case, the fact that finite difference numerical solutions are approximate time-stepping solutions involving accumulative numerical errors requires that numerical codes are tested against benchmark analytical solutions for accuracy and convergence. This is done for idealized cases where the assumptions of analytical solutions are respected. Therefore, in this chapter, analytical expressions of the 'one-line' model are improved to closer represent reality. In the following chapter, an improvement to the numerical solution of the 'one-line'

model is presented. Finally, in Chapter 6, the numerical solution is tested against the new improved analytical solutions derived in this chapter.

Specifically, this chapter is a contribution to relatively recent research that aims to relax one of the least realistic aspects of the 'one-line' analytical solutions to date. This is the common assumption that an unchanging and perpetual wave condition drives shoreline evolution. As seen in an overview of previous analytical work, presented in Section 2.2.2.3, analytical treatment of time varying wave conditions in the 1-line equation (Equation 2.20) was introduced by Larson *et al.* (1997) and later by Dean and Dalrymple (2002). As outlined in that section, the former study, using Laplace transforms, allows for a sinusoidally time-varying breaking wave angle at a single groyne and at a groyne compartment. Variation is expressed as a known function and is constrained at the location of the boundaries (groynes). The latter, aimed at investigating beach nourishment longevity, allows wave conditions to vary arbitrarily in time through a time-varying diffusion coefficient. Using Fourier decomposition of the shoreline position an analytical solution for an individual Fourier component is obtained, under the assumption of an initially straight, undisturbed shoreline. The lack of a more general analytical solution for the case of an arbitrary varying wave forcing prompted Reeve (2006) to develop a new semi-analytical solution for the case of a single groyne, which incorporated this effect in a relatively flexible manner. The Fourier cosine transform technique was used to derive the solution in terms of closed-form integrals. Time dependence was introduced through varying wave height and wave direction and through the adoption of a varying source/sink term.

The solution derived by Reeve (2006) provides a significant advance on previous analytical work. However, its applicability is restricted only to the case of a single groyne. In this study, new semi-analytical solutions, including time-varying forcing, for two important additional cases, are presented: (1) when the function of shoreline evolution is

known at a location along its length, e.g. a managed beach location and (2) between two groynes or headlands, perpendicular to the shoreline. Fourier techniques different to those used in Reeve (2006) were required to derive solutions for the cases presented here. In the former case, a Fourier sine transform is suitable and solutions are obtained in terms of closed-form integrals. In the latter, a bespoke finite Fourier cosine transform is devised and employed to obtain solutions as a Fourier series. Both solutions produce the spatial variability of the coastline explicitly with time in terms of its initial shape, the wave forcing, and a source/sink term which may vary in time and space. A further novelty in this study is the investigation of the effects of different forms of the diffusion coefficient on the shoreline evolution. Specifically, the impact of the diffusion coefficient of Equation 2.23 that relaxes the assumption of small angle of wave approach and explicitly includes wave angle variation in its formulation is examined in comparison with the widely used form of Equation 2.20 which assumes small wave angle and depends solely on the variation of the wave height.

The new solutions hold the general advantages of analytical solutions mentioned in Section 2.2.2.1. In fact, some of these advantages become greater since the response of the shoreline to more realistic wave conditions can be readily investigated and understood. In addition, they can provide benchmarks against which the accuracy and convergence of time-stepping numerical models under arbitrary time-varying wave inputs can be tested as it will be done in Chapter 6. As a result, confidence in the performance of numerical codes driven by time-varying waves can be increased. The present work introduces new important cases, thereby widening the scope of analytical investigations and the range of checks on computational codes.

In what follows, the 'one-line' relevant expressions needed for the derivation of the new solutions are referred, the analytical development to obtain the formal solutions along

with the methods implemented to provide numerical evaluation are given, example applications are presented, and finally, a discussion of the present work is carried out.

4.1 Theoretical framework

Following Reeve (2006) a 'one-line' model equation of the form of Equation 4.1 is taken as a starting point

$$\frac{\partial y}{\partial t} = \varepsilon(t)\frac{\partial^2 y}{\partial x^2} + r(t)y(x,t) + s(x,t) \qquad (4.1)$$

where r, s represent sources/sinks. The rationale behind the splitting of the source term in two parts, one dependent on the shoreline position, $r(t)y(x,t)$, and one independent of it, $s(x,t)$, is that solutions become more flexible in accommodating different aspects that are significant in the long-term shoreline management (Reeve, 2006).

The diffusion coefficient is estimated using two different forms, the most widely used small angle formulation of Equation 2.20 (where α_0 in Figure 2.2 is small) and the wide angle formulation of Equation 2.23 (where α_0 in Figure 2.2 can be wide ($<45^0$)). Both assume a small local shoreline orientation. The form of the diffusion coefficient in Equation 2.23 means that it is always less than that given in Equation 2.20 and so will lead to a more conservative evolution of the shoreline. In Reeve (2006) ε given by Equation 2.20 was used.

Following Reeve (2006), the amplitude of the longshore sand transport rate Q_0 (m^3/sec) is taken to be that of the routinely used CERC (1984) formula for the longshore sand transport rate (Equation 2.9). The value found by Schoones and Theron (1993) for the proportionality coefficient K of the CERC formula (K = 0.41 using H_s) is used (Section 2.2.1.3).

Reeve (2006) solved Equation 4.1 in the region $x>0$, $t>0$ subject to the initial condition given by Equation 4.2 and boundary conditions given by Equations 4.22, which

represents the boundary condition at a single impermeable groyne placed at $x = 0$, and 4.4 (see following section). As mentioned above, he used the Fourier cosine transforms technique to obtain the formal solutions.

4.2 Analytical solutions

4.2.1 Solution of shoreline change for known time evolution at a point

Here, solutions are obtained in the region $x>0$, $t>0$. The initial beach shape is arbitrary, with

$$y(x,0)=g(x) \qquad x>0 \qquad (4.2)$$

The alongshore point of known shoreline evolution is placed at $x = 0$. The boundary condition implemented for this case is

$$y(0,t) = h(t) \qquad t > 0 \qquad (4.3)$$

This condition is used to model the situation where the beach line is managed actively to maintain a particular beach width at a location, or where there is persistent bypassing of a groyne. The final condition, that the beach is undisturbed far away from the origin, is given by

$$y \to 0 \quad \text{as} \quad x \to \infty, \quad \textit{for} \quad t > 0 \qquad (4.4)$$

Equation 4.1 is solved subject to the initial condition given by Equation 4.2 and boundary conditions given by Equations 4.3 and 4.4. The functions $r(t)$, $s(x,t)$, $g(x)$, and $h(t)$ are arbitrary but known. The mathematical problem is solved through the use of Fourier sine transforms. Some basic definitions of Fourier sine transform follow (see e.g. Sneddon, 1972). The Fourier sine transform of a function, $f(x)$, is denoted by $\bar{f}(v)$, where v is the

transform variable, and the operation of taking a Fourier sine transform is denoted by $F_s[\ ]$.

Thus,

$$F_s[f(x)] = \bar{f}(v) = \int_0^\infty f(x)\sin(vx)dx \tag{4.5}$$

The inverse transform is defined by

$$F_s^{-1}[\bar{f}(v)] = f(x) = \frac{2}{\pi}\int_0^\infty \bar{f}(v)\sin(vx)dv \tag{4.6}$$

Three more expressions related to the Fourier sine transform are required to solve our system of equations. These are:

- The Fourier sine transform of the second derivative (see e.g. Sneddon, 1972)

$$F_s\left[\frac{\partial^2 f(x)}{\partial x^2}\right] = -v^2\bar{f}(v) + vf(0) \tag{4.7}$$

- A convolution theorem for a combination of cosine and sine transforms. If $\bar{f}(v)$ is the Fourier sine transform of $f(x)$ and $\tilde{g}(v)$ is the Fourier cosine transform of $g(x)$, then the convolution theorem required is (Sneddon, 1972)

$$\int_0^\infty \bar{f}(v)\tilde{g}(v)\sin(vx)dv = \frac{\pi}{4}\int_0^\infty f(\xi)\left[g(|\xi - x|) - g(\xi + x)\right]d\xi \tag{4.8}$$

- The definite integrals (see e.g. Gradshteyn and Ryzhik, 2000)

$$\frac{2}{\pi}\int_0^\infty ve^{-av^2}\sin(vx)dv = \frac{x}{2a^{3/2}\sqrt{\pi}}e^{-\frac{x^2}{4a}} \tag{4.9}$$

$$\frac{2}{\pi}\int_0^\infty e^{-av^2}\cos(vx)dv = \frac{1}{\sqrt{\pi a}}e^{-\frac{x^2}{4a}} \tag{4.10}$$

Applying the Fourier sine transform to Equations 4.1, 4.2, 4.3, and 4.4 gives

$$\frac{d\bar{y}(v,t)}{dt} = -(v^2\varepsilon(t) - r(t))\bar{y}(v,t) + v\varepsilon(t)h(t) + \bar{s}(v,t) \tag{4.11}$$

subject to the initial condition

$$\bar{y}(\nu,0) = \bar{g}(\nu) \tag{4.12}$$

where the overbar denotes sine transforms.

Equations 4.11 and 4.12 are solved using standard techniques, suitable for solving first order inhomogeneous ordinary differential equations (see e.g. Riley *et al.*, 1998). The solution to Equations 4.11 and 4.12 may be written as

$$\bar{y}(\nu,t) = \bar{g}(\nu)e^{-\int_0^t(\nu^2\varepsilon(u)-r(u))du} + \int_0^t e^{-\int_w^t(\nu^2\varepsilon(u)-r(u))du}(\nu\varepsilon(w)h(w)+\bar{s}(\nu,w))\,dw \tag{4.13}$$

where w is a dummy variable of integration running from time 0 to arbitrary time t. The general solution for $y(x,t)$ is obtained by taking the inverse Fourier sine transform of Equation 4.13. Here, this is written as

$$y(x,t) = F_s^{-1}\left[\bar{y}(\nu,t)\right] \equiv I_1 + I_2 + I_3 \tag{4.14}$$

where

$$I_1 = \frac{2}{\pi}\int_0^\infty \bar{g}(\nu)e^{-\int_0^t(\nu^2\varepsilon(u)-r(u))du}\sin(\nu x)d\nu \tag{4.15}$$

$$I_2 = -\frac{2}{\pi}\int_0^\infty\left(\int_0^t e^{-\int_w^t(\nu^2\varepsilon(u)-r(u))du}\nu\varepsilon(w)h(w)\,dw\right)\sin(\nu x)d\nu \tag{4.16}$$

and

$$I_3 = \frac{2}{\pi}\int_0^\infty\left(\int_0^t e^{-\int_w^t(\nu^2\varepsilon(u)-r(u))du}\bar{s}(\nu,w)\,dw\right)\sin(\nu x)d\nu \tag{4.17}$$

The inverse sine transform in Equations 4.15 and 4.16 can be performed analytically, which reduces the nesting of integrals in the solution. First, it is noted that the exponential part of the integral I_1 may be written in the form of a Fourier cosine transform

as in Equation 4.18. This is done by setting $a = \int_0^t \varepsilon(u)du$ in Equation 4.15 and using Equation 4.10.

$$e^{-\int_0^t v^2 \varepsilon(u)du} = F_c\left(\left\{\pi \int_0^t \varepsilon(u)du\right\}^{-1/2} e^{-\frac{x^2}{4\int_0^t \varepsilon(u)du}}\right) \tag{4.18}$$

Then, making use of Equation 4.8, Equation 4.19 may be obtained from Equation 4.15

$$I_1 = \frac{1}{2}\left\{\pi \int_0^t \varepsilon(u)du\right\}^{-1/2} e^{\int_0^t r(u)du} \int_0^\infty g(\xi)\left\{e^{-\frac{(x+\xi)^2}{4\int_0^t \varepsilon(u)du}} + e^{-\frac{(x-\xi)^2}{4\int_0^t \varepsilon(u)du}}\right\}d\xi \tag{4.19}$$

where ξ is a dummy variable. For Equation 4.16, Fubini's Theorem (see e.g. Haaser and Sullivan, 1971) may be employed to interchange the order of integration and get

$$I_2 = \frac{2}{\pi}\int_0^t e^{\int_w^t r(u)du} \varepsilon(w)h(w)\left(\int_0^\infty v e^{-\int_w^t v^2 \varepsilon(u)du} \sin(vx)dv\right)dw \tag{4.20}$$

setting now $a = \int_w^t \varepsilon(u)du$ in Equation 4.20 and using Equation 4.9, the former will take the form of Equation 4.21.

$$I_2 = \frac{x}{2\sqrt{\pi}}\int_0^t \left(\int_w^t \varepsilon(u)du\right)^{-3/2} e^{-\left(\frac{x^2}{4\int_w^t \varepsilon(u)du} - \int_w^t r(u)du\right)} \varepsilon(w)h(w)dw \tag{4.21}$$

In the above, the integral I_1 accounts for the initial shoreline configuration, the integral I_2 for the impact of the time varying wave conditions at $x = 0$ and the integral I_3 for the influence of the independent source term. The shoreline dependent source function, r,

appears in all terms. Although Equations 4.13 to 4.17 have similar forms to the ones derived by Reeve (2006), there are important differences. Firstly, the new solution is in terms of an inverse sine transform instead of cosine transform and secondly the second integral has an explicit dependence on the transform variable v. Despite the different boundary conditions and the different transform solution method, the term associated with the contribution of the initial shoreline shape is exactly the same in the case of a groyne or a fixed point (i.e. same as in Reeve (2006)). In contrast, I_2 now has a higher order term in the time integral of the diffusion coefficient and has an explicit dependence on the position coordinate, x.

The general solution for estimating shoreline change is given by the sum of Equations 4.17, 4.19, and 4.21. If $\varepsilon(t)$, $r(t)$, $s(x,t)$, $h(t)$ and $g(x)$ have simple functional forms then the integrals may be amenable to further analysis. Otherwise, their numerical evaluation is required.

The seeming complexity of the formal solutions is due to its generality. However, it also provides immediate insight to the contribution of different parts of the problem to the overall evolution of the shoreline. The first term arises from the departure of the initial shoreline shape from a straight line (which is taken as the line $y = 0$ without loss of generality). If the shoreline is initially straight then $g(x) = 0$ and the first term is zero. Similarly, the last term, I_3, is only non-zero if the source term is not zero. Finally, the second term, I_2, involves the diffusion coefficient and the boundary condition, $h(t)$.

4.2.2 Solution for shoreline adjustment within a groyne compartment

The case of shoreline change within a groyne or headland compartment is now solved. The boundary conditions are formulated at the locations of the groynes, at $x = 0$ and $x = a$ respectively, and are expressed by

$$\frac{\partial y(0,t)}{\partial x} = h(t) \qquad t > 0 \tag{4.22}$$

$$\frac{\partial y(a,t)}{\partial x} = f(t) \qquad t > 0 \tag{4.23}$$

The initial condition is given by Equation 4.2. To solve Equation 4.1 subject to the initial and boundary conditions a finite Fourier cosine transform is devised. Some basic definitions of the finite Fourier cosine transform follow (see e.g. Sneddon, 1972). Now, the finite Fourier cosine transform of a function, $f(x)$, is denoted by $\bar{f}(v)$, and the operation of taking a finite Fourier cosine transform is denoted by $F_c[\,]$. Thus,

$$F_c[f(x)] = \bar{f}(v) = \int_0^a f(x)\cos(\frac{v\pi x}{a})dx \tag{4.23}$$

The inverse transform is defined by

$$F_c^{-1}[\bar{f}(v)] = f(x) = \frac{1}{a}\bar{f}(0) + \frac{2}{a}\sum_{v=1}^{\infty}\bar{f}(v)\cos(\frac{v\pi x}{a}) \tag{4.24}$$

The finite Fourier cosine transform of the second derivative is given by

$$F_s\left[\frac{\partial^2 f(x)}{\partial x^2}\right] = (-1)^v\left(\frac{\partial y}{\partial x}\right)_{x=a} - \left(\frac{\partial y}{\partial x}\right)_{x=0} - \left(\frac{v\pi}{a}\right)^2 \bar{f}(v) \tag{4.25}$$

Applying the finite Fourier cosine transform to Equations 4.1, 4.2, 4.22, and 4.23 gives

$$\frac{d\bar{y}(v,t)}{dt} = -\left(\frac{\pi^2 v^2}{a^2}\,\varepsilon(t) - r(t)\right)\bar{y}(v,t) + \varepsilon(t)\big((-1)f(t) - h(t)\big) + \bar{s}(v,t) \tag{4.26}$$

subject to the initial condition

$$\bar{y}(v,0) = \bar{g}(v) \tag{4.27}$$

Equations 4.26 and 4.27 are solved using the "variation of parameters" method, giving

$$\bar{y}(v,t) = \bar{g}(v)e^{-\int_0^t (\frac{\pi^2 v^2}{a^2}\varepsilon(u)-r(u))du} + \int_0^t e^{-\int_w^t (\frac{\pi^2 v^2}{a^2}\varepsilon(u)-r(u))du} \left(\varepsilon(w)\left((-1)^v f(w) - h(w)\right) + \bar{s}(v,w)\right)dw \tag{4.28}$$

The general solution for *y(x,t)* is obtained by taking the inverse finite Fourier cosine transform of Equation 4.28. Here, this is written as

$$y(x,t) = F_c^{-1}\left[\bar{y}(v,t)\right] \equiv I_1 + I_2 + I_3 + I_4 \tag{4.29}$$

where

$$I_1 = \frac{1}{a}\bar{g}(0)e^{\int_0^t r(u)du} + \int_0^t e^{\int_w^t r(u))du} \varepsilon(w)\left[\left(f(w) - h(w)\right) + \bar{s}(0,w)\right]dw \tag{4.30}$$

$$\bar{g}(0) = \int_0^a g(x)dx \qquad \bar{s}(0,w) = \int_0^a s(x,w)dx$$

$$I_2 = \frac{2}{a}\sum_{v=1}^{\infty} \cos\left(\frac{v\pi x}{a}\right)\bar{g}(v)e^{-\int_0^t \left(\frac{\pi^2 v^2}{a^2}\varepsilon(u)-r(u)\right)du} \tag{4.31}$$

$$I_3 = -\frac{2}{a}\sum_{v=1}^{\infty} \cos\left(\frac{v\pi x}{a}\right)\int_0^t e^{-\int_w^t \left(\frac{\pi^2 v^2}{a^2}\varepsilon(u)-r(u)\right)du} \left[\varepsilon(w)\left((-1)^v f(w) - h(w)\right)\right]dw \tag{4.32}$$

$$I_4 = \frac{2}{a}\sum_{v=1}^{\infty} \cos\left(\frac{v\pi x}{a}\right)\int_0^t e^{-\int_w^t \left(\frac{\pi^2 v^2}{a^2}\varepsilon(u)-r(u)\right)du} \bar{s}(v,w)dw \tag{4.33}$$

The structure of the solution is slightly more complicated than in the earlier case. The initial shoreline shape appears in the term I_2, the boundary conditions at each groyne in term I_3, and the source function in term I_4. However, all components of the problem also occur together in the extra term I_1, which contains integrals only and no summations.

4.2.3 Numerical evaluation

In deriving the solutions, the initial conditions, wave sequence and source functions have all been retained as arbitrary functions. In general, these will not have analytical forms but will be specified numerically at discrete points. To evaluate the solutions it is necessary to perform the integrals and summations for the specified wave conditions. If these are specified as an analytical function of time then some further theoretical treatment may be possible.

Here, the case where the wave conditions are defined as a discrete time-series of values is considered. In this case, numerical integration methods are required to evaluate the solutions. For this reason, these solutions are referred to as 'semi-analytical'. The integrals are of relatively standard form for 'well-behaved' functions (i.e. functions which are bounded, continuous, and have continuous derivatives, except at a finite number of points), for which efficient and robust integration routines are readily available. The integrals with respect to u (Equations 4.17, 4.19, and 4.21) yield a number for a given value of t and closed-form integration formulae, i.e. integration formulae that use the value of the function at the endpoints of the integration, may be used for their evaluation. The numerical evaluation of the integral I_2, Equation 4.21, is problematic for when $w = t$. This may be handled by semi-open integration formulae.

Here, the Newton-Cotes formulae for open and semi-open integration (Press *et al.*, 1992) are used. The closed and semi-open formulae used in this study are the "alternative extended Simpson's rule" and "alternative extended extrapolative Simpson's rule" respectively. For any function $f(t)$ defined at discrete points $t_1, t_2, \ldots, t_n$, the bespoke closed and semi-open formulae are given respectively by

$$\int_{t_1}^{t_m} f(t)dx = \Delta t\left(\frac{17}{48}f_1 + \frac{59}{48}f_2 + \frac{43}{48}f_3 + \frac{49}{48}f_4 + (f_5 + \ldots + f_{n-4}) + \frac{49}{48}f_{n-3} + \frac{43}{48}f_{n-2} + \frac{59}{48}f_{n-1} + \frac{17}{48}f_n\right) + O\left(\frac{1}{n^4}\right) \quad (4.35)$$

$$\int_{t_1}^{t_m} f(t)dt = \Delta t\left(\frac{17}{48}f_1 + \frac{59}{48}f_2 + \frac{43}{48}f_3 + \frac{49}{48}f_4 + (f_5 + \ldots + f_{n-5}) + \frac{49}{48}f_{n-4} + \frac{63}{48}f_{n-3} - \frac{5}{48}f_{n-2} + \frac{109}{48}f_{n-1}\right) + O\left(\frac{1}{n^4}\right) \quad (4.36)$$

where $O(1/n^4)$ is an error term which signifies that the true answer differs from the estimate by an amount which is inversely proportional to the fourth power of the number of integration steps. The numerical evaluation of Equation 4.14 with all three integrals contributing to the result, for 6000 points alongshore, and for an output time of t = 400 hours with wave conditions specified every 1 hour, was extremely fast (a second or so) on a Pentium IV PC.

The same integration formulae were used for the numerical evaluation of the integrals appearing in Equation 4.29. When evaluating the summations in Equations 4.31, 4.32, and 4.33 a limit must be imposed on the number of terms used for the solution. The solutions exhibit "Gibbs Phenomenon". This behaviour is encountered in many practical applications where Fourier series are used to represent a function on a finite domain (Jerri, 1998). To reduce or eliminate Gibbs Phenomenon, filters have been developed (see e.g. Gottlieb and Shu, 1997). Here, a simple exponential filter is used, which was found to be satisfactory in clearing the results from unwanted oscillations. The numerical evaluation of Equation 4.32 (i.e. of the integral I_3, the only non-zero integral for the special case examined in the section "Applications and Results") was extremely fast ($\leq$2 sec) to evaluate the solution at t = 400 hours using a partial sum of 50 Fourier terms. The filtered series converged considerably faster than this as only about 30 Fourier terms were required to achieve convergence of the solutions.

4.3 Applications and Results

4.3.1 Input wave conditions

In the following, a time-series of hindcast wave conditions is used. It is based on the wave data described in Reeve (2006), but modified so that the wave angles represent realistic values at breaking. This time-series is a portion of about 17 days of a 27-year time-series, described in Reeve and Spivack (2004). The original time-series consisted of hourly hindcast waves for a location on the southeast of the UK over a period from 1971 to 1998. Deep water waves were hindcast using surface winds obtained from a global meteorological model. The waves were then transformed inshore to a fixed water depth, using a spectral refraction model. The transformations were performed using a constant water depth equivalent to the Mean High Water Spring tide. The resulting data set was expressed as time-series of the significant wave height, zero up-crossing wave period, and mean wave direction at hourly intervals. The data portion, used in this chapter, covers a time span of 400 hours, starting midnight January 1, 1972. Originally, this portion, as used in Reeve (2006), included waves with mean direction up to 85^0 relative to the shore normal, assuming a shore normal of 210^0. Here, the assumed value of the shore normal is kept the same but wave angles are reduced to 60% of their initial value, so that they do not exceed about 35^0. Thus, wave angle values resemble reasonable values at breaking as required by Equation 2.23. Time-series of ε are calculated using the wave time-series; assuming a water depth of 6m and a depth of closure of 10m (as in Reeve (2006)). In what follows, ε given by Equation 2.20 is denoted by ε_s, where the subscript "s" refers to the "small" angle approximation, whilst ε given by Equation 2.23 is denoted by ε_w, where "w" refers to the "wide" angle formulation.

Figure 4.1a shows the time-series of ε_s and ε_w, corresponding to the wave condition - sequence of significant wave height and of mean wave direction relative to the shoreline normal - shown in Figure 4.1b. In Figure 4.1b, a sequence of three storms is apparent, whilst waves arrive mostly from the west (positive angles) relative to the shoreline normal. Figure 4.1a illustrates the effect that the small wave angle approximation has on the diffusion coefficient. The peak value during the third storm is considerably larger than when the wide angle version of the coefficient is used.

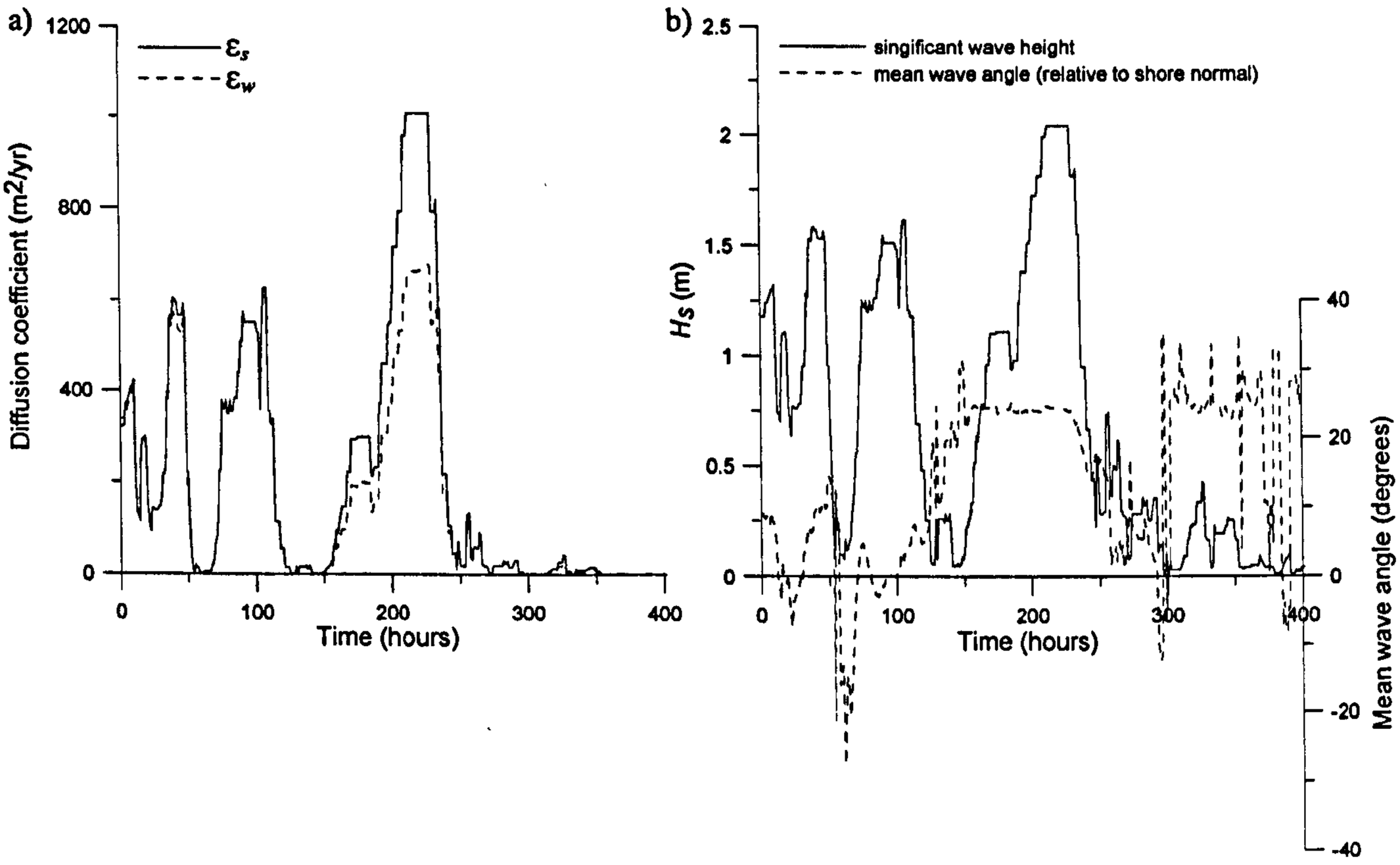

Figure 4.1 a) Time-series of diffusion coefficients, computed from the sequence of wave conditions shown in: b) Time-series of hourly nearshore wave heights and wave angles, from midnight January 1, 1972.

This time-series is used to illustrate the application of the new semi-analytical solutions for two main cases: (1) rectangular fill, and (2) groyne/headland compartment. In both cases, solutions are computed for both small and wide angle formulations for ε. These two cases of shoreline change are example cases and are not the only ones to which the general solutions maybe applied. For example, Zacharioudaki and Reeve (2007) applied

4.3 Applications and Results

4.3.1 Input wave conditions

In the following, a time-series of hindcast wave conditions is used. It is based on the wave data described in Reeve (2006), but modified so that the wave angles represent realistic values at breaking. This time-series is a portion of about 17 days of a 27-year time-series, described in Reeve and Spivack (2004). The original time-series consisted of hourly hindcast waves for a location on the southeast of the UK over a period from 1971 to 1998. Deep water waves were hindcast using surface winds obtained from a global meteorological model. The waves were then transformed inshore to a fixed water depth, using a spectral refraction model. The transformations were performed using a constant water depth equivalent to the Mean High Water Spring tide. The resulting data set was expressed as time-series of the significant wave height, zero up-crossing wave period, and mean wave direction at hourly intervals. The data portion, used in this chapter, covers a time span of 400 hours, starting midnight January 1, 1972. Originally, this portion, as used in Reeve (2006), included waves with mean direction up to 85^0 relative to the shore normal, assuming a shore normal of 210^0. Here, the assumed value of the shore normal is kept the same but wave angles are reduced to 60% of their initial value, so that they do not exceed about 35^0. Thus, wave angle values resemble reasonable values at breaking as required by Equation 2.23. Time-series of ε are calculated using the wave time-series; assuming a water depth of 6m and a depth of closure of 10m (as in Reeve (2006)). In what follows, ε given by Equation 2.20 is denoted by ε_s, where the subscript "*s*" refers to the "small" angle approximation, whilst ε given by Equation 2.23 is denoted by ε_w, where "*w*" refers to the "wide" angle formulation.

Figure 4.1a shows the time-series of ε_s and ε_w, corresponding to the wave condition - sequence of significant wave height and of mean wave direction relative to the shoreline normal - shown in Figure 4.1b. In Figure 4.1b, a sequence of three storms is apparent, whilst waves arrive mostly from the west (positive angles) relative to the shoreline normal. Figure 4.1a illustrates the effect that the small wave angle approximation has on the diffusion coefficient. The peak value during the third storm is considerably larger than when the wide angle version of the coefficient is used.

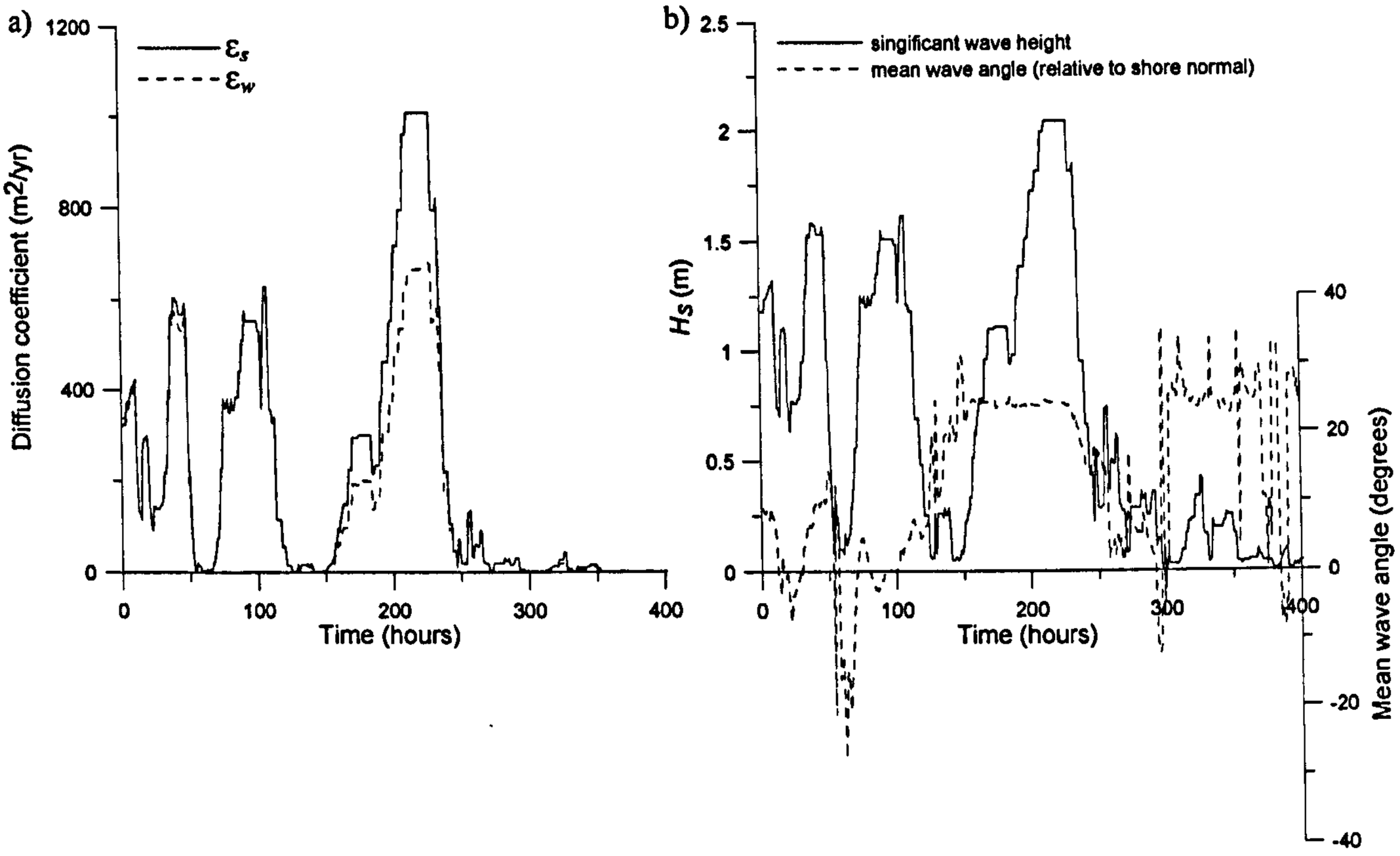

Figure 4.1 a) Time-series of diffusion coefficients, computed from the sequence of wave conditions shown in: b) Time-series of hourly nearshore wave heights and wave angles, from midnight January 1, 1972.

This time-series is used to illustrate the application of the new semi-analytical solutions for two main cases: (1) rectangular fill, and (2) groyne/headland compartment. In both cases, solutions are computed for both small and wide angle formulations for ε. These two cases of shoreline change are example cases and are not the only ones to which the general solutions maybe applied. For example, Zacharioudaki and Reeve (2007) applied

Equation 4.14 to the case of sand supplied to the corner of a fill to maintain its shape or beach evolution downdrift of a groyne with persistent bypassing. Simple cases of sea-level rise or of other sources/sinks of sediment along the shoreline may also be modelled.

4.3.2 Rectangular beach fill

A rectangular beach fill of extent between $x = a$ and $x = b$ with offshore extent y_0, is placed on a straight shoreline, as depicted in Figure 4.2. There are no sources or sinks of sediment, $s(x,t) = 0$ and $r(t) = 0$. Initial and boundary conditions are formulated as

$$y(x,0) = g(x) = \begin{cases} y_0 & a \le x \le b \\ 0 & x < a \quad x > b \end{cases} \qquad x > 0 \tag{4.37}$$

$$y(0,t) = h(t) = 0 \qquad t > 0 \tag{4.38}$$

Thus, in Equation 4.14, I_2 and I_3 equal zero and the solution considerably simplifies to yield

$$y(x,t) = I_1 = \frac{y_0}{2}\left[erf\left(\frac{a+x}{2\sqrt{\int_0^t \varepsilon(u)du}}\right) - erf\left(\frac{a-x}{2\sqrt{\int_0^t \varepsilon(u)du}}\right) - erf\left(\frac{b+x}{2\sqrt{\int_0^t \varepsilon(u)du}}\right) + erf\left(\frac{b-x}{2\sqrt{\int_0^t \varepsilon(u)du}}\right)\right] \tag{4.39}$$

If ε = constant then the integrals can be performed immediately and the solution evaluated analytically.

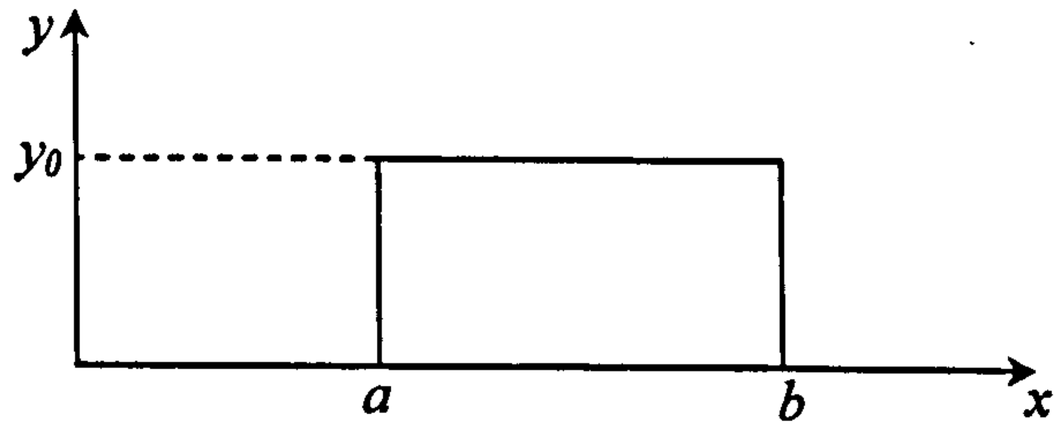

Figure 4.2 Illustrative definitions for the rectangular beach fill.

Figure 4.3 shows beach positions, computed with ε_s, at different times after the start of the wave sequence. Parameter values are a = 2300m, b = 3700m, and y_0 = 30m. The fill

is located away from the boundary condition at $x = 0$ so that its evolution is not affected by it within the time span used. The spatial domain is defined by $0 < x \leq 6000$m, with a discretisation of 1m resolution. In Figure 4.3a, the first three output times, t_1, t_2, and t_3 correspond to the ends of the three successive storms respectively whilst the last output time, t_4, is near the end of the time-series. Figure 4.3b depicts the evolution of just the tip of the beach nourishment for ε_s and ε_w and for every event in the wave sequence (i.e. output every hour). Progressive erosion of the fill in response to the higher waves in the time-series is shown. Points of interest include:

- Erosion of the fill during the third and most severe storm, i.e. within about 120 hours, is much more pronounced compared to erosion occurring within larger time-spans of lower waves, i.e. within 144 hours between the end of the third storm and the end of

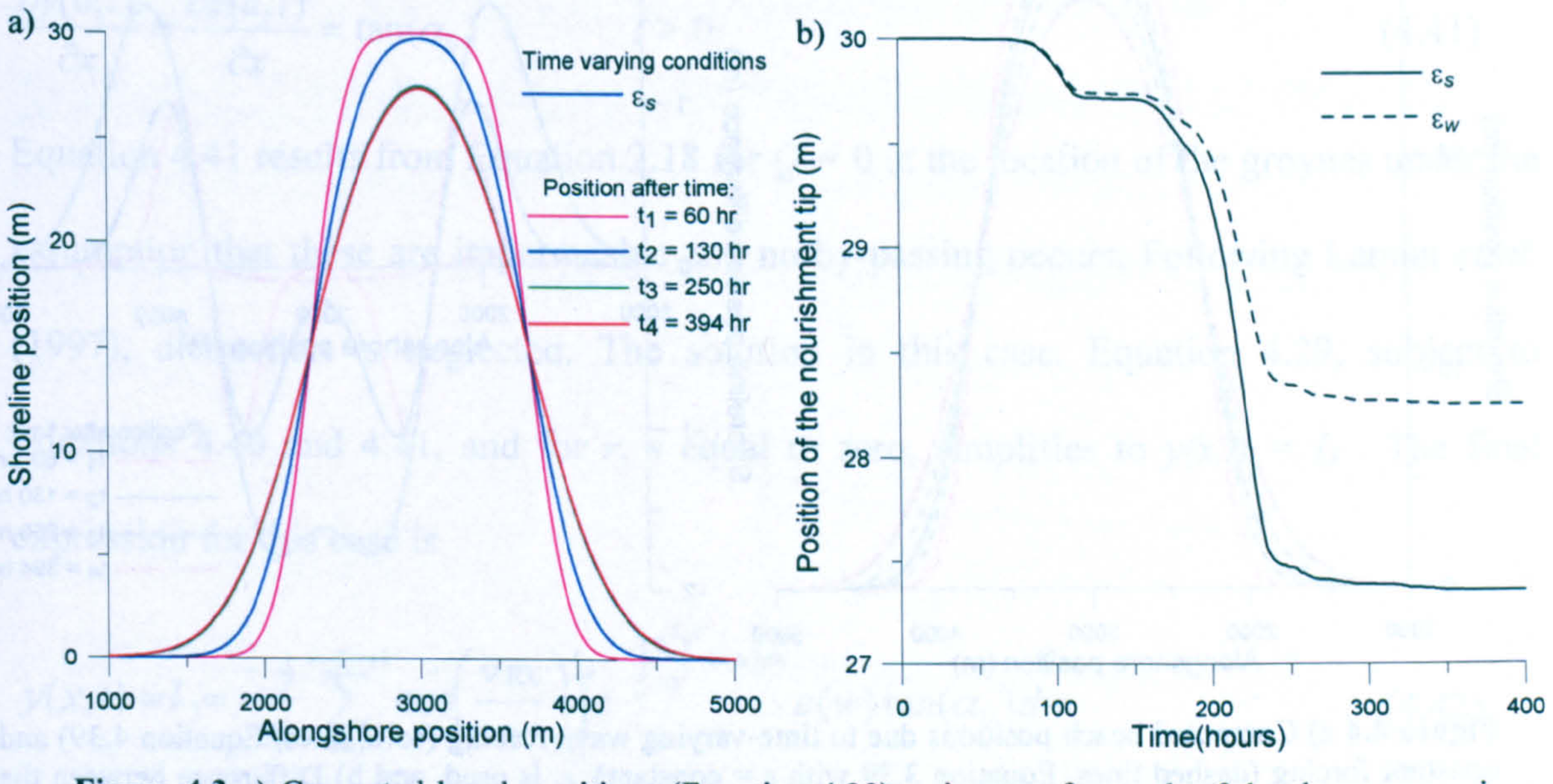

Figure 4.3 a) Computed beach positions (Equation 4.39), using ε_s, after each of the three successive storms and near the end of the time-series, and b) Positions of the beach nourishment tip computed using ε_s and ε_w respectively

the time-series. If an average erosion rate is assigned to the tip of the beach fill (x = 3000m) for different time-spans corresponding to different wave intensities, about

1.5% of daily beach loss takes place during the third storm (t_2 to t_3) whilst only about 0.05% of daily erosion occurs between the end of the third storm, t_3, and the end of the time-series, t_4, (ε_s is used for the calculations).

- The occurrence of higher wave angles during the third storm constrains the evolution of the fill when ε_w is used. This is evident in Figure 4.3b where the "slower" erosion of the tip with the use of ε_w is prominent during the third storm (which is manifested by the divergence of the ε_s and ε_w lines after the second output time, t_2). In terms of daily averages, during this storm the fill tip erodes 23cm less per day when ε_w is used.

Figure 4.4 compares results from the semi-analytical solution, Equation 4.39, and the purely analytical form for constant forcing. The time-series and the mean value of the ε_s over the period of 400 hours (ε_s = 210.28 m^2/hr) are used as input in Equation 4.39 and its

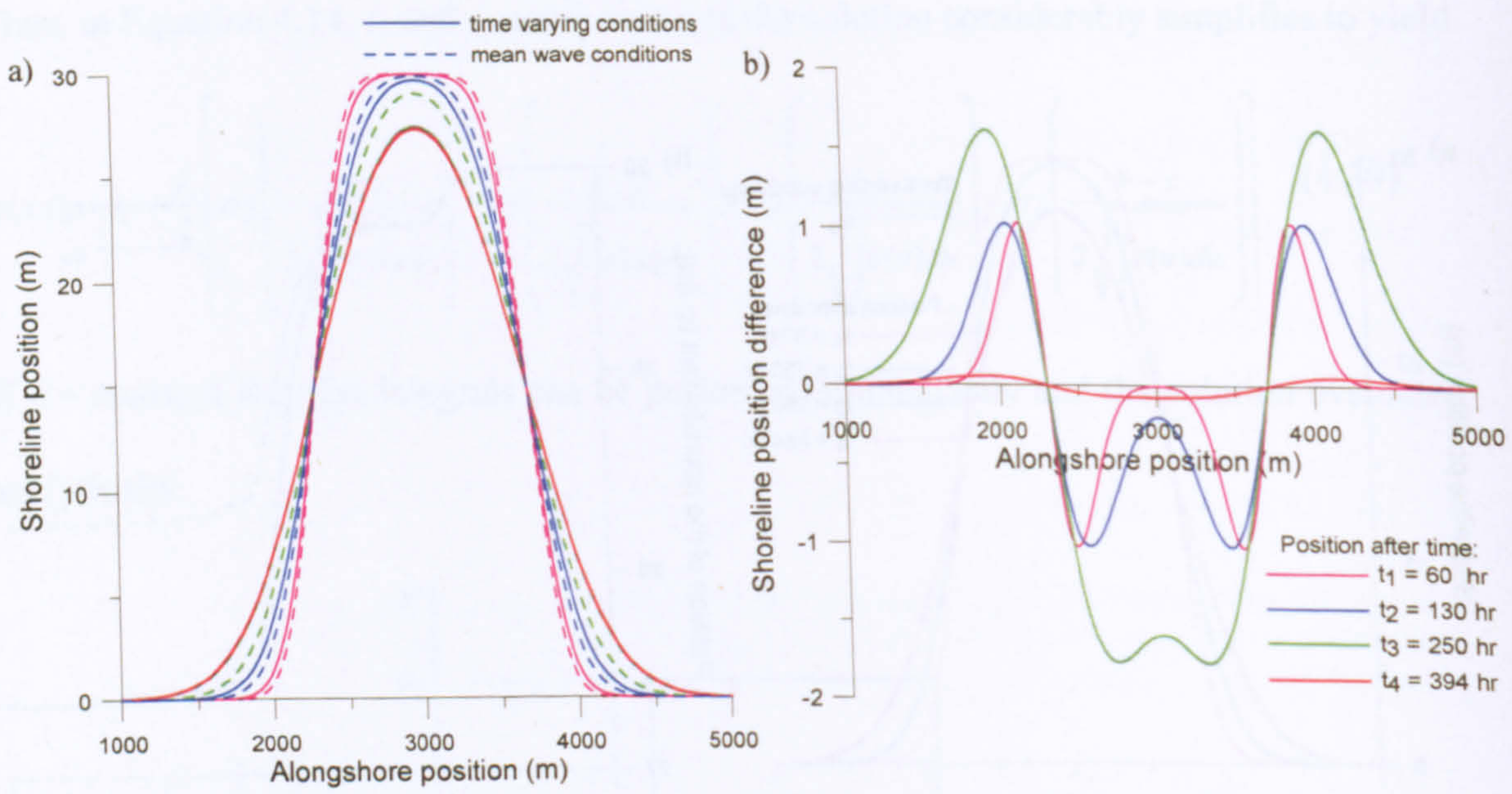

Figure 4.4 a) Computed beach positions due to time-varying wave forcing (solid lines, Equation 4.39) and constant forcing (dashed lines, Equation 3.39 with ε = constant), ε_s is used, and b) Difference between the shoreline positions computed using time-varying forcing and those computed using constant wave forcing, (legend relates to both parts of the Figure).

analytical form respectively. The plots show the two solutions for the five different instances t_1, t_2, t_3, and t_4. The two solutions are virtually indistinguishable at t_4. Figure 4.4

reveals that in what is a relatively small time span, there are significant differences between the semi-analytical and analytical solutions, particularly when the time-series deviates persistently from the average conditions, such as after the end of the second storm. As expected, faster erosion of the fill during storms and minor evolution during calm periods, illustrated when time variation is considered, cannot be depicted through the purely analytical solution which simply advances the shoreline in proportion to the time elapsed.

4.3.3 Groyne/headland compartment

The case of an initially straight shoreline within a groyne compartment of length *a*, where no sources/sinks of sediment exist, is defined by initial and boundary conditions as follows (see Equations 4.2, 4.22, and 4.23)

$$y(x,0) = g(x) = 0 \qquad x > 0 \tag{4.40}$$

$$\frac{\partial y(0,t)}{\partial x} = \frac{\partial y(a,t)}{\partial x} = \tan(\alpha_0) \qquad t > 0 \tag{4.41}$$

Equation 4.41 results from Equation 2.18 for $Q = 0$ at the location of the groynes under the assumption that these are impermeable and no by-passing occurs. Following Larson *et al.* (1997), diffraction is neglected. The solution in this case, Equation 4.29, subject to Equations 4.40 and 4.41, and for *r*, *s* equal to zero, simplifies to $y(x,t) = I_3$. The final expression for this case is

$$y(x,t) = I_3 = \frac{-4}{a} \sum_{v=1}^{v=2n+1} \cos\left(\frac{v\pi x}{a}\right) \int_0^t e^{-\int_w^t \frac{\pi^2 v^2}{a^2}\varepsilon(u)du} \varepsilon(w)\tan(\alpha_0)dw \tag{4.42}$$

Numerical solutions are examined for different partial sums and at four output times (same as above), corresponding to the end of each of the three consecutive storms shown in Figure 4.1, and to almost the end of the time-series respectively. The spacing between the groynes is taken to be 500m and a discretisation of 1m is adopted.

The Fourier series of Equation 4.42 was filtered using a 4th order exponential filter of the form (see e.g. Gottlieb and Shu, 1997)

$$filter = e^{-0.0000005v^4} \tag{4.43}$$

To choose a suitable form of the exponential filter, mean shoreline positions were calculated from the oscillatory solutions after a fixed oscillation pattern has been established. Then, the exponential form was determined on two criteria: (1) close resemblance of the computed filtered shoreline positions with the mean unfiltered ones, especially at alongshore locations where oscillation was minor (away from the boundaries), and (2) relatively fast convergence. The agreement between the filtered solution and the unfiltered one, averaged over one Gibbs cycle, was found to be very good with differences of up to 0.02% confined to within 10m from the boundary. Convergence was obtained within 26 to 32 Fourier terms, depending on the output time.

Figure 4.5 shows the simulated shoreline evolution for ε_s and ε_w, as it results after filtering. In this case, in contrast to the case of beach nourishment discussed before, the

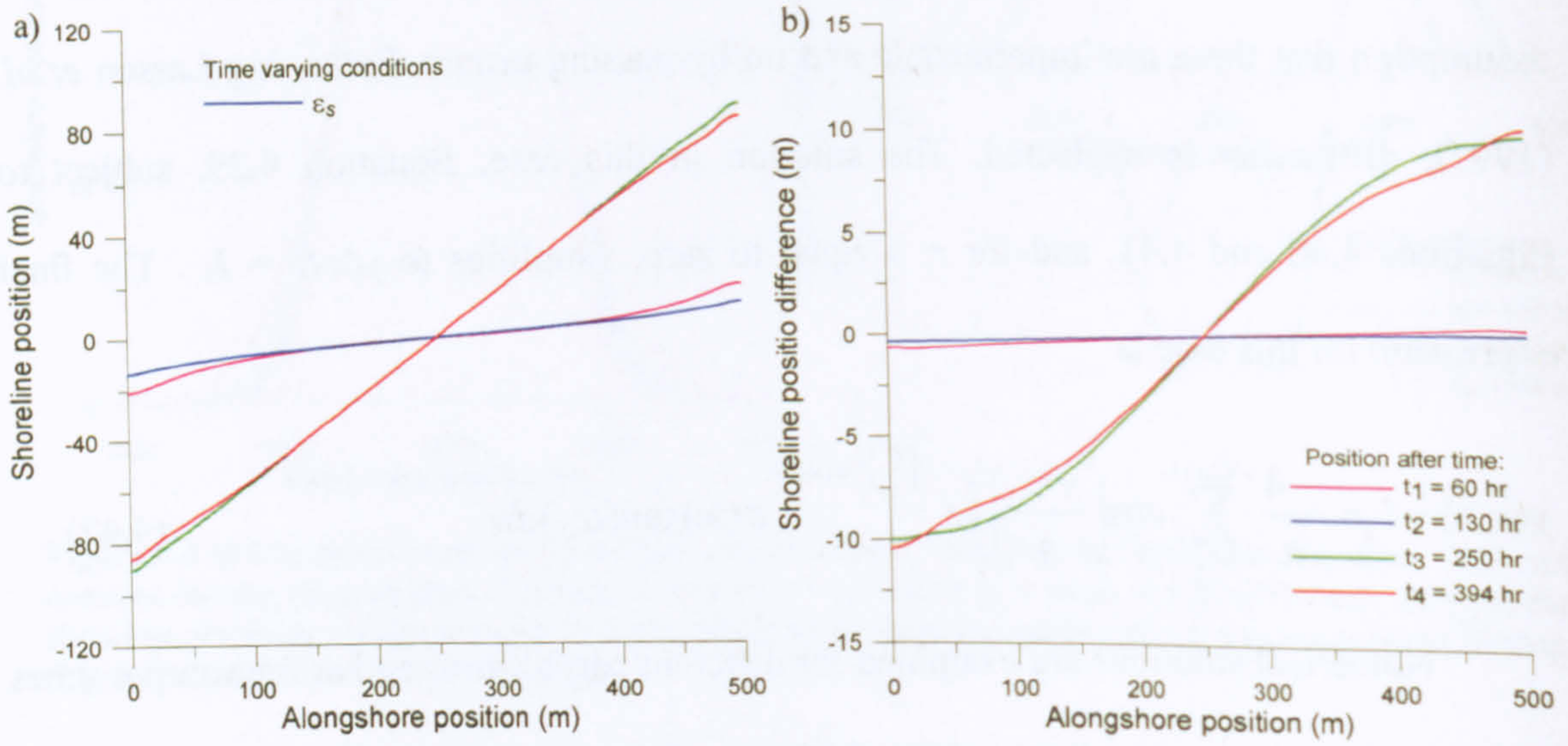

Figure 4.5 a) Computed shoreline evolution, using ε_s (solid lines) and ε_w (dashed lines), within two groynes which are assumed to be impermeable and of infinite length, (legend as in Figure 4.5b) and b) Difference between the shoreline positions computed using ε_s and those computed using ε_w.

importance of the variation of wave angle at the boundaries (Equation 4.41) is evident (Figure 4.5). Waves approaching from the west (from the left of the left hand groyne) are the predominant waves and cause shoreline retreat at the lee side of the left hand groyne. During the third and most severe storm (t_2 to t_3), when high waves from the west approach with highly oblique angles, shoreline recession is significantly enhanced. In contrast, during periods characterized by the occurrence of several waves from the east, such as during the second storm (t_1 to t_2), the shoreline slightly recovers.

The convergence properties of the solution are likely to be sensitive to variation of the different parameters involved, such as the spacing between the groynes and the time variation of the diffusion coefficient. However, the influence is expected to be confined very near the boundaries with minor impact away from them. Moreover, it should be born in mind that diffraction can have a significant effect near the groynes, so that its exclusion from the solutions presented here will anyway affect its accuracy near the boundaries. In this regard, it may be noted that even the more sophisticated numerical models encounter difficulties in capturing shoreline change within a groyne compartment near the groynes because of the curvature of the shoreline in this region (Hanson *et al.*, 2003; Weesakul *et al.*, 2004).

4.4 Discussion

In this chapter, new semi-analytical solutions to the 'one-line' model have been derived which, in contrast to earlier work, account for time varying wave forcing bringing analytical work closer to reality. The new solutions include wave conditions as explicit but arbitrary functions of time. Moreover, they allow for an initial shoreline shape that is an arbitrary function of alongshore distance, which in practice would be defined by a survey. The solutions also allow the effect of time-varying source terms to be included. Solutions

have been obtained for two specific but common cases: (1) a managed beach where there is a location with known evolution, and (2) shoreline evolution within a groyne compartment. In the former case, solutions were obtained using Fourier sine transform and are given in terms of the sum of three integrals. In the latter, a finite Fourier cosine transform was defined and used to obtain a solution that consists of the sum of three infinite Fourier series and one integral.

The new semi-analytical solutions are of a more complex form than the purely analytical expressions derived on the basis of the assumption of constant wave conditions. Nevertheless, their numerical evaluation is extremely fast. The Fourier series solutions (groyne compartment case) were found to converge rapidly. Gibbs phenomenon at points close to the groynes was readily and satisfactorily controlled using a standard filter. For the cases examined in this chapter it was found that solutions of practical use were obtained with about 30 terms. The convergence properties of the series solution are a function of the geometry of the problem being considered as well as the characteristics of the sequence of wave conditions driving the beach evolution. Results from a range of tests performed suggest that rapid convergence similar to that reported for the example described here, can be expected because of the Gaussian decay term multiplying the Fourier coefficients.

The extension of the theory to allow for a sequence of wave conditions means that the standard solutions for perpetual wave conditions are modified through a time-varying diffusion coefficient and through time varying boundary conditions. Here, solutions have been examined for two different forms of the diffusion coefficient. The first is valid for small wave angles and is dependent only on wave height, while the second is valid for large wave angles and is dependent on both wave height and angle. The general solutions derived in this chapter have been used to investigate the effect of the small angle approximation. It

is shown that the large angle formulation can have a subtle effect on the results, typically leading to a more conservative shoreline evolution.

The new solutions are sufficiently general so as to permit the investigation of a variety of factors that might impact the shoreline, such as storminess, sea-level change rates, or adaptive management policies. Moreover, they hold the general qualities of analysis, described in Section 2.2.2.1 whilst they provide a valuable tool to extend the range of solutions against which the accuracy and convergence of time-stepping finite difference numerical models can be tested.

In the remainder of this study, the new semi-analytical solutions will be used for the validation of a 'one-line' model, solved numerically via a very efficient numerical scheme, never used before in 'one-line' numerical modelling. Both, short-term validation, using the wave time-series employed for the purposes this chapter, and long-term validation, using long wave data sets obtained from climate models, will be performed.

Chapter 5

Method of Lines - Numerical solution to the 'one-line' model

In the preceding chapter, semi-analytical solutions of the 'one-line' model that can account for the time-variation of the wave forcing were derived. Although less strict in their assumptions than previous analytical expressions, they are still of limited engineering applicability. The main reason is their inability to cope with spatially varying wave characteristics – the result of shoaling, refraction, and diffraction – and complex geometries and boundary conditions, involving a number of diverse hard and/or soft engineering interventions on the beach. Also, they involve small angle approximations. As a result, to more accurately simulate shoreline evolution in complex natural environments a numerical model is needed. This can potentially account both for time and space variation, complex geometries and boundaries, could include simple refraction and diffraction routines, or could be coupled with other advanced numerical models (e.g. 2 or 3D refraction-diffraction models). In fact, the capabilities of a numerical 'one-line' model largely depend on its stage of development. This study is concerned with the very early stages of development of a numerical 'one-line' model for shoreline evolution. In particular, it focuses on the improvement of the numerical solution scheme of the model.

To date, explicit and implicit time-stepping finite differences have been used to solve the 'one-line' model numerically. As mentioned in Chapter 2 (Section 2.2.3.3), the explicit method is very attractive because it is extremely fast and easy to program. However, it is conditionally stable. In contrast, the implicit method is considerably more difficult to program, is slower to execute, but it is unconditionally stable so that it is often preferred to the explicit schemes. Yet, numerical errors increase with time step. Here, a different numerical method, known as the Method of Lines (MOL), is proposed for a more efficient solution of the continuity of sediment equation and associated expressions.

The basic concept of MOL is the conversion of an initial value Partial Differential Equations (PDEs) problem to an initial value Ordinary Differential Equations (ODEs) problem where a set of ODEs needs to be integrated in time (e.g. Schiesser, 1991). The fact that a wide range of ODE integrators of very high quality are readily available through software libraries (e.g. Fortran or Matlab libraries) is what makes MOL a particularly powerful and versatile technique and thus particularly attractive (Wouwer and Schiesser, 2005). A highly efficient numerical solution procedure based on MOL has been proposed by Hamdi *et al.* (2005) for the solution of Boussinesq-like equations in coastal engineering, related to nearshore evolution of the wave field. However, despite being a powerful technique, the method has not found its way to other coastal engineering problems or to coastal engineering practice.

The MOL solution procedure proposed in this study for the solution of the 'one-line' model has certain advantages over the explicit and implicit finite-difference numerical solution schemes used to date. Compared to the explicit finite-difference scheme, it has the advantage of being essentially unconditionally stable. Compared to the implicit finite-difference scheme, it is significantly easier to program and may retain its accuracy irrespectively of the user-specified time-step (not to be confused with the actual integration

stepsize used in the numerical algorithm). Execution speeds remain reasonable, close to those achieved with the explicit finite difference numerical scheme.

In what follows, a description of the MOL technique is given and an introduction to the different choices associated with this technique is made. Then, the specific MOL based numerical procedure used in this study for the solution of the 'one-line' model equations is presented. Some sensitivity analysis is performed. Further, the MOL procedure is compared against an explicit finite-difference code and the chapter closes with a discussion. In the following chapter, the present numerical code is tested for accuracy and convergence against the semi-analytical solutions derived in Chapter 3 for time-varying forcing.

5.1 The Method of Lines

The numerical MOL technique is appropriate for solving almost any initial value PDE problem of a general form

$$\partial \boldsymbol{u}/\partial t = \boldsymbol{f}(\boldsymbol{u}) \qquad x_L < x < x_R \tag{5.1}$$

where $\boldsymbol{u}$ is a vector of dependent variables, t is the initial value independent variable, $\boldsymbol{x}$ represents a three-vector (e.g. x, y, z) boundary value independent variable, and $\boldsymbol{f}$ is a spatial differential operator of the general form $\boldsymbol{f}(x, t, \boldsymbol{u}, \partial \boldsymbol{u}/\partial x, \partial^2 \boldsymbol{u}/\partial x^2, ...)$. Equation 5.1 can represent one, two, or three dimensional problems at it is in vector form (bold-face variables). In addition, although Equation 5.1 has a linear form, non-linear equations where $\boldsymbol{u}$ and its spatial derivatives in $\boldsymbol{f}$ are of a higher degree may also be solved by MOL (e.g. Wouwer *et al.*, 2001).

MOL solves equations of the form of Equation 5.1 in two steps:

- Spatial derivatives are approximated using finite differences or any other algebraic approximation technique.

- The resulting system of semi-discrete ODEs in the initial value variable is integrated in time, *t*.

This system of ODEs is of the general form

$$du/dt = g(u, t) \tag{5.2}$$

with initial condition

$$u(x, 0) = h(x) \tag{5.3}$$

and problem specific boundary conditions. Figure 5.1 illustrates the apparent reason why the method is called the Method of Lines. If for example a one-dimensional function *u(x, t)* is considered, its MOL numerical solution can be imagined to evolve along lines of fixed *x*. Ultimately, the solution of *u(x, t)* at a specific time *t* is a line connecting the corresponding values of *u(x, t)* on each individual vertical line of Figure 5.1.

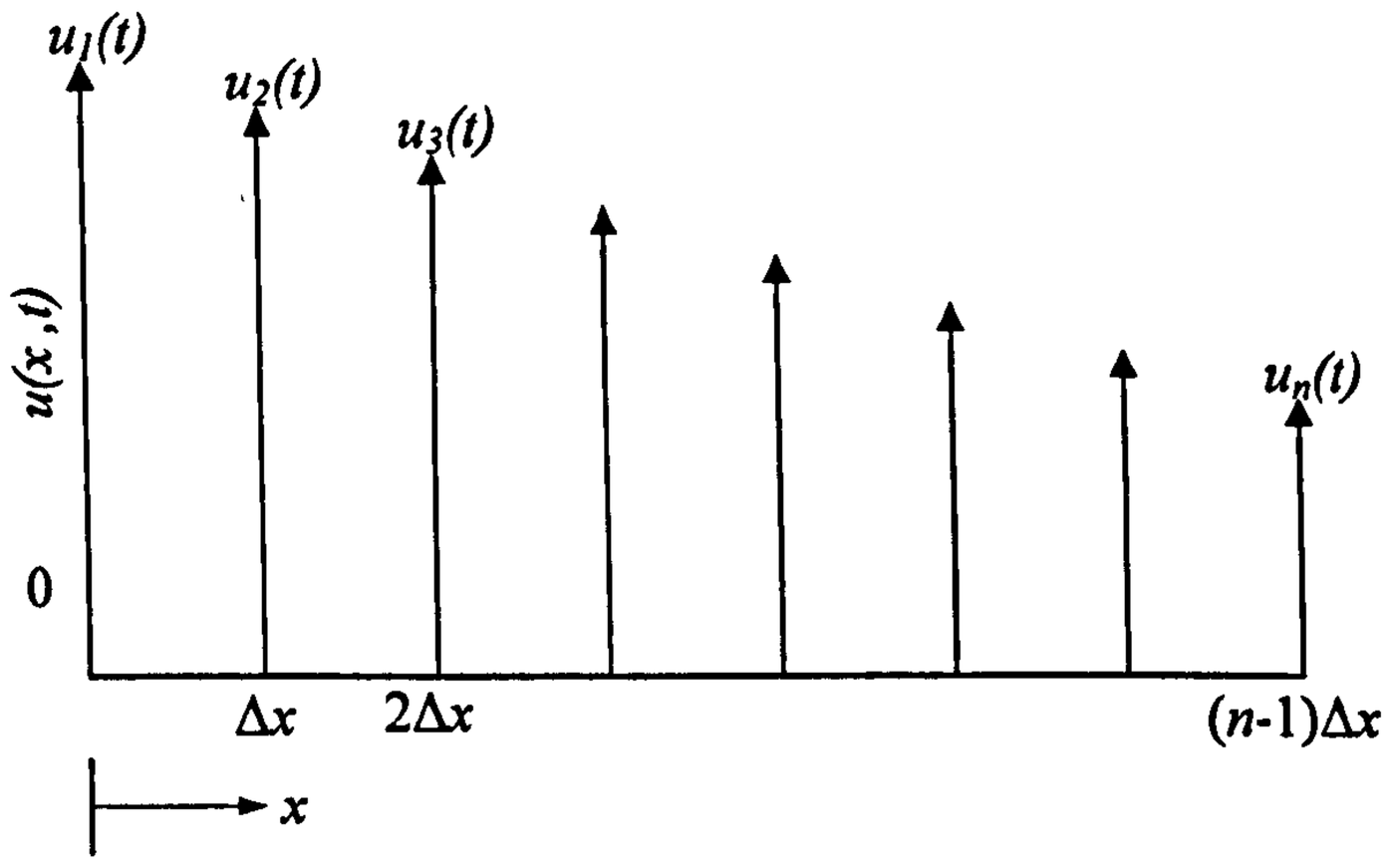

Figure 5.1 The origin of the name: 'numerical Method of Lines' (adapted from Schiesser, 1991).

An important part of the numerical solution procedures based on MOL is the choice of the discretisation technique for the spatial derivatives and the choice of the numerical ODE integrator. In fact, the method is one of the most acknowledged because of the wide variety of readily available spatial discretisation and ODEs integration routines of high quality. Moreover, since MOL coding closely resembles the problem equations, advanced

coding is possible, as switching to different 'off the shelf' routines needs minimal user effort. Thus, all the knowledge and practice relevant to initial value ODE problems may be applied to PDE problems through the MOL approach. Accordingly, the choice of spatial discretisation and time integration algorithms largely depends on the specific requirements of the problem under consideration. Thus, spatial approximations may for instance be performed with finite difference or finite element numerical schemes. Also, upwind, centered, or hybrid approximation approaches of different orders may be devised. Similarly, numerical integrators for smooth or stiff PDE problems, i.e. with solutions that do not change or do change abruptly in time respectively, may be used. These may have or not adaptive integration stepsize or order and allow for a fixed or a dynamic grid. By and large, stability and desired accuracy are the keys for choosing the spatial discretisation and ODE integration routines for any PDE problem.

A number of 'black box' algorithms based on the MOL numerical method may be found in libraries of software like Fortran or Matlab (e.g. NAG or DSS/2 library in Fortran). Alternatively, the user may choose to use numerical codes developed in text books (e.g. Press *et al.*, 1992; Schiesser, 1991) if a greater control over the numerical procedures is required. The latter approach is adopted in this study.

5.2 MOL solution of the 'one-line' model

5.2.1 System of ODEs

Here, the continuity of sediment, Equation 2.4, is solved using the MOL. Specifically, the following system of ODEs is integrated in time

$$\frac{dy_1}{dt} = \frac{1}{Dc}\left(\frac{Q_1 - Q_2}{\Delta x}\right) + \frac{1}{Dc} q_1 \qquad x_{LHB} < x < x_{RHB} \qquad t_0 < t < t_f \qquad (5.4)$$

$$\frac{dy_2}{dt} = \frac{1}{Dc}\left(\frac{Q_2 - Q_3}{\Delta x}\right) + \frac{1}{Dc} q_2$$

...

$$\frac{dy_N}{dt} = \frac{1}{Dc}\left(\frac{Q_N - Q_{N+1}}{\Delta x}\right) + \frac{1}{Dc} q_N$$

where LHB = Left Hand Boundary, RHB = Right hand boundary, t_0 and t_f are the initial and final time of integration respectively. The initial condition is given by

$$y_1(t_0) = y(1,0),\ y_2(t_0) = y(2,0),\ \ldots,\ y_N(t_0) = y(N,0) \qquad (5.5)$$

The boundary conditions are problem specific. Typically, they are given as functions of Q (Section 2.2.3.3). Apart from the LHS and RHS boundaries, internal constraints may be present. The above equations are solved on the staggered grid of Figure 2.6. The sediment transport rate, Q, is evaluated by Equation 2.18. The differential form of Equation 2.18 needed to complete the above system of ODEs is chosen to be

$$Q_i = Q_{0i} \sin\left\{2\left[a_{0i} - \arctan\left(\frac{y_i - y_{i-1}}{\Delta x}\right)\right]\right\} \qquad i = 1, 2, \ldots, N \qquad (5.6)$$

In the above equations, the first step of MOL which is the discretisation of the spatial derivatives has been performed. Simple first order upwind differences have been used as is customary in 'one-line' models to date (Section 2.2.3.3). What is left is the choice of the ODE integrator. This choice is explained below after some reasoning for retaining the first order upwind approximations of the spatial derivatives.

5.2.2 Spatial discretisation – Upwind differences

ODE time integrators can be of very high accuracy. Consequently, if the spatial approximations are of relatively low order, this will adversely affect the total accuracy of the MOL solution. Equations 5.4 and 5.6 above include simple first order upwind

approximations in the spatial domain. Thus, their accuracy is inversely proportional to Δx and the presence of numerical diffusion is quite likely (e.g. Wouwer *et al.*, 2001). A first step towards increasing the spatially dependant accuracy of the MOL solution would be to bring the approximations closer to the centre, e.g. centred differences, since the latter are generally of higher order. However, the problem under consideration is a conservation law problem which involves transport properties for which upwind differences have been found to impart the greatest numerical fidelity (e.g. Press *et al.*, 1992). Probably, a higher order upwind difference approximation would be possible (see e.g. Press *et al.*, 1992; Schiesser, 1991). Nevertheless, Q_i in Equation 5.6 may be bounded at several grid points along the spatial domain (e.g. by the presence of groynes) and not only at x_L and x_R. A discontinuity could be created at those points so that a higher order upwind approximation that uses several points alongshore would be likely to cross discontinuities and produce unreasonable results, similarly to centered difference approximations. As a result, aiming to keep the generality of the present 'one-line' model code, first order upwind differences were retained and no further investigation on alternatives of spatial derivatives discretisation was carried out.

5.2.3 ODEs time integrator – Bulirsch-Stoer method

The criteria for choosing the ODEs integrator are its accuracy and stability. The accuracy requirement is easily met in any up to date high quality ODEs integrator, where the user specifies the error tolerance in the inputs and the integrator adjust its stepsize to achieve the specified accuracy. Thus, error control is more or less automatic. On the other hand, the smoothness of the solutions of the PDE problem determines which ODEs integrator is better for stability. Thus, for stiff problems an implicit ODEs integrator is required for efficiency and stability. For smooth problems, explicit integrators are definitely

more efficient (Wouwer *et al.*, 2001) and have reasonable stability requirements. In the case of Equation 5.4, an explicit ODE integrator for smooth solutions was found to be suitable.

The ODEs integrator used in this study is known as the "Bulirsch-Stoer method" and according to Press *et al.* (1992) it is the best known technique for obtaining solutions of high accuracy with minimal computational effort. The method consists of three key elements which are:

- *Richardson's deferred approach to the limit.* This is the leading powerful idea of the Bulirsch-Stoer method. It consists of extrapolating a result computed with stepsize h to one that would have been obtained with a stepsize $h' << h$. Ultimately, the method aims to evaluate the solution that would be obtained had a stepsize $h = 0$ been used. The procedure is probably better illustrated in Figure 5.2. A big interval h is sequentially divided into finer and finer subintervals. The results obtained by the subdivisions are fitted by an analytic function which is used to extrapolate the answer to what would correspond to an essentially continuous time domain.

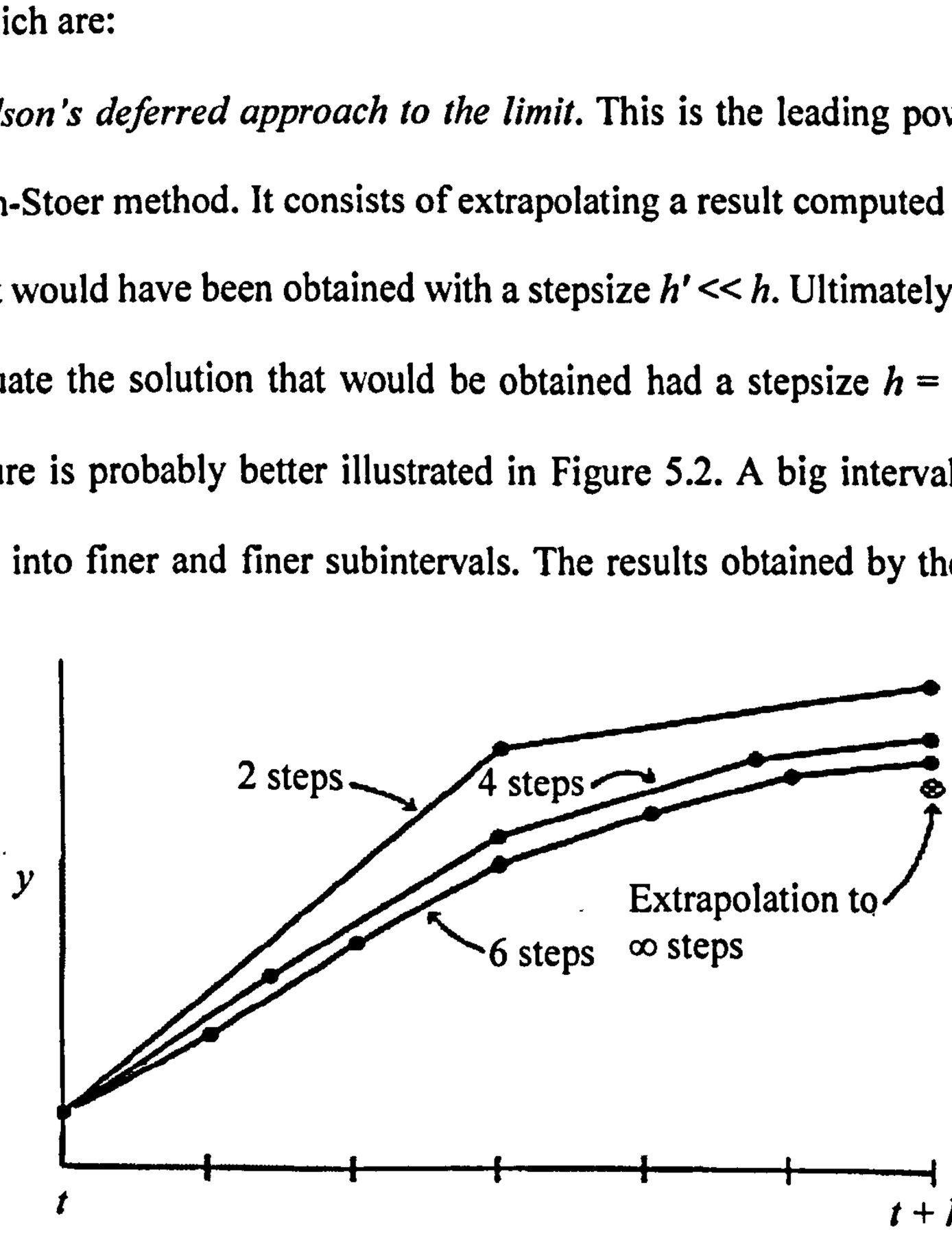

Figure 5.2 Richardson extrapolation as used in the Bulirsch-Stoer method (adapted from Press *et al.*, 1992)

- *Integration algorithm.* Integration in time is performed by the modified midpoint method.

- *Extrapolation function.* This is the fitting function used in "Richardson extrapolation" to extrapolate to $h = 0$. Here, polynomial extrapolation is used.

The numerical 'one-line' code was built in Fortran 77 with the basic Fortran modules needed for the Bulirsch-Sroer method obtained in full detail from Press *et al.* (1992). Full coding available in Schiesser (1991) was also of great help in developing a flexible and efficient numerical execution program. The following section gives an outline of the code structure and of its basic parameters. To facilitate reference to the above textbooks, subroutine names, symbols, and terminology in this chapter largely coincide with those found mainly in the work of Press *et al.* (1992) and then in Schiesser (1991).

5.2.4 Numerical code basics

The structure of the present 'one-line' Fortran code is depicted in Figure 5.3, where names of subroutines are enclosed by solid lines, names of input files by dashed blue lines and names of output files by dashed red lines. A brief description of each element of Figure 5.3 follows. The description omits mathematical details relevant to the integration of the ODEs. These can be found in Press *et al.* (1992).

<u>Input files</u>

DATA contains: (1) initial and final time of integration, t_0 and t_f respectively, (2) integration stepsize, h, (3) integration local error tolerance, *eps*, and (4) minimum stepsize allowed, *hmin*.

INFILE contains: (1) number of ODEs, *neqn*, (2) spatial grid cell size, *dx*, (3) parameters included in the sediment transport formulae (Equation 5.6), (4) depth of closure, (5) initial shoreline position, and (6) any values or indices related to boundary conditions and internal constraints.

WAVES contains: wave height, period, and direction.

The input files are read where the arrows point in Figure 5.3.

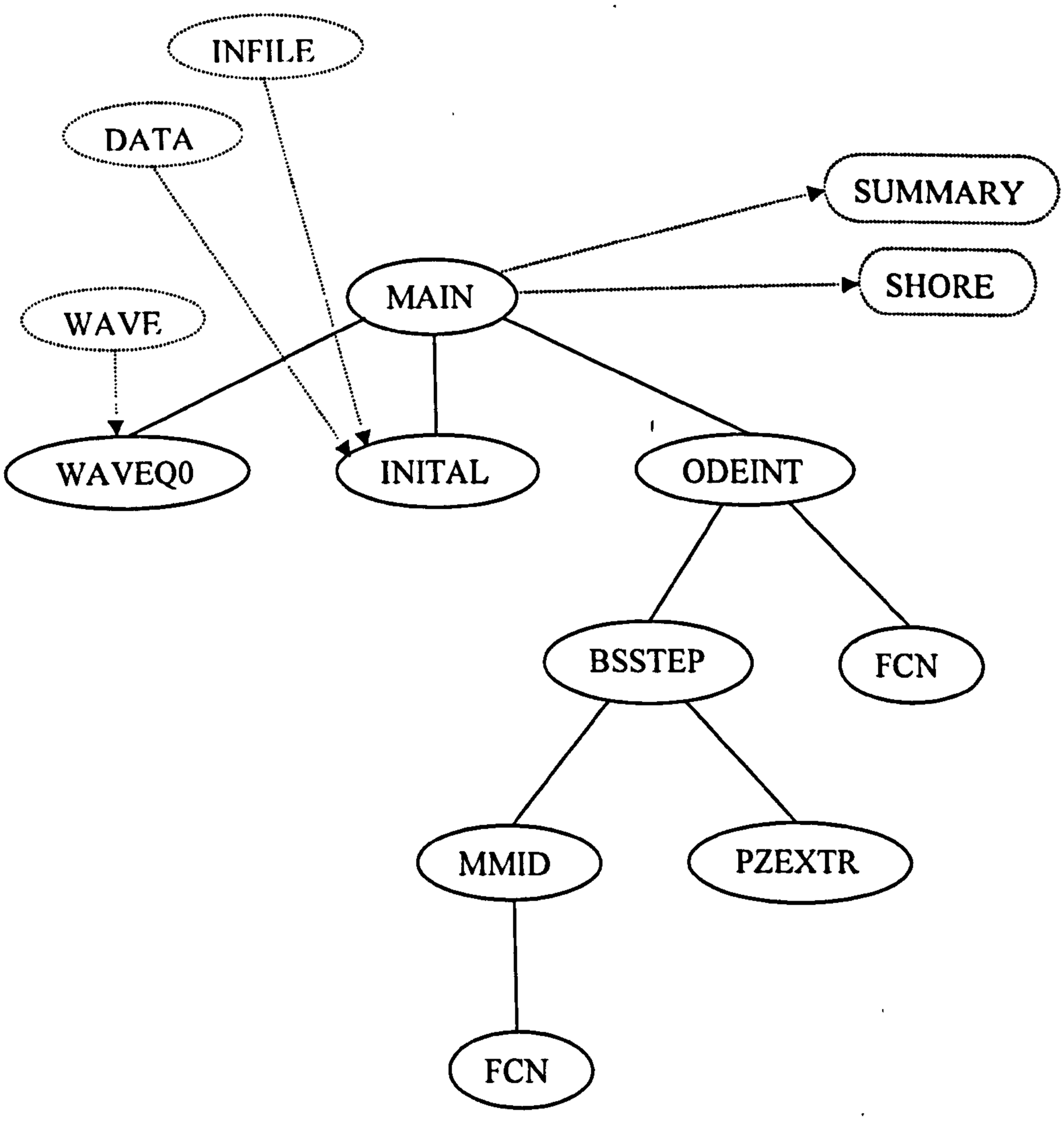

Figure 5.3 Main program structure of the 'one-line' model MOL based numerical solution

Subroutines

MAIN is the main program. It opens all input and output files. It obtains initial conditions read in INITAL and wave conditions read in WAVEQ0 which then become available throughout the program with the use of COMMON blocks. MAIN calls ODEINT in a loop from t_0 to t_f, in steps equal to h. In each call ODEINT produces the new values of the shoreline after h. The results, i.e. shoreline positions at intervals of h from t_0 to t_f are

written in the output file 'SHORE'. The output file 'SUMMARY' contains parameter values that may be adjusted in every program execution and may influence results and run times.

ODEINT is found in textbooks (e.g. Press *et al.*, 1992) as the "driver" routine. It starts and stops the integration, and stores intermediate results within one h if needed. The basic task of the routine is to return a solution that complies with the user specified error tolerance exactly after time h.

Integration of the ODEs and quality control of the solution is performed through BSSTEP, called in ODEINT, which is referred as the "stepper" routine. The "stepper" calls the "algorithm" routines, MMID and PEZXTR, where the basic formulae of the Bulirsch-Stoer method are implemented. Specifically, in MMID, the shoreline positions vector ($y_{1,\ldots,N}$) is integrated between t and $t + h'$, where h' is a stepsize variable, by a sequence of n substeps using the modified midpoint method. PEZXTR performs polynomial extrapolation of the discretized answer and provides extrapolated values and error estimates. The "stepper" routine, in an attempt to cross the user specified time interval, h, with user specified accuracy, *eps*, calls the "algorithm" routines in a loop that represents a sequence of values of n (n = 2, 4, 6,..., 16). The correction added to the MMID results between successive members of this sequence is taken as the error estimate and it is this value that should be less than or equal to *eps*. In each call, the "stepper" checks whether the predetermined *eps* is satisfied and accordingly accepts the solution or advances the loop. If the desired accuracy is not yet achieved after the end of a loop, BSSTEP reduces the stepsize to $h' < h$, and starts a new loop with n set back to $n = 2$. This procedure may be repeated until *eps* is satisfied. Then, control is passed to ODEINT along with the new shoreline positions at time $t_l + hdid$, where t_l denotes the start of an integration step in ODEINT and *hdid* is the stepsize accomplished in BSSTEP. Output is also *hdid* itself and

the next stepsize to be taken, *hnext*. If *hdid* = *h* then ODEINT returns to the main program and the solution is printed. Otherwise, ODEINT calls again BSSTEP to integrate the shoreline from t_1+ *hdid* to t_1 + *hdid* + *hnext*. In case t_1 + *hdid* + *hnext* overshoots $t_1 + h = t_2$ then *hnext* is reduced so that t_1 + *hdid* + *hnext* = t_2. BSSTEP may be called as many times as needed to cross the user specified *h* although a limit may be set by the user (*maxstp*). Overall, it is very important for the efficiency of the numerical code that BSSTEP takes the largest stepsize consistent with specified accuracy.

Last but not least is the subroutine FCN where the right hand side of Equation 5.4 is evaluated at the beginning of every integration step. Actually, FCN is the problem specification routine and along with WAVEQ0 (which evaluates Q_0 and a_0 for use in Equation 5.6) and INITAL are essentially the only subroutines that are user specified, acting as an interface between the user and the remainder of the code.

5.2.5 Model efficiency – Sensitivity analysis

The model efficiency, in terms of computation time and solution stability, along with its sensitivity and the sensitivity of the results to user defined key model parameters is examined in this section through a specific shoreline change problem. In particular, Equations 5.4 – 5.6 are solved for the common case where an initially straight shoreline is bounded by long, straight, impermeable groynes. Sediment sources/sinks are taken to be zero so that $q = 0$ in Equation 5.4. For this case, Equation 5.5 yields

$$y(1,0) = y(2,0) = \ldots, = y(N,0) = 0 \tag{5.7}$$

The boundary conditions, defined at the location of the groynes, are simply given by,

$$Q_1 = Q_{n+1} = 0 \tag{5.8}$$

and are directly superimposed in Equation 5.4. The amplitude of the sediment transport rate, Q_0 of Equation 5.6, is given by the CERC formula (Equation 2.9) with $K = 0.41$ as in Chapter 3. Similarly, a depth of closure of 10m is adopted.

The shoreline extent between the two groynes is 500m and is exposed to a constant nearshore wave condition, in time and alongshore, over a period of 984 hours. The constant wave characteristics are based on the shorter time-series used in Chapter 3. Thus, at a water depth of 6m, wave height is taken to be Hs = 1m, a value that is approximately equal to that producing the average wave energy of the time-series of Chapter 3. Similarly, a wave angle of $\alpha_0 = 14^0$ is adopted which gives the average value of the diffusion coefficient ε_w (for Hs = 1m) of the aforementioned time-series. These values are used directly in the calculation of Equation 5.6 since no refraction or diffraction are currently included in the model. Waves arrive from the left of the left hand groyne. The simulation period of 984 hours coincides with the time-scale of the problem under consideration, i.e. steady-state is observed after this time.

The above lead to $t_0 = 0$, t_f = 984hrs, and if $hmin = 0$, then h and eps remain to be specified in the DATA input file. Also, dx has to be determined in INFILE ($neqn$ = *dx/spatial domain extent*) and the problem is fully defined. Essentially, these three parameters, h, eps, and dx, are the only model parameters that may be adjusted for any specific coastal engineering problem. As a result, model sensitivity is tested with respect to their variation.

Model efficiency is monitored allowing for a quite stringent local error of 0.0001%. Hence, $eps = 10^{-6}$ is adopted and the model is run between t_0 and t_f at different intervals h and various dx values. Execution times for the different combinations of dx and h are shown in Table 5.1. Figure 5.4 depicts an example solution for dx = 25m and h = 1hr. The fast evolution of the shoreline towards equilibrium conditions is evident.

Table 5.1 Run times (sec) of the MOL solution of the 'one-line' model for different alongshore grid cell size, *dx*, and integration stepsize, *h*. *no solution obtained.

	***dx* (m)**						
***h* (hrs)**	**1**	**2**	**5**	**10**	**25**	**50**	**125**
1	≈ 8 min	70	10	2	<<1	<<1	<<1
3	≈ 7 min	55	8	"	"	"	"
6	"	51	6	"	"	"	"
8	"	"	"	"	"	"	"
12	"	"	"	"	"	"	"
24	"	50	5	"	"	"	"
984	*	49	<5	<1	"	"	"

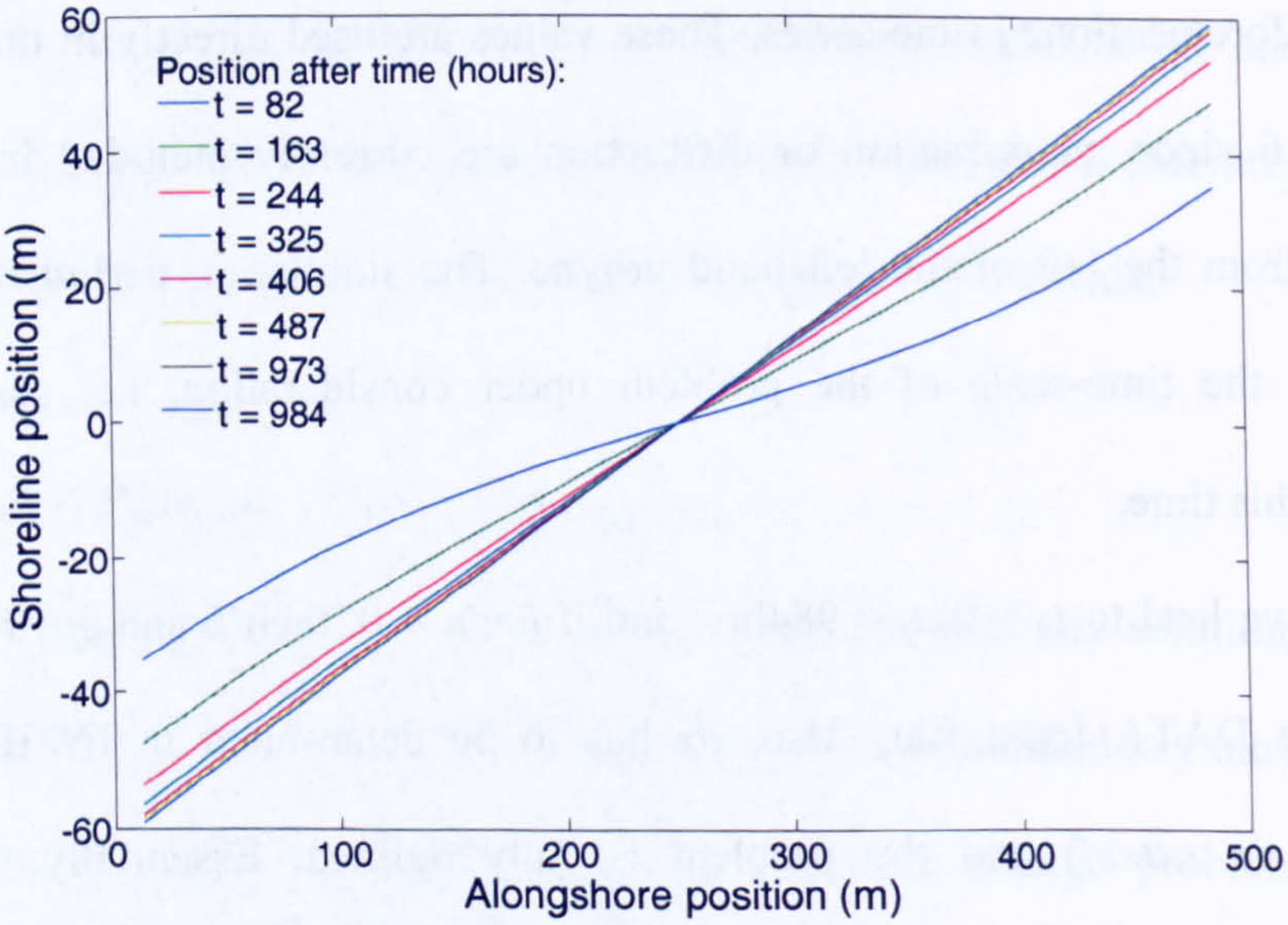

Figure 5.4 Shoreline evolution within a groyne compartment calculated with the MOL 'one-line' model for $dx = 25$m and integration stepsize $h = 1$.

Firstly, the consistency and stability of the solutions corresponding to each column of Table 5.1 (i.e. for fixed *dx* and varying *h*) was investigated at the various output times. Solutions were essentially the same with minor differences of maximum of 0.01m occurring sparsely at random times and alongshore positions. Furthermore, stability of the solutions was achieved for every combination of *h* and *dx*.

Table 5.1 clearly shows that execution time decreases with increasing *dx* and *h*. For $dx < 5$ significantly higher computation times are observed whilst for $dx = 1$m computation time is relatively large. An additional observation, not shown in Table 5.1, is that with decreasing *dx* and increasing *h*, the number of calls to BSSTEP routine from ODEINT, *maxstp*, generally increases. Ultimately, for $dx = 1$m and $h = 984$hrs execution is not completed even with *maxstp* = 100000. This situation is denoted in Table 5.1 by a star.

Increased computation time for decreasing *dx* is attributed to two reasons. The first apparent reason is that decreasing *dx* means more grid points alongshore, thus more ODEs to be integrated in time, which in turn translates to more computation. The second reason has to do with the stability of the ODEs integrator, in this case of the Bulirsch-Stoer method (Schiesser, 1991). As *dx* decreases the ODEs of Equation 5.4 become stiffer and smaller integration stepsizes, thus larger run times, are required to maintain stability. Smaller stepsizes result into more calls to the integration subroutine, BSSTEP, thus a larger value of *maxstp* (Press *et al.*, 1992; Schiesser, 1991).

Schiesser (1991) and Press *et al.* (1992) highlight the subtle effect *eps* can have on the results of a numerical MOL code. In the above runs, each shoreline position , $y_{1, 2, \ldots, N}$, was computed from the corresponding spatial derivatives of $\Delta Q_{1,2, \ldots N}/\Delta x$ with a relative accuracy of 10^{-6} (0.0001% error). Now, the sensitivity of the results to *eps* is tested by varying its value while *dx* and *h* are held constant. The value of $dx = 2$m was chosen in order to minimize the error associated with the spatial derivative approximation while keeping reasonable computation time (Table 5.1). The value of $h = 1$hr was adopted to increase output frequency and thus enhance error estimates between solutions of different *eps*. Table 5.2 contains the results. Its first column holds the solution pair on which comparison is performed. The second and third columns show the maximum and minimum difference respectively between corresponding shoreline positions throughout the output

files. Similarly, the fourth column shows the maximum Root Mean Square Error (RMSE) of corresponding shorelines in time. Table 5.3 shows run times for different *eps*.

Table 5.2 Comparison of MOL 'one-line' model solutions obtained with different user defined error tolerances, *eps* (dx = 2m, h = 1hr).

	Differences (m) between two corresponding solutions obtained with different *eps*		
pair of *eps*	**max difference**	**min difference**	**max RMSE**
10^{-14} and 10^{-12}	0	0	0
10^{-12} and 10^{-10}	0	0	0
10^{-10} and 10^{-8}	0.01	-0.01	0.0004
10^{-10} and 10^{-6}	0.02	-0.02	0.0054
10^{-10} and 10^{-4}	0.06	-0.06	0.0204
10^{-10} and 10^{-3}	0.25	-0.23	0.0479
10^{-10} and 10^{-2}	0.48	-0.51	0.0954
10^{-10} and 10^{-1}	53.15	-47.39	13.5360

Table 5.3 Run times for different *eps*.

eps	**Run time**
10^{-14}	107
10^{-12}	83
10^{-10}	81
10^{-8}	75
10^{-6}	70
10^{-4}	56
10^{-3}	56
10^{-2}	45
10^{-1}	30

Table 5.2 reveals that solutions start to change for *eps* $\geq 10^{-8}$ with their accuracy decreasing with increasing *eps*. For values of *eps* up to 10^{-2}, small changes in solution accuracy are noted whilst solutions become significantly erroneous for *eps* = 10^{-1}, which is

accompanied by a decrease in computation time (Table 5.3). For $eps < 10^{-8}$, where model output remains unchanged, solution error will be only due to the truncation error of the upwind approximation of the spatial derivatives of Equation 5.4. As expected, the more stringent the error tolerance specified, the more the computation time needed (Table 5.3).

The next step was to specify a stringent error tolerance, $eps = 10^{-10}$, to eliminate the error caused by the ODEs integration and to observe solution behavior obtained with constant h = 1hr and different dx. Solutions obtained with dx = 1m were compared with solutions obtained with dx = 5, 25, and 125m respectively at two alongshore locations, x = 62.5m and x = 187.5m. The calculated differences in shoreline positions are shown in Figure 5.5. Naturally, the solution differences increase as dx increases since the accuracy of the spatial approximations involved, and thus the accuracy of the solution in this case, is inversely proportional to dx. Figure 5.5 also depicts that larger differences are closer to the

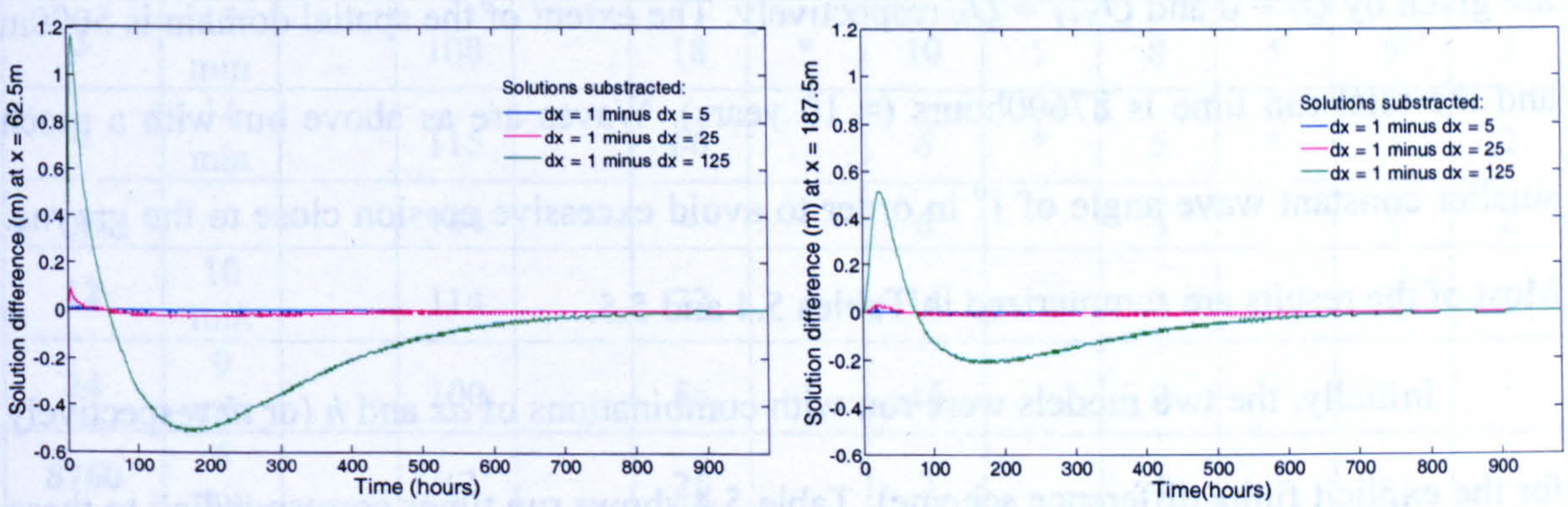

Figure 5.5 Differences between shoreline positions obtained with dx = 1m and dx = 5, 25, and 125m respectively at alongshore locations x = 62.5m (left) and x = 187.5m (right).

boundary (x = 62.5m) than away from it (x = 187.5m). Finally, it is apparent that solutions for different dx converge in time as the shoreline approaches its equilibrium shape. A more precise analysis of the accuracy of the solutions produced with the 'one-line' model based on MOL will be given later in Chapter 5, when numerical solutions for time-varying forcing will be compared against some of the approximate analytical solutions derived in

Chapter 4. Below the accuracy and performance of the MOL 'one-line' model is compared to an explicit finite difference 'one-line' numerical code.

5.2.6 MOL versus explicit and implicit finite difference 'one-line' models

Here, a 'one-line' model solved as common using the explicit finite difference numerical scheme (Section 2.2.3.3) is compared to the model of this study. The former model was developed by Chadwick *et al.* (2005). The purpose of this comparison is to perform a preliminary test of the accuracy of the MOL solution and to investigate whether there are any advantages in using this method. Here, the models are run for the case of a single groyne placed on an initially straight shoreline. No sediment may pass through or over the groyne and there are no other sources or sinks. For this case the initial condition is as in Equation 5.7 above whilst the boundary conditions at $x = 0$ and $x =$ alongshore extent are given by $Q_1 = 0$ and $Q_{N+1} = Q_N$ respectively. The extent of the spatial domain is 5000m and the total run time is 87600hours ($\approx$ 10 years). Waves are as above but with a much smaller constant wave angle of 1^0 in order to avoid excessive erosion close to the groyne. Most of the results are summarized in Tables 5.4 and 5.5.

Initially, the two models were run with combinations of *dx* and *h* (or *dt* respectively for the explicit finite difference scheme). Table 5.4 shows run times corresponding to these combinations. "M" denotes the MOL solution, "E" the explicit finite difference solution whilst the star denotes unstable solutions. A sensitivity analysis to *eps* revealed that for *dx* = 20m solutions remained identical for $10^{-4} < eps < 10^{-14}$. As a result, a value of $eps = 10^{-6}$ was adopted for the runs to ensure that integration accuracy surpasses spatial approximation accuracy.

An obvious advantage of the MOL solution is its largely increased stability (Table 5.4). As above, solutions are stable for relatively small *dx*s and for all the integration

stepsizes attempted. However, solution efficiency is significantly diminished for $dx < 20$m where a jump in computation time occurs. Nevertheless, for $dx = 10$m as an example, if a large h is adopted, e.g. $h = 8760$hrs which corresponds to a yearly output, the execution time is decreased to one-third ($\approx$ 6min) of that achieved with $h = 1$hr and is still within reasonable limits for a 10-year run. When the explicit finite difference method is stable, it is a faster method. However, the MOL solution often becomes faster for a larger user-specified stepsize where the finite difference technique is unstable.

Table 5.4 Run times (sec) of the MOL solution of the 'one-line' model (denoted with "M") and of the explicit finite difference solution (denoted with "E") for different alongshore grid cell size, dx, and time-step size, h. * solution is clearly unstable.

	***dx* (m)**											
***h* (hrs)**	**10**		**20**		**25**		**40**		**50**		**100**	
	M	**E**	**M**	**E**	**M**	**E**	**M**	**E**	**M**	**E**	**M**	**E**
1	18 min	*	57	*	46	20	29	13	24	11	13	6
3	15 min		108		18	*	10	5	8	5	5	3
6	14 min		115		66		6	*	5	*	3	2
8	-		144		-		6		3		3	2
12	10 min		114		72		14		2		2	1
24	9 min		100		56		15		9		1	*
8760	6 min		47		25		7		4		<1	

In contrast to what observed in the case examined in the previous section, MOL model run times for a constant dx do not monotonically decrease with increasing h. In this case, the general image is a run time increase at a certain user-specified integration stepsize that continues for a number of subsequent stepsizes till a decreasing trend is established again. As dx increases, the aforementioned increase takes place at a larger h. For instance it seems not to occur for $dx = 100$m. This result is most probably associated to the stability

properties of the method and is not examined further. However, it is highlighted that solutions did remain stable and essentially identical irrespectively of the value of h adopted.

Regarding the accuracy of the MOL solution, always with reference to the explicit finite difference solution, it was found that for any of the combinations of Table 5.4 the solutions obtained are largely the same between the two models. Any differences observed were due to a slight change of the finite difference solution with increasing dt. Figure 5.6, derived for dx = 100m, shows how the RMSE increases when solutions obtained with dt = 1hr and with the explicit finite difference method are compared with solutions of a progressively higher dt, dt = 3, 6, 8, …., 20hrs, at specific output times. The maximum RMSE that resulted from the comparison of yearly 'explicit' shorelines obtained using the aforementioned range of dt values is 0.0065m. In contrast, for any h < 40hrs, MOL solutions were identical so that max RMSE = 0m. Only for a very large user-specified integration stepsize, h = 8760hrs, were slightly different solutions obtained with max RMSE = 0.0028m.

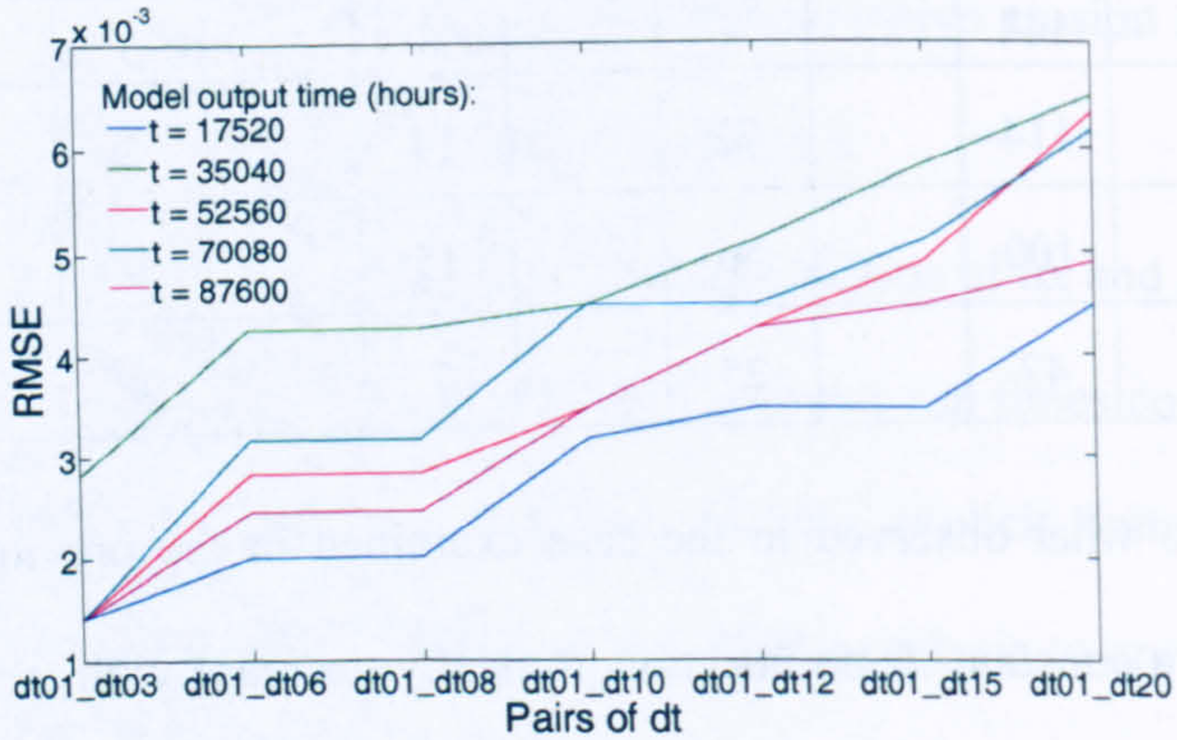

Figure 5.6 RMSE (m) between solutions obtained with dt = 1 and dt = 3, dt = 1 and dt = 6 hrs, etc, at five output times.

Unfortunately, an implicit finite difference numerical code (section 2.2.3.3) was not available to the author to fully compare it with the MOL based 'one-line' model. However, reference is made to Table 5.5 produced by Kraus and Harikai (1983) where the explicit

and implicit finite difference numerical schemes are compared for the same shoreline configuration problem as the one examined above. In this case, waves of constant wave height (1m) and direction (25^0) at the tip of the groyne were refracted and diffracted to the breaker line over a period of about 672hrs. The alongshore extent was taken to be 2000m with dx = 50m. The extended CERC formula of Equation 2.12 was used for the calculation of the sediment transport rate. In Table 5.5, the shoreline obtained with the explicit scheme and dt = 6hrs is used as the 'standard' for comparison and is denoted with a star.

Table 5.5 Comparison of explicit and implicit finite difference numerical schemes (adapted from Kraus and Harikai, 1983).

			$\frac{\Delta y - \Delta y^*}{\Delta y^*}$ (percent)		
Calculation method	***dt* (hr)**	**Comparative execution time**	**Adjacent jetty**	**Mid-beach**	**Adjacent fixed beach**
Explicit	2	2.81	-0.0	-0.0	-0.0
	3	1.88	-0.0	-0.0	-0.0
	4	1.41	-0.0	-0.0	-0.0
	6	1	0	0	0
	8	Unstable	-	-	-
Implicit	6	1.25	-0.7	-0.6	-0.0
	12	0.63	-1.5	-1.1	-0.7
	24	0.32	-2.9	-2.2	-1.4
	84	0.09	-10.1	-7.6	-6.5
	168	0.05	-19.4	-14.7	-13.7

An advantage of the MOL solution in comparison to the implicit finite difference numerical scheme is immediately clear from the results in Table 5.5. With the implicit finite difference scheme, solution accuracy deteriorates as dt increases, which is not the case when the MOL numerical scheme is used.

In the above, fixed wave conditions were considered, that is constant in time and constant alongshore. However, in engineering practice it is often the case that numerical 'one-line' models are run with waves that vary in time. If the study area consists of

essentially straight and parallel contours it can be reasonably assumed that time-varying nearshore waves remain constant alongshore. For more complex bathymetries, alongshore variation of nearshore wave characteristics becomes more important. Further, even if offshore waves are unchanged (e.g. average wave statistics are used as input), inshore waves will normally vary in time (even if slowly) because of feedback between the evolving local shoreline orientation and the process of nearshore wave transformation. In any case, the user-specified stepsizes (h or dt) of the numerical 'one-line' codes described will be determined by the frequency the wave input needs to be updated. Thus, very large stepsizes, for which it was found that the MOL based 'one-line' model is still stable without loss of accuracy, might not be appropriate.

5.3 Discussion

The 'one-line' model of shoreline change was solved for the first time with the "method of lines" numerical solution technique which converts an initial value PDE problem to an initial value ODE problem where a set of ODEs needs to be integrated in time. Following the steps of the MOL solution procedure, firstly, the spatial derivatives of the sediment transport rate in the continuity of sediment equation were approximated with first order upwind differences. Secondly, the Bulirsch-Stoer method as described in Press *et al.* (1992) was employed for the time integration of the resulting system of ODEs. The latter is a powerful, high precision, explicit ODE integrator with error control.

A sensitivity analyses, in terms of model efficiency and stability, was initially performed with respect to three user defined key parameters, the integration stepsize, h, the local integration error tolerance, *eps*, and the grid cell size, dx. A constant wave condition in time and space was used as input. As expected, execution time increased with decreasing

dx. Variation of *h* had a more complex effect on run times. In the first case of shoreline change examined (evolution within a groyne compartment over 984 hours), run times decreased monotonically with increasing *h*. In the second case (evolution near a single groyne over 10 years) run times seemed to decrease, increase, and then decrease again as *h* became larger. An increase in *dx* caused the turning point at which run times became larger to move to greater *h* values (e.g. for *dx* = 40m run time increase occurred at *h* = 24 hours). This result must have to do with the stability properties of the ODEs integrator and was not examined further. Run times generally increased with decreasing *eps*. In terms of stability and solution consistency, solutions were stable for any combination of *dx* and *h* attempted, including combinations of small *dx* and large *h* values. Furthermore, variation of *h* did not affect the results as solutions remained essentially unchanged even for extremely large user-specified integration stepsizes. On the other hand, the variation of *eps* did affect consistency with larger and larger *eps* leading to less accurate solutions. Obviously, the choice of *dx* did influence the results because of the dependence of the spatial approximation accuracy on this choice.

Although the above analysis infer the advantages of the MOL based 'one-line' model over the explicit and implicit finite difference 'one-line' numerical codes used to date, a direct comparison was performed with an explicit finite difference 'one-line' model whilst an indirect one was carried out with an implicit finite difference code. This was also necessary for a preliminary test on model accuracy since finite difference codes have been checked for accuracy and consistency against exact analytical solutions that assume constant forcing (Section 2.2.4). When the explicit finite difference scheme was stable solutions between this method and the MOL were essentially identical. However, the stability of the explicit finite difference solutions was found to be significantly decreased compared to the MOL solutions. In fact, MOL solutions can be thought as being

unconditionally stable; however, very small dx values cause the problem to become stiff so that a large computation time is required in the attempt of the explicit ODE integrator to maintain stability. Apart from increased stability, another advantage of the MOL based 'one-line' model is that solution accuracy does not deteriorate with increasing user-specified stepsize. However, this advantage is more important when MOL is compared to the implicit finite difference 'one-line' code as the effect of time-step, dt, on the solutions obtained with the explicit finite difference model is minor over the range of stable solutions. In terms of run times, the explicit finite difference 'one-line' code is generally faster. Nevertheless, execution times converge towards higher dx and larger h.

A final general advantage of the MOL numerical technique and also a definite advantage when compared to the implicit finite difference method is that it allows for easy and flexible programming of the 'one-line' model. In contrast to the complex implicit finite difference coding, MOL programming closely resembles the problem equations whilst boundary conditions are implemented simply, just as in the explicit finite difference solution scheme, minimizing complexities. This leads to a well structured and flexible code. Specifically, the user needs to specify initial conditions, boundary conditions, and specific problem mathematics (e.g. the equation used to estimate the sediment transport rate, Q) in three simple special-purpose routines. The rest are general-purpose routines that do not normally change with changing problem specification. In addition, general-purpose routines are readily available through textbooks or software libraries so that no particular effort from the programmer is required. Consequently, easy transition is permitted between different shoreline change problems. Easy transition is also permitted between different ODEs integrators or spatial derivative approximations if required. For example, if a relatively stiff shoreline problem is encountered, the user might wish to try an implicit ODEs integration algorithm for stiff problems.

Chapter 6

Numerical MOL versus semi-analytical solutions of the 'one-line' model

The accuracy and convergence of 'one-line' numerical models has been previously tested against analytical expressions which assume that an unchanging wave condition drives shoreline change (Hanson, 1987; Hanson and Larson, 1987). For example, Hanson (1987) compared exact solutions of shoreline change for different problem configurations with the explicit and implicit finite difference numerical codes built in the well-known 'one-line' model GENESIS. The results were summarized in Chapter 2, Section 2.2.4. In general, very good agreement was found when the assumptions of the analytical solutions, small angles and constant waves in time and space, were respected. Inevitably, discrepancies increased for problems involving larger angles of wave approach or/and larger local shoreline orientations. Nevertheless, no analytic solutions have been available to date to test the accuracy and convergence of numerical results obtained with wave forcing varying arbitrarily in time. In Chapter 4, explicit closed-form solutions of the 'one-line' model that account for the time-variation of the waves were derived, making it possible to perform a check of the numerical codes under these conditions. Such a check is carried out in this section. In particular, results from the MOL-based 'one-line' model

developed in this study are compared with results from the semi-analytical solutions of Chapter 4 for specific cases of shoreline change. It is noted that, under time-varying conditions, there is no guaranteed level of accuracy for the two methods. In addition, the methods are not strictly comparable because of the differing underlying assumptions; however, for suitable choice of test case the effects of the assumptions can be reduced to negligible proportions. For these reasons, no method is considered more accurate and an intercomparison is performed. The latter has the advantage that it is able to reveal how the discrepancy between semi-analytical and numerical solutions may vary with time in relation to the variation of the wave inputs, something that was not possible before when a constant wave condition had to be used for such a comparison.

In what follows the MOL-based 'one-line' numerical code is tested against the semi-analytical solutions of Chapter 4 for two cases: (1) a Gaussian shaped beach nourishment placed on an otherwise straight shore, and (2) within a groyne compartment. Discrepancies between the solutions are given mainly in terms of the Root Mean Square Error (RMSE). The comparison is performed on two wave input time-series: (1) very small angles of wave approach, and (2) occurrence of several high angled waves.

6.1 Problem specification

Two different wave input time-series were used to obtain solutions. These are the time-series of Chapter 4 and a modified version of it. In the modified time-series the wave angles are reduced to 10% of the values shown in Figure 4.1b. The resulting wave angle time-series is shown in Figure 6.1, where wave angles relative to the shoreline normal are 'small' ($< \pm 4°$). This is in line with assumptions of the analytical work and thus ensures a fair comparison.

Both the semi-analytical solutions and the numerical model at its present form do not account for nearshore wave transformation. Consequently, waves are taken to be constant alongshore and no feedback between changing shoreline orientation and nearshore wave characteristics is considered.

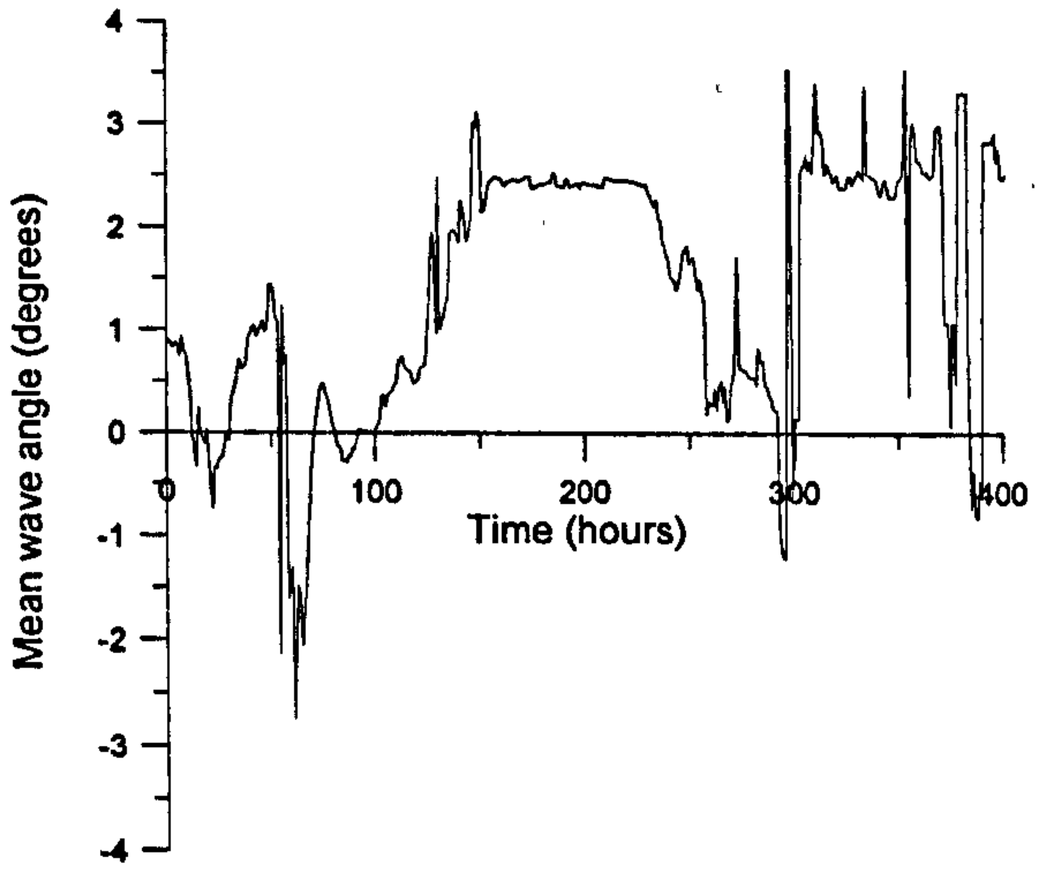

Figure 6.1 Time-series of hourly nearshore wave angles

Solutions are compared for two different cases of shoreline change. Firstly, shoreline evolution for $x > 0$ when the initial shoreline shape is that of a Gaussian beach nourishment is examined. This problem, like the problem of the rectangular beach nourishment examined in Chapter 4, Section 4.3.2, may be represented by the general form semi-analytical solutions of Section 4.2.1. For this case the initial condition is given by

$$y(x,0) = k\frac{1}{\sigma\sqrt{2\pi}}e^{-\frac{1}{2}\left(\frac{x-\mu}{\sigma}\right)^2} \tag{6.1}$$

where k is a proportionality coefficient, σ is the standard deviation of the Gaussian distribution and μ is its mean value. Boundary conditions are as in Equations 4.4 and 4.38. Without sources/sinks of sediment, the final solution to this problem is given by

$$I_1 = \frac{k}{2\sigma\pi\sqrt{2}}\left(\int_0^t \varepsilon(u)du\right)^{-\frac{1}{2}} \int_0^\infty e^{-\frac{1}{2}\left(\frac{\xi-\mu}{\sigma}\right)^2} \left(e^{-\frac{(x-\xi)^2}{4\int_0^t \varepsilon(u)du}} - e^{-\frac{(x+\xi)^2}{4\int_0^t \varepsilon(u)du}} \right) d\xi \qquad (6.2)$$

For the particular problem of this section a spatial extent of 12000m is adopted with a discretisation of 1m. In addition, k = 15000, σ = 200m, and μ = 6000m. These parameter values generate a smooth Gaussian hump centered at the middle of the spatial domain away from the boundaries. This unconstrained example of beach change, where a smooth initial shoreline irregularity tends to diffuse with time, is a suitable problem for the comparison of the semi-analytical and numerical solutions in terms of accuracy and convergence. This is because the small angle approximations inherent in the analytical solutions are initially well respected and are even more respected with time as the irregularity is smoothed out.

Shoreline evolution within a groyne compartment is the second case examined. The problem is defined in Chapter 4, Section 4.3.3, by Equations 4.40-4.43. Parameter values are as in Chapter 4 (see also Figure 4.5). For this case, the comparison of the semi-analytical and numerical solutions might be more sensitive. This is because the presence of constraints on the flow of sediments and the existence of a prevailing wave direction are expected to lead to increasingly tilted shorelines with time, exhibiting larger local shoreline orientations which could violate the small angle assumptions inherent in the semi-analytical work. Nevertheless, for small wave angles and not large time spans, this effect is expected to be minor.

6.2 Results

6.2.1 Small wave angle time-series

Firstly, results obtained with the small wave angle time-series of Figure 6.1 as input are presented. For this time-series, $\varepsilon_s \cong \varepsilon_w$ (Sections 2.2.2.2). Here, ε_s is used in the semi-analytical expressions for consistency with previous studies of comparison between analytical and numerical solutions of the 'one-line' model (e.g. Hanson and Larson, 1987). The case of the Gaussian beach nourishment, described above, is initially examined. Figure 6.2 shows the RMSE between semi-analytical and numerical output shorelines at every output time (output step-size = 1hr). The numerical shorelines were obtained for dx = 2m and $eps = 10^{-10}$. The first value corresponds to a very good spatial resolution which increases the accuracy of the MOL output and enhances error estimates when this is compared to the semi-analytical output. At the same time, it does not require excessively big run times (run time ≈ 5 min). The second value corresponds to a very stringent local integration error tolerance which guarantees that spatial approximation accuracy is the only

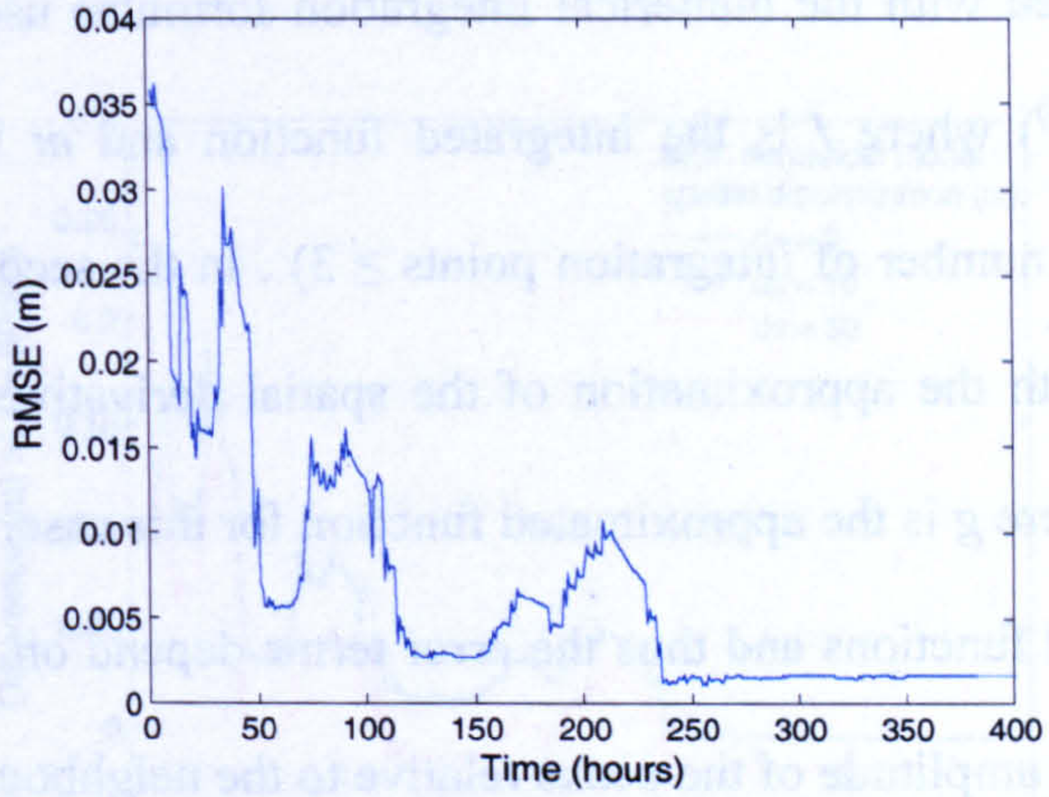

Figure 6.2 Evolution of the RMSE (m) between semi-analytical and MOL numerical output.

source of error in the MOL solutions. An integration stepsize of h = 1hr was adopted to solve both semi-analytical and numerical expressions.

Figure 6.2 reveals an excellent agreement between the semi-analytical and numerical solutions with a maximum RMSE of about 0.035m. Maximum RMSE values occur within the first output times whilst discrepancies clearly decrease with time. This decrease is far from linear. Specifically, RMSE peaks are evident in the figure, which exactly coincide with periods of stormy waves in the time-series (see Figure 4.1). In contrast, RMSE is relatively low and essentially constant during periods of low wave activity. This variation of RMSE with changing wave characteristics (in this case mostly with changing wave height rather than wave angle since the latter is kept very small) is introduced to the results because of the form of the error terms associated with the two kinds of solutions, semi-analytical and numerical. In the first case, for h = 1hr, the order of the error term associated with the numerical integration formulae used to solve Equation 6.2 is given by $O(f^{(m)})$ where f is the integrated function and m is the order of the f derivative ($m > 4$ for a number of integration points ≥ 3) . In the second case, the order of the error associated with the approximation of the spatial derivatives of Equation 5.4 is given by $O(dx\, g^{(2)})$ where g is the approximated function for this case. In summary, in both cases, the approximated functions and thus the error terms depend on the wave height and angle. In Figure 6.2, the amplitude of the peaks relative to the neighbouring constant RMSE values can provide a rough idea of how variation in wave characteristics may affect the error terms and the resulting discrepancy between the solutions.

Nevertheless, it would not be correct to say that one approach is more accurate that the other especially when extremely small differences such as those represented in Figure 6.2 are found. This is because, on one hand, the error introduced by the small angle approximations of the semi-analytical solutions is largely unknown and may surpass the

error of the aforementioned numerical approximations, and, on the other hand, the MOL error is a cumulative one in contrast to the semi-analytical error, hence it is expected that it will increase in time. The relative importance of these errors in time is difficult to estimate. It could be, for example, that after a certain amount of fill diffusion, there is an interchange of the relative accuracy of the two different solutions.

Figure 6.3 depicts the time evolution of the difference between the two solutions, semi-analytical and numerical, at one alongshore location, x = 6000m, which corresponds to the tip of the beach fill. This difference is calculated for numerical solutions obtained with three different values of dx discretization, dx = 2m (as in Figure 6.2), dx = 10m, and dx = 50m respectively. The larger the dx the worse the numerical model resolves the curvature of the shoreline and the poorer the solutions. Generally, the figure shows that for a shoreline of 30m at the peak, an agreement to within less than 1% is achieved between the two solutions.

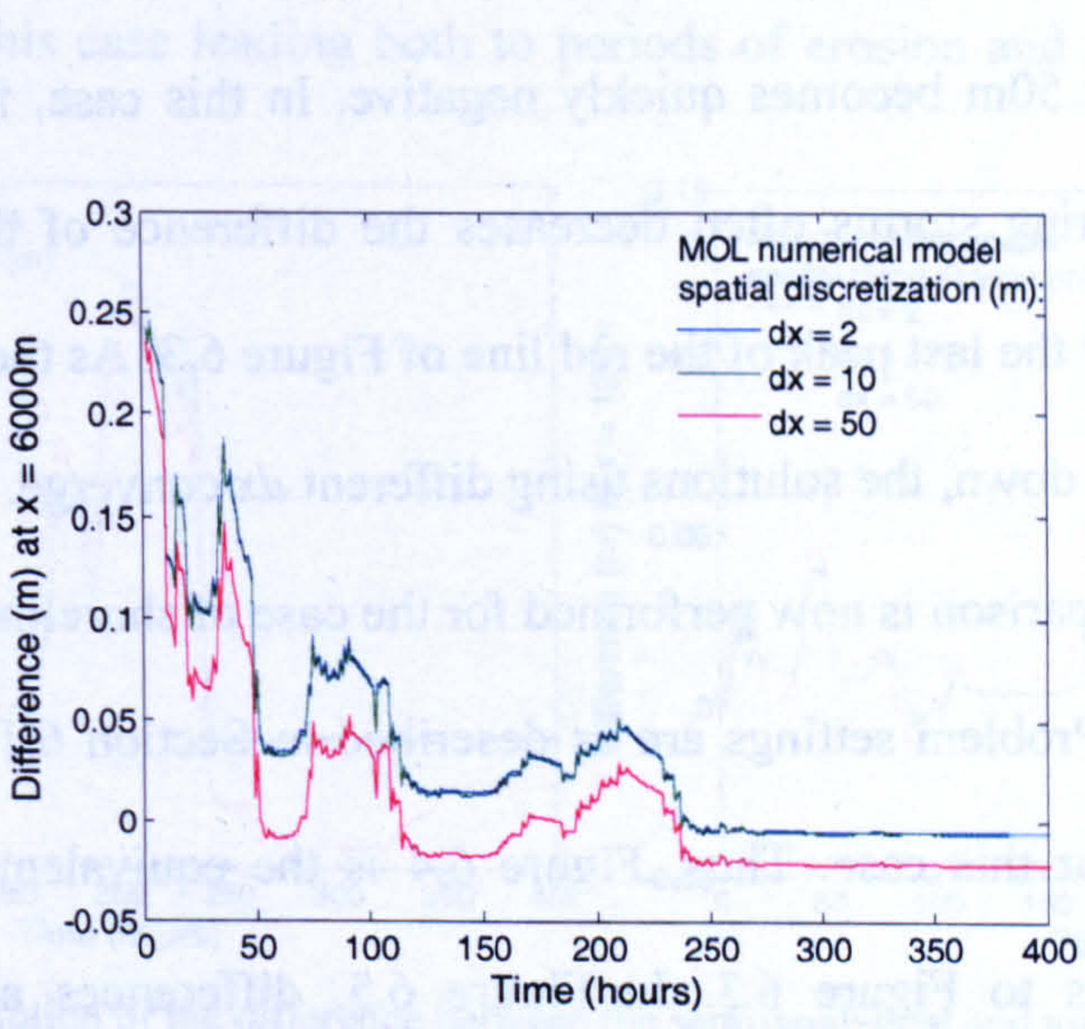

Figure 6.3 Time evolution of the difference between the semi-analytical and numerical solution at x = 6000m. The discrepancy is calculated for three different MOL solutions obtained with dx = 2, 10, and 50m respectively.

Initially the semi-analytical solution is above the numerical one, i.e. semi-analytical solution > numerical solution (the differences in Figure 6.3 correspond to the calculation:

semi-analytical solution – numerical solution). The coarser the *dx* discretization, the more peaked the shape of the fill, and the smaller this initial difference. Focusing on the blue line of Figure 6.3 which corresponds to the most accurate numerical solution (smaller *dx*), it is observed that the aforementioned initial discrepancy is decreasing with time till it becomes negative after $t \approx$ 240hrs. It is at this time that the positions of the two solutions interchange, i.e. the numerical solution falls above the semi-analytical. This suggests that overall the semi-analytical solution diffuses faster than the numerical. However, the peaks along the line indicate that this is not always the case and that during periods of increased wave activity, the numerical solution responds stronger causing greater erosion of the fill, increasing the difference between the two solutions. A larger *dx* in the numerical model causes the tip of the beach fill to evolve slower, so that the interchange in the relative position of the semi-analytical and numerical shorelines is faster. This is why the line corresponding to dx = 50m becomes quickly negative. In this case, faster erosion of the numerical solution during storms often decreases the difference of the two solutions as shown, for instance, by the last peak of the red line of Figure 6.3. As the fill diffuses further and its evolution slows down, the solutions using different *dx* converge.

The above comparison is now performed for the case of shoreline evolution within a groyne compartment. Problem settings are as described in Section 6.1. Similar figures as above are presented for this case. Thus, Figure 6.4 is the equivalent of Figure 6.2 and Figure 6.5 corresponds to Figure 6.3. In Figure 6.5, differences are plotted for two alongshore positions, x = 75m away from the left hand groyne, and x = 125m away respectively.

Again, Figure 6.4 shows excellent agreement between the semi-analytical and MOL numerical solutions. However, higher RMSE values are reached in this case compared to the Gaussian fill case examined above. RMSE maximum is about 0.2m. The variation of

RMSE in time largely follows the wave height variation of Figure 4.1b. Nevertheless, this

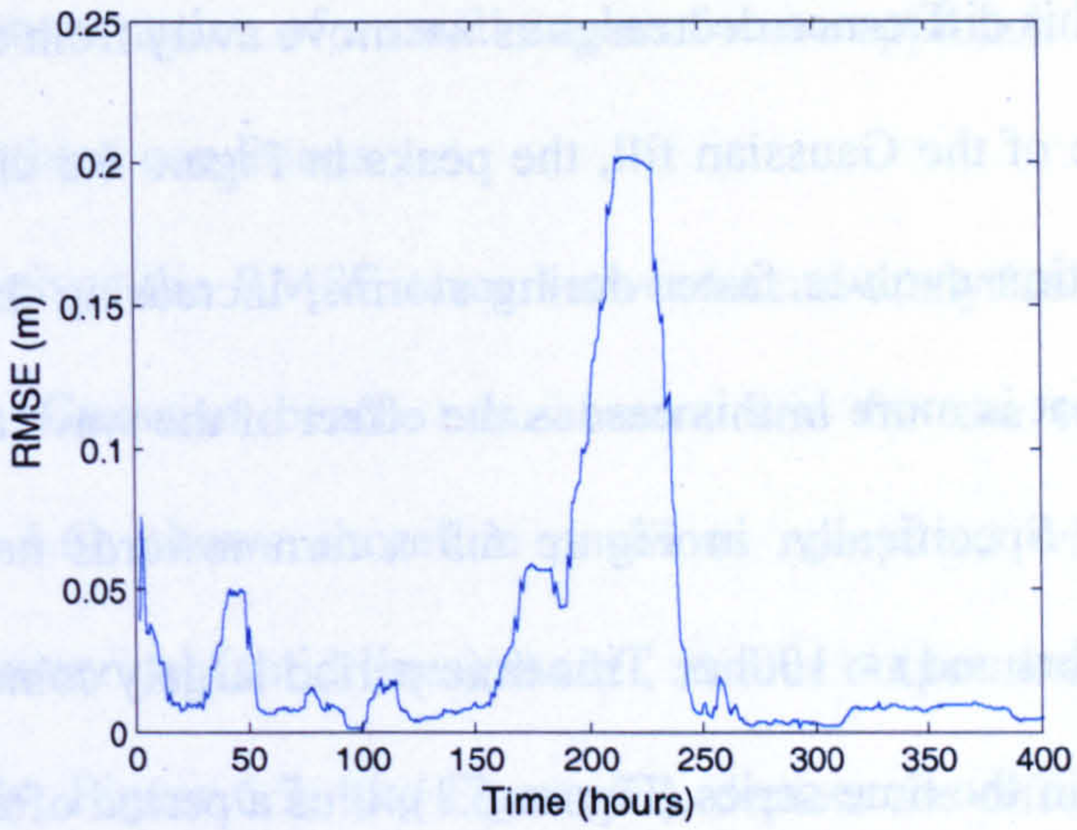

Figure 6.4 Evolution of the RMSE (m) between semi-analytical and MOL numerical output.

resemblance is not as good as the one shown in Figure 6.2 and in contrast to that figure no clear trend in time exists in Figure 6.4. This result is due to the more important role of wave angle variation in this case leading both to periods of erosion and accretion in contrast to

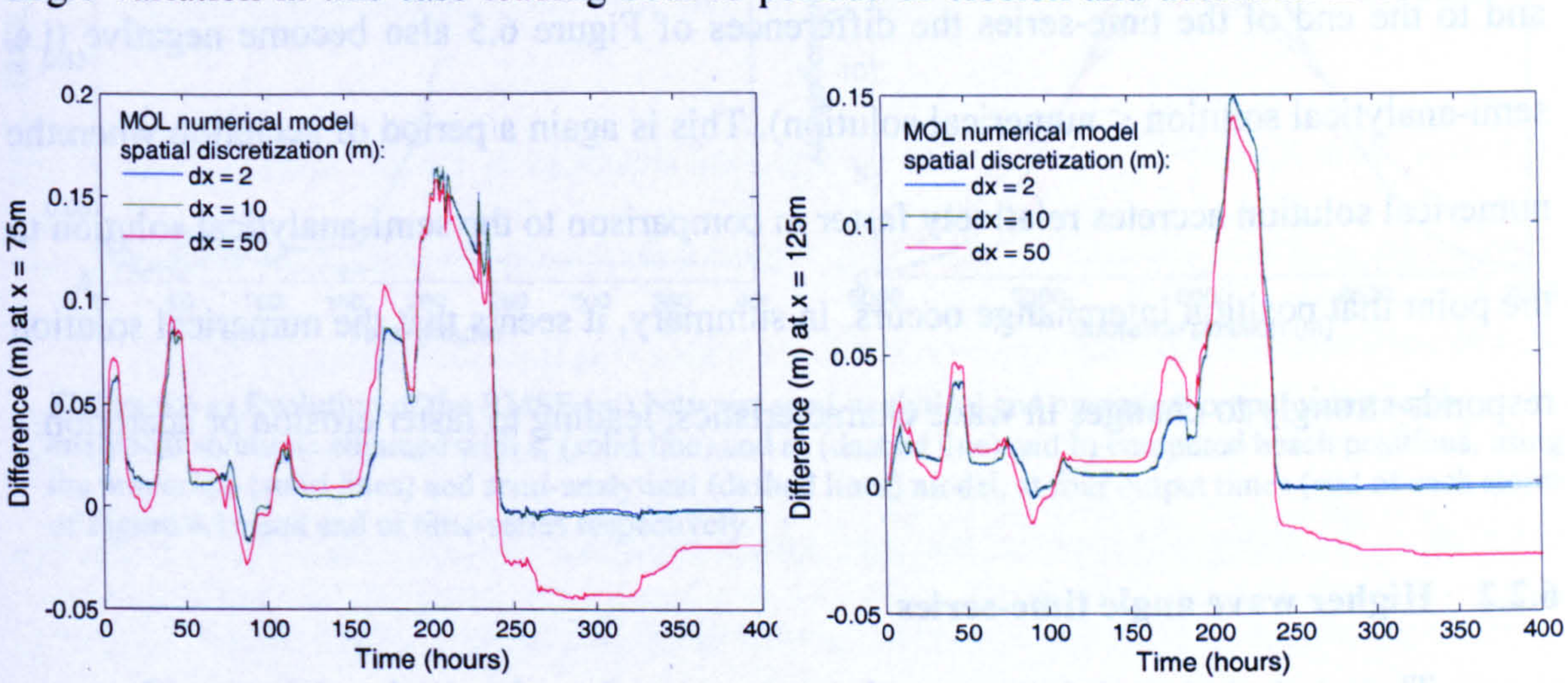

Figure 6.5 Time evolution of the difference between the semi-analytical and numerical solution, at $x =$ 75m (left) and x = 125m (right). The discrepancy is calculated for three different MOL solutions obtained with dx = 2, 10, and 50m respectively.

the case examined above where only diffusive/erosional trends are present. This is explained better in the following paragraph. Figure 6.5 shows the larger the dx the larger

the difference between semi-analytical and numerical output for this case of shoreline change. In addition, this difference decreases as we move away from the boundaries.

As in the case of the Gaussian fill, the peaks in Figure 6.5 clearly suggest that the MOL numerical solution evolves faster during storms, increasing the difference between the two solutions. What is more in this case is the effect of the wave angle variation on the observed differences. Specifically, in Figure 6.5 a turn towards negative differences is shown between $t \approx 80$hrs and $t \approx 100$hrs. This time period largely coincides with a period of negative wave angles in the time-series (Figure 6.1), thus a period of accretion near the left groyne (see Figure 4.5a, Chapter 4, for some indication of evolution patterns for this problem, i.e. accretion versus erosion). According to Figure 6.5, during this period, the numerical solution accretes relatively faster than the semi-analytical solution causing an interchange in the relative position of the output shorelines. After the end of the third storm and to the end of the time-series the differences of Figure 6.5 also become negative (i.e. semi-analytical solution < numerical solution). This is again a period of accretion when the numerical solution accretes relatively faster in comparison to the semi-analytical solution to the point that position interchange occurs. In summary, it seems that the numerical solution responds strongly to changes in wave characteristics, leading to faster erosion or accretion.

6.2.2 Higher wave angle time-series

The same two scenarios were also used to test the performance of the two solution methods for higher wave angles, ie. the time-series of Figure 4.1b, without any wave angle modification. This time-series contains several storms with highly oblique waves, so that the small angle approximation of the semi-analytical work is likely to give a relatively poor accuracy. The effect of this deviation from the assumptions of the semi-analytical expressions on the discrepancy between analytical and numerical output is examined

briefly in this section. Here, both ε_s and ε_w are used to obtain semi-analytical solutions since the latter relaxes the assumption of a small angle of wave approach and thus is expected to perform better under these conditions.

Figure 6.6a gives the RMSE error between semi-analytical and numerical output for the case of the Gaussian beach nourishment and for the two different diffusion coefficients. Figure 6.6b shows shoreline positions computed with the semi-analytical (dashed lines) and numerical (solid lines) model, at four output times (same as in Chapter 4), and for ε_s. Finally, Figure 6.7, like Figure 6.3, depicts the difference between the two solutions at x = 6000m alongshore and for the two different diffusion coefficients.

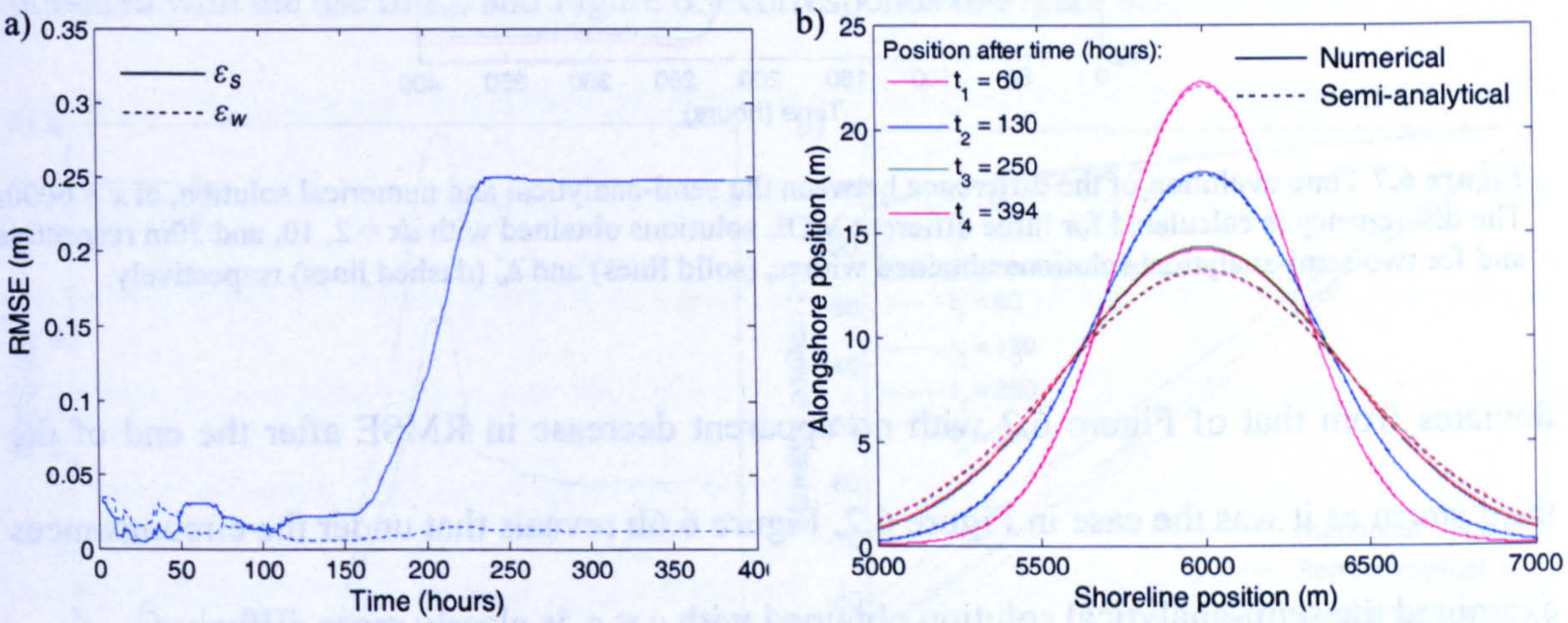

Figure 6.6 a) Evolution of the RMSE (m) between semi-analytical and numerical output using semi-analytical solutions obtained with ε_s (solid line) and ε_w (dashed line) and b) computed beach positions, using the numerical (solid lines) and semi-analytical (dashed lines) model, at four output times (end of each storm of Figure 4.1b and end of time-series respectively.

Figure 6.6a shows that the agreement between semi-analytical and numerical solutions is still very good. In fact, with the use of ε_w the magnitude and pattern of the RMSE is very similar to the one of Figure 6.2. When ε_s is used this pattern substantially changes. Most evidently, a significant increase in RMSE occurs from the beginning of the third storm of Figure 4.1b to the end of it, after which RMSE values stay essentially constant to the end of the time-series. The maximum RMSE value reached with ε_s is around

0.25m. When comparison is made with Figure 6.2, it becomes obvious that the difference in RMSE pattern and magnitude is due to the higher wave angles encountered in the time-series used herein. For instance, the third storm during which RMSE evidently increases is accompanied by persistently high angled waves. Even with the use of ε_w the RMSE pattern

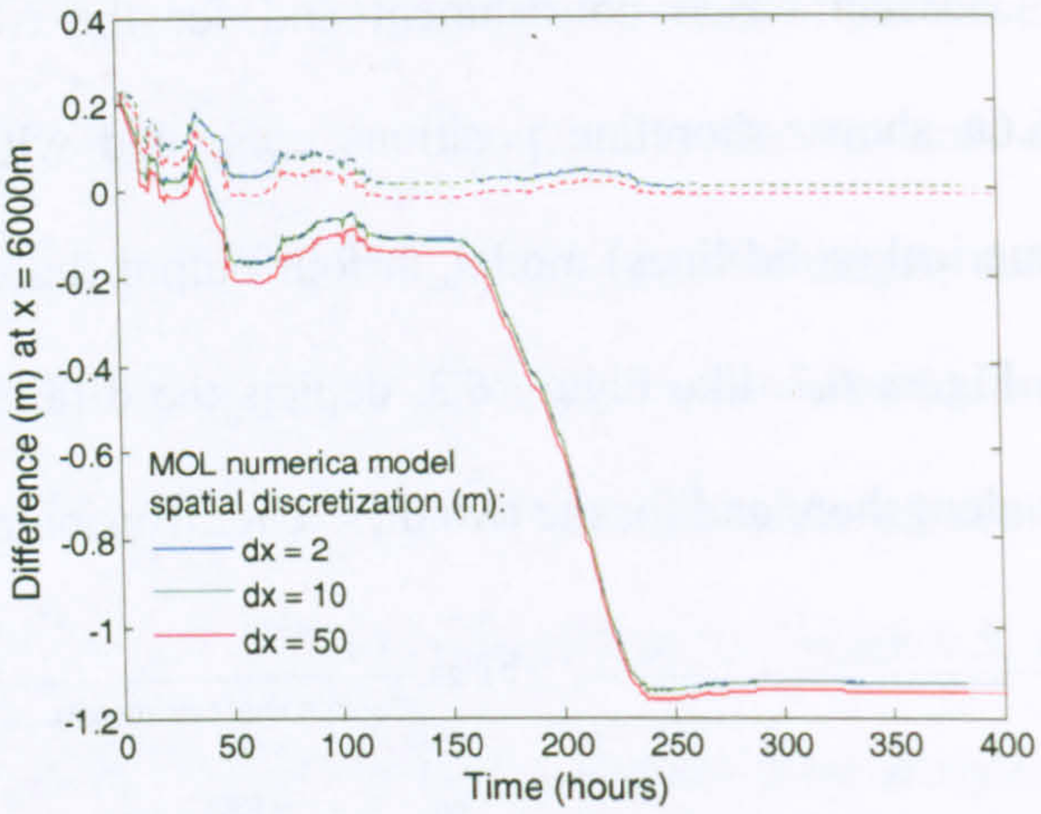

Figure 6.7 Time evolution of the difference between the semi-analytical and numerical solution, at x = 6000m. The discrepancy is calculated for three different MOL solutions obtained with dx = 2, 10, and 50m respectively and for two semi-analytical solutions obtained with ε_s (solid lines) and ε_w (dashed lines) respectively.

deviates from that of Figure 6.2 with no apparent decrease in RMSE after the end of the third storm as it was the case in Figure 6.2. Figure 6.6b reveals that under the circumstances examined the semi-analytical solution obtained with $\varepsilon = \varepsilon_s$ is clearly more diffusive.

Figure 6.7 also helps to understand better the discrepancies observed by revealing the sign of the difference between the semi-analytical and numerical solutions. Initially, the differences obtained with the use of ε_s in the semi-analytical solution (solid lines) are discussed and compared to those of Figure 6.3. Here, a much quicker interchange of the position of the two solutions occurs (after about 20hrs for the line corresponding to dx = 2m), with the semi-analytical solution eroding faster than the numerical one. As before, the initial peaks of the figure, up to about 130hrs indicate faster erosion of the numerical solution. However, this is now the case only when storms are accompanied by low wave

angles. During the third storm (after t ≈ 150hrs) when wave angles become persistently high, the diffusion caused by the semi-analytical solution is more severe than that caused by the numerical, in contrast, to what it has been observed up to this point. When wave heights are considerably low the difference between the two solutions remains largely constant even if high angles occur. The pattern of the differences observed with ε_w used in the semi-analytical solution is largely as in Figure 6.3

As in Section 6.2.1, the same analysis as above is carried out for the case of shoreline evolution within a groyne compartment. Figure 6.8a corresponds to Figure 6.6a, Figure 6.8b corresponds to Figure 6.6b with the addition of the semi-analytical solution obtained with the use of ε_w, and Figure 6.9 corresponds to Figure 6.7.

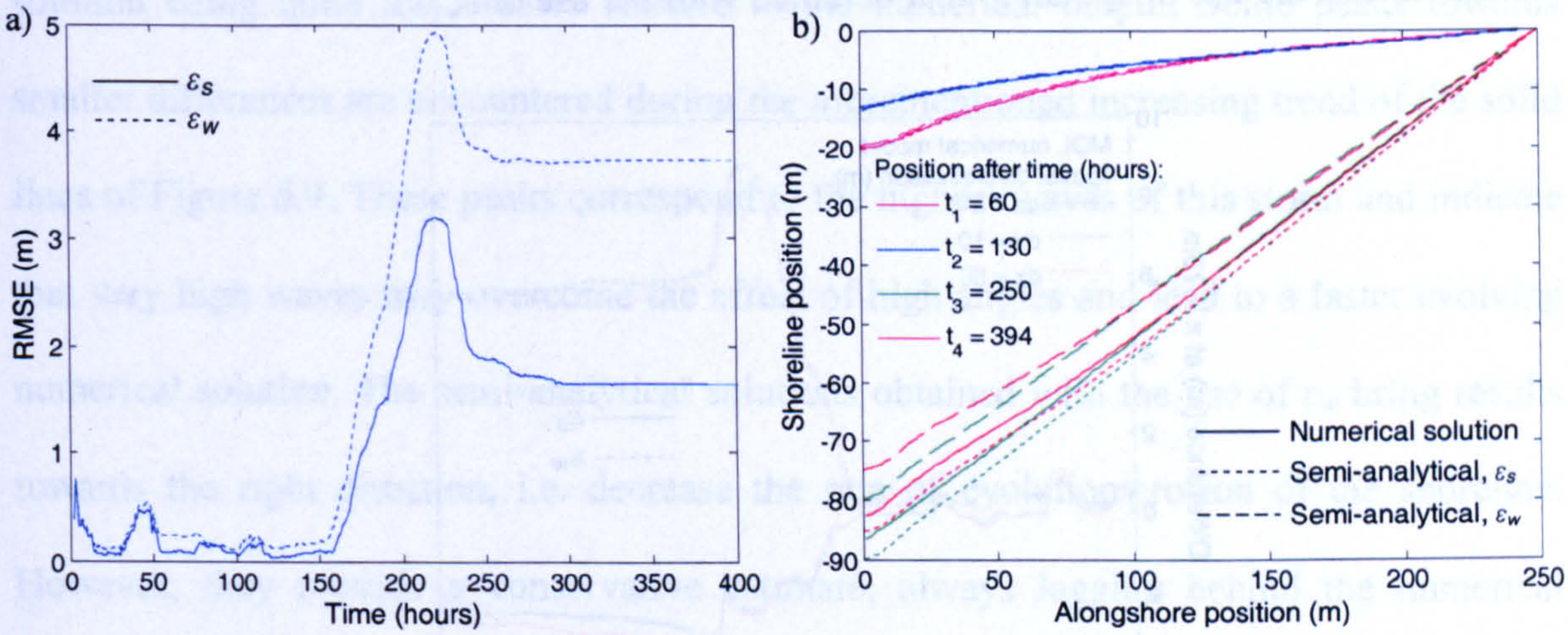

Figure 6.8 a) Evolution of the RMSE (m) between semi-analytical and numerical output using semi-analytical solutions obtained with ε_s (solid line) and ε_w (dashed line) and b) computed beach positions, using the numerical (solid lines) model, and the semi-analytical with ε_s, (dotted lines) and ε_w (dashed lines), at four output times (end of each storm of Figure 4.1b and end of time-series respectively).

Figure 6.8a shows that the semi-analytical and numerical solutions still agree quite well, although there is an obvious increase in RMSE in comparison to the situation when waves of small wave angle were input in the models (Figure 6.4) and in comparison to the evolution of the Gaussian beach fill examined before. As in the case of the Gaussian fill

evolution, the pattern of the RMSE variation is different to that of Figure 6.4, with a substantial increase in RMSE during the third storm and a relatively much smaller decrease after it. In terms of numbers, in Figure 6.8a, the value of RMSE from t = 150hrs (start of third storm) to t = 220hrs (peak of the third storm) increases by 31 times compared to 20 times in Figure 6.4. This result is for ε_s. In contrast to the case of the Gaussian nourishment (Figure 6.6a), when ε_w is used, the RMSE error is higher than that obtained with ε_s. Further, the discrepancy between the two lines of Figure 6.8a increases slightly in time. This result is the reverse of what it was expected, as the latter diffusion coefficient is supposed to be more accurate for larger wave angles. Figure 6.8b shows that the numerical solution falls somewhere in the middle between the two semi-analytical solutions, being closer to the one obtained with the use of ε_s than to that obtained with the use of ε_w.

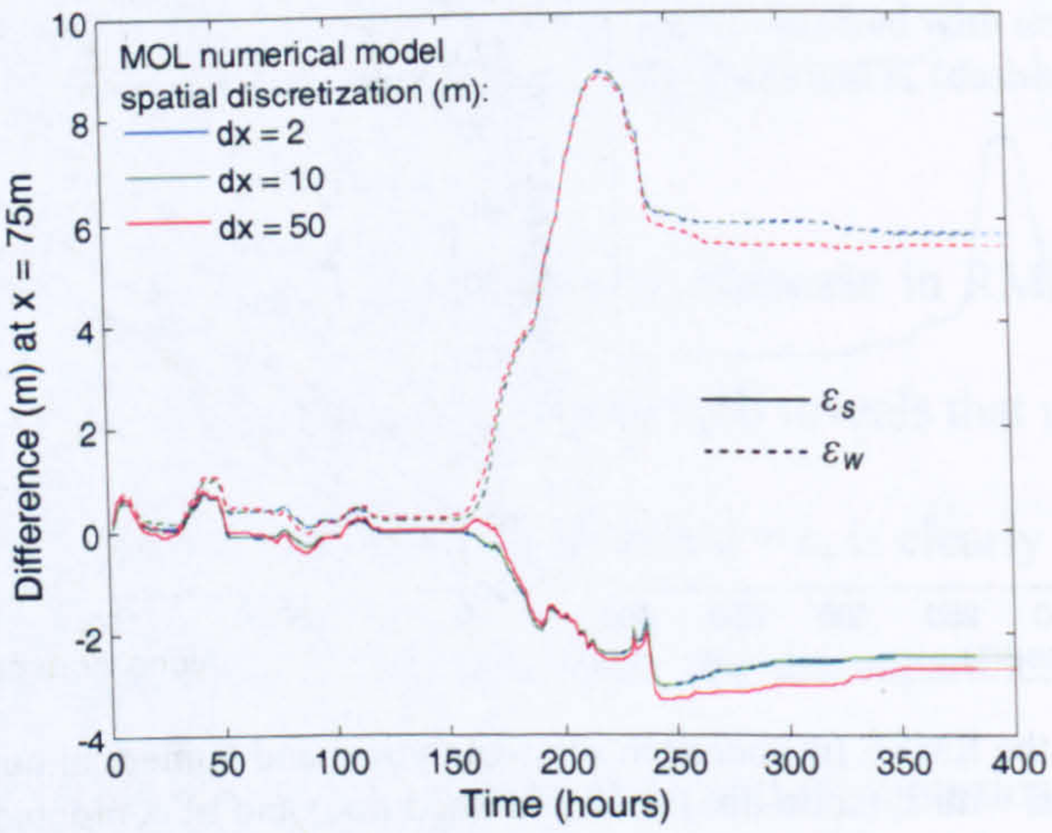

Figure 6.9 Time evolution of the difference between the semi-analytical and numerical solution, at x = 6000m. The discrepancy is calculated for three different MOL solutions obtained with dx = 2, 10, and 50 respectively and for two semi-analytical solutions obtained with ε_s (solid lines) and ε_w (dashed lines) respectively.

Figure 6.9 shows trends similar to the case of the Gaussian nourishment (i.e. Figure 6.7 compared to Figure 6.3). In general, the effect of the higher wave angles in the time-series is to speed up the evolution of the semi-analytical solution obtained with the use of ε_s relative to that of the numerical solution; the larger the dx the slower the relative evolution

of the numerical solutions. Specifically, focusing on the lines corresponding to ε_s in Figure 6.9, it is observed that up to the third storm the shape of the variation of the differences is very similar to that of Figure 6.5 (left) although a faster interchange in the relative position of the two solutions occurs, indicating a higher erosional potential for the semi-analytical solution. The most evident change is again during the third storm when the difference between the two solutions clearly increases. This increase is in the opposite direction (opposite sign) compared to Figure 6.5 (left). In other words, when low wave angles (Figure 6.1) were input in the models, the numerical solution was more erosive relative to the semi-analytical solution during the high waves of the third storm; in contrast, the high wave angles encountered during this storm reverse this result leading to the numerical solution being quite less erosive relative to the numerical output. Some peaks towards smaller differences are encountered during the aforementioned increasing trend of the solid lines of Figure 6.9. These peaks correspond to the highest waves of this storm and indicate that very high waves may overcome the effect of high angles and lead to a faster evolving numerical solution. The semi-analytical solutions obtained with the use of ε_w bring results towards the right direction, i.e. decrease the rate of evolution/erosion of the shoreline. However, they provide a conservative estimate, always lagging behind the numerical solution by a greater distance compared to that by which the semi-analytical solutions with ε_s overtake the numerical results. This is why the differences of Figure 6.9 that correspond to ε_w evolve in the opposite direction of those that correspond to ε_s and are of greater magnitude.

The reason why the use of ε_w produces higher RMSE errors between the semi-analytical and numerical results for this case of shoreline change is not straightforward. Calculations of the sediment transport rate Q computed with three sediment transport formulae, one used in the numerical model (Equation 2.18), one used to derive the semi-

analytical model with $\varepsilon = \varepsilon_s$ (Equation 2.19), and one used to derive the latter with $\varepsilon = \varepsilon_w$ (Equation 2.22), respectively, revealed that for a wide range of local shoreline orientation $(\partial y/\partial x)$ values, the values of Q computed with Equation 2.19 are closer to those computed with Equation 2.18 (the one containing no small angle assumptions) than those computed with Equation 2.22. For example, for constant Q_0 and a constant $\alpha = 10^0$ the range of $\partial y/\partial x$ within which the above observation is valid is 0.06-0.26. For constant $\alpha = 30^0$ this range becomes 0.19-0.5 (0.5 is the maximum value attempted). In fact, the lower limit of this range increases linearly with wave angle. Such local shoreline orientation values are encountered as the shoreline adjusts within the groyne compartment and are the reason for the higher RMSE obtained with the use of ε_w. In the case of the evolution of the Gaussian nourishment, the Gaussian hump evolves towards lower values of $\partial y/\partial x$ so that the above observation on the values of Q is no longer valid after $\partial y/\partial x$ becomes small enough. Indeed, Figure 6.6a shows that the RMSE corresponding to ε_w is initially bigger than that corresponding to ε_s (over about the first 50hrs) but it becomes smaller with time.

6.3 Discussion

In this chapter, the 'one-line' semi-analytical solutions derived in Chapter 4, which account for time-varying wave conditions, were compared to the numerical solutions of the MOL based 'one-line' numerical model, which was developed in Chapter 5. Input to the models were two different wave time-series respectively, the first incorporating only small wave angles relative to the global shoreline orientation, the second including several highly oblique waves. Semi-analytical solutions obtained both with the use of ε_s and ε_w were used in the analysis for the latter case whilst only ε_s solutions were used for the former case. Results from the two models, semi-analytical and numerical, were compared for two cases

of shoreline change: (1) unconstrained evolution of a smooth Gaussian hump, and (2) evolution within a groyne compartment. It was not attempted to assign a higher accuracy to one or the other model, since both consist approximations with largely unquantifiable errors for the case where wave conditions are arbitrary functions of time.

Excellent agreement between the two solutions was found for the small wave angle time-series, since the 'small angle approximations' of the analytical work are achieved in this case. The agreement was somewhat better for the Gaussian nourishment evolution than for shoreline change within a groyne compartment. This is attributed to larger local shoreline orientations associated with the latter case. For both cases, it was found that high waves in the time-series cause the numerical solution to evolve faster relative to the semi-analytical solution. Thus, in the case of the Gaussian fill, storms caused faster spreading of the fill. In the case of the groyne compartment, they caused faster erosion or accretion depending on the wave direction relative to the shore normal. In this case, even during periods of relatively low wave activity, the numerical solution responded faster to changes in the direction of the flow, e.g. faster transition from erosion to accretion relative to the semi-analytical output. In the case of the Gaussian fill evolution, it was observed that in the long-term, the semi-analytical solution is slightly more diffusive than the numerical. This is in agreement with Hanson (1987) who found that for this case of shoreline change, the analytic solution produced an overestimation of the fill erosion although the small wave angle assumption was not violated.

Good agreement between the two solutions was found when the wide-angle wave time-series was used as input in the models. However, as expected, this agreement was clearly less good than that found above because of the violation of the small angle assumptions of the semi-analytical solutions in this case. Hanson and Larson (1987) demonstrated that the error caused by linearizing the transport equation is an overestimation

of the speed of shoreline response. In both of the problems examined herein, high wave angles caused the semi-analytical shoreline evolution to speed up relative to the solutions obtained by the numerical MOL solution. Nevertheless, very high waves in the time-series were able to overcome the effect of high wave angles.

When ε_w was used along with the wide-angle time-series as input, in accordance with what would have been expected, the agreement between semi-analytical and numerical solutions improved in the case of the Gaussian fill. However, in contrast to expectations, this agreement became worse in the case of shoreline evolution within a groyne compartment. This result was found to be because of a high sensitivity of the ε_w semi-analytical solutions to the value of the local shoreline orientation. Adopting values of constant wave angle it was revealed that there is a corresponding threshold shoreline orientation value above which the agreement between ε_w semi-analytical solutions and numerical solutions is less good that the agreement of the latter with ε_s semi-analytical solutions. For wave angles between 5^0 and 40^0, this threshold value varied linearly between 0.03 and 0.25. In general, the use of ε_w brought semi-analytical results towards the right direction, i.e. decreased the rate of evolution/erosion of the shoreline. However, they always lagged behind the numerical solution by a greater distance compared to that by which the semi-analytical solutions with ε_s overtook numerical results.

The analysis presented in this chapter adds to previous work on the comparison between analytical and numerical solutions in the sense that the effect of the variation of the wave characteristics in time on the discrepancy between different solutions could be investigated. For example, in short, the observations of this chapter include:

- High wave heights have a subtle effect on the results by increasing the rate by which the numerical shoreline evolves relative to the rate of evolution of the semi-analytical output.

- High wave angles can often prevent this effect as they cause analytical solutions to speed up as a result of the violation of the assumption of 'small' angles.
- Whether 1 or 2 will dominate depends on the severity of the storm.
- ε_w might be a worse approximation than ε_s in certain cases of shoreline change.

Chapter 7

Wave climate scenarios

The 'one-line' semi-analytical and numerical models, developed in Chapters 4 and 5 respectively will be used in Chapter 8 to investigate how the evolution of a hypothetical sandy shoreline stretch might change in response to different future wave climate scenarios (2071-2100) relatively to its 'present' evolution (1961-1990). Since nearshore wave conditions at or near breaking are required as input to the models (Section 2.2.3.4), the aim of this chapter is to describe the original data sets available and the methodology adopted to obtain the nearshore wave climate scenarios, used directly in the 'one-line' climate runs of Chapter 8. Specifically, this chapter describes wind data sets, obtained from climate models at a single offshore location, the hindcast of corresponding deep water wind waves, and their transformation to a single inshore location. Model calibration processes are explained and brief wave data statistics are presented. Essentially this chapter constitutes the methodology chapter (excluding decision on parameter values directly relevant to the 'one-line' model simulations) of an impact assessments study – impact of climatic changes in wave characteristics on shoreline evolution – the results of which are presented in Chapter 8.

As with all climate impact assessment studies, the present study (Chapters 7 and 8) involves assumptions, limitations, and considerable uncertainty. These will be slowly revealed going through the methodology and will be discussed at the end of this chapter and in Chapter 8 along with the advantages of the present approach. If the reader wishes at this point to have a more complete idea of the procedures, limitations, and advantages related to the present work, they are prompted to the introduction of Chapter 8 and the last two sections of this chapter. Here, only the basic concept that largely determines the methodology adopted is highlighted. This is the interest of this study on the different relative effect the various wave climate scenarios ('present' versus future) have on shoreline evolution rather than the actual accuracy of each scenario, essentially the accuracy of the 'control' time-series against measurements or other 'actual' data. As a result, model validation procedures are not of great importance. Instead, it is important to ensure that realistic wave conditions are used in the analysis. This concept is in agreement with the adoption of a hypothetical shoreline stretch.

7.1 Methodology - data

7.1.1 Wind climate scenarios

Wind output from a number of time-slice (30-year) experiments (Table 7.1), done within the frame of the PRUDENCE project (Section 3.2.5), is used in this study. Data come from one RCM called HIRHAM (Christensen *et al.*, 1996) at two spatial resolutions, 12km and 50km respectively. Wind output frequency is 3 hours. Only A2 SRES scenario was available at 12km resolution. Both A2 and B2 scenarios (Section 3.2.1) were available at 50km resolution. At 50km resolution, output from HIRHAM driven by two GCMs was

obtained. One is the HadAM3H (Pope *et al.*, 2000) which is a high resolution (≈ 120km) AGCM. The other is the ECHAM4/OPYC (Roeckner *et al.*, 1996) which is a coarser resolution (≈ 300km) AOGCM. Simulations driven by the former GCM will be referred as HIRHAM-H (-H12 if at 12km resolution and -H50 if at 50km) in the text whilst those driven by the latter GCM will be referred as HIRHAM-E (-E50). These two experiments also differ with respect to the monthly mean SSTs used to drive the climate models and the nature of the wind output. In the first experiment (HIRHAM-H) the SSTs used in the 'control' experiment are monthly mean observations whilst instantaneous winds are output. In the second experiment (HIRHAM-E) SSTs are taken directly from the driving AOGCM whilst 3-hourly average winds are output. The use of observed SSTs better constrains a GCM towards the observed climate (Christensen and Christensen, 2007). Climate model wind output was available only for one model realization (Section 3.2.4) for each experiment shown in Table 7.1.

Table 7.1 Climate model time-slice experiments used in this study

RCM	AGCM	SRES	Control period	Scenario period	Resolution	Abbreviations	
						control	scenario
HIRHAM	HadAM3H	A2	1961-1990	2071-2100	12km	C12	A12
HIRHAM	HadAM3H	A2	1961-1990	2071-2100	50km	HC50	HA50
HIRHAM	HadAM3H	B2	1961-1990	2071-2100	50km		HB50
HIRHAM	ECHAM4	A2	1961-1990	2071-2100	50km	EC50	EA50
HIRHAM	ECHAM4	B2	1961-1990	2071-2100	50km		EB50

Wind data consisted of the zonal, *u*, and meridional, *v*, components of the wind vector at two offshore locations corresponding to the two horizontal RCM resolutions. The data location for the 12km resolution climate experiment is at 50.5246° North and -1.6410° East whilst for the 50km resolution experiments is at 50.5965° North and -1.5942° East. Location coordinates correspond to the middle of the grid cells (e.g. 12km x 12km grid cell for the 12km resolution experiment) and are situated at the south central coast of England,

offshore from Poole Bay. At the eastern end of the Bay lies Hengistbury Head. The latter is fronted by a shoreline stretch which, at the start of this study, was thought to be well suited for one-line modelling applications. This, along with the fact that a relatively rich set of beach profile and wave data existed at the site, were the reasons the aforementioned data points were chosen. Nevertheless, as already mentioned, a hypothetical shoreline stretch was employed for this study. This is because of 'one-line' modelling complications at the site, described in Section 8.2.

Figure 7.1 depicts the wind data locations (green dots) along with the extent of the corresponding grid cells, the blue box for the 12km resolution and the whole figure extent for the 50km resolution. Both cells embrace a UK Met Office wave hindcast point (red dot) which is located at 50.50° North and -1.66° East, at 33m water depth (Ordinance Datum Newlyn (ODN)). Nearshore, the red dot denotes a refraction point, located at Hengistbury Head, at 50.7097° North and -1.7493° East, and at 3.53m water depth (ODN). Offshore

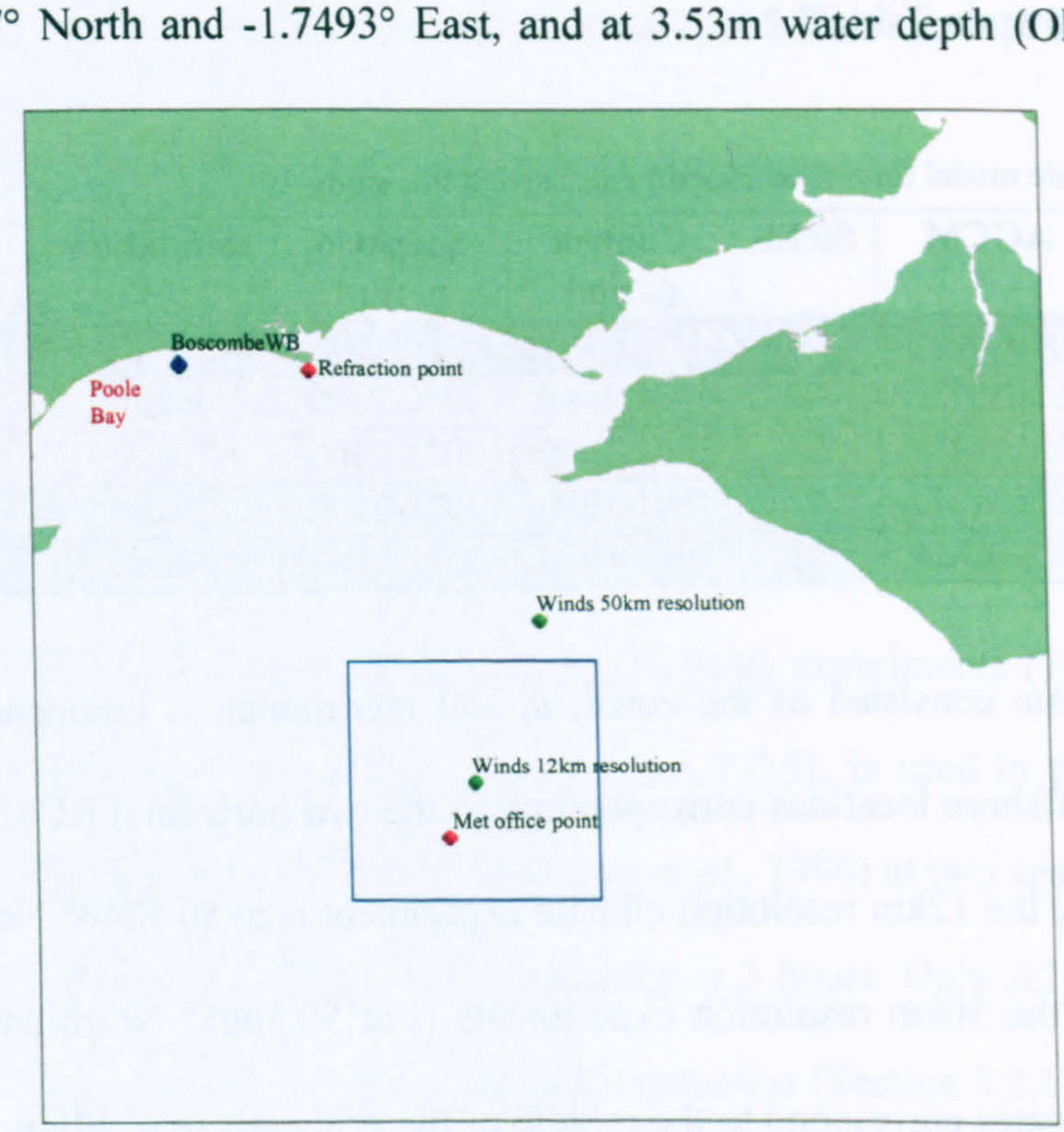

Figure 7.1 Wave data locations offshore Poole Bay including 1) locations of RCM wind data (green dots), 2) the Met office hindcast data location (offshore red dot), 3) a nearshore refraction point (inshore red dot), and 4) a nearshore wave buoy (blue dot).

waves will be transformed to this point in this study. The blue dot represents a directional wave buoy placed at about 11m water depth. The latter will not be used herein.

All the 30-year time-series of 3-hourly winds corresponding to the different simulations of Table 7.1 are used in the following analysis. This starts with the hindcast of deep water wind waves and continues with their inshore transformation. Thus, 30-year time-series of 3-hourly nearshore wind waves are generated which directly correlate to the different experiments of Table 7.1.

7.1.2 SANDS software and other data

The Shoreline and Nearshore Data System (SANDS) was used in this study to retrieve, store, and manipulate data. This is a sophisticated user friendly software, developed by Halcrow Ltd, where a large amount of data of varying nature related to the coastal zone (e.g. winds, waves, currents, beach profiles, bathymetric profiles) can be stored, monitored, and analyzed. The most powerful features of SANDS include: (1) input data can be analyzed to establish links between forcing and response and (2) data and statistics can be visualized through graphs, diagrams, roses, etc, and locations through GIS mapping. Details on the capabilities of SANDS may be found on the SANDS website (http://www.halcrow.com/software/solutions/sands_home.asp, 2007).

SANDS is presently used by a number of city councils and some coastal research institutions who store data in the software and often make it freely available to the wider research community. Data for the southern coast of England, including the study area, come mainly from the Strategic Regional Coastal Monitoring Programmes, funded by DEFRA, and are managed and disseminated by the Channel Coastal Observatory (http://www.channelcoast.org/, 2008). Quality controlled data used in this study belong to

the Poole Bay City Council and were made available through the Channel Coastal Observatory in SANDS format. The data consists of:

- A 17-year time-series of 3-hourly hindcast waves (wave height, period, and direction) at the Refraction point of Figure 7.1. The time-series covered the period 01/07/1988 – 31/12/2005.
- A 'refraction coefficients' file for the transformation of deep water waves from the Met Office point of Figure 7.1 to the Refraction point.
- Tidal constituents for the prediction of nearshore tidal levels, needed for the nearshore wave transformation.

The first data set was used to 'calibrate/validate' the deep water wave hindcast. The second and third data sets were used to perform the wave transformation of the deep water hindcast waves to the Refraction point through the SANDS software. The process of offshore wave hindcast and inshore wave transformation are outlined below.

7.1.3 Deep water wave hindcast

A parametric, point hindcast model, based on modified SMB hindcast expressions which account for non-coincident wind and wave directions for fetch limited waves, is used in this study to hindcast deep water waves for the full set of wind data described in Section 7.1.1. The model was described in Chapter 2, Section 2.2.3.4., and its basic formulae are documented in Donelan (1980) and CERC (1977). In what follows, it is referred as the SMB-Donelan model.

To calculate deep water wave characteristics (wave height, period, and direction) the model requires wind speed and direction as input. These were obtained through the u and v components of the wind vector using the simple formulae

$$\text{Wind speed} = (u^2 + v^2)^{1/2}$$

$$\text{Wind direction} = \arctan(u/v) + k$$

where $k = 0$ for $u, v > 0$, $k = 360°$ for $v > 0$ and $u < 0$, and $k = 180°$ for $v < 0$ and $u > 0$ or $u < 0$.

Required model input is also the fetch lengths extending from the hindcast location to the surrounding coastline in radials at specified direction intervals. Here, fetch lengths were calculated for the Met Office point (Figure 7.1). This was done under the assumption that winds corresponding to the climate model locations (green dots in Figure 7.1) would remain approximately the same at the Met Office point. This assumption was made because the 'transformation coefficients' file (Section 7.1.2) used in the SANDS wave transformation module specifically links the Met Office point to the Refraction point of Figure 7.1. The validity of the assumption is expected to be strong for the 12km resolution winds and to deteriorate somewhat for the 50km resolution winds because the middle of the grid cell in this case is further away from the Met Office point. Table B1 (Appendix B) shows the directions (degrees from North) at which fetches were estimated and the corresponding fetch lengths (kilometres). The table contains 39 fetch limits with spacing between 3^0 and 15^0, chosen to best represent changes in the distance between the hindcast location and the surrounding coastline (Figure 7.2). Most frequent spacing is around 9^0. For the fetch limit interval 228^0-257^0, the radials extend to the Atlantic Ocean (i.e. no land interception), (Figure 7.2). For this interval, the value of 1000km fetch length was chosen through model calibration (see Section 7.1.5).

In addition to the inputs, a number of parameters have to be specified by the user in the model. These are:

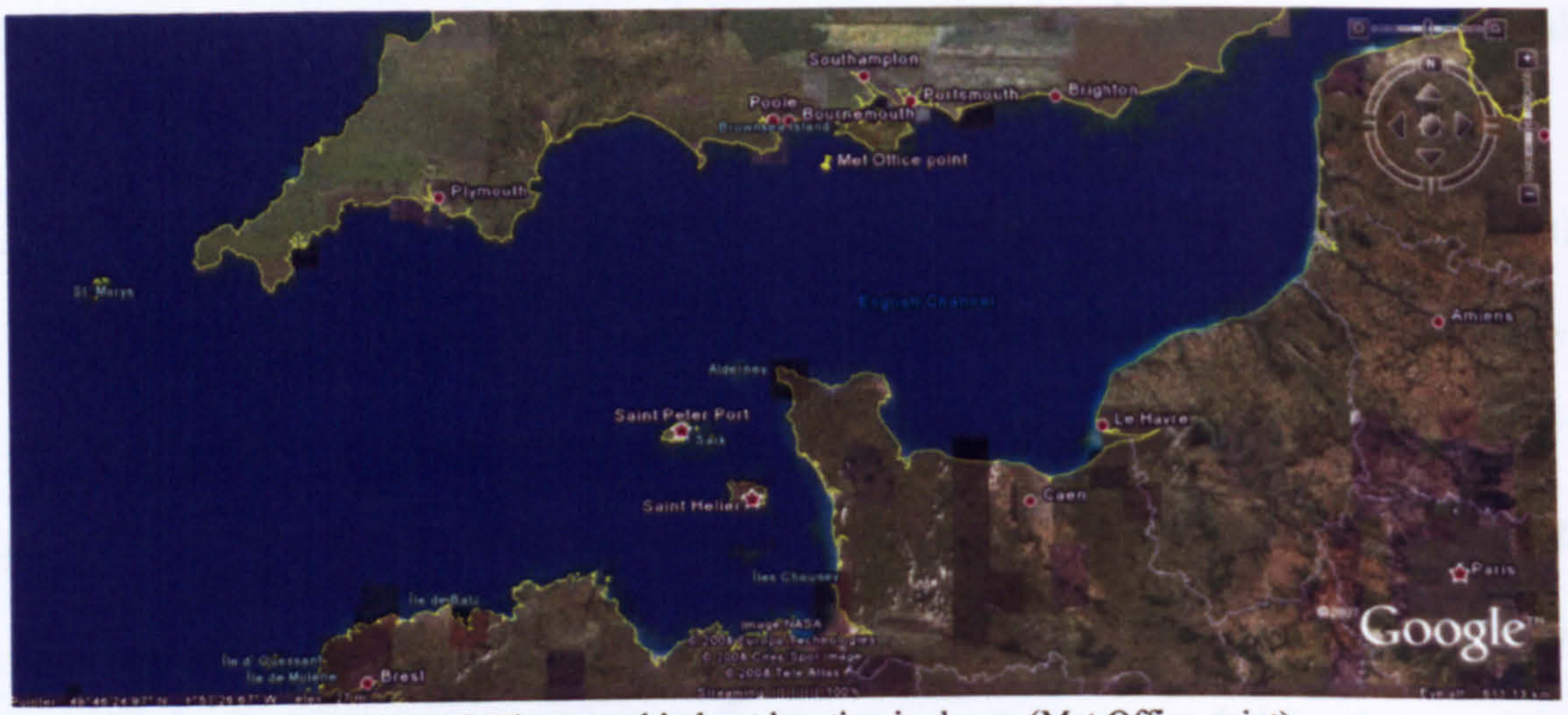

Figure 7.2 The English Channel. The wave hindcast location is shown (Met Office point).

- *Wind convergence angle*: Defines regions of constant wind speed and direction associated with fetch calculations.
- *Use of average or minimum wind speed in back-stepping process*: Back-stepping from the new wind record to successive previous records is performed to estimate wind duration. If successive records are within the "wind convergence angle" an average wind direction and an average or minimum wind speed (user's choice) are calculated. The wave due to the averaged wind is hindcasted.
- *Rate of decay exponent*: Rate at which wave energy decays if the wind drops or changes direction.
- *Use of effective or straight fetch lengths*: Effective fetch lengths, in contrast to straight lengths, account for the narrowness of the fetch lengths, e.g. in small lakes.

The "wind convergence angle" is typically taken to be between 15^0 and 45^0. According to CERC (1984) wind direction is very likely to be constant within 15^0, likely enough within 30^0, and less likely within 45^0 (not uncommon value in engineering practice). The "wind convergence angle" is used in the model to estimate wind duration, i.e. the period over which the wind causes the wave to grow (unless of very low speed). For the "rate of decay

exponent", a linear rate is typically assumed although this parameter is normally found by model calibration as no correct or most appropriate value exists (Kamphuis, 2000). Regarding "effective fetch lengths", these would be more appropriate for restricted water bodies rather than the open see where "straight fetch lengths" work well (CERC, 1984). The final values of the parameters were determined through model calibration (see Section 7.1.5). Hindcast wave files were input in SANDS for subsequent inshore wave transformation. Wave files consisted of the significant wave height, H_s, peak period, T_p, and mean wave direction, θ_0.

7.1.4 Inshore wave transformation

The SANDS wave transformation module was used in this study to predict inshore wave characteristics (H_s, T_p, and α) from the offshore hindcast wave data, described above, through the use of known wave refraction and tidal data. The full set of offshore hindcast wave data (30-year time-series of 3-hourly waves corresponding to the climate experiments of Table 7.1) was transformed inshore in SANDS. Approximately 15min were required for the transformation of each of the 30-year time-series.

As mentioned above, transformation took place from the Met Office point in deep water to the Refraction point at 3.53m water depth (Figure 7.1). Nearshore tidal levels, required over the wave transformation periods, were predicted in SANDS from known tidal constituents (62 constituents) at the Bournemouth tide gauge, located at 50.7127 North and -1.8653025 East. Ultimately, transformation was performed through the use of a wave transfer coefficient file, generated with the REFPRO ray back-tracking spectral wave energy transformation model (Section 2.2.3.4). The refraction coefficient file, linking the Met Office point to the Refraction point, was readily available (i.e. no additional REFPRO runs needed to be done by the user). Since SANDS wave transfer files are linked to

specific locations, incorporation of sea-level rise would alter the depth at these locations so that 'modeled' wave conditions for the 'control' and 'scenario' runs would not be directly comparable. Consequently, a constant mean sea-level (MSL) was assumed for the transformation of all wave climate scenarios. Thus, the effect of sea-level rise (SLR) on the nearshore transformation of future waves (Section 3.1) was not taken into account in this study, introducing uncertainty in the estimation of differences between 'present' and future shoreline evolution (Chapter 8). Such an effect could be partly incorporated through the use of the Bruun Rule (Section 8.3.3), described in Section 3.3.1 Further uncertainties relate to the exclusion of any bathymetric changes over time and of potential changes in tidal range in the future.

7.1.5 Wave hindcast model calibration

Offshore wind or wave data were not available to this study to validate the climate model output or to calibrate/validate the output of the SMB-Donelan model at the Met Office offshore point. The only data available for the wave hindcast model calibration was the 17-year (1988-2005) hindcast wave time-series (3-hourly) at the Refraction point (Section 7.1.2). This time-series was generated by transforming inshore deep water hindcast waves obtained at the Met Office point, using the 25km resolution Met Office European Waters wave model (EMO for the remainder of this study). Transformation was carried out in SANDS as above: Therefore, calibration of the SMB-Donelan model was done by maximizing the agreement between SMB-Donelan and EMO transformed waves at the Refraction point.

Being a hindcast, the EMO nearshore time-series is also associated with a number of inaccuracies (Bradbury *et al.*, 2004). As a result, comparison of hindcast waves against hindcast waves could only lead to approximate model calibration/validation. Nevertheless,

the EMO model has been extensively validated and has shown reasonable agreement with measurements (Bradbury *et al.*, 2004). Yet, the comparison between SMB-Donelan and EMO model output is further constrained by differences in calculation methods and incorporated processes. The main differences of EMO model include:

- Different spatial resolution which may affect grid integrated model input and output.
- JONSWAP spectrum is used.
- Different frequency and directional resolution (22.5^0).
- Incorporation of swell from distance sources (the Atlantic in this case).
- Incorporation of wave energy dissipation due to breaking.

In addition, winds produced by climate models, input to SMB-Donelan, are of different accuracy to those produced by mesoscale Numerical Weather Prediction (NWP) models, input to EMO. Climate model output is usually less accurate (Section 3.2.6.2). To conclude, fitting SMB-Donelan waves against EMO waves is appropriate only in the sense of maximizing the realism of the former model output or in other words of generating wave climate scenarios as close to reality as possible. This rationale was adopted for the calibration of the SMB-Donelan model.

The higher resolution (12km) 'control' wave climate scenario, C12, was used for the above comparison. The latter was performed in terms of annual means and maximum values with the focus on the agreement of H_s rather than T_p or α (inshore wave direction) which will be more affected by the presence of swell. Since only two years of overlap (1989-1990) existed between the two time-series, SMB-Donelan model calibration aimed to closely reproduce the range of annual means and inter-annual variability of the subsequent 17 years EMO results.

The range of inshore wave directions used for back-tracking in REFPRO is 131^0-204^0 for this location. Anything outside this range is a very low period deep water wave

that retains its offshore values at the nearshore location. These corresponded to calm waves (Figure 7.3) for which H_s = 0.2m, lower limit assigned by the wave transformation model. All waves of H_s = 0.2m were treated as calms with H_s, T_p, and α = 0. After a sensitivity analysis of the SMB-Donelan model to the variation of the parameters defined in Section 7.1.3 and to the fetch length from the sector 228^0-257^0 (Table B1) corresponding to the opening of the English Channel to the Atlantic Ocean (Figure 7.2) the parameter values of Table 7.2 were chosen as those that give the best agreement with EMO data. Figure 7.3 shows the resulting annual means of the inshore wave characteristics (and maxima for H_s) for the two different time-series and the annual percentage of calm events (H_s = 0m). Table 7.3 shows some basic statistics of the two time-series as a whole and Figure 7.4 shows associated wave roses. The wave roses do not include calm waves.

The combination of parameter values in Table 7.2 is not unique. Results from different combinations could also be 'reasonable' since the mean wave statistics associated solely with wind waves (or 'local swell') at the area are not well known for a more comprehensive comparison. In general, an increase in the wind convergence angle leads to an increase in the yearly mean H_s accompanied by a decrease in its maximum values. However, Bradbury *et al.* (2004) have found that EMO underestimates max H_s so that even higher values than those shown by the upper red line in Figure 7.3a would be expected. Moreover, a lower mean of the SMB-Donelan output wave heights is normal. This is because the model does not account for swell which overall lead to higher waves (Hawkes *et al.*, 1997), and because climate model winds have been found to be weaker than actual winds (Section 3.2.6.2), a result however found with data of a daily resolution. The effect of using minimum wind speed in the back-stepping process or of increasing the rate of decay exponent or of using effective fetches is to decrease the wave heights. In turn, lower waves result in strengthening the directional bin of 150^0-165^0 at the expense of the

dominant wave direction of 180^0-195^0 as shown in the 'actual' wave rose of Figure 7.4 (left). Decreasing the fetch length from the Atlantic has the same effect. Thus, although the

Table 7.2 Parameter values adopted in the SMB-Donelan deep water wave hindcast

Parameter	**Value**
Wind convergence angle	15^0
Use of average or minimum wind speed in back-stepping process	Average
Rate of decay exponent	0.2
Use of effective or straight fetch lengths	Straight fetch lengths
Fetch length from 228^0-257^0	1000km

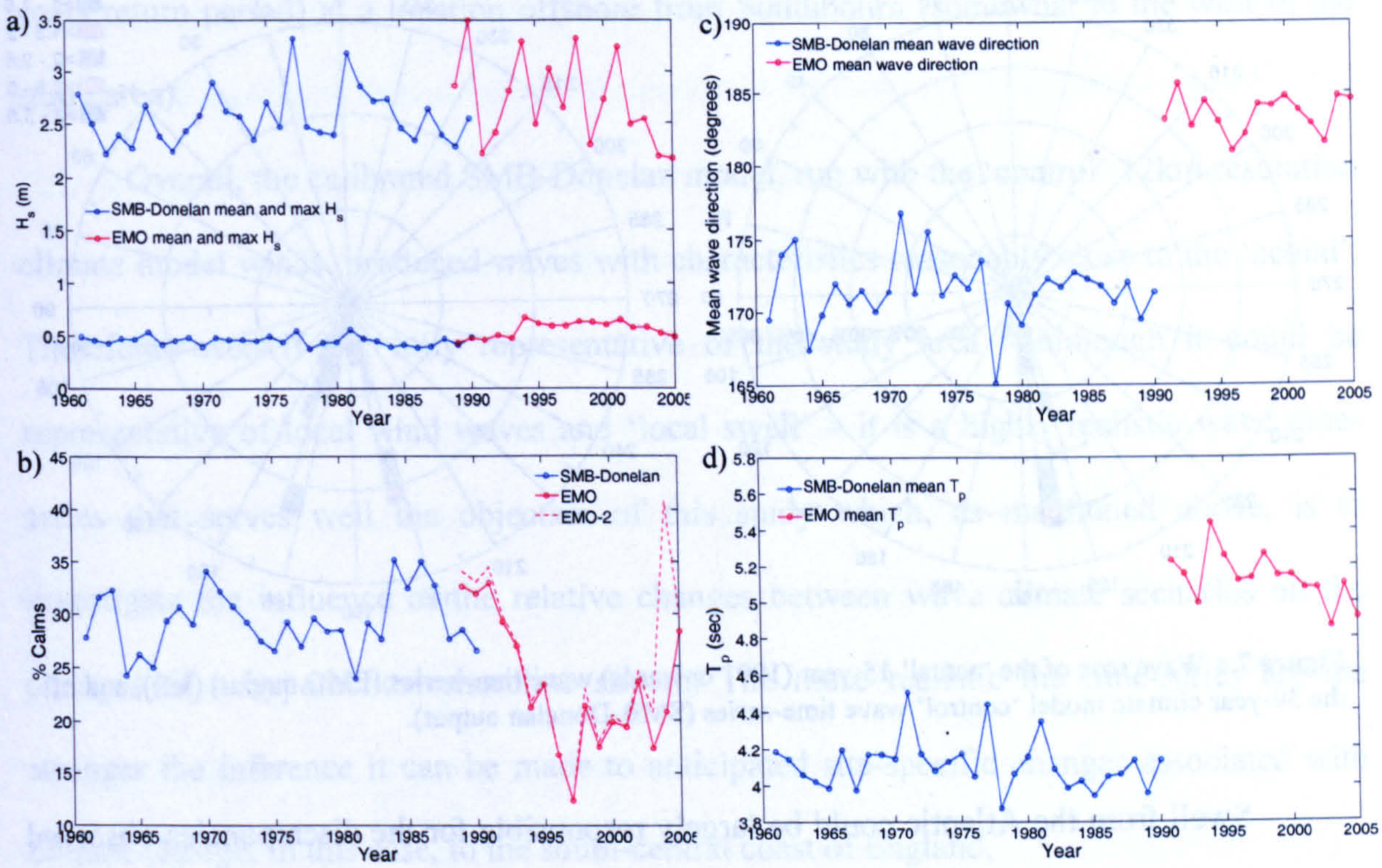

Figure 7.3 a) yearly mean maximum and mean H_s corresponding to SMB-Donelan (12km 'control' wave climate scenario) and EMO model (NWP driven waves) output respectively, b) yearly percentage of calm waves for the two time-series; EMO line excludes missing values from the analysis, EMO-2 dashed line replaces missing values with calms. Similarly c,d) yearly mean wave direction and T_p respectively (EMO data for years 1989 and 1990 are discarded because of an error in the prediction of wave direction before May 1990 (Halcrow, 2004)).

adopted value of 1000km is somewhat unrealistic (Kamphuis (2000) suggests that wind speed and direction are unlikely to be constant over fetch lengths greater than 500km), it does produce results closer to the 'actual' ones.

Table 7.3 Basic statistics of the 12km 'control' wave climate scenario (output from SMB-Donelan model (SMB in the table)) and of the 25km 'actual' wave climate (output from EMO model).

	SMB H_s	EMO H_s	EMO H_s*	SMB α	EMO α	SMB T_p	EMO T_p	Offshore SMB H_s
Min	0	0	0	146.6	149.3	3	3	0
Max	3.31	3.49	3.49	196.4	195.6	8.33	12.05	6.92
Mean	0.45	0.56	0.55	171.5	183.9	4.15	5.23	1.22
Median	0.35	0.45	0.44	165.7	187	4.32	4.52	1.05
Standard deviation	0.46	0.5	0.5	14.87	9.4	1.15	1.47	0.87
Range	3.31	3.49	3.49	49.77	46.23	5.33	9.05	6.92

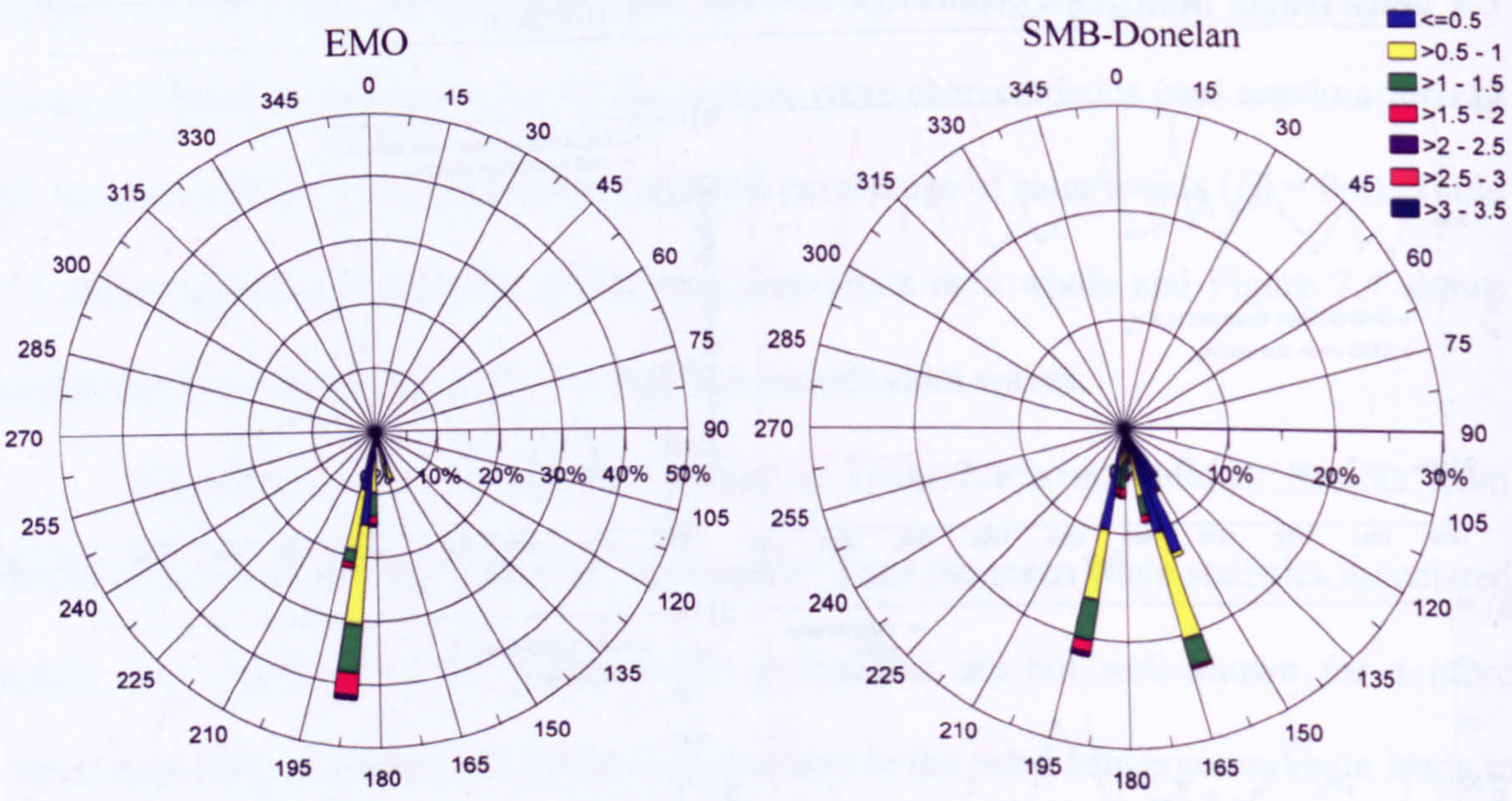

Figure 7.4 Wave rose of the 'actual' 15-year (1991 onwards) wave time-series (EMO output) (left), and of the 30-year climate model 'control' wave time-series (SMB-Donelan output).

Swell from the Atlantic could be largely responsible for the discrepancies observed between EMO and SMB-Donelan output since swell occur about 45% of the time at the study area (Hawkes *et al.*, 1997). Omission of swell from the SMB-Donelan model explains well the observed shift in prevailing wave direction to the south-southeast and the lower mean T_p values (Figures 6.3 and 6.4). Indeed, studies on the wave regime of the study area do support that local wind waves approach mainly from the south-southeast (SCOPAC, 2003) with the south-southwest approach being also dominant. Table 7.3 shows a shift of 12.4^0 in mean wave direction and of 21.3^0 in median. Also, a higher spread in the

directions of the SMB-Donelan waves is evident in Figure 7.4 and is expressed by the higher standard deviation in Table 7.3. This could be further associated with the finding that climate models tend to produce winds of a higher spread than actual (Section 3.2.6.2). Mean T_p is about 20% lower and so is the mean wave height (Table 7.3). A higher percentage of calm events is encountered in the C12 wave time-series (SMB-Donelan output). The offshore max H_s of 6.92m (Table 7.3) agrees well with a study by Halcrow (1999) which found that max H_s varies between 5.5m (1 year return period) and 7.4m (50 years return period) at a location offshore from Southbourn (somewhat to the west of the study area).

Overall, the calibrated SMB-Donelan model, run with the 'control' 12km resolution climate model winds, produced waves with characteristics reasonably close to the 'actual'. Therefore, even if not fully representative of the study area – although it could be representative of local wind waves and 'local swell' – it is a highly realistic wave time-series that serves well the objective of this study which, as mentioned above, is to investigate the influence of the relative changes between wave climate scenarios on the changes of a hypothetical shoreline stretch. The more realistic the time-series are the stronger the inference it can be made to anticipated site-specific changes associated with climate change. In this case, to the south-central coast of England.

7.2 Monthly means and the significance of their differences

In Chapter 8, discussion on relative shoreline change in response to the various wave climate scenarios (Table 7.1) is in terms of monthly statistics. Here, it is ensured that such comparisons are justified, i.e. that there are significant differences in the input time-series to the 'one-line' model or in other words in the monthly wave statistics of the

'control' and 'scenario' climate simulations. Besides, monthly information on the forcing conditions is required to better understand and explain the changes examined in Chapter 8. In particular, in this section, the monthly mean values of the significant wave height, H_s, and of the mean wave direction are calculated for the different wave scenarios and are then tested in suitable pairs for significant differences. A conventional robust hypothesis test on the difference in means of two samples, known as the two-sample *t*-test, is performed.

The two-sample *t*-test can show if two independent samples having a normal distribution with unknown equal (or, optionally, unequal) variances, have the same mean or not. The mathematics of the test can be found in most relevant textbooks (e.g. Freund, 1992) and are not of immediate interest to this study. Here, the inputs and outputs of the *t*-test are summarized with reference to the Matlab software command

$$[h, p, ci] = \text{ttest2}(x, y, alpha)$$

where the inputs are within the parentheses on the right hand side, the outputs within the brackets on the left, and where "ttest2" denotes the two-sample *t*-test. The test accepts or rejects the 'null-hypothesis' that the two input samples, x, y, have equal means at a user specified significance level, *alpha*. The latter can be interpreted as the probability of rejecting the 'null-hypothesis' when it is actually true. For example, for a common value of *alpha* = 0.05 there is a 5% probability that the test result is false. Rejection or acceptance of the 'null-hypothesis' depends on the p value, which is the probability of obtaining by chance a value of the test statistic as extreme or more extreme than the value computed from the sample. If $p > alpha$ the test accepts the 'null-hypothesis'. In this case $h = 0$. If $p <$ *alpha* the test rejects the 'null hypothesis' and $h = 1$. The final output, *ci*, denotes the range of mean values with a 100(1-alpha)% probability of containing the true mean of the difference $x - y$ (Mathworks, 2001).

The t-test assumes that the data follow a normal distribution, that no serial autocorrelation exists (i.e. subsequent values in the sample are independent), and that the simulation is statistically stationary. The first assumption may be ignored for relatively large samples (Mathworks, 2001). The third assumption, although the 30-year future simulations are not stationary because of the gradually increasing greenhouse gas forcing, is also overlooked after Räisänen *et al.* (2003) who suggested that this effect is expected to be small. However, serial autocorrelation may severely impact on the test performance by causing the test to find significant differences when there are not any (Zwiers and von Storch, 1995). The climate data do exhibit autocorrelation. Its brief characteristics and a simple way around it are described below.

Figure 7.5 (left) shows the temporal autocorrelation of the significant wave height, H_s, and mean wave direction over 5 days (40 lags) for the 12km resolution 'control' wave

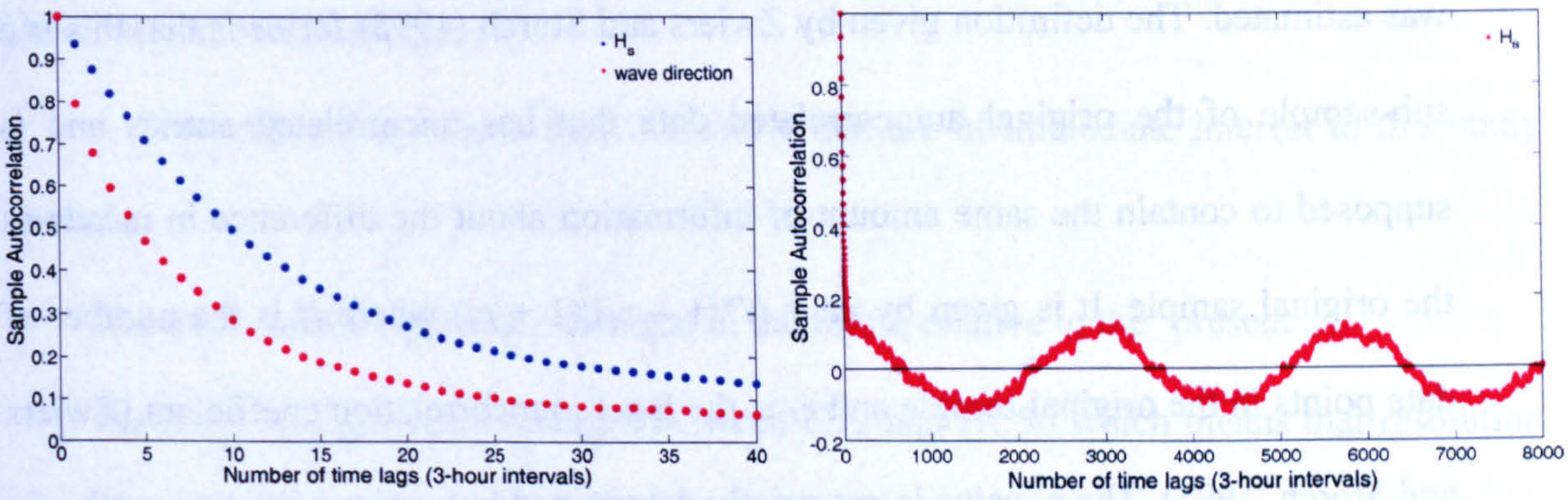

Figure 7.5 Temporal autocorrelation of the wave height, H_s, and the mean wave direction at lags from 3 hours to 5 days for the 12km resolution 'control' wave climate (C12) (left), and temporal autocorrelation of H_s only at lags from 3 hours to 500 days (right).

time-series (C12). Figure 7.5 (right) shows the autocorrelation of H_s over 1000days (8000 lags). The former indicates that the data come from an underlying autoregressive model with moderate autocorrelation (i.e. the decrease in autocorrelation is close to linear; however noise is present) (http://www.itl.nist.gov/div898/handbook/, 2006). The latter shows that the autocorrelation of H_s has a sinusoidal pattern that is repeated with a period

of one year (2880 lags = 360 days). This indicates that the observed autocorrelation is the result of a yearly cycle in the time-series. A very similar autocorrelation pattern was found for all climate experiments (Table 7.1).

Fitting a statistical model to the data and performing the *t*-test on the remaining random variations could be a solution to the problem of autocorrelation. However, this approach is fairly elaborate and of unnecessary complexity for the purpose of this study which is the simple identification of significant differences in the samples' monthly means. Instead, a simple, 'clean', and straightforward approach is adopted herein. This is to take sub-samples from the original sample so that the autocorrelation disappears. Specifically, the procedure followed here consists of two main steps:

- After the original 30-year time-series were separated by month (i.e. time-series of 30 consecutive Januaries etc), the equivalent sample size, *ne*, for each individual sample was estimated. The definition given by Zwiers and Storch (1995) for *ne* is that this is a sub-sample of the original autocorrelated data that has uncorrelated entries and is supposed to contain the same amount of information about the difference in means as the original sample. It is given by $ne = N^*(1 - r_1)/(1 + r_1)$ where N is the number of data points in the original sample and r_1 is the lag-1 autocorrelation coefficient (Zwiers and Storch, 1995). The r_1 value is not strictly determined but varies within a month of a year and between years. Here, it is taken to be the largest autocorrelation coefficient estimated throughout the sample between two neighboring wave records. This keeps *t*-test results to the conservative side.
- A random sub-sample of size equal to the equivalent sample size, *ne*, was taken from each individual original sample and suitable pairs (e.g. 'present' versus future conditions for each experiment of Table 7.1) were compared for differences in monthly means by performing the *t*-test with significance level *alpha* = 0.05. This step was

repeated 1000 times, each time with different (or not) random subsamples taken from the original samples. The aim was to assign a confidence level to the *t*-test output through examination of the percentage of *t*-tests that reject the 'null-hypothesis' out of the 1000 *t*-tests in total. Thus, the higher this percentage the higher the evidence that the associated means are indeed significantly different.

Results for the different climate experiments are summarized in Table 7.4, where the aforementioned percentages for each month and comparison pair are shown. Red values are for percentages > 50% and indicate a significant difference. The significant wave height, H_s, is split into two parts for the comparisons, corresponding to waves of direction greater than 178^0 and less than 178^0 respectively. This is done to facilitate interpretation of the results in Chapter 8 where 'one-line' simulations are made for a shoreline with a normal of 178^0. Figure 7.6 shows the monthly means to which the *t*-test results correlate and reveals the direction of the changes.

Primarily, observations from Table 7.4 that are of immediate interest to this study include:

- There are indeed significant changes in the future relative to the 'present'.
- There are no significant changes between C12 and HC50 which means that resolution effects on the results are not superimposed on the effect of a changing atmosphere.
- Significant changes between HC50 and EC50 appear in several months indicating a high influence of the driving global climate model on the results or/and the effect of using average 3-hourly winds in the analysis (HIRHAM-E output) instead of instantaneous winds (HIRHAM-H output).

These observations justify exploration of the impact of climatic changes in wave conditions on future shoreline evolution (Chapter 8) whilst they give some guidance on the relative

Table 7.4 *t*-test null-hypothesis rejection percentages (i.e. 100*(number of *t*-tests with $h = 1$)/1000) for each month and comparison pair. Red values (percentage > 50%) indicate significant differences. Climate simulation abbreviations are as in Table 7.1.

	Month											
	1	**2**	**3**	**4**	**5**	**6**	**7**	**8**	**9**	**10**	**11**	**12**
H_s (direction > 178^0)												
C12-A12	8.7	4.6	4.1	36.6	35.3	6.5	20	24.8	62.2	22	31.8	54.6
HC50-HA50	11.3	5.2	21.8	5.8	49.3	18.6	7.5	9.3	37.6	39	23.6	48.4
HC50-HB50	39.8	6.5	23.6	18.4	14.5	12.3	5.1	4.8	4.2	21	22.1	15.1
HA50_HB50	71.6	4.7	69.1	10.8	18.6	6.6	12.8	16.6	21.5	7.6	58.7	13.7
EC50-EA50	5.7	4.1	4.4	47.9	34.4	23	44.8	11.9	88.2	73	31.8	2.9
EC50 –EB50	3.8	10.2	18.3	20.3	4.6	49.8	46.2	12.2	67.6	73	68.1	15.9
EA50-EB50	5	10.6	14.7	10.9	29.4	10.6	2.4	4.2	9.5	4.9	9.1	13.8
C12-HC50	4.7	12.6	4	8.6	4.6	4.7	13.6	22.3	9.3	15	49.9	23.8
HC50-EC50	5.1	29.2	9.4	14.5	13.4	62.4	54.5	8.2	50.8	65	92.6	29.4
H_s (direction < 178^0)												
C12-A12	53.6	36.1	20.3	29.5	5.4	4.4	33.2	84.5	90.1	34	37.9	15.4
HC50-HA50	25.3	17.8	4.6	3.8	9.4	19.8	4.5	76.6	55.6	39	59.6	7.9
HC50-HB50	6	41	9.2	19.2	6.1	4.4	5.1	29.9	33.9	5.2	45.8	16.5
HA50_HB50	23.3	8.8	10.7	18.7	12.6	17.1	4.1	16.4	15.5	28	6.1	4
EC50-EA50	20.7	62.4	22.9	5.7	37.5	82.6	88.3	100	80.9	5	16.5	37.1
EC50 –EB50	12	60.3	3.3	5.6	12.5	36.4	34.3	79	13.8	6.9	5.5	10.9
EA50-EB50	5.1	5.6	32.6	4.9	11.8	30.3	35.9	49.7	42.6	14	8.9	19.3
C12-HC50	12.2	4.5	4.5	5.2	8.9	12.3	5.9	6.1	13.6	37	33.9	35.3
HC50-EC50	84.2	36	50.6	99.6	65.4	87.1	90.5	80.8	32.6	87	71.9	43.9
Wave direction												
C12-A12	79.9	84.3	66.9	78.7	37.5	13.9	14.9	99.9	81.4	14	7.2	24.4
HC50-HA50	89	88.5	82.5	19.2	25.5	20.8	26.4	99.7	76.1	18	10.5	21.2
HC50-HB50	7.3	70.8	4.4	13.6	6.3	8	23.5	78.4	16.7	15	9	4.8
HA50_HB50	83.8	9.1	76.8	6.8	13.6	11.4	4	45.8	92.6	4.4	20.1	15.3
EC50-EA50	7.8	5.1	5.5	6.3	14.6	70.4	51.6	100	17.2	8.7	29	11.4
EC50 –EB50	11.7	60.1	62.2	11.5	5.9	14.3	18.2	100	36.4	12	4.3	38
EA50-EB50	3.9	58.6	55.5	5.6	8.7	37.4	12.9	9.5	7.9	4.6	42	16.1
C12-HC50	7.1	5.2	4.8	16.9	11	4.9	4.9	3.6	5.8	8.4	7.4	10.3
HC50-EC50	53.7	5.7	19.7	74.1	23	97.7	94.6	100	98.6	100	70.7	39.9

magnitude of the changes expected from the different experiments. In the remainder of this study a greater focus will be given on the HIRHAM-H12 experiment because of its higher resolution which is thought to impart a higher 'accuracy'. Lower 'accuracy' is associated

with the 50km resolution experiments mostly because of their inability to well resolve extremes but also because a considerable amount of land is incorporated in the grid cell

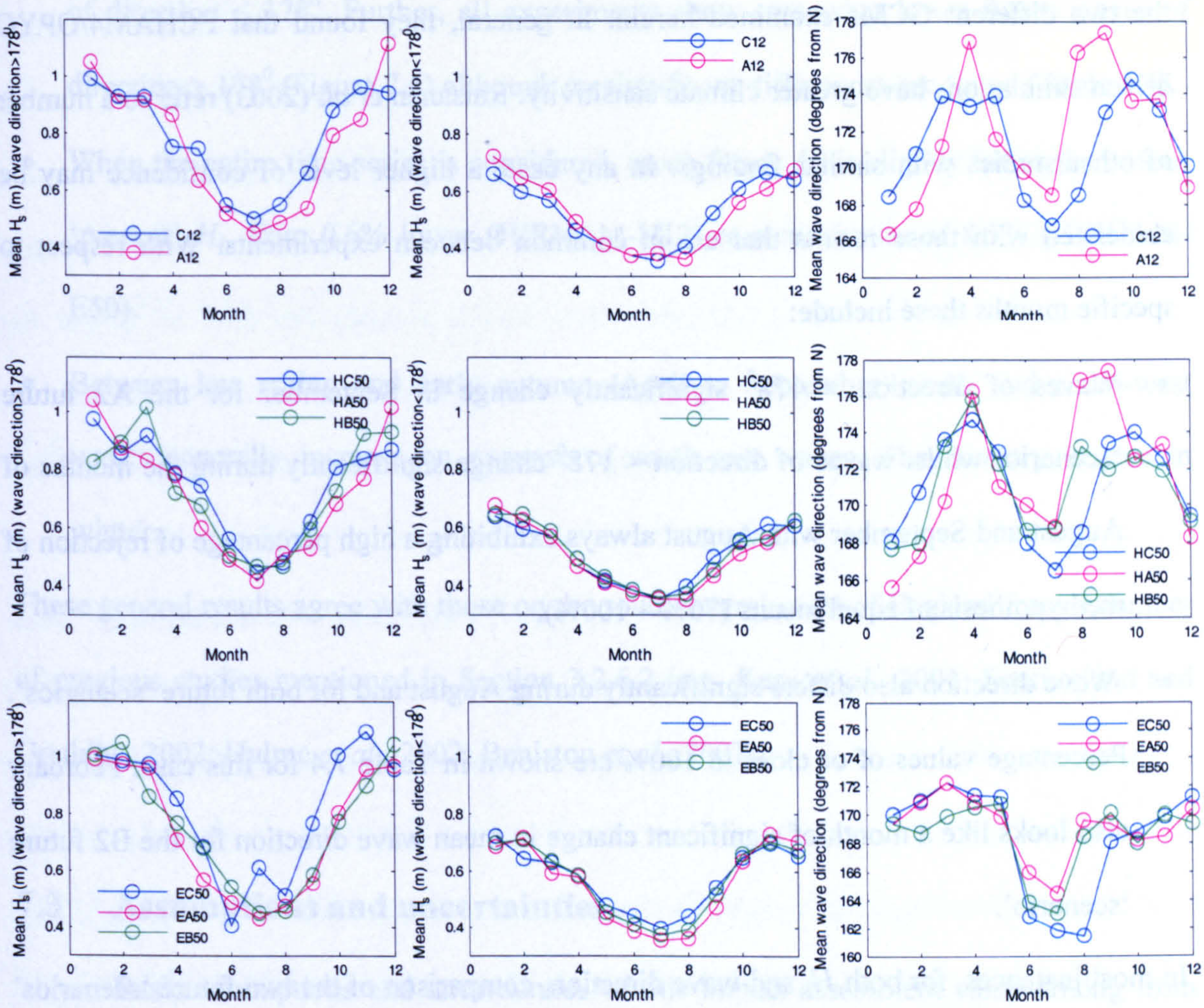

Figure 7.6 Mean monthly values of: 1) H_s for waves of direction > 178^0 (left column), 2) H_s for waves of direction < 178^0 (middle column), and 3) wave direction for all waves (right column). The HIRHAM – H12, HIRHAM – H50, and HIRHAM – E50 experiments are shown respectively from top to bottom.

over which climate model wind predictions have been found to be less reliable (Section 3.2.6.2). Also, as mentioned in Section 7.1.1, the ECHAM4/OPYC driven experiment is more prone to errors because, in contrast to the HadAM3H driven experiments, it does not use observed sea-surface conditions.

Similar results (Table 7.4) are found between experiments of different resolution. However, as already inferred from the above discussion, this is not the case between

experiments driven by different global climate models (GCM). Räisänen *et al.* (2003) also found significant divergence in wind speed output from a RCM when this was driven by the two different GCMs examined herein. In general, they found that ECHAM4/OPYC driven simulations have greater climate sensitivity. Raisanen *et al.* (2003) refer to a number of other studies with similar findings. In any case, a higher level of confidence may be associated with those results that are in common between experiments. With respect to specific months these include:

- Waves of direction > 178^0 significantly change in September for the A2 future 'scenario' whilst waves of direction < 178^0 change significantly during the months of August and September with August always exhibiting a high percentage of rejection of the hypothesis of equal means (76% – 100%).
- Wave direction also differs significantly during August and for both future 'scenarios'. Percentage values of or close to 100% are shown in Table 7.4 for this case. February also looks like a month of significant change in mean wave direction for the B2 future 'scenario'.

In most instances, for both H_s and wave direction, comparison of the two future 'scenarios' (highlighted in green in Table 7.4) results into fewer significant differences than those found between 'control' and A2 'scenario' but not necessarily between 'control' and B2 'scenario'.

Other general conclusions drawn out of Table 7.4, Figure 7.6, and additional analysis include:

- Prevailing winter waves are generally higher in the future than in the 'present'.
- Prevailing autumn waves, including August, are lower in the future.

- Summer and spring waves are largely unchanged in terms of H_s apart from the HIRHAM-E simulation which indicates lower future waves during summer for waves of direction < 178^0. Further, all experiments show somewhat lower future waves of direction > 178^0 (Figure 7.6) although no significant differences are found (Table 7.4).
- When the entire time-series is considered, mean future H_s is slightly lower than mean 'present' H_s, from 0.6% lower (HIRHAM-H12) to a maximum of 8.5% (HIRHAM-E50).
- Between late spring and early autumn (April to September) south and south-west waves generally increase on expense of south-east waves. The contrary is true in winter.

These general results agree with those on the south-central coast of England from a number of previous studies mentioned in Section 3.2.6.2 (e.g. Kaas *et al.*, 2001; Southerland and Gouldby, 2002; Hulme *et al.*, 2002; Beniston *et al.*, 2007).

7.3 Assumptions and uncertainties

Basic assumptions and uncertainties of this impact assessment study arising from the methodology described above are summarized in this section. Alongside, when appropriate, some reassurance is given on the magnitude of the uncertainty or the significance of the assumption implications. Assumptions and uncertainties include:

- A small part of the uncertainties in climate scenarios, outlined in Section 3.2.4, are addressed here. Two future scenarios, one RCM at two resolutions (only one scenario (A2) available at the higher resolution), and two driving GCMs are used in the assessment. However, a number of other future scenarios are possible whilst numerous RCMs and driving GCMs exist. Nevertheless, the A2 and B2 future scenarios used

herein are thought to embrace the greatest part of the variability of possible futures. Furthermore, as mentioned in Section 3.2.4, qualitative results from different RCMs are often in agreement. Thus, the greatest part of the climate scenarios uncertainty is expected to be due to the differential results obtained from different driving GCMs.

- Further to the above, only one realization of the climate model simulations is used, hence, uncertainty due to 'natural'/unforced climate variability is not directly accounted for (Section 3.2.4). However, statistical tests are able to assess the magnitude of the noise expected due to natural variability and compare it with the magnitude of the signal, i.e. 'true' climatic changes (Räisänen *et al.*, 2003). The *t*-test performed in this study has this ability.
- The impact of SLR on 'present' and most importantly future nearshore wave characteristics is ignored. So is the impact of potential changes in tidal characteristics. However, Halcrow (2004) found through a wave transformation study at the area that an increase of 250mm in sea-level by 2053 resulted in little change in inshore wave climate. They suggested though that reduced wave attenuation (Section 3.1) could be more important under greater SLR and more extreme waves. In any case, they support that such changes are small compared to those caused by changes in the offshore wave climate in response to altered future wind patterns.
- The bathymetry over which waves travel inshore is taken to be unchanged in time.
- Swell is excluded from the analysis and generated 'present' wind-wave time-series for input to the 'one-line' simulations are realistic but not necessarily entirely representative of the study area. However, the reasonable resemblance of the hindcast wave climate to the 'actual' (a hindcast including swell) wave climate along with the close agreement of the present output with literature on wind-wave climate at the area

support that the offshore wave-time-series produced by the climate model winds is highly realistic. As a result, strong inference to site-specific changes expected in the future can be made.

- Although the wave time-series produced in this study are non-stationary, the assumption of stationary data inherent in the *t*-test was ignored. As mentioned above, this decision was made after Räisänen *et al.* (2003) who suggested that this effect is expected to be small.

7.4 Discussion

A set of 30-year 3-hourly wind time-series obtained from few climate model experiments were used to hindcast deep water waves that were then transformed inshore forming a corresponding set of 30-year 3-hourly nearshore wave time-series that will be used as input in 'on-line' model simulations in Chapter 8. The time-series correspond to two time periods, the 'present' or 'control' period (1961-1990) and the future or 'scenario' period (2071-2100). Wave hindcast was done at a single offshore point using the SMB-Donelan model which employs simple hindcast expressions. Wave transformation was carried out to a single inshore location through the SANDS software, which uses readily available 'wave transfer' files, generated by a ray back-tracking spectral wave energy transformation model (REFPRO), to transform waves between specific offshore and inshore locations. Finally, a hypothesis test was performed on the nearshore wave data to explore whether monthly mean wave characteristics change significantly in the future.

In the context of this study, the differential effect of different climate scenarios is investigated along with the differential effect of different RCM resolutions or/and driving GCMs. However, the higher (12km) resolution climate simulation available receives the

greatest focus as it can better capture climate variability and extremes. Little attention was paid to the validation of the generated wave time-series against actual wind-waves at the site. Instead, it was ensured that the time-series are statistically similar to the hindcast data available for the site. This is because the interest of this study is on the relative change in shoreline response under the various wave climates rather than the accuracy of model predictions.

Similarly to all climate impact assessment studies, the present study is characterized by non-trivial uncertainty. This is related to the uncertainty in climate scenarios and to the exclusion from the analysis of a number of processes that could have an impact, severe or not, on the results. SLR, changes in tidal characteristics, changes in bathymetry, and swell are main processes that were ignored in the methodology described. Nevertheless, despite the uncertainty, which to a certain degree in unavoidable, there are a number of advantages pertaining to the present study. These include:

- It is amongst one of the very few studies that investigate the potential impact of changes in future wave fields on shoreline evolution (Section 3.3.3). Therefore, it helps to improve understanding on the potential magnitude of change under altered offshore wave heights and directions in the future.
- It is the only such study that uses climate model scenarios instead of incremental. As mentioned in Section 3.2.2, the former scenarios are presently considered as the best available since they are based on physical considerations and explicitly account for changes in greenhouse gases in the atmosphere (see Appendix A, Table A3).
- It uses climate model winds of a high spatial (down to 12km) and temporal resolution (3-hourly); the author is not aware of other studies that have been carried out using climate model winds at higher resolution (> 50km spatial resolution; 6-hourly to daily

temporal) for the prediction of future wave climate. The high resolution captures both changes in temporal variability and in the mean, i.e. changes in the frequency and intensity of stormy conditions and changes in the prevailing wind climate, which are both important in the assessment of the impact of different future wave scenarios on shoreline evolution.

- In addition to the above, the present study uses simple, but fast and straightforward software that allows for the full set of data to be used and analyzed without need for data reduction (e.g. binned wave data or other wave time-series summary statistics). This further enhances estimations of shoreline change (e.g. Le Mehauté and Soldate, 1978; Kamphuis, 2000; Southerland and Gouldby, 2002). For instance, SANDS needed about 15mins to transform a 30-year 3-hourly wave time-series inshore over real bathymetry. This means that a great number of lengthy data-sets can be efficiently transformed this way. In contrast, any sophisticated wave model would need a significant amount of time to perform such a task unless data were considerably reduced though statistical analysis. Especially if absolute accuracy is less important than relative accuracy, such as in this study, a modelling approach like the one used herein is probably more appropriate.
- As in the majority of studies on climate change to date, the present study uses one realization of the climate models. Thus, the effect of changes in natural variability is not directly accounted for. However, the magnitude of the noise expected due to natural variability is estimated herein through statistical considerations (hypothesis tests) and compared with the magnitude of the signal, i.e. 'true' climatic changes (Räisänen *et al.*, 2003).

Chapter 8

Shoreline change under future wave climate scenarios

As explained in Chapter 7, this chapter uses the 'one-line' modelling techniques developed in Chapters 4 and 5 to investigate changes in the evolution of a hypothetical stretch of shoreline under the various nearshore wave climate scenarios produced in the previous chapter. The numerical 'one-line' model of Chapter 5 is mainly used to obtain the results. This is because this model is free from 'small angle approximations' inherent in the semi-analytical 'one-line' expressions of Chapter 4. Nevertheless, to extend the work of Chapter 6 where the two models, semi-analytical and numerical, were compared for relatively short-period runs, the analytical 'one-line' approach is used for the simulation of one climate model experiment (HIRHAM-H12) in order to assess the relative performance of the two models in the very long-term (30 years).

Results on shoreline change are given in terms of monthly and seasonal alongshore statistics. The potential for significant changes in mean future shoreline positions, and in the shoreline positions' distribution relative to 'present' means and distributions, is estimated at individual alongshore locations through hypothesis testing, using the *t*-test and *ks*-test respectively. Focus is on the higher resolution climate experiment, HIRHAM-H12,

since, as previously explained (Section 7.2), input data resulting from this experiment are expected to be the most 'accurate'. However, results obtained from other experiments/scenarios are also described, especially when differences are notable. Expected deviations from the HIRHAM-H12 predicted change are also inferred by the results summarized in Table 7.4 and Figure 7.6 in the previous chapter. No direct consideration of SLR is examined although its effect is briefly explored through the inclusion of the Bruun Rule in the sediment continuity equation.

Most of the assumptions and uncertainties but also benefits from this work were described in Chapter 7 (summarized in Sections 7.3 and 7.4). Some extra uncertainty is now added because of the assumptions of the 'one-line' model and its deterministic implementation. Nevertheless, it is important to highlight that both climate change and decadal modelling uncertainty are by and large unavoidable, yet climate change assessments are highly important. Compared to previous work, the main advantages of the present study are the increased realism of future scenarios along with a better representation of climate variability and extremes. It is also intended to improve understanding of potential implications of climate change on shoreline evolution.

In what follows, the specific shoreline evolution problem examined along with the formulae and parameters used in the 'one-line' simulations are described initially. Monthly and seasonal shoreline statistics are then explained and output corresponding to the various input wave climate scenarios is presented. Semi-analytical 'one-line' model output is then compared with output from the numerical model. The assumptions and uncertainties of the present study follow and the chapter ends with a discussion of the findings.

8.1 Model formulae and parameters

The equation solved by the numerical model is the continuity of sediment equation as given by Cowell *et al.* (2003) (Equation 3.2, Section 3.3.1) but with all local source terms (q) set to zero. The global source term (first term on the right hand side) which corresponds to changes in mean sea-level with time is activated only when SLR is considered (see Section 8.3.3); otherwise it is also set to zero. The sediment transport formula used is the well-known CERC formula in its simplest form (Equation 2.9 or 5.6 in differential form). A depth of closure, D_c, of 10m and an active profile length, L, of 1100m were assumed. These values would suggest an intermediate profile. Parameters in the CERC formula were set as: $K = 0.41$ (Section 2.2.1.3), water depth = 3.53m which is the reference depth of the input waves, $\rho_s = 2650 kg/m^3$ (quartz-density sand), $\rho = 1020 kg/m^3$ (sea-water density), and $\sigma = 0.6$ (Komar, 1998). Diffraction is neglected and wave characteristics are assumed constant alongshore.

The case of shoreline evolution examined is that of an initially straight shoreline that is bounded on the right hand side by a long impermeable groyne. For this case, the initial condition is given by $y(x,0) = 0$. The left hand boundary (LHB) and right hand boundary (RHB) conditions were set as $Q_1 = Q_2$ and $Q_{N+1} = 0$ respectively (see Figure 2.5), where the former represents a pinned beach and the latter states that no sediment is passing through or over the long groyne. The shoreline extent was taken to be 15000m which was big enough to ensure that the assumption of a pinned beach at the LHB has no affect on the results. Other model parameters (see Section 5.2.4 for a list of inputs required by the 'one-line' numerical model solved with the Method of Lines) were set as: $dx = 30$m, $neqn = 500$, $h = 3$hrs which corresponds to the wave input temporal resolution, $eps = 10^{-6}$ which is the maximum value of the error tolerance below which results remained unchanged, and *hmin*

= 0. All 30-year 3-hourly nearshore time-series of significant wave height, H_s, and mean wave direction, α, corresponding to the climate model experiments of Table 7.1 (Chapter 7) were simulated. Input wave directions were adjusted relative to the shoreline normal which was taken to be 178^0.

The situation described is hypothetical. Nevertheless, it retains some of the features of the shoreline fronting Hengistbury Head (area shoreward of the Refraction point of Figure 7.1). Specifically, the stretch of shoreline extending from the eastern tip of Poole Bay to about 1500m to the west is relatively straight and bounded on the right hand side by a long groyne. Although one could think Hengistbury Head as a suitable case study for the present impact assessment, there are a number of factors that largely complicate 'one-line' modelling applications at the area. Of these, the most important is that incoming waves (Figure 7.4, left) are to the east of the actual shoreline normal of 202^0 causing alongshore sediment transport to the west and erosion at the long groyne, a situation opposite to the one observed. Indeed, it has been suggested (Halcrow, 2004) that eastward transport due to tidal currents dominates wave induced transport to the west causing net accretion at the long groyne. Other complications, mainly associated with ill-defined sources/sinks of sediment, especially in the very long term, include: (1) input from cliff erosion, (2) bypassing of the long groyne and input of sediment on the LHB (where short groynes appear to the west), (3) replenishment works, and (4) presence of shingle in the sand mixture. As a result, if all of the above factors were to be incorporated significant complexity would be introduced but with no improvement in uncertainty estimates making site-specific modelling of little benefit, a situation valid for a great deal of coastlines. A hypothetical case, like the one examined herein, can still provide qualitative results, describing expected general trends at the site and at the south-central coast of England in general.

A number of values of the shoreline normal have been tried before adopting the value of 178^0. Initially, the true shoreline normal of 202^0 was attempted with which excessive erosion (often greater than 250m over a single month) adjacent to the long groyne was computed. Reasonable values of shoreline change (< 250-300m) over the 30-year period simulations were obtained for angles of shoreline normal in the range of 175^0 - 180^0. The chosen value of 178^0 has the interesting property that shoreline evolution changes from accretion during the 'control' period to erosion during the 'scenario'; and the sensitivity of longshore transport to wave direction is more easily seen. Although net drift direction and rates of net accretion or erosion are highly sensitive to the choice of the shoreline orientation, hypothesis tests on the significance of shoreline changes under the different wave climate scenarios are of a lower sensitivity to this parameter. Thus, despite small changes in the *p* values, significant differences in monthly mean shoreline positions or their distribution appear largely within the same time and space domain (i.e. within the same months and for the same alongshore positions). It was found that significant differences were mostly reduced when the shoreline normal deviated from 178^0, i.e. when both 'control' and 'scenario' exhibited a common trend of erosion or accretion.

As mentioned in the introduction, the same shoreline evolution problem was also solved using semi-analytical solutions of the kind derived in Chapter 4. The particular problem examined herein, i.e. shoreline change at a single groyne, was solved by Reeve (2006) whose work Chapter 4 extended. To solve this problem analytically, the initial condition is as above whilst boundary conditions are given by Equations 4.4 and 4.22 where $h(t) = \tan(\alpha_0)$ for $Q = 0$ (see Equation 4.41). The latter equation corresponds to the boundary condition at the location of the groyne, placed now at $x = 0$m alongshore. Since the solution is obtained for $x > 0$, $x = 0$m corresponds to the LHB of the solution domain in contrast to the numerical model setting where the groyne location signified the RHB.

However, this is easily fixed since results from the two models at different alongshore positions are simply mirroring each other relative to the middle (7500m) of the spatial domain. The equation solved, as given by Reeve (2006), is

$$I_2 = \frac{1}{\sqrt{\pi}} \int_0^t \left(\int_w^t \varepsilon(u)du \right)^{-1/2} e^{-\left(\frac{x^2}{4\int_w^t \varepsilon(u)du} - \int_w^t r(u)du \right)} \varepsilon(w)\tan(\alpha_0)dw \qquad (8.1)$$

This is the equivalent of Equation 4.21 in Chapter 4. Similarly to that chapter, the integrals I_1 and I_3 needed for the full solution (Equation 4.14) equal zero for this case of shoreline change. Temporal discretization was 3 hours, as above.

8.2 Monthly/Seasonal means and the significance of their difference

This section explores whether significant changes in mean shoreline positions or in shoreline positions' distribution are expected in the future. The analysis is done primarily in terms of monthly and then in terms of seasonal statistics. In particular, the procedure adopted involves the following steps. Initially, 'one-line' simulations are performed for each individual 30-year time-series but with the shoreline set back to its initial shape after each single month or season in the time-series is simulated (i.e. for each year there are 12 or 4 shoreline shape outputs, one for each month or season respectively). Therefore, for each wave climate time-series each month or season consists of 30 shoreline position values at each alongshore location, one for each year. The mean of these 30 values is computed alongshore, giving monthly or seasonal means. For certain location (see following paragraph), a *t*-test is performed to estimate whether significant differences exist in mean shoreline positions of 'control' and 'scenario' runs. The test was described in Section 7.2. A Kolmogorov-Smirnov test, *ks*-test, is also carried out in this chapter. This is a

conventional non-parametric test which compares the distribution of two samples, in this case, the distribution of the 30 shoreline positions corresponding to a particular month or season and alongshore location for two wave climate time-series. Test inputs and outputs are as summarized in Section 7.2 for the *t*-test except for the *ci* term (see the *t*-test Matlab command in Section 7.2) which is not applicable in this case. Now, the 'null hypothesis' is that the two samples come from the same distribution. Like the *t*-test, the *ks*-test performs better when no serial autocorrelation exists, which is the case in this problem. The mathematics of the test can be found in established statistical textbooks (e.g. Freud, 1992).

Results are presented in Figure 8.1 where all the statistics are visualized. The figure corresponds to one particular month. The monthly shoreline statistics for the two wave climate time-series, 'control' (blue lines) and 'scenario' (pink lines), are depicted. These include: (1) the average shoreline position alongshore (solid lines), (2) the median shoreline position alongshore (thick dashed lines), and (3) the standard deviation of the shoreline positions alongshore. Superimposed are the results of the hypothesis tests carried out at alongshore locations where the standard deviation of both 'control' and 'scenario' shoreline positions is greater than 2m. Test results are depicted as vertical lines at the aforementioned locations, labeled with the corresponding tests' *p*-values and are plotted only for *p*-values < 0.05, thus at significance level *alpha* ≤ 0.05. Results with $0.025 < p < 0.05$ are in cyan colour, with $0.0125 < p < 0.025$ are in orange-brown colour, and with $p < 0.0125$ are in red colour. The limits of the lines associated with the *t*-test output (dotted lines) correspond to the confidence interval bounds, *ci*, computed for *alpha* = 0.025. Lines related to the *ks*-test (dashed vertical lines) are of constant length. Equivalent plots are drawn to describe the seasonal statistics.

The structure of the plot of Figure 8.1 is informative in a number of ways. Firstly, rather than using arbitrary levels of significance, *alpha*, to arrive at definite conclusions on

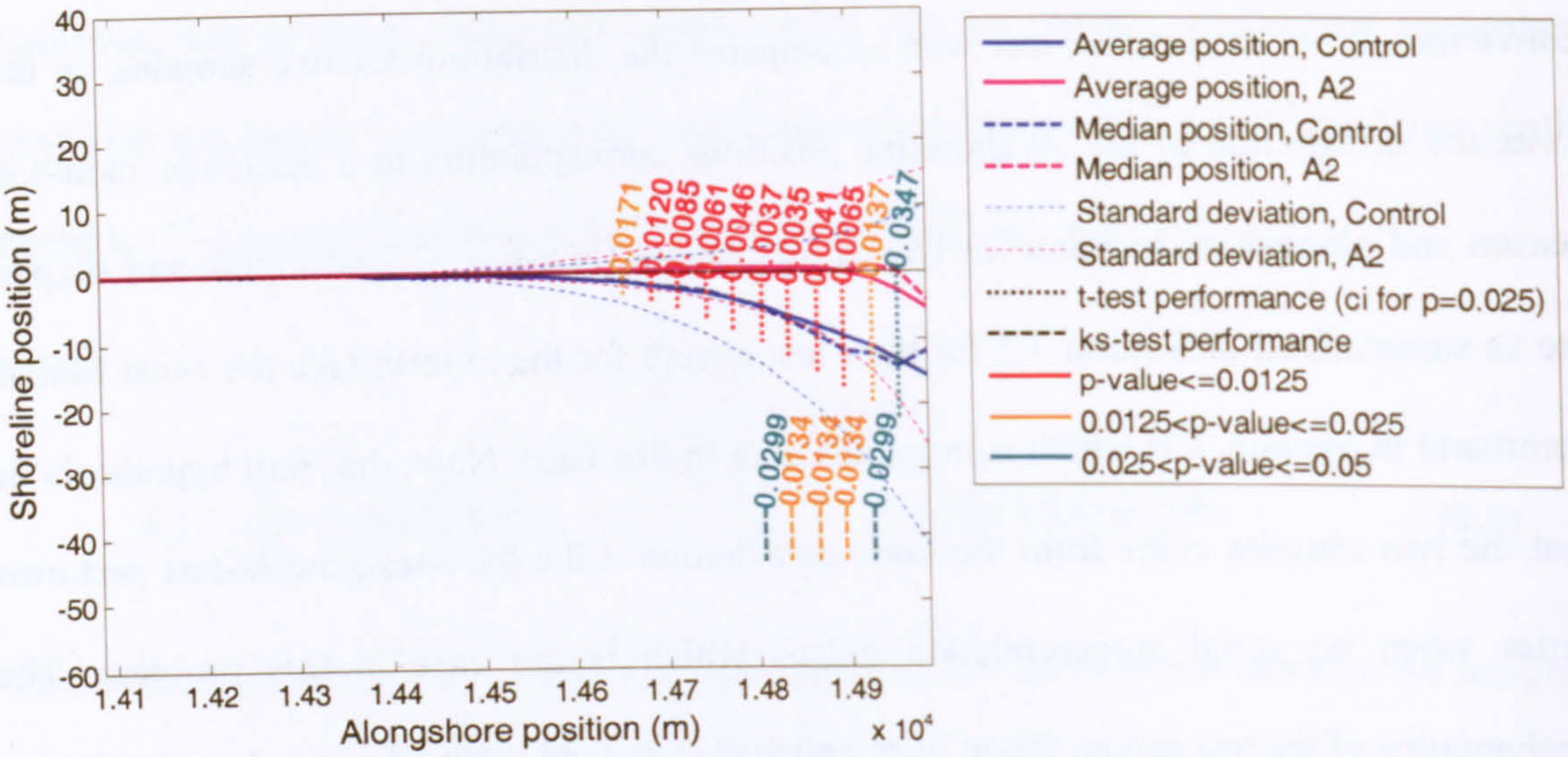

Figure 8.1 Shoreline monthly statistics corresponding to two wave climate time-series, 'control' (blue lines) and 'scenario' (pink lines) respectively: mean shoreline position (solid lines), median position (thick dashed lines), and positions' standard deviation (thin dashed lined). Hypothesis test results (vertical lines): *t*-test (dotted lines) and *ks*-test (dashed lines). *T*-test line limits indicate confidence intervals, *ci*, for $p < 0.025$. Cyan, orange, and red colours (*p* values and lines) signify different levels of significance, *alpha* (< 0.05).

whether two means or distributions are indeed significantly different, the *p*-values are given so that the degree of evidence against the hypothesis of equal means or distributions can be assessed. Lower *p* values indicate higher signal intensity and correspond to a higher degree of evidence against the 'null-hypothesis'. The coloured *p*-value bands of Figure 8.1 help to directly identify the degree of confidence associated with every test result. Furthermore, by mapping the *p*-values alongshore the spatially variable effect of a future wave climate on shoreline position changes can be assessed. The direction of change and the often differential variability between 'control' and 'scenario' in monthly shoreline positions can also be deduced from the plot. Figure 8.1, viewed in conjunction with Table 7.4 and Figure 6.6, can be used to establish links between changes in forcing characteristics and future shoreline changes.

To better assess whether changes in future significant wave heights or wave directions are more responsible for the observed changes in shoreline positions, the above

procedure was repeated twice more with modified wave input time-series. Firstly, wave height variation was replaced with a constant wave height value, common for 'control' and 'scenario'. The wave height that reproduced the average value of the wave energy for the 'control' C12 time-series was adopted in the 'one-line' simulations. Secondly, the wave angle variation in the original time-series was replaced with a constant wave angle. The mean wave angle of the 'control' C12 time-series was used for both 'control' and 'scenario' simulations.

A problem arising from the above procedure is one known in statistics as "multiple comparisons" or "multiple testing" problem. It occurs when statistical tests are used repeatedly leading to a potential increase in the experiment-wide significance level alpha, i.e. the probability of incorrectly rejecting the null-hypothesis due to chance (false positives) increases (e.g. Miller, 1981). For example, if *alpha* = 0.05 and one test is performed at a single alongshore location, the probability of it giving a false positive by chance is 5%. If n tests are performed at n alongshore locations the above probability changes according to the relation: $alpha = 1 - (1\text{-}alpha_{\text{per comparison}})^n$. Thus, if for instance 20 tests are carried out (≈ max number of alongshore locations where a test is performed in this study), the probability of false positives becomes 64% (*alpha* = 0.64). A common correction to this problem is to consider that the highest accepted individual p-value is $p = alpha/n$ so that the overall *alpha* does not exceed the desired limit (e.g. 0.05). This is known as the Bonferroni correction. However, this correction has been found to be very stringent, leading to several false negatives when comparisons are dependent, e.g. in this study alongshore positions are the product of a shoreline model and are highly correlated. In fact, no correction is needed when data are fully correlated. For correlated outcome something between full Bonferroni correction and no correction at all should be applied (http://home.clara.net/sisa/bonhlp.htm, 2007). Here, to keep things simple, the p-values are

shown alongshore so that, as above, one can investigate the degree of evidence associated with each change without necessarily declaring this change as significant.

8.3 Results

8.3.1 Monthly

Figures 8.2 and 8.3 show the results obtained for the HIRHAM-H12 climate change experiment. Figure 8.2 shows monthly means, medians, standard deviations, and hypothesis test results for all twelve months and when both H_s and wave direction, α, vary. Figure 8.3 shows results when a constant H_s (0.65m) is adopted (above the blue line) and when a constant α (171.47^0) is adopted respectively (below the blue line). Only months with test p values < 0.05 appear in the figure. Figure 8.2, apart from showing months of potentially significant change ($p < 0.05$), also serves to illustrate whether 'control' or 'scenario' are relatively more erosive or accretive for every individual month.

In terms of relative shoreline evolution, Figure 8.2 shows that during winter and spring the A2 future wave climate is more erosive than the C12 'present' wave climate with the exception of April. During late summer and autumn the A2 'scenario' is generally more accretive than the 'control'. For a few months, notably March, Aug, and September, C12 and A12 cause shoreline evolution in opposite directions. The observed patterns agree well with the mean monthly values of the input wave characteristics (wave height and direction) shown in Figure 7.6. In fact, the above trends in shoreline evolution may be largely explained just by looking at the mean monthly values of the wave direction in Figure 7.6. In general, mean shoreline position differences do not exceed 25m.

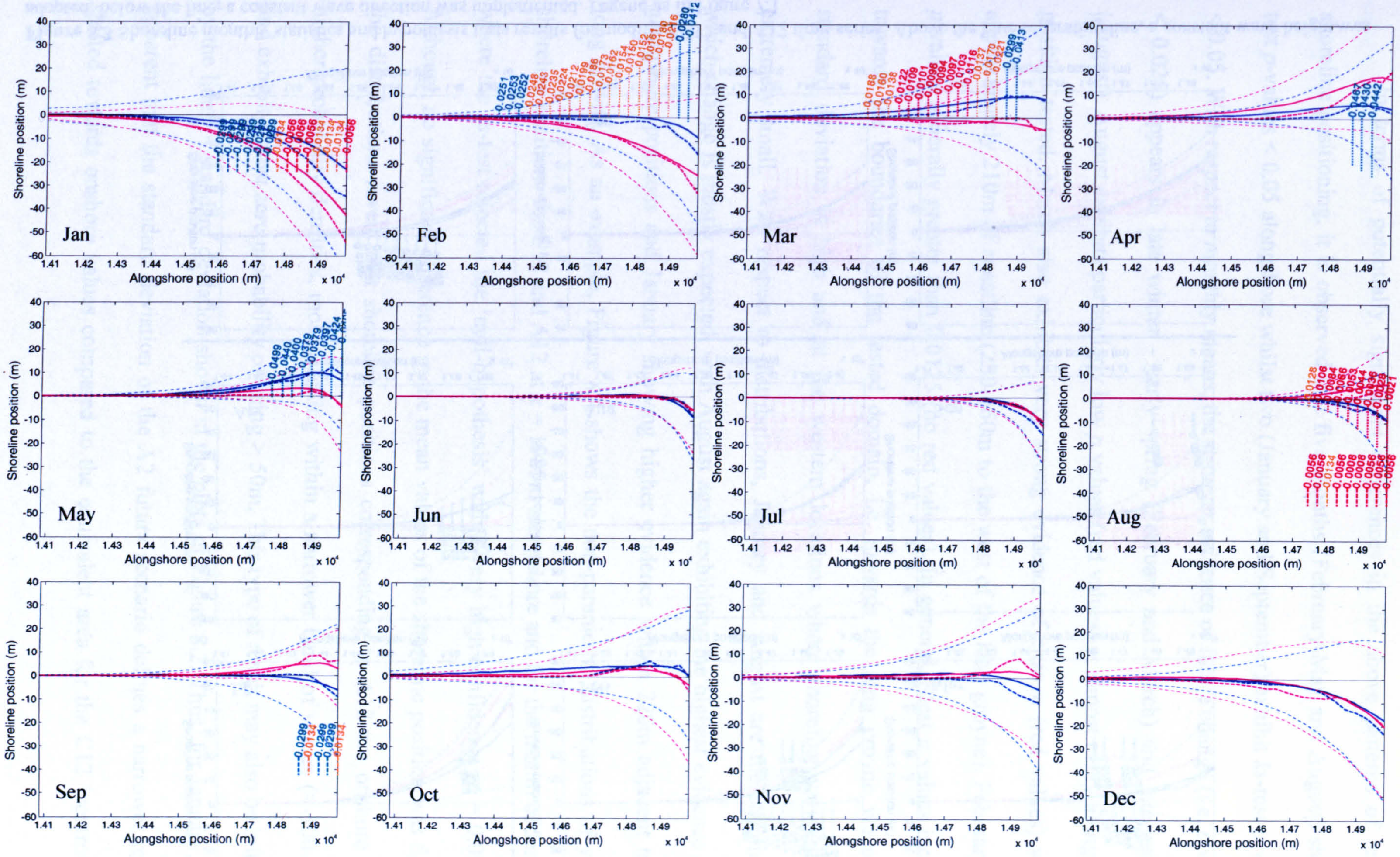

Figure 8.2 Shoreline monthly statistics and hypothesis test results for C12 and A12 wave time-series. Legend as in Figure 8.1

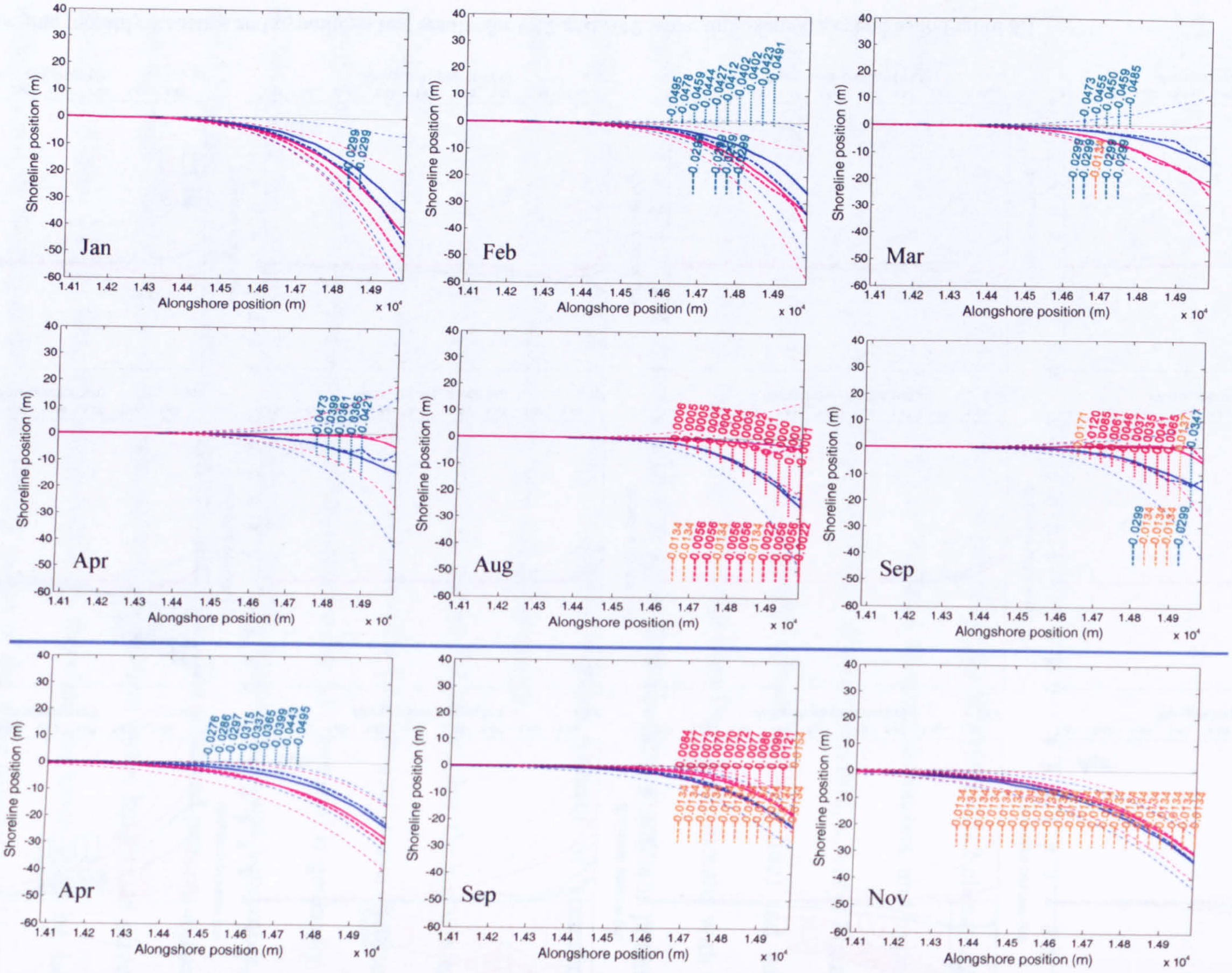

Figure 8.3 Shoreline monthly statistics and hypothesis tests results for modified C12 and A12 time-series. Above the blue separating line, a constant wave height was adopted, below the line, a constant wave direction was implemented. Legend as in Figure 7.1

In terms of potentially significant differences in the above patterns of relative shoreline positioning, it is observed that five months (February-May and August) show *t*-test *p*-values < 0.05 alongshore whilst two (January and September) exhibit *ks*-test *p*-values < 0.05. With respect to monthly means, the stronger evidence of future change (i.e. *p* values < 0.025) appears in late winter - early spring (February and March) and late summer (August). August exhibits particularly low *p* values (red values) at almost every alongshore position tested. March also exhibits very strong evidence of change (red values) within approximately 210m of coastline (250-460m to the west of the long groyne). February has *p* values generally greater than 0.0125 (no red values). In general, *t*-test *p* values increase towards the boundaries of the tested domain, i.e. towards the long groyne where the standard deviation is high and at the western locations where shoreline variability is extremely small. With respect to distributions, January and August are the months for which change is mostly expected, with August again exhibiting the highest evidence at all alongshore positions and January showing higher evidence within 220m adjacent to the long groyne. As an example, Figure 8.4 shows the non-parametric distributions of yearly shoreline positions for C12 and A12 at x = 1985m alongshore and for the month of January where the *ks*-test rejected the 'null-hypothesis' with a very high confidence (p = 0.0056). Although no significant difference in the mean values of the shoreline position was found, the distributions reveal that shoreline positions corresponding to A12 are onshore with higher probability densities, mostly falling within a narrower band of values (≈-100-5m), and exhibit almost zero probability of being > 50m. This type of result may also be inferred by the lines of standard deviation shown in the plots of Figure 8.2. Thus, for January, it is apparent that the standard deviation of the A2 future scenario defines a narrower region shifted towards onshore values compared to the equivalent area for the C12 'control'. A

less broad band of yearly shoreline position values for the A12 simulation is the case for several months.

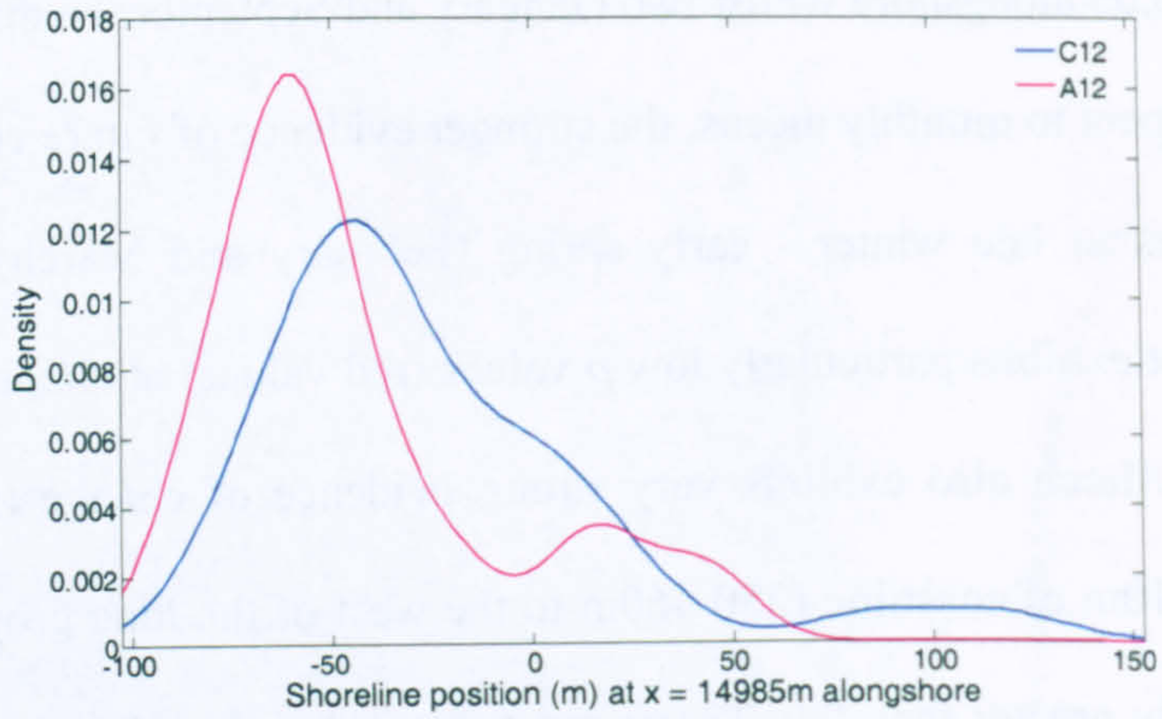

Figure 8.4 Yearly shoreline position distribution for C12 and A12 at x = 1985m alongshore and for the month of January.

Figure 8.3 suggests that the changes found in Figure 8.2 are mostly caused by future changes in wave direction rather than in wave height. In fact, for every month that exhibited changes in shoreline positions at significance level lower than 5% ($p < 0.05$) when the original time-series were input in the 'one-line' model, no change of 'significance' was found when a constant wave direction was adopted for the simulations. September is the only exception. In contrast, with the exception of May, changes of 'significance' were found for the above months when a constant wave height was adopted (first two rows of Figure 8.3). Changes in both mean shoreline position and shoreline positions' distribution was often the case. Nevertheless, results indicate that it is the combination of the variation in wave height and direction that enhance or suppress differences in Figure 8.2. Thus, in winter and spring changes found due to wave direction variation alone are of smaller 'significance' than those found when both wave height and direction varied. In addition, evidence of change in Figure 8.2 is present at alongshore locations for which no evidence of change exists when either the wave height or the wave

direction was kept constant (Figure 8.3). For example, Figure 7.6 shows that in January wave direction for the 'scenario' A12 is veered eastwards relative to the 'control' C12 and Table 7.4 shows that this veering is 'significant'. Thus, greater erosion west of the long-groyne is expected under the A12 future. However, changes in future wave direction alone (Figure 8.3) were not able to reproduce the more 'significant' changes in shoreline positions distributions found at several alongshore locations when both wave height and wave angle varied (Figure 8.2). It is the significant westward shift of the mean wave direction in combination with the significant increase in the mean wave height of waves of direction $< 178^0$ during this month (Figure 7.6 and Table 7.4) that can explain the above pattern. May is an example of a similar effect, despite the fact than no changes of 'significance' were found when the input time-series were compared (Table 7.4 and Figure 7.6) and the same was true when the two wave characteristics were varied individually to obtain shoreline positions (Figure 8.3), a decrease in mean wave height from the west along with a shift in mean wave direction to the east for the A12 'scenario' combine to produce some evidence of greater erosion in the future. In contrast, in September, the variation of each of the wave characteristics individually generates strong evidence of future shoreline change; however, the evidence decreases when the two are combined because the largely significant veering of the future mean wave direction to the west is accompanied with a significantly lower mean wave height from this direction (Figure 7.6 and Table 7.4), thus establishing an opposite shoreline trend.

The coarser resolution HIRHAM-H50 experiment gave results similar to those obtained above for the 'control' and A2 'scenario'. Except for March, during winter and spring somewhat lower p values were obtained and at fewer locations. In March and August stronger evidence of change was found with this coarser resolution. Results for the HIRHAM-E50 experiment are shown in Figure 8.5. A considerably different picture of

'significant' shoreline changes than the one described above is evident in the figure (left column). Now, evidence of change appears only during the summer months (June – August) and is particularly high (red values) throughout this season. Changes in both mean shoreline positions and shoreline positions' distribution appear at most of the alongshore locations tested. *P*-values are generally very low with $p << 0.0125$ for most of the cases. Particularly for August the number resolution adopted to illustrate the *p*-values (5 decimal points) was not enough to capture the non-zero part of the values. August is the only month where evidence of change is in agreement with the other two climate experiments. Similarly to them, changes of maximum of 25m in mean shoreline position were found.

The second column of Figure 8.5 shows that when a constant wave height is adopted in the simulations, *p*-values > 0.05 are found over summer exactly as above. The last two columns of the figure show that when a constant wave direction is adopted July and August still show evidence of change but not June. Such evidence is also present in May, September, and October. Due to wave angle variation alone changes appear stronger in August (100% 'null-hypothesis' rejection percentage in Table 7.4) compared to those found due to wave height variation solely over this month. The contrary is true for July (88.3% rejection percentage for waves of direction $< 178^0$ in Table 7.4 compared to 51.6% for wave direction). The combined variation of the wave characteristics leads to somewhat weaker changes in July whilst somewhat stronger changes are obtained in August, signifying opposite and parallel trends respectively caused by individually varying the two wave characteristics. These patterns show once more that when 'significant' changes in shoreline positions are obtained because of wave angle variation alone, it is most probable that changes of similar strength will result if wave height variation is incorporated. On the other hand, when 'significant' changes are obtained because of wave height variation alone,

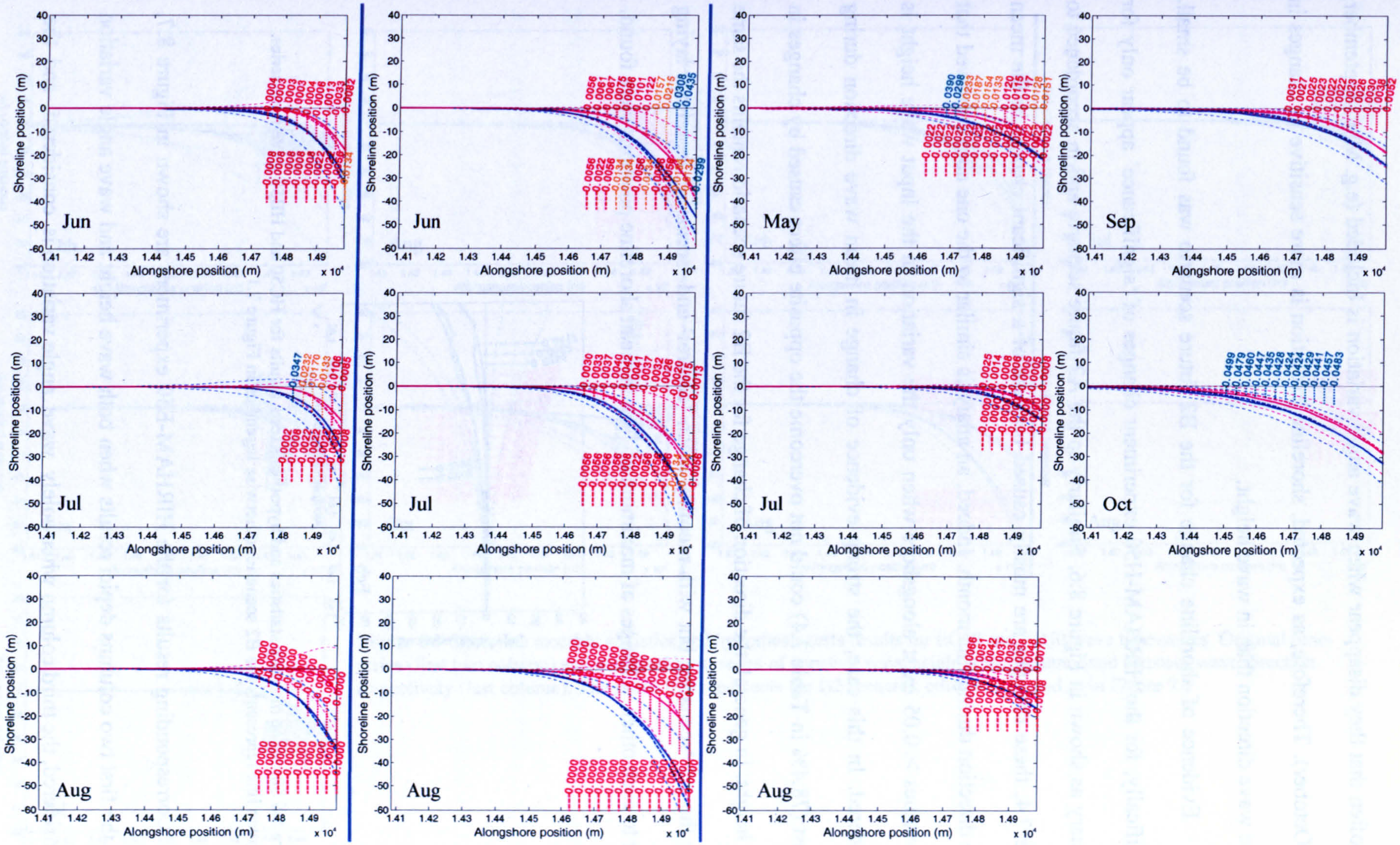

Figure 8.5 Shoreline monthly statistics and hypothesis tests results for EC50 and EA50 wave time-series. Original time-series (first column) and modified time-series of constant wave height (second column) and constant wave direction respectively (last two columns).

it is often that they disappear when wave angle variation is included (e.g. May, September, and October). Therefore, as expected, shoreline evolution is more sensitive to changes in future wave direction than in wave height.

Evidence of shoreline change for the B2 future scenario was found to be small. Specifically, for the HIRHAM-H50 experiment changes of 'significance' appear only for February as shown in Figure 8.6. Similarly to the A2 future scenario and in accordance to Table 7.4, these changes are mostly caused because of a significant change in the mean wave direction during this month. Indeed, an analysis similar to the one above showed that no p-values > 0.05 exist alongshore when only the variation in the input wave height is considered. In this case, the strong evidence of change in mean wave direction during August (78.4% in Table 7.4) could not overcome the opposite effect caused by changes in wave height. In general, the direction of change for the B2 future scenario remains the same as for the A2 'scenario' but with monthly mean 'control' and 'scenario' shorelines laying closer to each other. Changes of maximum of 13m in mean shoreline positions were found.

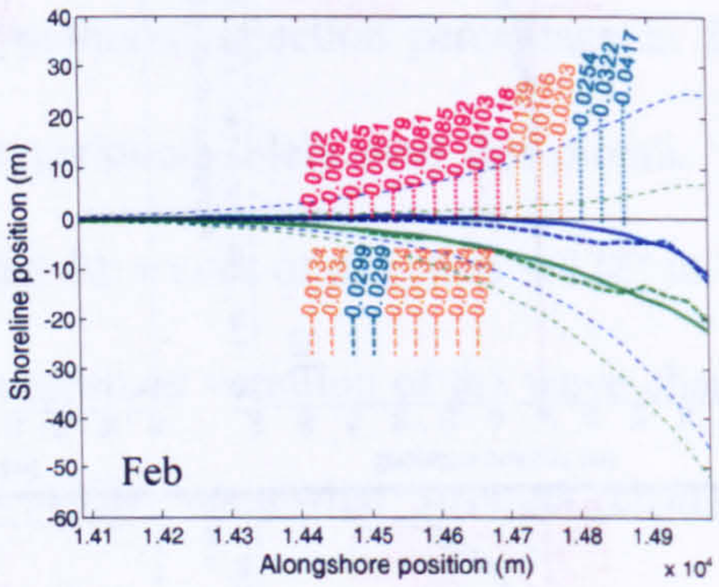

Figure 8.6 Shoreline monthly statistics and hypothesis tests results for HC50 and HB50 wave time-series. The green line represents the B2 scenario, otherwise legend as in Figure 7.1.

Corresponding results for the HIRHAM-E50 experiment are shown in Figure 8.7, where the first two columns depict results when both wave height and wave angle variation are considered, the third column when solely wave angle variation is considered, and the

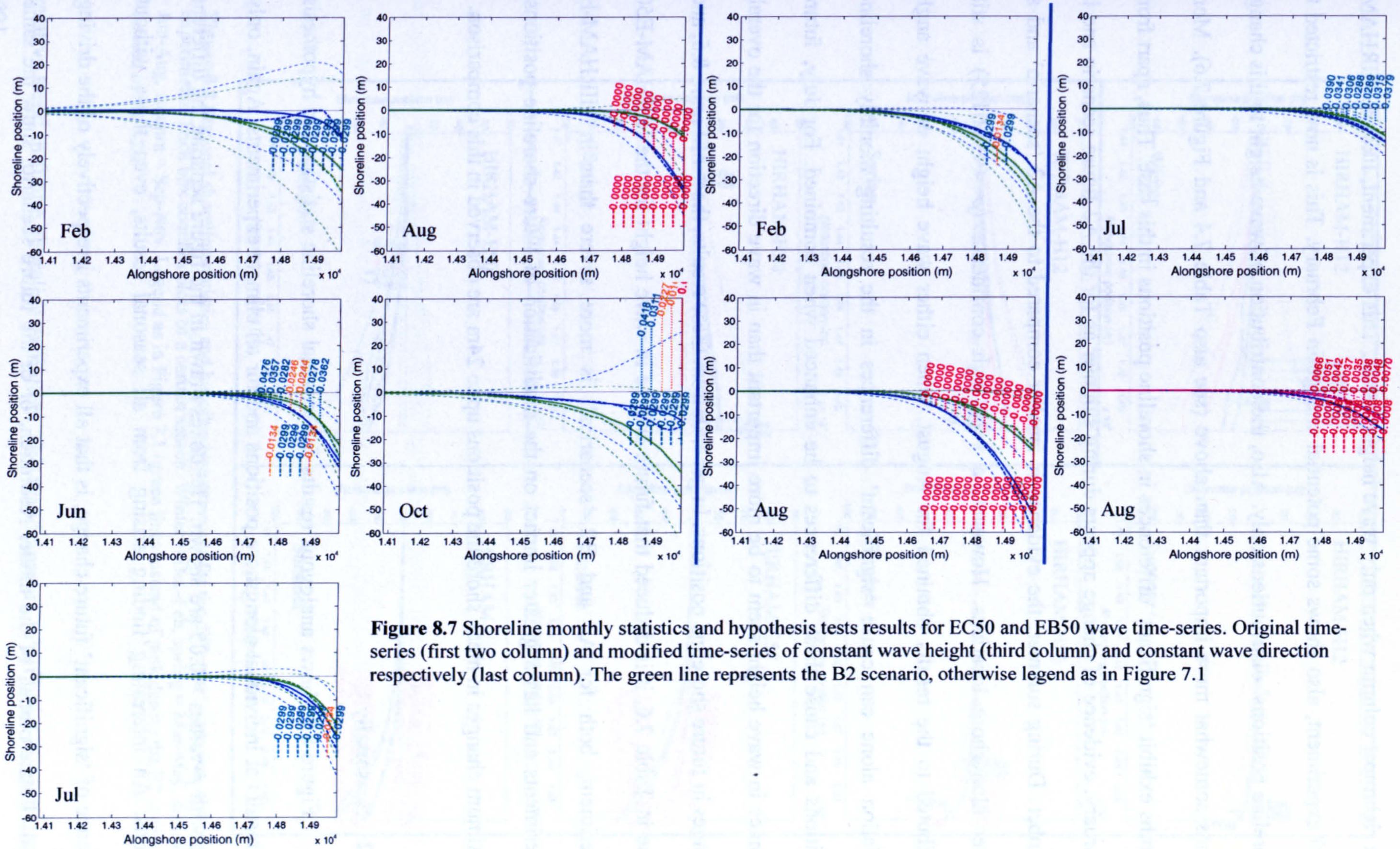

Figure 8.7 Shoreline monthly statistics and hypothesis tests results for EC50 and EB50 wave time-series. Original time-series (first two column) and modified time-series of constant wave height (third column) and constant wave direction respectively (last column). The green line represents the B2 scenario, otherwise legend as in Figure 7.1

last rightmost column when only wave height varies. This experiment, like the HIRHAM-H50 experiment, also shows some potential change in February. This is now restricted to shoreline positions' distributions only. Also, the contribution of wave height to this change seems somewhat more important than above (see also Table 7.4 and Figure 7.6). More months exhibit 'significant' differences in shoreline positions in this case. Thus, apart from February, evidence of change appears during summer as for the A2 future scenario and in October. During summer, the evidence is smaller compared to the A2 'scenario' and at fewer alongshore locations. However, a very high confidence ($p << 0.0125$) is still attributed to the results obtained for August, when either wave height or wave angle variation alone can cause 'significant' differences in the resulting monthly shoreline positions and cause these differences to be enhanced when combined. For July, future changes in wave height seem to be more important than in wave direction for the overall changes in future shoreline positions. In general, from these results, those of Figure 8.5, and those in Table 7.6, it is deduced that future change in wave height for the HIRHAM-E50 experiment, both for A2 and B2 'scenarios', is more severe than in HIRHAM-H experiments and has a greater impact on the modification of future shoreline positions. Maximum changes in mean shoreline positions up to 24m are observed in this comparison.

8.3.2 Seasonally

Figure 8.8 shows analogous results for seasonal shoreline statistics and hypothesis test results at individual alongshore positions and for all climate experiments. Again, only plots with p-values > 0.05 are shown. The boxes drawn in the figure separate the different seasons. An interesting finding arising from all seasonal results, even those without evidence of 'significant' future change, is that all experiments irrespectively of the driving global climate model, of the model resolution, or of the future scenario, show the same

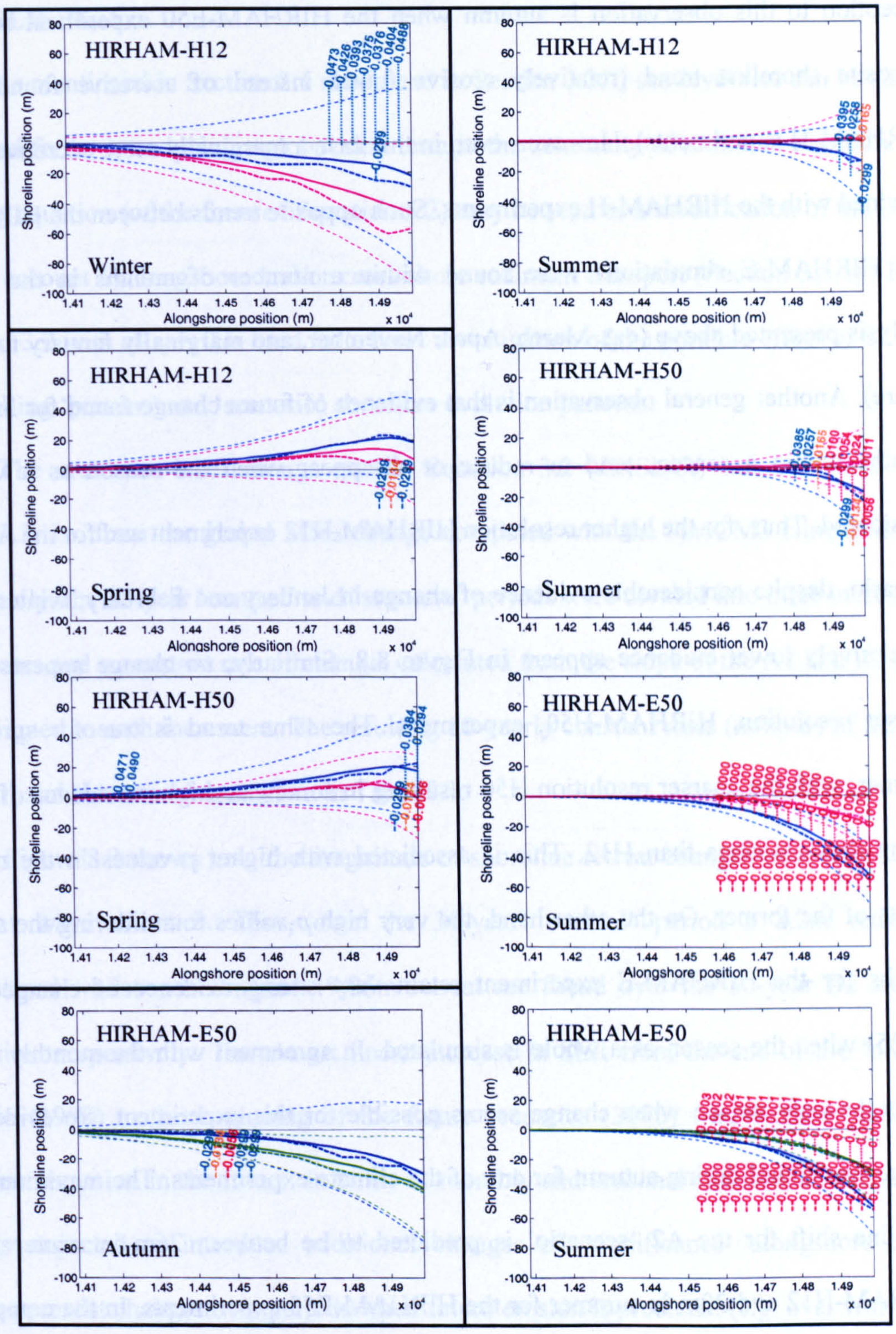

Figure 8.8 Seasonal shoreline statistics and hypothesis tests results for the different 'scenarios' and climate experiments. Each box contains plots of a certain season. Winter = Dec-Feb, spring = Mar-May, summer = Jun-Aug, autumn = Sep-Nov. Legend as in Figure 7.1 (green lines instead of pink denote the B2 scenario instead of the A2).

relative trend in future shoreline evolution. This trend appears in different magnitudes. An

exception to this observation is autumn when the HIRHAM-E50 experiment reveals an opposite shoreline trend (relatively erosive future instead of accretive found for the HIRHAM-H experiments). However, even in this case a marginally more accretive trend in obtained with the HIRHAM-H experiments. Such opposite trends between the HIRHAM-H and HIRHAM-E simulations were found within a number of months in the monthly analysis presented above (e.g. March, April, November, and marginally January for the A2 future). Another general observation is that evidence of future change found for individual months within a season, tend to reduce or disappear when the season as a whole is considered. Thus, for the higher resolution HIRHAM-H12 experiment and for the A2 future scenario, despite considerable evidence of change in January and February, winter change of relatively lower evidence appears in Figure 8.8. Similarly, no change appears for the coarser resolution, HIRHAM-H50, experiment. The same trend is true for spring and summer, with the coarser resolution H50 resulting in somewhat higher evidence of change during these seasons than H12. This is associated with higher *p*-values in the monthly results of the former. On the other hand, the very high *p*-values found during the summer months for the HIRHAM-E experiment retain very strong evidence of change ($p << 0.0125$) when the season as a whole is simulated. In agreement with the monthly results, this is the only season when change seems possible for this experiment. No evidence of change was found during autumn for any of the climate experiments. The maximum mean shoreline shift for the A2 'scenario' is predicted to be between 26m in winter for the HIRHAM-H12 and 30m in summer for the HIRHAM-E50 experiments. In the comparison of the 'present' with the B2 future scenario, evidence of change appears only for the HIRHAM-E50 experiment and essentially only in summer ($p << 0.125$). Weak evidence of different shoreline positions' distribution is also present in autumn.

8.3.3 SLR effect

As mentioned in Section 8.1 above and in Section 3.3.1, sea-level rise can be simply accounted for by introducing a global sink term in the continuity of sediment equation. The resulting equation (of the form of Equation 3.2) may be seen as a modification of the Bruun Rule to account for longshore and/or cross-shore sediment transport (Section 3.3.1). Here, Equation 3.2 with all $q = 0$ is used for a brief investigation of the possible effect of SLR on the resulting 'present' and 'scenario' shoreline evolution patterns.

The mean sea-level change rate in Equation 3.2 ($\partial MSL/\partial t$) was estimated from Figure 3.3, i.e. from the global MSL change computed with the HadCM3 climate model. Specifically, the 30-year 'control' and 'scenario' periods were divided into three increments of 10 years and a constant rate of change, calculated from the slope of the A2 and B2 lines, was assigned to each increment. The resulting 10-yearly constant rates (m/hour) of SLR for 'control' and 'scenarios' are shown in Table 8.1.

Figure 8.9 shows how the magnitude of shoreline retreat changes over time for the different wave climates. Thus, over the 30-year 'control' period a 2.2m retreat is encountered whilst a 13.2m and 19.25m retreat are found over the 30-year B2 and A2 'scenarios' respectively. The almost linear increase in SLR from the end of the 'present' scenario (1990) to the beginning of the future scenarios (2070) would cause additional shoreline recession in the future. In terms of monthly and seasonal statistics an accelerated SLR is expected to introduce additional changes of 'significance' alongshore and/or enhance present changes over periods when future erosion is predicted (e.g. over winter and spring in Figure 8.8). On the other hand, a decrease of changes of 'significance' is expected over periods when future accretion is predicted (e.g. August in Figure 8.8). However, such a simplified consideration of SLR ignores its effect on wave shoaling and refraction patters as mentioned in Section 7.3 and only accounts for shoreline perpendicular waves acting

closer to the shore due to deeper water. In addition, for the same future scenarios a wide range of SLR is predicted by the different climate models (vertical bars on the right hand side of Figure 3.3).

Table 8.1 10-yearly constant sea-level rise rates

	SLR (m/hour)		
	CONTROL	**A2**	**B2**
1960-1970	$2.31481E^{-08}$		
1970-1980	$3.47222E^{-08}$		
1980-1990	$1.73611E^{-07}$		
2070-2080		$5.78704E^{-07}$	$4.05093E^{-07}$
2080-2090		$6.94444E^{-07}$	$4.62963E^{-07}$
2090-2100		$7.52315E^{-07}$	$5.20833E^{-07}$

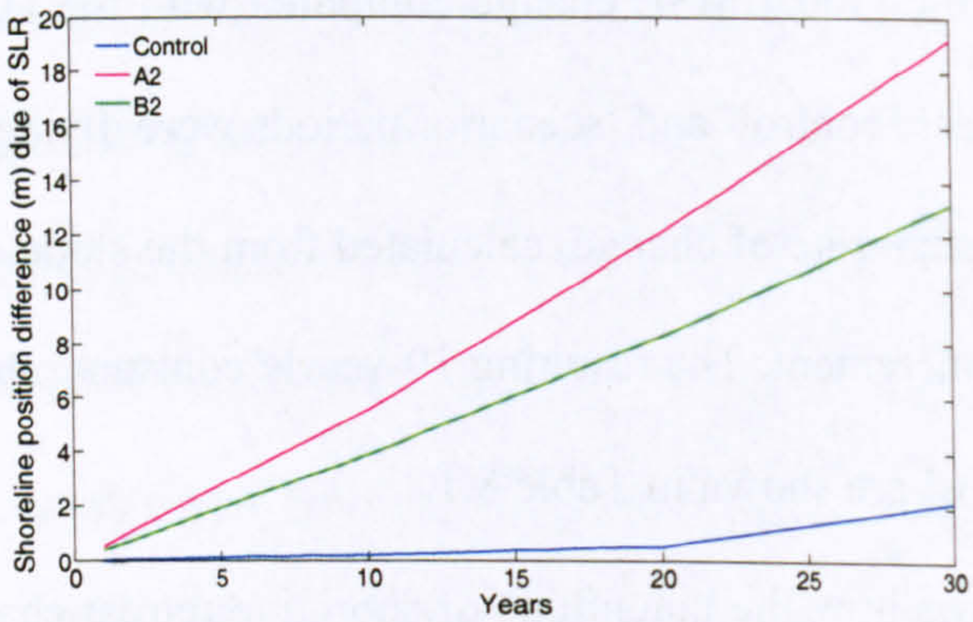

Figure 8.9 Shoreline position change (erosion) alongshore because of SLR versus time.

8.3.4 Comparison with semi-analytical model output

The 'one-line' semi-analytical solution described in Section 8.1 was used to simulate shoreline evolution for the HIRHAM-H12 experiment and results were compared to those obtained with the numerical model. In terms of monthly and seasonal statistics, results were found to be extremely close to those shown in Figures 8.2 and 8.8. Figure 8.10 shows the evolution of the RMSE (m) between the two solutions, semi-analytical (ε_s and ε_w respectively) and numerical, over a complete 30-year simulation corresponding here to the C12 'control' wave time-series. Model output at intervals of 30 days is compared. The

figure shows an increase of the RMSE in time, reaching a maximum value of 6.56m towards the end of the time-series. Slightly smaller, essentially negligibly different RMSE is obtained with the use of ε_w.

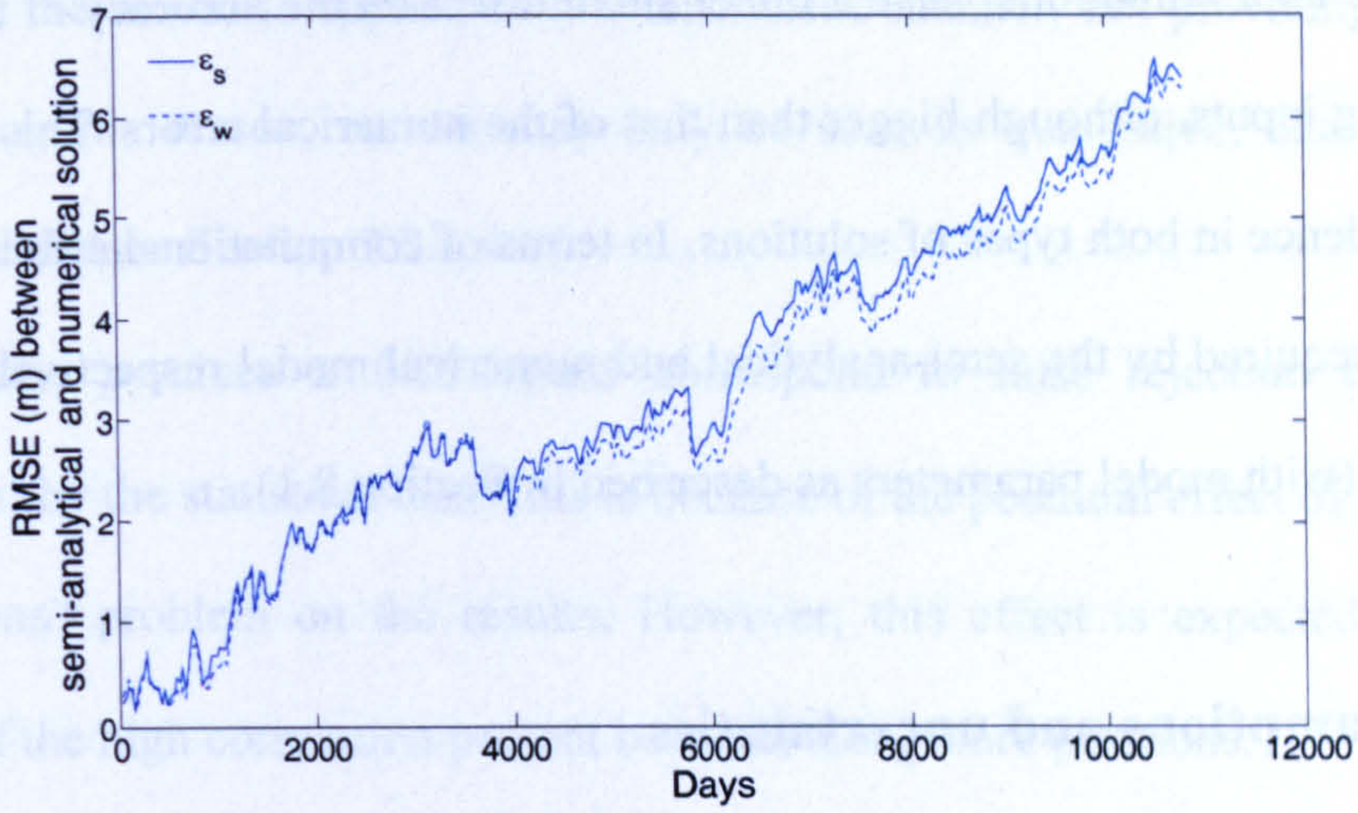

Figure 8.10 Evolution (over 30 years) of the RMSE (m) between semi-analytical and MOL numerical output.

Here, the situation is similar to the one of Figure 6.8, Chapter 6, i.e. to shoreline evolution within a groyne compartment, where both erosional and accretional trends are present and where several high angles of wave approach relative to the shoreline normal occur. Thus, as discussed in Chapter 6, the increase in RMSE with time is a combination of the assumptions and errors associated with the two different 'one-line' models Firstly, the small angle approximation inherent in the semi-analytical solution is often violated with waves of direction > 15^0 largely dominant relative to waves of direction < 15^0. As a result, a frequent overestimation of the shoreline evolution rate by the semi-analytical solution would lead to an increasingly bigger deviation from the numerical solution. Secondly, the numerical error, in contrast to the semi-analytical one, is cumulative. Thus, an increasing numerical diffusion associated with the specific numerical scheme adds to the deviation observed. A 30-year simulation with modified, largely decreased wave angles relative to the shoreline normal (max $|$wave angle $|$ < 15^0) resulted in a maximum RMSE (m) of

0.08m indicating that errors due to 'small wave angle approximations" are potentially much more important than errors due to numerical diffusion. In any case, for such a long-term simulation the error between the two solutions is still considered small suggesting that 'small angle approximations' have a rather small effect on the accuracy of the results under time-varying inputs, although bigger than that of the numerical errors. This result increases one's confidence in both types of solutions. In terms of computational efficiency, 35sec and 3min were required by the semi-analytical and numerical model respectively to complete a 30-year run (with model parameters as described in Section 8.1).

8.4 Assumptions and uncertainties

Extending Section 7.3, additional basic assumptions and uncertainties of this impact assessment study that arise from the use of the 'one-line' model and the specific methodology adopted are summarized in this section. These include:

- Waves at a reference water depth of 3.53m are input in the models and wave characteristics are assumed to be constant alongshore. This assumption would be a reasonable approximation of a shore with nearly straight parallel contours. Diffraction is neglected.
- The assumption of a constant depth of closure, D_c, inherent in the 'one-line' models is often violated in the very long time-scale when net profile translation might occur (Section 2.2.1.5). Specifically, D_c has been found to increase with time. Thus, a different value of D_c might be appropriate for the 'scenario' simulations disregarding the fact that D_c might change even within the 30-year runs.

- No sources or sinks of sediments are considered. In a site-specific application future changes in the sediment budget are to be expected and might considerably influence the results.
- In general, the model is applied in a deterministic manner, not providing uncertainty bounds. For this reason, results may only be seen as qualitative, aiming to reveal general trends (see Section 2.2.3.4.1).
- Occasionally, *p*-values ≤ 0.05 could correspond to false rejection of the 'null-hypothesis' by the statistical test. This is because of the potential effect of the "multiple comparisons" problem on the results. However, this effect is expected to be small because of the high correlation present between alongshore positions.

8.5 Discussion

The potential effect of a changing wave climate due to climate change on future shoreline evolution was explored in this chapter. Using climate model based 'present' wave conditions (1961-1990) and 'scenarios' (2071-2100) to run the 'one-line' model individually for every month and season within each of the 30-year time-series (i.e. setting the shoreline to its initial shape after each month or season was executed), monthly and seasonal statistics of the 'present' and future shorelines were generated. Hypothesis tests were then performed to identify any potential for changes of significance between 'present' and future statistics, in particular, changes in the mean shoreline values and shoreline positions' distributions alongshore. Thus, for example, one could find that future scenarios of offshore wave heights and directions (the parameters examined herein) result in winter shorelines moved 'significantly' shorewards (i.e. indicating the presence of an erosional trend) relative to 'present'. This trend could be even in the opposite direction to the existing

one. Then, one should plan to count for the possible adverse consequences of such a trend. For instance, at Hengistbury Head (area behind the Refraction point at Figure 7.1) significantly enhanced erosion during a certain period (e.g. a month or a season) might violate a safety threshold beyond which a breach through the low cliff line is highly possible. If this happened a tidal inlet to Christchurch Harbour (to the east of Poole Bay in Figure 7.1) would be established separating Hengistbury Head from the mainland (Halcrow, 2004; SCOPAC, 2003). SLR would be expected to act in addition to changes in offshore wave climate to generally enhance trends of future erosion or reduce future accretional trends predicted with wave climate changes alone.

All climate experiments of Table 7.1 were used in the analysis. The latter was performed on a hypothetical stretch of shoreline consisting of a long straight shoreline bounded at one side by a long impermeable groyne. The main findings may be summarized as:

Medium-high A2 future scenario

- HIRHAM-H12 experiment shows substantial evidence of shoreline change relative to control shoreline statistics primarily in late winter months (January and February), early spring (March) and later summer (August). Change also appears in later spring and early autumn (September) but is associated with a lower degree of confidence.
- HIRHAM-H50 experiment leads to very similar results with slightly lower *p*-values (i.e. stronger evidence of change) in early spring (March) and late summer (August) and slightly weaker for the rest of the months.
- HIRHAM-E50 experiment shows very strong evidence of future change ($p << 0.0125$) but only through summer (June-August).

- August is the only month the three experiments agree on showing very strong evidence of future shoreline change, suggesting that regional climate model resolution has a much smaller effect on the results than that of the driving global model. This is a common result found in several studies (e.g. Räisänen *et al.*, 2003)
- Seasonally, for the HIRHAM-H experiments, evidence of change is smaller than that found for individual months within a season. The H12 experiment shows changes of 'significance' mainly in winter and summer and less in spring. *P*-values are generally > 0.025. The H50 experiment produces changes of higher 'significance' in spring and summer (several *p*-values < 0.0125 in summer) but no such change is predicted for winter. HIRHAM-E50 experiment in accordance with its monthly results shows very strong evidence of change in summer ($p << 0.0125$).

Medium-low B2 future scenario

- Smaller evidence of change is predicted for this future scenario which usually produces shorelines lying between the 'control' and A2 'scenario' shorelines.
- HIRHAM H50 experiment shows changes of 'significance' only in February.
- HIRHAM E50 experiment agrees with HIRHAM H50 for February, however showing change of considerably smaller 'significance' during this month. Also, as for A2, changes appear 'significant' for every summer month, particularly for August. Some change is also present in October.
- Seasonally, only the HIRHAM-E50 experiment produces evidence of future change and essentially only for summer where $p << 0.0125$.

General

- Shoreline changes of 'significance' are closely linked to 'significant' changes in future wave direction. Less to those in wave height. The latter normally acts to enhance or

reduce changes due to wave direction variation alone but is rarely able to produce a 'significant' difference in shoreline positions if considered on its own, i.e. if wave direction is kept constant. Wave height impact on shoreline evolution modification is found to be more important for the HIRHAM-E50 experiment for which strong evidence of future H_s mean change was found.

- All experiments agree in the direction of shoreline evolution in response to the future scenarios relative to the 'present' for all seasons except from autumn (relative erosion in winter and spring and accretion in summer).

Overall, the above results suggest that it is difficult to arrive at concrete conclusions about changes in future shoreline evolution patterns because of the output variability produced by experiments driven by different global climate models. In addition to this uncertainty, uncertainties described in Sections 7.3 and 8.4 lessen the degree of confidence in the results. However, such an analysis still helps to suggest that certain changes are more probable than others. For example, that winter shoreline erosion in the future relative to the 'present' is much more likely than relative accretion or that future offshore wave climate will most probably cause relative shoreline accretion during summer which might be partly compensated because of SLR. Investigation of a greater number of emission scenarios and mainly climate model experiments would help to improve the degree of confidence in these types of result. To this extent, a simple, straightforward, and efficient methodology like the one adopted in this study could easily accommodate a broad range of models and scenarios.

To end with, it is highlighted that studies on potential shoreline change due to climate change are still very rare and have traditionally used incremental scenarios that often lack of realism. Never before has climate model output been used in future shoreline assessments. Also some assessments of changes in future wave climate, and occasionally

alongshore drift rates, have used climate model output of a much coarser resolution both in time and space.

Chapter 9

Conclusions and recommendations

In this final chapter of the thesis, the work carried out throughout this document is encapsulated to provide the reader with a concise but clear image of its aims, pathways, benefits, and findings. Initially, the fundamental objectives of the study are given along with those elements of the work that largely determined the root followed to achieve these objectives. The fact that the present work is associated with non trivial uncertainty is emphasized. Then, a brief background summary is given stressing the points that are central to the research carried out. The gaps or deficits of existing work this study aimed to fill in are listed next. Alongside, the related improvements/extensions of the present work are mentioned. Conclusions of this study are highlighted through the use of square bullets and are divided in the four major investigation themes of this study: analytical 'one-line' modelling; numerical 'one-line' modelling; intercomparison of the two modelling types; wave climate impact on the shoreline. The methodology associated with each of these themes is briefly outlined. Finally, further research is suggested that should improve the results of the present work or extend it to make it more comprehensive.

9.1 Study aims and characteristics

The present study has been primarily focused on the assessment of the impact of changes in wave climate (wave height and direction), caused by climate change, on the evolutionary patterns of the shoreline. The study further aimed at improving the 'one-line' model for shoreline change, i.e. the tool used to achieve its primary objective. Therefore, a substantial part of this work has been on the development of the analytical and numerical solutions of the model.

Key methodological elements of the study include:

- The original data sets relevant to the forcing used in this study are site-specific; however, the case of shoreline change examined is hypothetical.
- As a consequence, the results obtained are not site-specific but rather broadly representative of coastlines of a similar setting to the one hypothesized, similar forcing mechanisms, and future changes in wave characteristics of a comparable magnitude.
- The hypothesized case of shoreline change is one that is appropriate for 'one-line' modeling applications.
- Interest is on relative shoreline changes between 'present' or 'control' evolution and future or 'scenario' evolution.
- As a result, the accuracy of the 'control' wave climate against actual observations is not of importance; instead, the use of realistic wave conditions is important.
- Simple, fast, and straightforward techniques are proposed that are capable of accommodating a wide range of scenarios, i.e. very long wave time-series, with minimum computational effort and without need for data reduction, thus retaining the precise wave characteristics.
- Results are qualitative given in terms of general trends.

When looking at the present work, one has to bear in mind that no data and no methods are currently available to predict accurately the impact of climate change on the evolution of the coastal zone. At these time-scales, predictions are difficult and inherently uncertain. However, they are necessary for efficient SMPs. As a result, existing studies involve a number of assumptions and simplifications, and a significant degree of uncertainty so that they can only be seen as highly approximate qualitative approaches. The same is true for this study, which serves as an early, interim assessment of future shoreline change until better methods and data become available or the methodology suggested is elaborated to account for a greater part of the uncertainty involved in predicting future shoreline change. Meanwhile, the work presented herein contributes to the understanding of the magnitude and direction of shoreline position changes expected to occur in response to a changing wave climate and proposes simple but often preferable methods to this problem.

9.2 Background thesis summary

The need for incorporating the effects of climate change, especially SLR and changes in wave climate, in the predictions of shoreline change has been highlighted in this thesis. Difficulties and uncertainties associated with long-term predictions were mentioned and current approaches were outlined. The shoreline change modeling approach used in this study, i.e. the 'one-line' model, was reviewed in detail. Furthermore, a review was carried out on climate change. This included its potential effects on the coastal environment; the methods associated with the development of climate change scenarios; SLR, wind and wave climate scenarios for the UK; and the description of studies that have investigated the impact of the aforementioned climatic variables on future modifications of the littoral drift and the shoreline.

It has been shown that decadal predictions of shoreline change are extremely difficult because of the high complexity of the coastal system and the uncertainty associated with climate change, the latter being the sum of the uncertainty in the magnitude of climate change and in the associated modeling of atmospheric forcing and ocean response. Current approaches to long-term prediction of shoreline evolution are mathematical or non-mathematical (e.g. statistical extrapolation). The former are highly preferred because, in contrast to the latter, they may account for changes in the statistics of the forcing, they are objective, they typically require a smaller amount of data, and they are cheap. It has been shown that amongst existing mathematical models for the prediction of shoreline change, behaviour-oriented models, the 'one-line' model, and hybrid models can be applied for decadal predictions. The former are of restricted generality. The latter involve not well established parameterization or various processes and require large funds to be applied. This makes the 'one-line' model the best option for decadal shoreline change predictions when results need to be broadly representative, data availability is limited, and resources are restricted - issues that pertain to the present work.

This simplified model, based on the concept of a constant equilibrium beach profile, has proven its skill in various applications. It performs best at open, sandy shores, shaped predominately by wave-induced alongshore transport. This is the kind of coastal environment the present study has focused on. Analytical and numerical solutions to the model exist. The former involve small angle approximations and are for idealized cases of shoreline change. The latter may be applied to complex conditions. Nevertheless, the two types of solutions are complementary and both important.

It has been stressed that the 'one-line' model is far from perfect and its basic assumptions might be violated in the very long-term, especially under the effects of climate change. For example, in several cases, a steepening of the beach profile has been observed

under SLR. Such a steepening would render the assumption of a constant equilibrium beach profile invalid. Similarly, assumptions of any model for shoreline change are at risk when the models are applied to predict the distant future. The greater the time-scale simulated the larger the uncertainty associated with the model output.

The review on climate change scenarios for the UK revealed that future SLR acceleration is considered certain whilst there is strong evidence that the wave climate will change around the British Isles. Nevertheless, it has been highlighted, that even if change in the variable of interest is undisputed, uncertainty is significant, so that a wide range of possible futures, i.e. a number of future scenarios for the same variable, exist. Therefore, uncertainty estimates of climate change impact assessment studies improve as the number of scenarios accounted for increases. For the derivation of climate change scenarios, a number of techniques exist. These are broadly divided into mathematical and non-mathematical. Comprehensive, physically-based mathematical models are the ones preferred for reasons that are similar to those described for the case of shoreline evolution modelling. For example, the fact that non-mathematical approaches do not explicitly relate to greenhouse forcing is a severe drawback of these approaches and can lead to the generation of unrealistic future scenarios.

Climate change mathematical models differ in their formulation and resolution. Differences in formulation are responsible for a great deal of the uncertainty associated with climate change scenarios. Differences in resolution mainly determine how well fine scale processes are simulated. The higher the resolution the better these are resolved. In consequence, climate variability and extremes are better captured. The latter are very important for regional impact assessment studies. Therefore, higher resolution climate model output form RCMs is essential for these studies. Coarser resolution GCM output is sufficient for the assessment of large-scale processes and is needed to drive the RCMs.

Climate model simulations are computationally expensive, particularly the regional ones. As a result, the models are run for limited areas or/and restricted time periods.

The number of studies on the impact of climate change on wave climate, littoral drift and shoreline evolution is steadily growing. Several studies already exist on future changes in offshore wave climate. Few have evaluated nearshore changes in wave characteristics and associated modifications in the littoral drift. With respect to future changes in shoreline positions, a substantial amount of studies exist on the effect of SLR on this variable. These are mostly based on simplified calculations using the Bruun Rule. However, studies that have explicitly investigated the impact of a changing wind wave climate on shoreline evolution are still very scarce. These have only used incremental scenarios, which, as explained, are generated by changing the variable of interest incrementally by plausible but arbitrary amounts. The 'one-line' model has been applied in these studies. Relatively coarse resolution GCM wind fields or incremental scenarios have been used in the studies of the impact of climate change on wave climate and littoral drift.

9.3 Shortcomings of existing work fulfilled in the present study

Identified gaps or deficits of existing climate change impact assessment studies are listed below. A statement of the related improvements/extensions of this study follows after each gap/deficit is introduced.

1. Scarcity of studies on the effect of a changing wave climate on shoreline evolution, thus, limited understanding of the problem. This study uses alternative methods and data sets for the investigation of this effect. Further insight is obtained on the order of shoreline change that could be expected under a realistic range of change in future wave characteristics.

2. Use of incremental - thus possibly unrealistic - wave climate scenarios in the aforementioned studies. This study generates future wave climate scenarios from physically-based climate model wind output. These should be of a higher quality and lead to improved estimates of potential future shoreline change.
3. Use of a coarse resolution climate model output in studies that aimed to assess relative changes in wave climate and littoral drift between present and future. This study uses high spatial and temporal resolution climate model output, the highest employed to date. As a result, the wave climate scenarios produced are expected to be of a higher quality with a better representation of short-term variability and extremes.

As explained, this work further aimed to improve its basic tool, i.e. the 'one-line' model. Shortcomings in the analytical and numerical solutions of the model were treated. These include:

1. Most analytical solutions make the assumption that a constant, perpetual wave condition drives shoreline change. This is highly unrealistic since it is the cumulative effect of storm and non-storm events that determines shoreline positions. Time variation of the wave forcing has been considered before by two studies but in a limited way. In short, the variation of the waves has been described either by a specific function and only at the boundaries of the domain or only a single frequency of the shoreline movement was simulated assuming an initially straight shoreline. Here, new flexible semi-analytical solutions are derived that account for wave conditions that vary arbitrarily in time, for an initial shoreline shape that is an arbitrary function of alongshore distance, and for source/sinks of sediment.
2. The explicit time-stepping finite difference numerical solution of the 'one-line' model is unstable. The implicit time-stepping finite difference solution, although unconditionally stable, decreases in accuracy with increasing time-step. In addition, it

is difficult to program. Here, the aforementioned problems were overcome by solving the model with the powerful and versatile 'Method of Lines' numerical solution scheme.

3. Numerical 'one-line' models have not been compared against analytical models under time-varying wave conditions because of the lack of analytical solutions under these conditions. Consequently, there has been a lack of understanding on how the discrepancy between the two solutions varies with time in relation to the variation of the wave inputs. This study has gained insight into this discrepancy through a comparison of the new numerical code with the new semi-analytical solutions.

9.4 Methodology outline and Conclusions

9.4.1 New semi-analytical solutions of the 'one-line' model

Fourier transform techniques were used to derive the new solutions. Two common cases of shoreline change were solved: (1) when the function of shoreline evolution is known at a location along its length, and (2) within a groyne/headland compartment. The solutions are given in terms of closed-form integrals or converging Fourier series. They are semi-analytical in the sense that numerical integration is required. Advantages and disadvantages of the new solutions include:

- They hold the general advantages of analysis but are much closer to reality than previous analytical work since shoreline response to a sequence of storm and non-storm events can be simulated. This response can depart substantially from that predicted when a time-average condition is employed.

- They provide a valuable tool for extending the range of solutions against which the accuracy and convergence of time-stepping numerical models can be tested.
- They are of sufficient generality so as to permit investigation of a variety of factors that might impact the shoreline, such as storminess, sea-level change rates, or simple adaptive management policies.
- They allow for the use of diffusion coefficient formulae that explicitly account for wave angle variation. Examination of the effect of such a diffusion coefficient showed that it can have a subtle effect on the results (see Section 9.4.3).
- Compared to earlier analytical solutions, a weakness of the new solutions is that they are of increased complexity - yet very efficient to calculate - and have non-accumulative small errors associated with the numerical integration required for their evaluation.

9.4.2 MOL numerical solution of the 'one-line' model

In the specific MOL based numerical procedure used herein, the spatial derivatives of the sediment transport rate in the continuity of sediment equation were approximated with first order upwind differences as common, and the resulting system of ODEs was integrated in time using the high precision Bulirsch-Stoer time integrator with error control. A sensitivity analysis to key parameters of the method and a comparison of MOL solutions with explicit and implicit finite difference solutions of the 'one-line' model revealed the following advantages and disadvantages of the MOL solutions:

- In contrast to the explicit finite difference solutions, the MOL solutions were found to be 'unconditionally' stable. Stability problems appear for very small values of dx and are indicated by large run times. Thus, the practical applicability of the MOL method over such grid-size values is reduced.

- The MOL solutions are almost identical to the explicit finite difference solutions when these are stable. However, in contrast to the implicit finite difference solutions, the accuracy of the MOL solutions is not affected by the user specified time-step. This is because the actual integration stepsize of the MOL numerical scheme is controlled internally so that user-specified accuracy is always met.
- In contrast to the complex implicit finite difference coding, MOL programming of the 'one-line' model is simple and flexible. The user may switch to different shoreline change problems, ODEs integrators, or spatial approximations with minimal effort. The abundance of very high quality ODEs integrators that are readily available is a general advantage of the MOL method and is what makes the method particularly attractive at the first place.
- One might consider as a weakness of the MOL based code the fact that it executes slower than the explicit finite difference code. Nevertheless, execution times are comparable and converge towards higher dx and larger user-specified integration stepsizes.

9.4.3 Intercomparison between the semi-analytical and MOL solutions

No higher accuracy was assigned to any of the methods since both are approximate with largely unquantifiable errors for the case where wave conditions vary arbitrarily in time. Solutions were compared for two cases of shoreline evolution: (1) smooth Gaussian hump, and (2) groyne compartment. Two versions of a 400 hours wave sequence were used as input: (1) consisting of very small angles of wave approach, and (2) containing several high angled waves. Two diffusion coefficients were considered. One which allows only for small angles of wave approach, ε_s, and one which allows for wider angles, ε_w. Results which conform to previous work and new findings are listed below:

- Excellent agreement was found between semi-analytical and numerical results when the 'small-angle approximations' of the analytical work were achieved, i.e. for the small wave angle time-series. Good agreement, despite clearly less good than in the aforementioned case, was found between the two solutions for the wide-angle wave time-series because of the violation of the small-angle assumption of the semi-analytical solutions. These results are in agreement with earlier work and were largely expected.
- Agreement between the two solutions was better for the case of the smooth Gaussian hump than for the case of the groyne compartment. This is attributed to larger local shoreline orientations associated with the latter case.
- In accordance with earlier work, it was shown that the error caused by linearizing the transport equation is an overestimation of the speed of shoreline response. Thus, high wave angles caused the semi-analytical shoreline evolution to speed up relative to the numerical. Nevertheless, the present work revealed that high wave heights have a subtle effect on the results by increasing the rate by which the numerical shoreline evolves relative to the rate of evolution of the semi-analytical output. For significantly high waves, numerical solutions may evolve faster than analytical even if these waves approach the shore with high angles.
- In contrast to what would have been expected, the use of ε_w in the semi-analytical solutions proved to be a worse approximation than the use of ε_s for certain cases of shoreline change. This is because of the high sensitivity of the former diffusion coefficient to the value of the local shoreline orientation. Specifically, above a threshold value of this parameter and within a certain range, approximations with ε_w became worse. For wave angles between 5^0 and 40^0, this threshold value varied linearly between 0.03 and 0.05.

9.4.4 Wave climate scenarios and associated relative shoreline changes

Reference to the "Study aims and characteristics", Section 9.1, helps to understand the methodological choices described below. In summary, the procedure for generating nearshore wave climate scenarios for input in 'one-line' simulations followed the following steps:

- Wind data from three RCM (HIRHAM) time-slice experiments consisting of the 'control' (1961-1990) and 'scenario' (2071-2100) time-slices, were obtained. Experiments varied with respect to their resolution (12km and 50km) or the driving GCM (HadAM3H and ECHAM4/OPYC). Output has been for the SRES A2 and B2 emission scenarios. Data were located at the south-central coast of England (offshore from Poole Bay).
- Deep water waves were hindcast from the wind data using the SMB-Donelan point hindcast model which accounts for non-coincident wind and wave directions.
- Waves were transformed to a single nearshore location (Hengistbury Head) using SANDS software which in turn uses the REFPRO ray back-tracking spectral wave energy transformation model.
- A *t*-test was performed to identify significant differences between 'control' and 'scenario' mean monthly nearshore wave characteristics (wave height and direction).

SLR, changes in tidal characteristics, changes in bathymetry, swell, and alongshore variation of the wave characteristics were neglected in the analysis.

The nearshore wave climate scenarios were directly input in the 'one-line' model. A hypothetical shoreline segment of 268^0 azimuth was implemented. The model was run individually for every month and season within each of the 30-year time-series to produce monthly and seasonal statistics of 'control' and 'scenario' shorelines. *T*-tests and *ks*-tests were performed for individual alongshore positions to identify whether some evidence of

change between 'present' and future statistics exists. Stronger or weaker evidence of shoreline modification has been inferred from the *p*-values of the hypothesis tests.

Conclusions related to the wave climate statistics are recapitulated below. These are expected to be representative of the south-central coast of England, where the original data are located. General trends and relative differences of significance are referred only for those cases when the various climate model experiments produce results that are in agreement. Thus:

- In general, in the future, prevailing winter waves (Dec-Feb) are higher, autumn waves (Sep-Nov) including August are lower, and summer and spring waves are largely unchanged. The long-term mean H_s is slightly lower in the future, 0.6% to 8.5% for the HIRHAM-H12 and the HIRHAM-E50 experiments respectively. These general trends conform to a number of previous studies.
- From April to September south and southwest waves generally increase on expense of southeast waves. The contrary is true in winter.
- Significant differences in long-term mean H_s between 'present' and A2 'scenario' have been found in September. Such differences in wave direction have been found in August and are associated with a very high degree of confidence. For the B2 'scenario' wave direction changes significantly in February.
- For both H_s and wave direction, the comparison of future scenarios, A2 versus B2, results into fewer significant differences than those found between 'control' and A2 but not necessarily between 'control' and B2.
- In agreement with earlier studies, climate model resolution was found to have a small effect on the results but the choice of the driving GCM had a significant influence. However, it should be kept in mind that this result could be partly caused because of the

different way wind was treated in the two experiments (HIRHAM-H50 and HIRHAM-E50).

Conclusions related to the shoreline statistics may be summarized as:

- As expected, the layout of the evidence of future change in shoreline positions is similar for the two experiments driven by the same GCM but considerably diverges between experiments driven by different GCMs, thus preventing high confidence in the results. Nevertheless, particularly for seasonal output, the three experiments mostly agreé in the direction of 'future' shoreline evolution relative to the 'present'. Thus, greater erosion in winter and spring and greater accretion in summer has been predicted.
- In general, for the A2 emission scenario, evidence of change is stronger in later winter (Jan-Feb), early spring (Mar) and late summer (Aug) for the HIRHAM-H experiment and through summer for the HIRHAM-E experiment. Thus, August is the only month when common results between experiments were obtained. Also, this is the month when evidence of change is the strongest for all experiments.
- For the B2 emission scenario, weaker evidence of change is predicted with the mean B2 shorelines normally lying between the 'control' and A2 shorelines. There was agreement amongst the experiments that some change is evident in February. Otherwise, it is only the HIRHAM-E experiment that resulted in strong evidence of change during summer.
- In general, for entire seasons the evidence of future change appeared weaker than that corresponding to individual months. Summer is the only season for which the three experiments agree that shoreline change is highly possible in the future.
- Shoreline changes of 'significance' are more linked to 'significant' changes in future wave direction than in wave height. The impact of the latter was found to be increased for the HIRHAM-E experiment for which strong evidence of future H_s mean change was found.

- Shoreline position variability in response to future wave climate scenarios was found to be equal or smaller than the 'present' variability.

9.5 Recommendations for future research

There are several research possibilities that could improve or extend the work presented herein. In fact, climate change impact assessment studies may be divided in two broad categories: (1) those that pursue an holistic approach to the problem by incorporating the greatest possible number of scales and processes that could be of relevance to the problem under consideration, e.g. advanced 'system' models in combination (or not) with non-mathematical approaches, and (2) those that simplify the problem and study one or two processes of interest in isolation. Specific advantages and disadvantages of each of these approaches were described in this study, which focused in the simplified approach to achieve its objectives. Here, priority research directions are suggested that are mostly related to the simplified approach to the problem of climate change and shoreline evolution. These include:

- **Increase of the number of climate model experiments used in the analysis.** This is probably the most obvious research direction to improve the kind of results obtained from the methods used herein and to arrive to more concrete conclusions about the effect of a changing wave climate on future shoreline positions. By incorporating the greatest possible number of experiments, carried out for different emission scenarios, with different RCMs and most importantly different driving GCMs, one can assign a weight to each of the results produced by each of these experiments. For example, if a specific result appears for the majority of climate model simulations, the probability to observe this result in the future should be greater and a higher weight should be applied to it. In

this way, one's confidence in certain outputs should increase relative to one's confidence in others.

- **Probabilistic modelling.** Following Ruggiero *et al.* (2006), the Monte Carlo technique can be used to generate several wave time-series from the original climate model based wave scenarios and to run the 'one-line' model in a probabilistic manner. In this way, shoreline change prediction probability distribution functions can be produced. Following Cowell *et al.* (2006) and Dickson *et al.* (2007) uncertainty in profile shapes and magnitude of shoreline recession can also be studied by varying the future values of 'closure depth' in the 'one-line' model simulations.

- **Estimation of the temporal evolution of the statistics.** It would be beneficial if the statistical analysis of the significance of the differences between 'present' and 'future' shorelines would be performed using shorter period averages as well as longer. This is because the signal intensity is expected to vary temporally so that such an analysis would provide some information on the temporal evolution of the abovementioned significance.

- **Extreme analysis of the wave input.** Such an analysis can assess whether future changes in the frequency and/or intensity of storms or changes in the prevailing wave climate are more important in causing shoreline changes of significance.

- **Incorporation of water levels – feedback between changing shoreline orientation and nearshore wave characteristics.** The impact of SLR and possibly tidal changes on nearshore wave transformation can be accounted for with fairly small additional effort. SANDS software in combination with a simple refraction model, coupled to the 'one-line' numerical code, can be used to achieve this task. Specifically, SANDS software allows the user to define the MWL used in the wave transformation routine. Changing

its value would mean that different water depths would correspond to the Refraction point. From this point waves should be transferred to a reference depth further inshore through the refraction routine of the 'one-line' model, assuming that bottom contours parallel the shoreline orientation. This would also be a way to simply account for the feedback between changes in shoreline orientation and wave characteristics near breaking, assuming constant bathymetry seawards the Refraction point.

- **Incorporation of swell.** Incorporation of swell waves would require wind data over a large domain. For example, if swell was to be hindcast for the specific data location of this study wind data over the northeast Atlantic would be required. In addition, the employment of a higher dimension, more computationally intensive wave hindcast model would be needed. Nevertheless, incorporation of swell is thought to be important, particularly in site specific studies where the swell component is strong.
- **Investigation of the impact of future changes in wave period.** Apart from wave height and direction, the impact of future changes in wave period on shoreline response can be added in the analysis through the adoption of a sediment transport formula that contains this parameter, e.g. Kamphuis' (Equation 2.10) instead of CERC formula.

Appendix A

Table A1 Main features of the models validated in the study of Szmytkiewicz *et al.* (2000) (adopted from Szmytkiewicz *et al.*, 2000)

Feature	GENESIS	LITPACK	SAND94	UNIBEST
2-D bathymetry	necessary in full run; not used in simplified run	required only for determination of representative profile(s)	necessary	required only for determination of representative profile
Variability of seabed properties along shore profile	not taken into account	taken into account	not taken into account	not taken into account
Wave input parameters	significant	root-mean-square	significant	significant
Wave chronology	taken into account	taken into account	taken into account in full run; not taken into account in simplified run	not taken into account
Wave transformation	"mild slope" equation - type in full run; linear refraction/shoaling in simplified run	e.g., Battjes–Janssen	Battjes–Janssen	Battjes–Janssen
Diffraction around structures	taken into account	taken into account	not taken into account	not taken into account
Longshore current	not modelled	Longuet–Higgins type	Longuet–Higgins type	Longuet–Higgins type
Longshore sediment transport	CERC-type formula	DHI model	Bijker, Grant–Madsen, Ackers–White, van Rijn	Engelund–Hansen, Bijker, van Rijn, Bailard, CERC
Beach nourishment	taken into account	taken into account	taken into account	taken into account
Groins, jetties	taken into account	taken into account	taken into account	taken into account
Offshore breakwaters	taken into account	taken into account	not taken into account	not taken into account
Seawalls, revetments	taken into account	taken into account	taken into account	taken into account

Table A2 The characteristics of the four future social and emission scenarios for the UK (adopted from FORESIGHT, 2003)

	Present day	World Markets	National Enterprise	Local Stewardship	Global Sustainability
Social values		Internationalist, libertarian	Nationalist, individualist	Localist, co-operative	Internationalist, communitarian
Governance structures		Weak, dispersed, consultative	Weak, national, closed	Strong, local, participative	Strong, co-ordinated, consultative
Role of policy		Minimal, enabling markets	State-centred, market regulation to protect key sectors	Interventionist, social and environmental	Corporatist, political, social and environmental goals
Economic development		High growth, high innovation, capital productivity	Medium-Low growth, low-maintenance innovation, economy	Low growth, low innovation, modular and sustainable	Medium-High growth, high innovation, resource productivity
GPD growth per year	2.5%	3.5%	2%	1.25%	2.75%
Total investment – % of GDP	19%	22%	18%	16%	20%
Agricultural activity (% of total activity)	2%	1%	2%	3%	1.5%
Newly developed land – hectares per year	6,500	6,000	4,500	1,000	3,000
UKCIP global emissions associated with each scenario		High emissions	Medium-High emissions	Medium-Low emissions	Low emissions

Table A3 The role of various types of climate scenarios and an evaluation of their advantages and disadvantages according to the five criteria described below the table. Note that in some applications a combination of methods may be used (e.g. regional modelling and a weather generator) (adopted from IPCC WG1, 2001).

Scenario type or tool	Description/Use	Advantages[a]	Disadvantages[a]
Incremental	• Testing system sensitivity • Identifying key climate thresholds	• Easy to design and apply (5) • Allows impact response surfaces to be created (3)	• Potential for creating unrealistic scenarios (1, 2) • Not directly related to greenhouse gas forcing (1)
Analogues: Palaeoclimatic	• Characterising warmer periods in past	• A physically plausible changed climate that really did occur in the past of a magnitude similar to that predicted for ~2100 (2)	• Variables may be poorly resolved in space and time (3, 5) • Not related to greenhouse gas forcing (1)
Instrumental	• Exploring vulnerabilities and some adaptive capacities	• Physically realistic changes (2) • Can contain a rich mixture of well-resolved, internally consistent, variables (3) • Data readily available (5)	• Not necessarily related to greenhouse gas forcing (1) • Magnitude of the climate change usually quite small (1) • No appropriate analogues may be available (5)
Spatial	• Extrapolating climate/ecosystem relationships • Pedagogic	• May contain a rich mixture of well-resolved variables (3)	• Not related to greenhouse gas forcing (1, 4) • Often physically implausible (2) • No appropriate analogues may be available (5)
Climate model based: Direct AOGCM outputs	• Starting point for most climate scenarios • Large-scale response to anthropogenic forcing	• Information derived from the most comprehensive, physically-based models (1, 2) • Long integrations (1) • Data readily available (5) • Many variables (potentially) available (3)	• Spatial information is poorly resolved (3) • Daily characteristics may be unrealistic except for very large regions (3) • Computationally expensive to derive multiple scenarios (4, 5) • Large control run biases may be a concern for use in certain regions (2)
High resolution/stretched grid (AGCM)	• Providing high resolution information at global/continental scales	• Provides highly resolved information (3) • Information is derived from physically-based models (2) • Many variables available (3) • Globally consistent and allows for feedbacks (1,2)	• Computationally expensive to derive multiple scenarios (4, 5) • Problems in maintaining viable parametrizations across scales (1,2) • High resolution is dependent on SSTs and sea ice margins from driving model (AOGCM) (2) • Dependent on (usually biased) inputs from driving AOGCM (2)
Regional models	• Providing high spatial/temporal resolution information	• Provides very highly resolved information (spatial and temporal) (3) • Information is derived from physically-based models (2) • Many variables available (3) • Better representation of some weather extremes than in GCMs (2, 4)	• Computationally expensive, and thus few multiple scenarios (4, 5) • Lack of two-way nesting may raise concern regarding completeness (2) • Dependent on (usually biased) inputs from driving AOGCM (2)
Statistical downscaling	• Providing point/high spatial resolution information	• Can generate information on high resolution grids, or non-uniform regions (3) • Potential,for some techniques, to address a diverse range of variables (3) • Variables are (probably) internally consistent (2) • Computationally (relatively) inexpensive (5) • Suitable for locations with limited computational resources (5) • Rapid application to multiple GCMs (4)	• Assumes constancy of empirical relationships in the future (1, 2) • Demands access to daily observational surface and/or upper air data that spans range of variability (5) • Not many variables produced for some techniques (3, 5) • Dependent on (usually biased) inputs from driving AOGCM (2)
Climate scenario generators	• Integrated assessments • Exploring uncertainties • Pedagogic	• May allow for sequential quantification of uncertainty (4) • Provides 'integrated' scenarios (1) • Multiple scenarios easy to derive (4)	• Usually rely on linear pattern scaling methods (1) • Poor representation of temporal variability (3) • Low spatial resolution (3)
Weather generators	• Generating baseline climate time-series • Altering higher order moments of climate • Statistical downscaling	• Generates long sequences of daily or sub-daily climate (2, 3) • Variables are usually internally consistent (2) • Can incorporate altered frequency/intensity of ENSO events (3)	• Poor representation of low frequency climate variability (2, 4) • Limited representation of extremes (2, 3, 4) • Requires access to long observational weather series (5) • In the absence of conditioning, assumes constant statistical characteristics (1, 2)
Expert judgment	• Exploring probability and risk • Integrating current thinking on changes in climate	• May allow for a 'consensus' (4) • Has the potential to integrate a very broad range of relevant information (1, 3, 4) • Uncertainties can be readily represented (4)	• Subjectivity may introduce bias (2) • A representative survey of experts may be difficult to implement (5)

[a] Numbers in parentheses under Advantages and Disadavantages indicate that they are relevant to the criteria described. The five criteria are: (1) *Consistency* at regional level with global projections; (2) *Physical plausibility and realism*, such that changes in different climatic variables are mutually consistent and credible, and spatial and temporal patterns of change are realistic; (3) *Appropriateness* of information for impact assessments (i.e., resolution, time horizon, variables); (4) *Representativeness* of the potential range of future regional climate change; and (5) *Accessibility* for use in impact assessments.

Table A4 Regional sea level rise allowances (adopted from DEFRA, 2006).

Administrative or Devolved Region	*Assumed Vertical Land Movement (mm/yr)*	*Net Sea-Level Rise (mm/yr)*				*Previous allowances*
		1990-2025	*2025-2055*	*2055-2085*	*2085-2115*	
East of England, East Midlands, London, SE England (south of Flamborough Head)	-0.8	4.0	8.5	12.0	15.0	6mm/yr* constant
South West and Wales	-0.5	3.5	8.0	11.5	14.5	5 mm/yr* constant
NW England, NE England, Scotland (north of Flamborough Head)	+0.8	2.5	7.0	10.0	13.0	4 mm/yr* constant

Table A5 Climate-change and management scenarios used in SCAPE models (adopted from Dickson *et al.*, 2007)

Climate-change and management scenarios	
Climate-change scenarios (2000-2100)	
Sea-level rise	
Low	0.2 m higher by 2100 (no change in rate of SLR)
Medium	0.45 m higher by 2100
High	1.2 m higher by 2100
Offshore wave conditions	
Low	no change
Medium	7% increase in winter wave height by 2100
High	10% increase in winter wave height by 2100
High +	High, plus clockwise rotation of the wave rose (10^0)
High –	High, plus anticlockwise rotation of the wave rose (10^0)
Management scenarios (2000-2100)	
1 Defend the whole coastline	100% of cliffed coast defended
2 Maintain existing defences	71% of cliffed coast defended
3 Managed retreat 1 (by 2030 structures removed from small towns)	34% of cliffed coast defended
4 Managed retreat 2 (by 2030 structures removed from larger towns/industry i.e., Overstrand, Mundesley, Bacton Gas Terminal)	16% of cliffed coast defended
5 Remove defences	0% of cliffed coast defended

Appendix B

Table B1 Fetch limits in degrees from North (bold) and associated fetch lengths in km (e.g. 22.8 km fetch length corresponds to radials between 1^0 and 10^0)

1	**10**	**19**	**28**	**37**	**46**	**55**	**64**	**73**	**79**
22.8	16.91	18.16	27.06	19.63	20.75	22.08	23.49	114.3	209.71
88	**97**	**106**	**115**	**124**	**133**	**143**	**152**	**162**	**173**
205.75	198.8	172.34	148.75	145.01	156.05	138.71	121.83	82.46	82.81
184	**195**	**199**	**202**	**209**	**213**	**228**	**257**	**262**	**270**
80.19	128.95	202.58	84.88	118.17	242.86	1000	128.08	120.55	49.72
278	**286**	**294**	**301**	**311**	**327**	**336**	**345**	**360**	
49.86	24.77	21.53	22.09	25.46	25.01	23.05	23.03		

References

Abernethy, C.L, and Gilbert, G., 1975. Refraction of wave spectra. Hydraulics Research Station, Wallingford Report INT117, May 1975.

Alexander, L.V., Tett, S.F.B., and Jónsson, T., 2005: Recent observed changes in severe storms over the United Kingdom and Iceland. *Geophysical Research Letters*, 32, L13704, doi:10.1029/2005GL022371.

Andrew, C. J. F., 1999. Bibliographic review of nearshore wave models. Report DSTO-GD-0214, Maritime Operations Division Aeronautical and Maritime Research Laboratory.

Ashton, A., Murray, A.B., and Arnailt, O., 2001. Formation of coastline features by large-scale instabilities induced by high-angle waves. *Nature*, 414: 296-300.

Bagnold, R.A., 1963. Mechanics of marine sedimentation. In: M.N.Hill (Editor), The Sea, Vol.3. The earth beneath the sea. Interscience, New York, pp. 507-528.

Bakker, W.T. and Edelman, T., 1965. The coastline of river deltas. *Proceedings of the 9th International Conference on Coastal Engineering*, ASCE, pp 199-218.

Bayram, A., Larson, M., Miller, H.C., Kraus, N.C., 2001. Cross-shore distribution of longshore sediment transport: comparison between predictive formulas and field measurements. *Coastal Engineering*, 44: 79-99.

Beersma, J., Rider, K., Komen, G., Kaas, E., and Kharin, V., 1997. An analysis of extra-tropical storms in the North Atlantic region as simulated in a control and 2xCO_2 time-slice experiment with a high resolution atmospheric model. *Tellus*, 49A: 347-361.

Bell, R.G., Hume, T.M., and Hicks, D.M., 2001. Planning for climate change effects on coastal margins. New Zealand Ministry for the Environment, Wellington, New Zealand, 73 pp.

Beniston, M., Stephenson, D. B., Christensen, O. B., Ferro, C. A. T., Frei, C., Goyette, S., Halsnaes, K., Holt, T., Jylha, K., Koffi, B., Palutikof, J., Scholl, R., Semmler, T., and Woth, K., 2007. Future extreme events in European climate: an exploration of regional climate model projections. *Climatic Change*, 81 (Supplement 1), 71-95.

Beniston, M., Tol, R.S.J., Delcolle, R., Hormann, G., Iglesias, A., Innes, J., McMichael, A.J., Martens, A.J.M., Nemesova, I., Nicholls, R.J., and Toth, F.L., 1998. Europe. In: Watson, R.T., Zinyowera, M.C., and Moss, R.H. (Editors), The Regional Impacts of Climate Change - An Assessment of Vulnerability. Cambridge University Press, Cambridge, UK, pp. 149-186.

Bird, E.C.F., 1985. *Coastline Changes*. John Wiley and Sons, New York, 219 pp.

Bird, E.C.F., 1993. *Submerging coasts: the effects of a rising sea level on coastal environments*. John Wiley and Sons, Chichester, UK, 184 pp.

Birkemeier, W.A., 1985. Field data on seaward limit of profile change. *Journal of Waterway, Port, Coastal, and Ocean Engineering*, 111(3): 598-612.

Bishop, C.T., 1983. Comparison of manual wave prediction models. *Journal of the Waterway Port Coastal and Ocean Division*, 109(1): 1–17.

Bodge, K.R. and Kraus, N.C., 1991. Critical examination of longshore transport rate magnitude. *Coastal Sediments `91*, ASCE, pp. 139-155.

Bodge, K.R., 1992. Representing equilibrium beach profiles with an exponential expression. *Journal of Coastal Research*, 8: 47-55.

Bonnett, T., 2002. Mathematical modelling of shoreline evolution. Fourth Year Project, University of Nottingham, School of Mathematical Sciences, 59 pp.

Bouws, E., Jannink, D., and Komen, G., 1997. The increasing wave height in the North Atlantic Ocean. *Bulletin of the American Meteorological Society*, 77(10): 2275-2277.

Bradbury, A.P., Mason, T.E., and Holt, M.W., 2004. Comparison of the Performance of the Met Office UK-Waters Wave Model with a Network of Shallow Water Moored Buoy Data. *Proceedings of the 8th International Workshop on Wave Hindcasting and Forecasting*, Hawaii.

Bretschneider, C. L., 1952. Revised wave forecasting relationships. *Proceedings of the 2nd International Conference on Coastal Engineering*, pp. 1-5.

Bretschneider, C. L., 1958. Revisions in wave forecasting: deep and shallow water. *Proceedings of the 6th International Conference on Coastal Engineering*, pp. 30-67.

Bruun, P., 1954. Coast erosion and development of beach profiles. Technical Memorandum No. 44. Beach Erosion Board, U.S. Army Corps of Engineers.

Bruun, P., 1962. Sea level rise as a cause of shore erosion. *Journal Waterways and Harbours Division*, 88(1-3): 117-130.

Bruun,P., 1988. The Bruun Rule of erosion by sea-level rise: a discussion of large-scale two and three-dimensional usages. *Journal of Coastal Research*, 4: 627-648.

Burgess, K., Jay, H., and Hosking, A., 2004. Futurecoast: Predicting the future coastal evolution of England and Wales. Journal of Coastal Conservation, 10(1): 65-71.

Capobianco, M, Larson, M., Nicholls, R.J., Kraus, N.C., 1997. Depth of closure: a contribution to the reconciliation of theory, practice, and evidence. *Coastal Dynamics `97*, pp. 507-515.

Capobianco, M., De Vriend, H. J., Nicholls, R. J., and Stive, M. J. F., 1999. Coastal area impact and vulnerability assessment: The point of view of a morphodynamic modeller. *Journal of Coastal Research*, 15(3): 701-716.

Carslaw, H. and Jaeger, J., 1959. *Conduction of heat in solids*. Oxford: Clarendon Press.

CERC, 1977. Shore protection manual. Coastal Engineering Research Center, U.S. Corps of Engineers, Vicksburg.

CERC, 1984. Shore protection manual. Coastal Engineering Research Center, U.S. Corps of Engineers, Vicksburg.

Chadwick, A. J., Morfett, J., and Borthwick, M., 2004. *Hydraulics in Civil and Environmental Engineering*. E & F N Spon, London, 644 pp.

Chadwick, A.J., Karunarathna, H., Gehrels, R. O'Brien, D. and Dales, D., 2005. A New Analysis for the Coastal Processes for the Slapton Barrier Beach System. *Maritime Engineering*, ICE, 158(4): 147-161.

Christensen, J. H. and Christensen, O. B., 2007. A summary of the PRUDENCE model projections in European climate by the end of this century. *Climatic Change*, 81(Supplement 1): 7-30.

Christensen, J. H., Carter T.R., and Giorgi, F., 2002. PRUDENCE employs new methods to assess European climate change. *Eos, Transactions American Geophysical Union*, 83(13): 147.

Christensen, J.H., Christensen, O.B., Lopez, P., van Meijgaard, E., and Botzet, M., 1996. The HIRHAM4 Regional Atmospheric Climate Model. DMI Scientific Report No. 96-4, DMI, Copenhagen.

Cooper, J. A. G. and Pilkey, O. H., 2004. Sea-level rise and shoreline retreat: time to abandon the Bruun rule. *Global and Planetary Change*, 43: 157-171.

Cooper, J.A.G. and Pilkey, O.H., 2004. Alternatives to the mathematical modelling of beaches. *Journal of Coastal Research* 20(3): 641-644.

Cotton, P.D., Carter, D.J.T., Allan, T.D., Challenor, P.G., Woolf, D., Wolf, J., Hargreaves, J.C., Flather, R.A., Bin, L., Holden, N., and Palmer, D., 1999.

JERICHO - The impact of a changing wave climate on our coasts. Technical Report, BNSC LINK project R3/003, Satellite Observing Systems, UK.

Cowell, P.J. and Bruce, T.G., 2006. Discussion on: Pilkey, O.H. and Cooper, J.A.G., 2006. Discussion of: Cowell, P.J., Thom, G., Jones, A., Everts, C.H., and Simanovic, D., 2006. Management of uncertainty in predicting climate-change. Journal of Coastal Research, 22(1): 232-245. Journal of Coastal Research, 22(6): 1577-1579. *Journal of Coastal Research*, 22(6): 1580-1584.

Cowell, P.J., Stive, M.J.F., Niedoroda, A.W., Swift, D.J.P., De Vriend, H.J., Buijsman, M.C., Nicholls, R.J., Roy, P.S., Kaminsky, G.M., Cleveringa, J., Reed, C.W., and De Boer, P.L., 2003. The coastal track (Part 2): an applications of aggregated modelling to lower-order coastal change. *Journal of Coastal Research*, 19(4): 828-848.

Cowell, P.J., Thom, G., Jones, A., Everts, C.H., and Simanovic, D., 2006. Management of uncertainty in predicting climate-change. *Journal of Coastal Research*, 22(1): 232-245.

Crank, J., 1975. *The mathematics of diffusion*. Oxford: Clarendon Press.

Dabees, M., and Kamphuis, W.J., 1998. ONELINE, a numerical model for shoreline change. *Proceeding of the 26th International Conference on Coastal Engineering*, ASCE, pp. 2668-2681.

Davidson-Arnott, G.D., 2005. Conceptual model of the effects of sea level rise on sandy coasts. *Journal of Coastal Research*, 21(6): 1166-1172.

De Vriend, H. J., 2003. On the prediction of aggregated-scale coastal evolution. *Journal of Coastal Research*, 19(4): 757-759.

De Vriend, H.J., Capobianco, M., Chesher, T., de Swart, H.E., Latteux, B, Stive, M.J.F., 1993. Approaches to long-term modelling of coastal morphology: a review. *Coastal Engineering*, 21: 225-269.

Dean, R.G. and Dalrymple, R.A., 2002. *Coastal processes: with engineering applications*. Cambridge University Press, Cambridge, 487 pp.

Dean, R.G. and Maurmeyer, E.M., 1983. Models for beach profile response. In: Komar, P.D., (Editor), Handbook of Coastal Processes and Erosion. CRC Press, Boca Raton, Florida, pp. 151-166.

Dean, R.G., 1977. Equilibrium beach profiles: characteristics and applications. *Journal of Coastal Research*, 7(1): 53-84.

Dean, R.G., 1983. *CRC handbook of coastal processes and erosion*. P.D. Komar, ed., CRC Press, Inc., Boca Raton, Florida.

Dean, R.G., 1990. Beach response to sea level change. "Ocean Engineering Science". In: Le Méhauté, B. and Hanes, D.M., (Editors), The Sea. John Wiley and Sons, NY. Vol 9, pp. 869-887.

DEFRA, 2006. Flood and coastal defence guidance FCDPAG3 economic appraisal supplementary note to operating authorities – climate change impacts. <http://www.defra.gov.uk/environ/fcd/pubs/pagn/fcdpag3/>.

Dickson, M., Walkden, M., and Hall, J. W., 2007. Systematic impacts of climate change on an eroding coastal region over the twenty-first century. *Climatic Change*, 84(2): 141-166.

Dodd, N. and Brampton, A. H., 1995. Wave transformation models: A project definition study. Report SR 400, HR Wallingford, Wallingford, 24 pp.

Donelan, M. A., Hamilton, J., and Hui, W. H., 1985. Directional spectra of wind-generated waves. *Philosophical Transactions of the Royal Society of London*, Serries A, 315: 509-562.

Donelan, M., 1980. Similarity theory applied to the forecasting of wave heights, periods and directions. *Canadian Coastal Conference*, Burlington, Canada, pp. 47-61.

Dong, P. and Chen, H., 1999. A probability method for predicting time-dependent long-term shoreline erosion. *Coastal Engineering*, 36: 243-261.

Dong, P. and Chen, H., 2001. Wave chronology effects on long-term shoreline erosion predictions. *Journal of Waterway, Port, Coastal, and Ocean Engineering*, 127(3): 186-189.

Douglas, B.C., Kearney, M.S., and Leatherman, S.P., 2001. *Sea level rise: history and consequences*. Academic Press, San Diego, US, 232 pp.

Eitner,V., 1996. Geomorphological response of the East Frisian barrier islands to sea-level rise: an investigation of past and future evolution. *Geomorphology*, 15: 57-65.

Environmental Agency, 1999. The state of the environment of England and Wales: coasts. Environmental Agency Report. Stationary Office, London, 201 pp.

Falqués, A. and Calvete, D., 2005. Large scale dynamics of sandy coastlines: Diffusivity and instability. *Journal of Geophysical Research*, 110, C03007, doi:10.1029/2004JC002587.

Falqués, A., 2003. On the diffusivity in coastline dynamics. *Geophysical Research Letters*, 30(21): 2119.

Falqués, A., 2006. Wave driven alongshore sediment transport and stability of the Dutch coastline. *Coastal Engineering*, 53: 243-254.

Feyen, L., Dankers, R., Barredo, J.I., Kalas, M., Bódis, K., Roo, A. Lavalle, C., 2006. Flood risk in Europe in a changing climate. Institute of Environment and Sustainability, PESETA Project, Report EUR 22313 EN, 20 pp.

Forbes, D. L., Orford, J. D., Taylor, R. B., and Shaw, J., 1997. Interdecadal variation in shoreline recession on the Atlantic coast of Nova Scotia. *Proceedings of the Canadian Coastal Conference '97*, Guelph, Ontario, Canadian Coastal Science and Engineering Association, Ottawa, ON, Canada, pp. 360-374.

FORESIGHT, 2003. Future flooding. Executive summary. Flood and Coastal Defence Project of the Foresight programme, Office of Science and Technology, UK, 59 pp.

Freund, J.E., 1992. *Mathematical Statistics*. Prentice Hall, Inc, New Jersey, 576 pp.

Gallagham, D. P., Saint-Cast, F., Nielsen, P., and Baldock, T. E., 2006. Numerical solutions of the sediment conservation law; a review and improved formulation for coastal morphological modelling. Coastal Engineering, 53: 557-571.

Galvin, G.J. and Eagleson, P.S., 1965. Experimental study of longshore currents on a plane beach. CERC Technical Memo No. 10, U.S. Army Corps of Engineers.

Goda, Y., 2000. *Random seas and design of maritime structures*. Advanced Series of Ocean Engineering, Vol.15, World Scientific Publishing, Singapore, 443 pp.

Goreau, T.J., Hilbertz, W., and Hakeem, A. Azeez A., 2004. Web resource. http://www.globalcoral.org/MALDIVES%20SHORELINES.%20GROWING%20A%20BEACH.htm, 01/05/2004.

Gottlieb, D. and Shu, C.-W., 1997. On the Gibbs phenomenon and its resolution. *SIAM Review*, 39(4): 644-668.

Gradshteyn, I.S. and Ryzhik, I.M., 2000. *Table of integrals, series and products*. Academic Press, San Diego, 1163 pp.

Gravens, M.B., Kraus, N.C., Hanson, H., 1991. GENESIS: generalized model for simulating shoreline change. Report 2, Workbook and System User's Manual. U.S. Army Corps of Engineers.

Grevemeyer, I., Herber, R., and Essen, H.H., 2000. Microseismological evidence for a changing wave climate in the northeast Atlantic Ocean. *Nature*, 408: 349-352.

Grijm, W., 1961. Theoretical forms of shoreline. *Proceedings of the 7th International Conference on Coastal Engineering*, ASCE, pp. 219-235.

Gulev, S.K. and Hasse, L., 1999. Changes in wind waves in the North Atlantic over the last 30 years. *International Journal of Climatology*, 19: 1091-1117.

Günther, H., Rosenthal, W., Stawarz, M., Carretero, J.C., Gomez, M., Lozano, L., Serrano, O., and Reistad, M., 1998. The wave climate of the Northeast Atlantic over the period 1955-1994: the WASA wave hindcast. *The Global Atmosphere and Ocean System*, 6: 121-163.

Haaser, N.B. and Sullivan, J.A., 1971. *Real Analysis*. Van Nostrand Reinhold, New York, 341 pp.

Halcrow Ltd, 2004. Poole Bay and harbour strategy study- Assessment of flood and coast defence options - Poole Bay. Halcrow report, 57 pp.

Halcrow Maritime, 1999. Poole and Christchurch Bays Shoreline Management Plan. Report to Poole Bay and Christchurch Bay Coastal Group (Lead Authority: Bournemouth Borough Council) Volume 2: Physical Environment.

Halcrow, 2002. Futurcoast [CD-ROM]. Produced for Department for Environment, Food, and Rural Affairs (DEFRA).

Hallermeier, R.J., 1981. A profile zonation for seasonal sand beaches from wave climate. *Coastal Engineering*, 4: 253-277.

Hamdi, S., Enright, W. H., Ouellet, Y., and Schiesser, W. A., 2005. Method of lines solutions of the extended Boussinesq equations. *Journal of Computational and Applied Mathematics*, 183: 327-342.

Hands, E.B., 1983. The Great Lakes as a test model for profile responses to sea level changes. In: Komar, P.D., (Editor), Handbook of Coastal Processes and Erosion. CRC Press, Boca Raton, Florida, pp. 179-189.

Hanson, C. and Goodness, C.M., 2004. Predicting future changes in wind. Climate Change Research Unit, University of East Anglia, Norwich, NR4 7TJ.

Hanson, H. and Kraus, N.C., 1991. Numerical simulation of shoreline change at Lorain, Ohio. *Journal of Waterway, Port, Coastal, and Ocean Engineering*, 117: 1-18.

Hanson, H. and Larson, M., 1987. Comparison of analytic and numerical solutions of the one-line model of shoreline change. *Coastal Sediments `87*, ASCE, pp. 500-514.

Hanson, H. and Larson, M., 1998. Seasonal shoreline variations by cross-shore transport in a one-line model under random waves. *Proceeding of the 26th International Conference on Coastal Engineering*, ASCE, pp. 2682-2695.

Hanson, H., 1987. GENESIS-A generalized shoreline change numerical model for engineering use. Ph.D. Thesis, Dept. of Water Resources Eng., Lund Inst. of Tech./Univ. of Lund, Report No. 1007, 206 pp.

Hanson, H., Aarninkhof, S., Capobianco, M., Jimenez, J.A., Larson, M., Nicholls, R.J., Plant, N.G., Southgate, H.N., Steetzel, H.J., Stive, M.J.F., de Vriend, H.J., 2003. Modelling of coastal evolution on yearly to decadal time scales. *Journal of Coastal Research*, 19(4): 790-811.

Hanson, H., Larson, M., Kraus, N.C., 2001. A new approach to represent tidal currents and bathymetric features in the one-line model concept. *Coastal Dynamics `01*, pp. 173-181.

Hanson, H., Larson, M., Kraus, N.C., Capobianco, M., 1997. Modelling of seasonal variations by cross-shore transport using one-line compatible methods. *Coastal Dynamics `97*, pp. 893-902.

Hawkes, P.J., Bagenholm, C., Gouldby, B.P, and Ewing, J., 1997. Swell and bi-modal wave climate around the coast of England and Wales. Report SR 409, HR Wallingford.

Hoffman, J.D., 2001. *Numerical methods for engineers and scientists*. Marcel Dekker, Inc. 823 pp.

Holt, T., 1999. A classification of ambient climatic conditions during extreme surge events off Western Europe. *International Journal of Climatology*, 19: 725-744.

Hosking, A. and McInnes, R., 2002. Preparing for the impacts of climate change on the Central South Coast of England: a framework for future risk. *Journal of Coastal Research*, 36(SI): 381-389.

Houghton, J. T., Meira Filho, L. G, Callander, B. A., Harris, N., Kattenberg, A., and Maskel, K., editors. *Climate change 1995: the Science of Climate Change.* Cambridge University Press, Cambridge, UK.

Hulme, M. and Carter, T.R., 2000. The changing climate of Europe. In: Parry M.L., (Editor), Assessment of Potential Effects and Adaptations for Climate Change in Europe: The Europe ACACIA Project. Jackson Environmental Institute, University of East Anglia, Norwich, UK, 324 pp.

Hulme, M. and Jenkins, G. J., 1998. Climate change scenarios for the UK: scientific report. UKCIP Technical Report No.1, Climate Research Unit, Norwich, UK, 50 pp.

Hulme, M., Jenkins, G.J., Lu,X., Turnpenny, J.R., Mitchell, T.D., Jones, R.G., Lowe, J., Murphy, J.M., Hasell, D., Boorman, P., McDonald, R., and Hill, S., 2002. Climate change scenarios for the United Kingdom: the UKCIP02 scientific report. Tyndall Centre for Climate Change Research, School of Environmental Sciences, University of East Anglia, Norwich, UK, 120 pp.

Inman,D.L. and Bagnold,R.A., 1963. Littoral processes. In: M.N.Hill (Editor), The Sea, Vol.3. The earth beneath the sea. Interscience, New York, pp. 529-553.

IPCC SRES, 2000. Special report on emissions scenarios (SRES). A special report of working Group III of the Intergovernmental Panel on Climate Change. Cambridge University Press, Cambridge, UK, 559 pp.

IPCC WG1, 2001. Climate change 2001: the scientific basis. Contribution of the Working Group I to the Third Assessment Report of the Intergovernmental Panel on Climate Change. Cambridge University Press, Cambridge, UK, 881 pp.

IPCC WG1, 2007. Climate change 2007: the physical science basis. Contribution of the Working Group I to the Fourth Assessment Report of the Intergovernmental Panel on Climate Change, Cambridge University Press, Cambridge, UK, 940 pp.

IPCC WG2, 2001. Climate change 2001: impacts, adaptation and vulnerability. Contribution of the Working Group II to the Third Assessment Report of the Intergovernmental Panel on Climate Change. Cambridge University Press, Cambridge, UK, 1000 pp.

Jayakumar and Mahadevan, R., 1993. Numerical simulation of shoreline evolution using a one-line model. *Journal of Coastal Research*, 9(4): 915-923.

Jenkins, G and Lowe, J., 2003. Handling uncertainties in the UKCIP02 scenarios of climate change. Hadley Centre Technical Note 44, 15 pp.

Jenkins, M., and Keehn, S., 2001. Effects of beach nourishment of equilibrium profile and depth of closure. *Coastal Dynamics `01*, pp. 888-897.

Jerri, A. J., 1998. *The Gibbs phenomenon in Fourier analysis, splines and wavelet approximations*. Kluwer Academic Publishers, Dordrecht, 376 pp.

Kaas, E. and Andersen, U., 2000. Scenarios for extra-tropical storm and wave activity: methodologies and results. ECLAT-2 Blue Workshop, Climate Scenarios for Water Related and Coastal Impact, KNMI, Netherlands.

Kaas, E., Andersen, U., Flather, R.A., Willimas, J.A., Blackman, D.L., Lionello, P., Dalan, F., Elvini, E., Nizzero, A., Malguzzi, P., Pfizenmayer, A., von Storch, H., Dillingh, D., Phillipart, M., de Ronde, J., Reistad, M., Midtbø, K.H.,Vignes, O., Haakenstad, H., Hackett, B., Fossum, I., Sidselrud, L., 2001. Synthesis of the

STOWASUS-2100 project: regional storm, wave and surge scenarios for the 2100 century. Danish Climate Centre Report 01–3, 27 pp.

Kamphuis, J.W., 1991. Alongshore sediment transport rate. *Journal of Waterway, Port, Coastal, and Ocean Engineering*, 117: 624-640.

Kamphuis, J.W., 2000. *Introduction to coastal engineering and management.* World Scientific Publishing Co. Pte. Ltd., 437 pp.

Karambas, Th.V., de la Pena, J.M., Christopoulos, S., Santas, J.C., Krestenitis, Y.N., 2001. Malagueta beach case: Nourishment characteristics, field surveys and numerical simulation. *Coastal Dynamics `01*, pp. 182-191.

Komar, P.D. and Inman, D.L. 1970. Longshore sand transport on beaches. *Journal of Geophysical Research*, 75(30): 5914-5927.

Komar, P.D. and McDougal, W.G., 1994. The analysis of beach profiles and nearshore processes using the exponential beach profile form. *Journal of Coastal Research*, 10: 59-69.

Komar,P.D., 1998. *Beach processes and sedimentation.* Prentice Hall, Inc, New Jersey, 544 pp.

Kraus, N.C. and Harikai, S., 1983. Numerical model of the shoreline change at Oarai Beach. *Coastal Engineering*, 7: 1-28.

Kraus, N.C., Isobe, M., Igarashi, H., Sasaki, T.O., Harikaw, K., 1982. Field experiments on longshore transport in the surf zone. *Proceeding of the 18th International Conference on Coastal Engineering*, ASCE, pp. 969-988.

Kumar, S.V., Anand, N.M., Chandramohan, P., Naik, G.N., 2002. Longshore sediment transport rate-measurement and estimation, central west coast of India. *Coastal Engineering*, 48: 95-109.

Lanfredi, N.W., Pousa, J.L., and d'Onofrio, E.E.D., 1998. Sea-level rise and related potential hazards on the Argentine Coast. *Journal of Coastal Research*, 14(1): 47-60.

Larson, M. and Kraus, N.C., 1989. SBEACH: numerical model for simulating storm induces beach change. Technical Report CERC-89-9, U.S. Army Corps of Engineers.

Larson, M., 2005. Numerical modeling. In: Schwartz, M. (Editor), Encyclopedia of Coastal Science, pp. 730-733.

Larson, M., Capobianco, M., Jansen, H., Rozynski, G., Southgate, H. N., Stive, M., Wijnberg, K. M., and Hulscher, S., 2003. Analysis and modeling of field data on coastal morphological evolution over yearly and decadal time scales. Part 1: Background and linear Techniques. *Journal of Coastal Research*, 19(4): 760-775.

Larson, M., Hanson, H., Kraus, N.C., 1987. Analytical solutions of the one-line model of shoreline change. Technical Report CERC-87-15, USAE-WES, Coastal Engineering Research Center, Vicksburg, Missisippi.

Larson, M., Hanson, H., Kraus, N.C., 1997. Analytical solutions of one-line model for shoreline change near coastal structures. *Journal of Waterway, Port, Coastal, and Ocean Engineering*, 123(4): 180-191.

Larson, M., Kraus, N. C., and Hanson, H., 2006. Simulation of regional longshore sediment transport and coastal evolution - the "cascade" model. Proceedings of the 28th International Conference on Coastal Engineering, ASCE, Cardiff, Wales, pp. 2612-2624.

Le Mehauté, B and Soldate, M., 1977. Mathematical modelling of shoreline evolution. CERC Miscellaneous Report No. 77-10, USAE-WES, Coastal Engineering Research Center, Vicksburg.

Le Mehauté, B and Soldate, M., 1978. Mathematical modelling of shoreline evolution. *Proceeding of the 16th International Conference on Coastal Engineering*, ASCE, pp. 1163-1179.

Le Mehauté, B. and Brebner, A., 1961. An introduction to coastal morphology and littoral processes. Report 14, Department of Civil Engineering, Queen's University, Kingston, Ontario, Canada.

Leatherman, S.P., Zhang, K., and Douglas, B.C., 2000. Sea level rise shown to drive coastal erosion. *EOS Transactions, American Geophysical Union*, 81(6): 55-57.

Leggett, J., Pepper, W.J., and Swart, R.J., 1992: Emissions scenarios for IPCC: An update. In: Houghton, J.T., Callander, B.A., Varney, S.K., (Editors.), Climate Change 1992. The Supplementary Report to the IPCC Scientific Assessment. Cambridge University Press, Cambridge.

Longuet-Higgins, M.S., 1952. On the statistical distribution of the height of sea waves. *Journal of Marine Research*, 11: 245-266.

Lorenzo, E. and Teixeira, L., 1997. Sensitivity of storm waves in Montevideo (Uruguay) to a hypothetical climate change. *Climate Research*, 9: 81-85.

Lunkeit, F., Fraedrich, K., and Bauer, S., 1998. Storm tracks in a warmer climate: Sensitivity studies with a simplified circulation model. *Climate Dynamics*, 14: 813-826.

Mathworks, 2001. Statistics toolbox. Matlab user's guide, Version 5.

Mearns, L. O., Mavromatic, T., Tsvetsinskaya, E., Hays, C., and Easterling, W., 1999. Comparative responses of EPIC and CERES crop models to high and low resolution climate change scenario. *Journal of Geophysical Research*, 104(D6): 6623-6646.

Mearns, L. O., Rosenweig, C., and Goldberg, R., 1997. Mean and variance change in climate scenarios: methods, agricultural applications, and measures of uncertainty. *Climatic Change*, 35: 367-396.

Miller R.G., 1981. *Simultaneous statistical inference*. Springer, New York.

Minura, N. and Nobuoka, H., 1995. Verification of Bruun Rule for the estimate of shoreline retreat caused by sea-level rise. *Coastal Dynamics 95*, ASCE, pp. 607-616.

Miura, M., Uda, T., and Serizawa, M., 2006. Theoretical extrapolation of open boundary condition of one-line model. *Proceedings of the 30th International Conference on Coastal Engineering*, San Diego, California, USA, pp. 3442-3454.

Murray, A. B. and Ashton, A., 2004. Extending 1-line modeling approach to explore emergent coastline behaviors. *Proceedings of the 29th International Conference on Coastal Engineering*, National Civil Engineering Laboratory, Lisbon, Portugal, pp. 2035-2047.

Nicholls, R. J., Watkinson, A., Mokrech, M., Hanson, S., Richards, J., Wright, J., Jude, S., Nicholson-Cole, S., Walkden, M., Hall, J., Dawson, R., Stansby, P., Jacoub, G. K., Rounsvell, M., Fontain, C., Acosta, L., Lowe, J., Wolf, J., Leak, J., Dickson, M., and Balson, P., 2007. Integrated coastal simulation to support shoreline management planning. *Flood and Coastal Management Conference*, University of York, UK.

Nicholls, R.J. and Wilson, T., 2001. Integrated impacts on coastal areas and river flooding. In: Holman, I.P. and Loveland, P.J. (Editors), Regional Climate Change Impact and Response Studies in East Anglia and North West England (RegIS). Final report of MAFF project no. CC0337, 360 pp.

Nicholls, R.J., 2000. Coastal zones. In: Parry, M.L., (Editor), Assessment of Potential Effects and Adaptation for Climate Change in Europe: The Europe ACACIA Project. Jachson Environmental Institute, University of East Anglia, Norwich, United Kingdom, 324 pp.

Nicholls, R.J., and Birkemeier, W.A., 1997. Morphological and sediment budget controls on depth of closure at Duck, NC. *Coastal Dynamics `97*, pp. 497-505.

Nicholls, R.J., Birkemeier, W.A., Lee, G., 1998. Evaluation of depth of closure using data from Duck, NC, USA. *Marine Geology*, 148: 179-201.

Nicholls,R.J., 2002. Rising sea levels: potential impacts and responses. In: Hester, R. and Harrison, R.M., (Editors), Global Environmental Change. Issues in Environmental Science and Technology, Number 17, Royal Society of Chemistry, Cambridge, pp. 83-107.

Ozasa, H. and Brampton, A.H., 1980. Mathematical modelling of beaches backed by seawalls. *Coastal Engineering*, 4(1): 47-64.

Paskoff,R.P., 2004. Potential implications of sea-level rise for France. *Journal of Coastal Research*, 20(2): 424-434.

Payo, A., Baquerizo, A., and Losada, M. A., 2004. Uncertainty assessment of long term shoreline prediction. *Proceedings of the 29th International Conference on Coastal Engineering*, Lisbon, Portugal, pp. 2087-2096.

Peerbolte, E.B., de Ronde, J.G., de Vrees, L.P.M., Mann, M., and Baarse, G., 1991. Impact of sea-level rise on society: a case study for the Netherlands. Final Report, Delft Hydraulics and Rijkswaterstaat, Delft and the Hague.

Pelnard-Considère, R., 1956. Essai de theorie de l'evolution des forms de rivages en plage de sable et de galets: 4th Journees de l'Hydraulique, les Energies de la Mer, Question III, Rapport No. 1: 289-298.

Perlin, M., 1979. Predicting beach planforms in the lee of breakwater. *Coastal Structures '79*, ASCE, pp. 792-808.

Pilkey, O.H., Young, R.C., and Bush, D.M., 2000. Comment of sea level rise shown to drive coastal erosion. *EOS Transactions*, 81(3): 437-441.

Pope, V.D., Gallani, M.L., Rowntree, P.R., and Stratton, R.A., 2000. The impact of new physical parameterizations in the Hadley Centre climate model: HadAM3. *Climate Dynamics*, 16: 123–146.

Press, W. H., Teukolsky, S. A., Vettering, W. T., and Flannery, B. P., 1992. *Numerical recipes in Fortran: the art of scientific Computing*. Cambridge University Press, Cambridge.

Price, W. A., Tomlinson, D. W., and and Willis, D. H., 1972. Predicting changes in the plan shape of beaches. *Proceedings of the 13th International Conference on Coastal Engineering*, ASCE, pp. 1321-1329.

Pryor, S.C., Barthelmie, R.G., and Kjellström, E., 2005: Potential climate change impact on wind energy resources in northern Europe: Analyses using a regional climate model. *Climate Dyn*amics, 25: 815–835.

Räisänen, J., Hansson, U., Ullerstig, A., Döscher, R., Graham, L. P., Jones, C., Meier, M., Samuelsson, P., and Willén, U., 2003. GCM driven simulations of recent and future climate with the Rossby Centre coupled atmosphere - Baltic Sea regional climate model RCAO. RMK No.101, Rossby Centre, SMHI.

Reeve, D.E. and Spivack, M., 2004. Probabilistic Methods for Morphological Prediction. *Coastal Engineering*, 51(8-9): 661-673.

Reeve, D.E., 2006. Explicit expression for beach response to non-stationary forcing near a groyne. *Journal of Waterway, Port, Coastal and Ocean Engineering*, 132: 125-132.

Regnauld, H., Binois, S., Fouque, C., and Lemasson, L., 1999. Micro- to mesoscale evolution of beaches in response to climatic shift: observation and conceptual modelling (Brittany, France). *Geologie en Mijnbouw*, 77: 323-332.

Reinen-Hamill, R.A., 1997. Numerical modelling of the Canerbury Regional Bight. The use of a shoreline evolution model for management and design purposes. *Pacific Coasts and Ports `97: Proceedings of the 13th Australasian Coastal and Ocean Engineering Conference*, pp. 359-364.

Richmond, B.M., Mieremet, B., and Reiss, T.E., 1997. Yap Islands coastal systems and vulnerability to potential accelerated sea-level rise. *Journal of Coastal Research*, 24(SI): 153-173.

Riley, K. F., Hobson, M. P., and Bence, S. J., 1998. *Mathematical methods for physics and Engineering: a comprehensive guide*. Cambridge University Press, Cambridge, 1028 pp.

Roeckner, E., Arpe, K., Bengtsson, L., Christoph, M., Claussen, M., Dümenil, L., Esch, M., Giorgetta, M., Schlese, U., and Schulzweida, U., 1996. The atmospheric general circulation model ECHAM-4: Model description and simulation of present-day climate. MPI Report 218, Max-Planck-Insitut für Meteorologie, 90 pp.

Rowell, D. P., 2006. A demonstration of the uncertainty in projections of the UK climate change resulting from regional model formulation. *Climatic Change*, 79(3-4): 243-257.

Ruggiero, P., List, J., Hanes, D., and Eshleman, J., 2006. Probabilistic shoreline change modeling. *Proceedings of the30th International Conference on Coastal Engineering*, San Diego, California, USA, pp. 3417-3429.

Rummukainen, M., Bergström, S., Persson, G., Rodhe, J. and Tjernström, M., 2004: The Swedish Regional Climate Modelling Programme, SWECLIM: a review. *Ambio*, 33: 176–182.

Schiesser, W.E., 1991. *The numerical method of lines: Integration of partial differential equations*. Academic Press, Inc, 326 pp.

Schoones, J.S. and Theron, A.K., 1993. Review of the field-data base for longshore sediment transport. *Coastal Engineering*, 19: 1-25.

Schoones, J.S. and Theron, A.K., 1994. Accuracy and applicability of the SPM longshore transport formula. *Proceeding of the 24th International Conference on Coastal Engineering*, pp. 2595-2609.

SCOPAC, 2003. Poole harbour entrance to Hengistbury Head (Poole Bay). SCOPAC Sediment transport study, 42 pp.

SCOR, 1991. The response of beaches to sea level changes: a review of predictive models. Report of the Scientific Committee of Ocean Research Working Group 89. *Journal of Coastal Research*, 7(3): 895-921.

Slott, J. M., Murray, A.B., Valvo, L., and Ashton, A., 2005. Shoreline response to climate change and human manipulations in a model of large-scale coastline change. *Eos Trans. AGU*, 86(52), Fall Meet. Suppl., Abstract H51C-0387.

Sneddon, I.H., 1972. *The use of integral transforms*. McGraw-Hill, Inc, 539 pp.

Soulsby, R.L., Sutherland, J., and Brampton, A.H., 1999. Coastal steepening, the UK view. HR Wallingford Report TR 91.

Southgate, H. N., Wijnberg, K. M., Larson, M., Capobianco, M., and Jansen, H., 2003. Analysis of field data of coastal morphological evolution over yearly and decadal timescales. Part 2: Non-linear techniques. *Journal of Coastal Research*, 19(4): 776-789.

Southgate, H.N. and Capobianco, M., 1997. The role of chronology in long-term morphodynamics. *Coastal Sediments `97*, ASCE, pp. 943-952.

Steetzel, H.J., 1995. Prediction of development coastline and outer deltas of Wadden coast for the period 1990-2040. WL/ DELFT HYDRAULICS report H1887, (in Dutch).

Steetzel, H.J., de Vroeg, H., van Rijn, L.C, Stam, J., 2000. Long-term modelling of the Holland coast using a multi-layer model. *Proceeding of the 27th International Conference on Coastal Engineering*, pp. 2942-2955.

Stive, M. J. F., Roelvink, D. A., and De Vriend, H. J., 1990. Large scale coastal evolution concept. The Dutch coast. *Proceedings of the 22nd International Conference on Coastal Engineering*, ASCE, New York, USA, pp. 1962-1974.

Stive, M.J.F., 2004. How important is global warming for coastal erosion? *Climatic Change*, 64: 27-39.

Stive, M.J.F., Aarninkhof, S.G.J., Hamm, L., Hanson, H., Larson, M., Wijnberg, K.M., Nicholls, R.J., and Capobianco, M., 2002. Variability of shore and shoreline evolution. *Coastal Engineering*, 47: 211-235.

Sutherland, J. and Goulby, B., 2002. Vulnerability of coastal defences to climate change. *Water and Maritime Engineering*, 156(WM2): 137-145.

Sutherland, J. and Wolf, J., 2002. Coastal defence vulnerability 2075. Report SR 590, 30 pp.

Szmytkiewicz, M., Biegowski, J., Kaczmarek, L. M., Okròj, T., Ostrowski, R., Pruszak, Z., Ròżyńsky, G., and Skaja, M., 2000. Coastline changes nearby harbours structures: comparative analysis of one-line models versus field data. *Coastal Engineering*, 40: 119-139.

Szmytkiewicz, M., Biegowski, J., Kaczmarek, L. M., Okròj, T., Ostrowski, R., Pruszak, Z., Ròżyński, G., Skaja, M., and Zeidler, R. B., 1998. Comperative analysis of

coastline models. Final Report, DWW-1149, Rijkswaterstaat Delft, C2-30-VAL, IBW PAN Gdańsk.

Taylor, J. A., Murdock, A. P., and Pontee, N. I., 2004. A macroscale analysis of coastal steepening around the coast of England and Wales. *The Geophysical Journal*, 170(3): 179-188.

Thieler, E.R., Pilkey, Young, R.S., Bush, D.M., Chai, F., 2000. The use of mathematical models to predict beach behaviour for U.S. coastal engineering: A critical review. *Journal of Coastal Research*, 16(1): 48-67.

Thompson, C. J., 2006. Forward Developments Ltd. Napier City Council EnvC W029/2006. New Zealand Environment Court.

Uguccioni, L., Deigaard, R., and Fredsoe, J., 2006. Instability of a coastline with very oblique wave incidence. *Proceedings of the 30th International Conference on Coastal Engineering*, San Diego, California, USA, pp. 3542-3553.

Van Straaten, L.M.J.U., 1961. Directional effects of winds, waves, and currents along the Dutch North Sea coast. *Geologie en Mijnbouw*, 40: 333-346 (Part 1) and 363-391(Part 2).

Walkden, M. and Dickson, M., 2006. The response of soft rock shore profiles to increased sea-level rise. Tyndall Centre for Climate Change Research, Working Paper 105.

Walkden, M. J. A. and Hall, J. W., 2005. A predictive mesoscale model of the erosion and profile development of soft rock shores. *Coastal Engineering*, 52: 535-563.

Walsh, K.J.E., Betts, H., Church, J., Pittock, A.B., McInnes, K.L., Jackett, D.R., and McDougall, T.J., 2004. Using sea level rise projections for urban planning in Australia. *Journal of Coastal Research*, 20(2): 586-598.

Walton, T.L. and Chiu, T.Y., 1979. A review of analytical techniques to solve the sand transport equation and some simplified solutions. *Coastal Structures `79*, ASCE, pp. 809-837.

Walton, T.L., 1994. Shoreline solution for tapered beach fill. *Journal of Waterway, Port, Coastal, and Ocean Engineering*, 120(6): 651-655.

WAMDIG, 1988: The WAM model - A third generation ocean wave prediction model. *Journal of Physical Oceanography*, 18: 1775-1810.

Weesakul, S. and Rasmeemasmuang, T., 2002. Numerical computation of grenulate bay shape. *Proceedings of the 28th International Conference on Coastal Engineering*, ASCE, Cardiff, Wales, pp. 3259-3271.

Weesakul, S., Pokavanich, T., and Yee Win, T., 2004. Numerical modelling of dynamic equilibrium bay shape. *Proceedings of the 29th International Conference on Coastal Engineering*, National Civil Engineering Laboratory, Lisbon, Portugal, pp. 2220-2231.

Willis, D. H., 1977. Evaluation of alongshore transport models. *Proceeding of Coastal Sediments '77*, ASCE, pp. 350-365.

Wind, H.G., 1990. Influence functions. *Proceedings of the 21thInternational Conference on Coastal Engineering*, ASCE, pp. 3281-3294.

Wolf, J. and Woolf, D., 2005. Waves and climate change in the sea of the Herbides. *ISOPE 2005*, Seoul, South Korea, 19-24 June, pp. 9.

Wouwer, A. V and Schiesser, W. A., 2005. Special Issue on the method of lines: Dedicated to Keith Miller. *Journal of Computational and Applied Mathematics*, 183: 241-244.

Wouwer, A. V, Saucez, Ph, and Schiesser, W. A., 2001. *Adaptive method of lines*. Chapman & Hall/CRC, 432 pp.

Young, R.S., Pilkey, O.H., Bush, D.M., Thieler, E.R., 1995. A discussion of the Generalized Model for Simulation Shoreline Change (GENESIS). *Journal of Coastal Research*, 11(3): 875-886.

Zacharioudaki, A. and Reeve, D. E., 2007. Explicit formulae of shoreline change under time-varying forcing. *Proceedings of the Conference on River, Coastal and Estuarine Morphodynamics: RCEM2007*, Twente, Netherlands, pp. 1067-1074.

Zhang, K., Douglas, B.C., and Leatherman, S.P., 2000. Twentieth-century storm activity along the U.S. east coast. *Journal of Climate*, 13: 1748-1761.

Zhang, K., Douglas, B.C., and Leatherman, S.P., 2004. Global warming and coastal erosion. *Climatic Change*, 64: 41-58.

Zwiers, F. W. and von Storch, H., 1995. Taking serial correlation into account in tests of the mean. *Journal of climate*, 8: 336-351.

http://home.clara.net/sisa/bonhlp.htm, 2007. Simple Interactive Statistical Analysis (SISA).

http://peseta.jrc.es/index.html, 2007. Projection of Economic impacts of climate change in Sectors of the European Union based on boTtom-up Analysis (PESETA project).

http://prudence.dmi.dk/, 27/10/2007. Prediction of Regional scenarios and Uncertainties for Defining EuropeaN Climate change risks and Effects (PRUDENCE project). Project EVK2-CT2001-00132 in the EU 5th Framework program for Energy, environment, and sustainable development.

http://solidearth.jpl.nasa.gov/PAGES/sea01.html, 06/12/2003. NASA. Solid Earth Sciences Working Group (SESWG).

http://web.dmi.dk/pub/STOWASUS-2100/, 2005. Regional STOrm, Wave and SUrge Scenarios for the 2100 century (STOWASUS 2100 project).

http://www.channelcoast.org, 2008. Channel Coastal Observatory. Data courtesy from the Channel Coastal Observatory.

http://www.halcrow.com/software/solutions/sands_home.asp, 2007. Halcrow Ltd.

http://www.itl.nist.gov/div898/handbook/ , 18/07/2006. NIST/SEMATECH e-Handbook of Statistical Methods.

http://www.ukcip.org.uk/, 2007. UK Climate Impacts Programme (UKCIP project).